

Welcome to

Novel strategies for high-granularity and radiation hardness LGAD sensors and front-end electronics

Michele CASELLE
(KIT)
michele.caselle@kit.edu

KSEIT

MENU

1) Novel High-Spatial and Time Resolution Sensor Technologies
(lecture 1)

Planar silicon sensor, 3D-sensor and LGAD

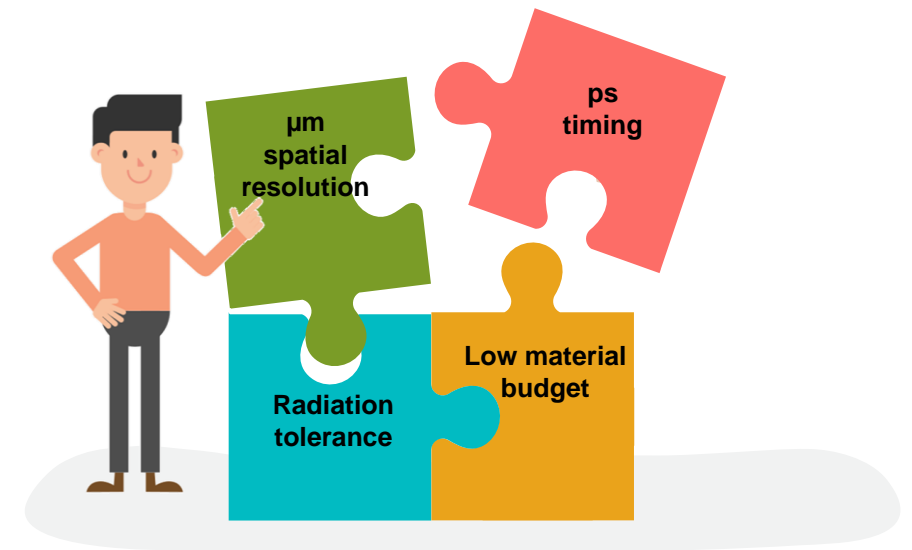
2) Readout Electronics Circuits and Strategies (lecture 2)

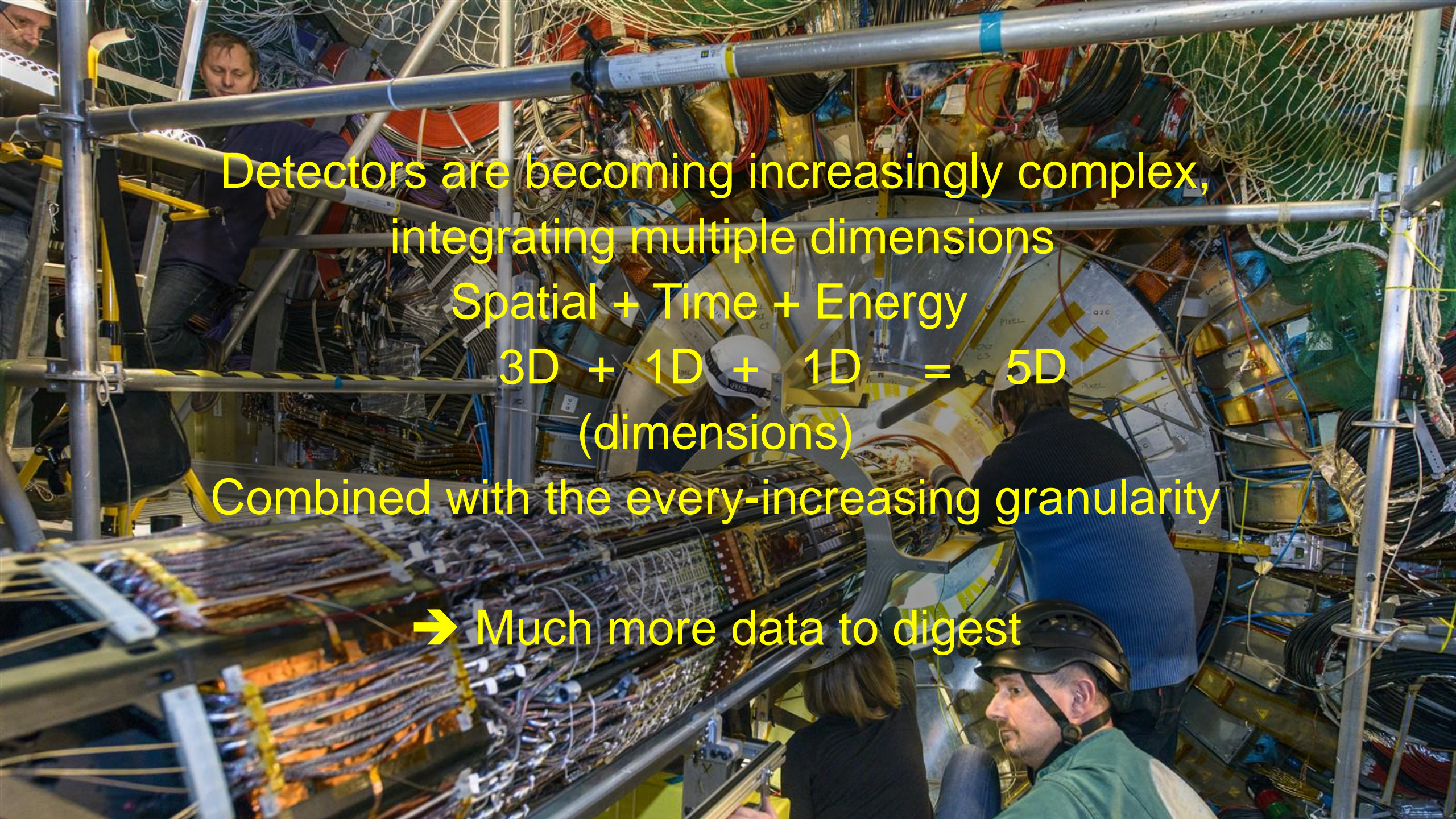
Amplification, timestamp logic, time-to-digital converters (TDCs)

First lecture

The 4D challenge

- Is it possible to build a detector with concurrent excellent time and position resolution?
- Can we provide in the same detector and readout chain:
 - Ultra-fast timing resolution [~ 10 ps]
 - Precision location information [10's of μm]





Detectors are becoming increasingly complex,
integrating multiple dimensions

Spatial + Time + Energy

$3D + 1D + 1D = 5D$
(dimensions)

Combined with the every-increasing granularity

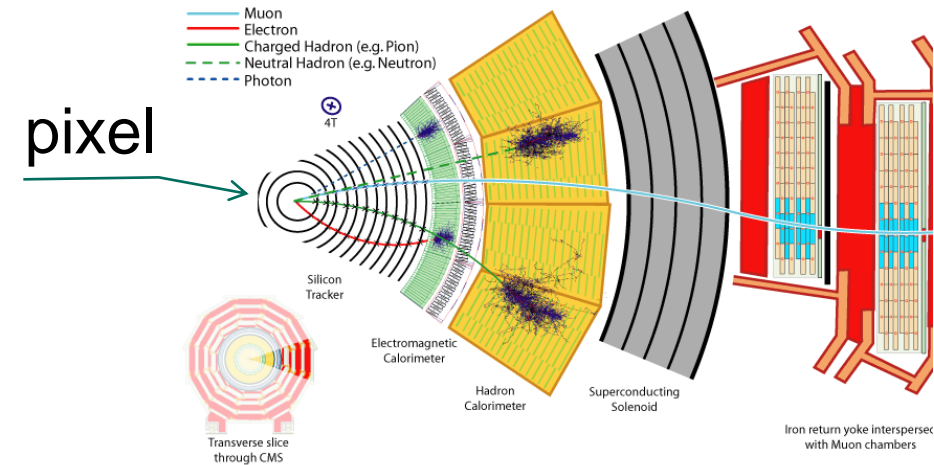
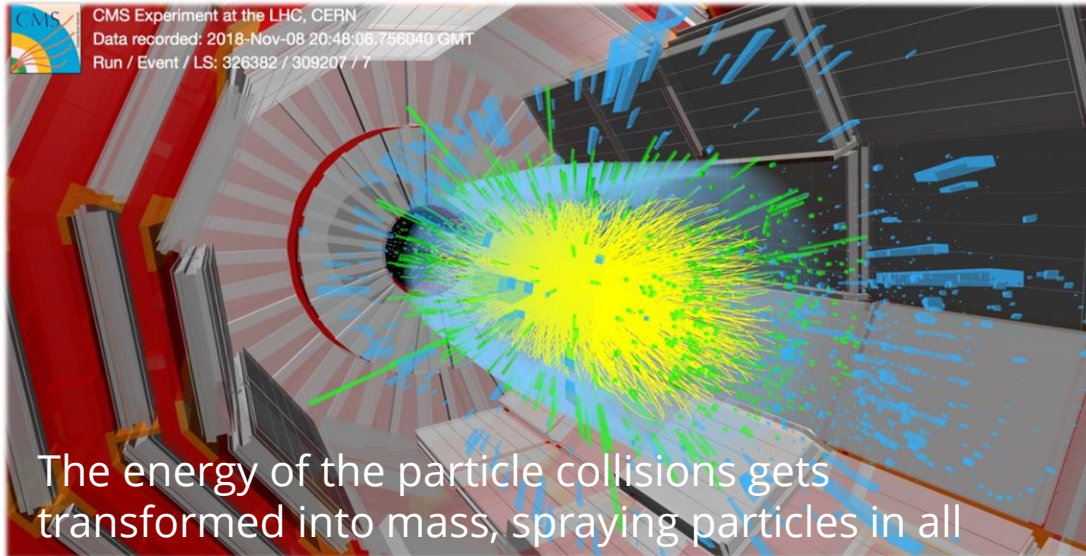
→ Much more data to digest



Why the time is important in
future HEP detector ?

CERN's Large Hadron Collider (LHC)

LHC is the most powerful and largest particle accelerator in the world

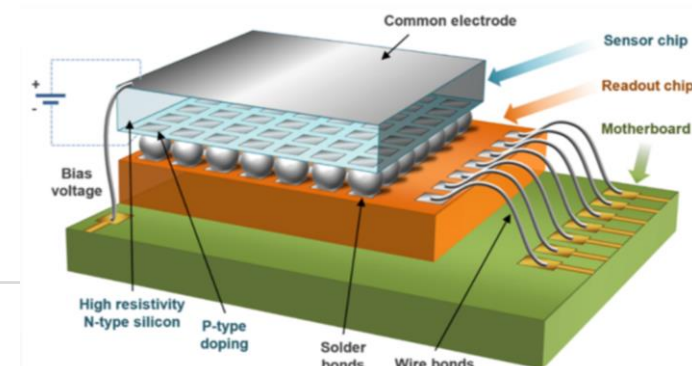


The detector is shaped like a cylindrical onion, with several concentric detection layers

■ Innermost detector layer consists of silicon pixel detector, requirements are:

- High-pixel granularity (resolution few μm)
- Time-resolution (25 ns, 40 M collision/sec)
- Large detector (several m^2)
- Operating in extremely harsh environment (10 million billions C)

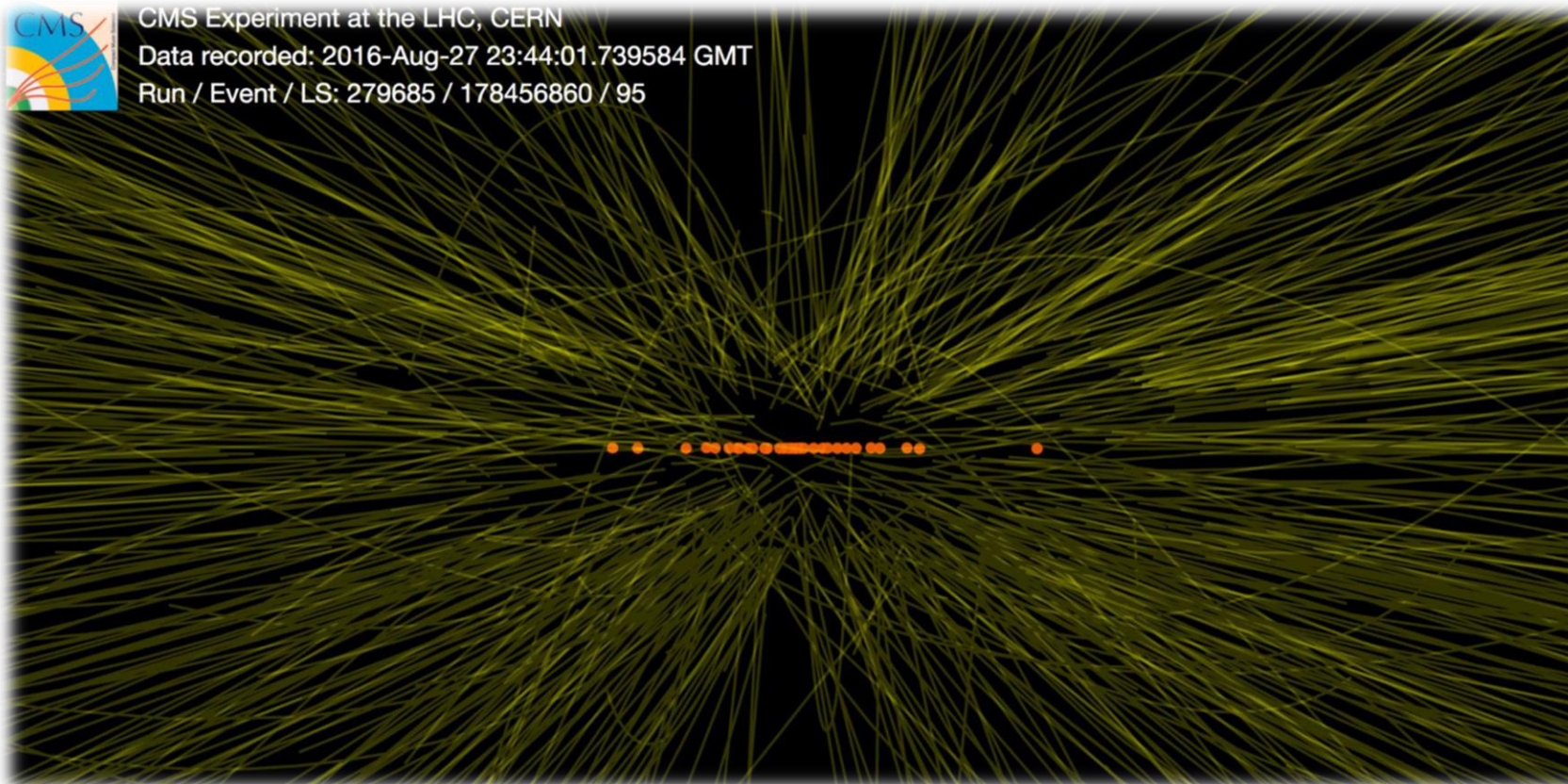
Hybrid pixel detector



Why the *time* is important ?

Pileup at collider experiments

- At each bunch crossing multiple collisions may happen (events)
- A primary vertex is associated to each event



[Collision events recorded by CMS in 2016 - CERN Document Server](#)

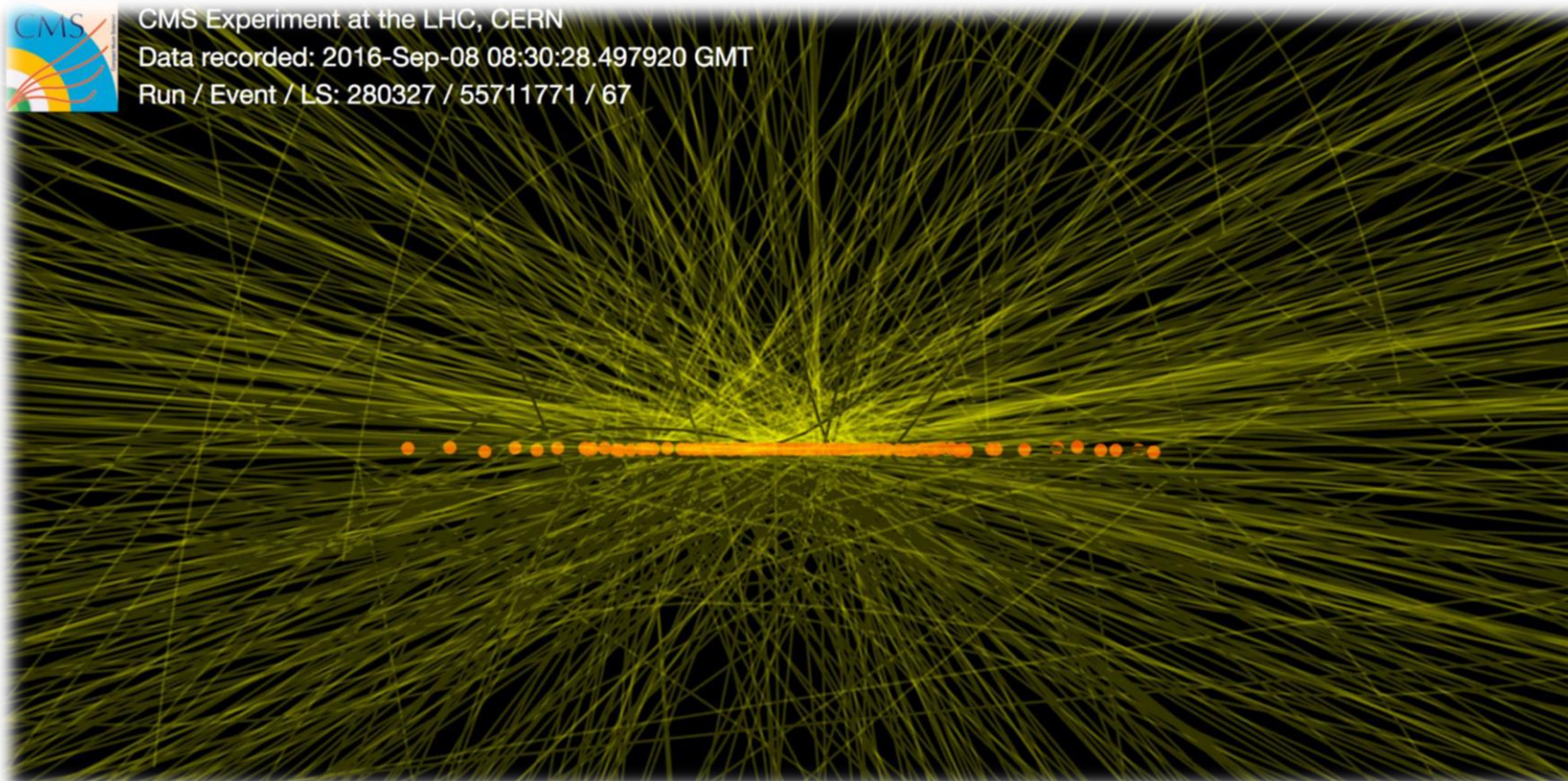
Event at CMS with 30 reconstructed vertices

Increasing the luminosity also the number of events increases

Why the *time* is important ?

Pileup at collider experiments

- At each bunch crossing multiple collisions may happen (events)
- A primary vertex is associated to each event



[Collision events recorded by CMS in 2016 - CERN Document Server](#)

Event at CMS with 86 reconstructed vertices

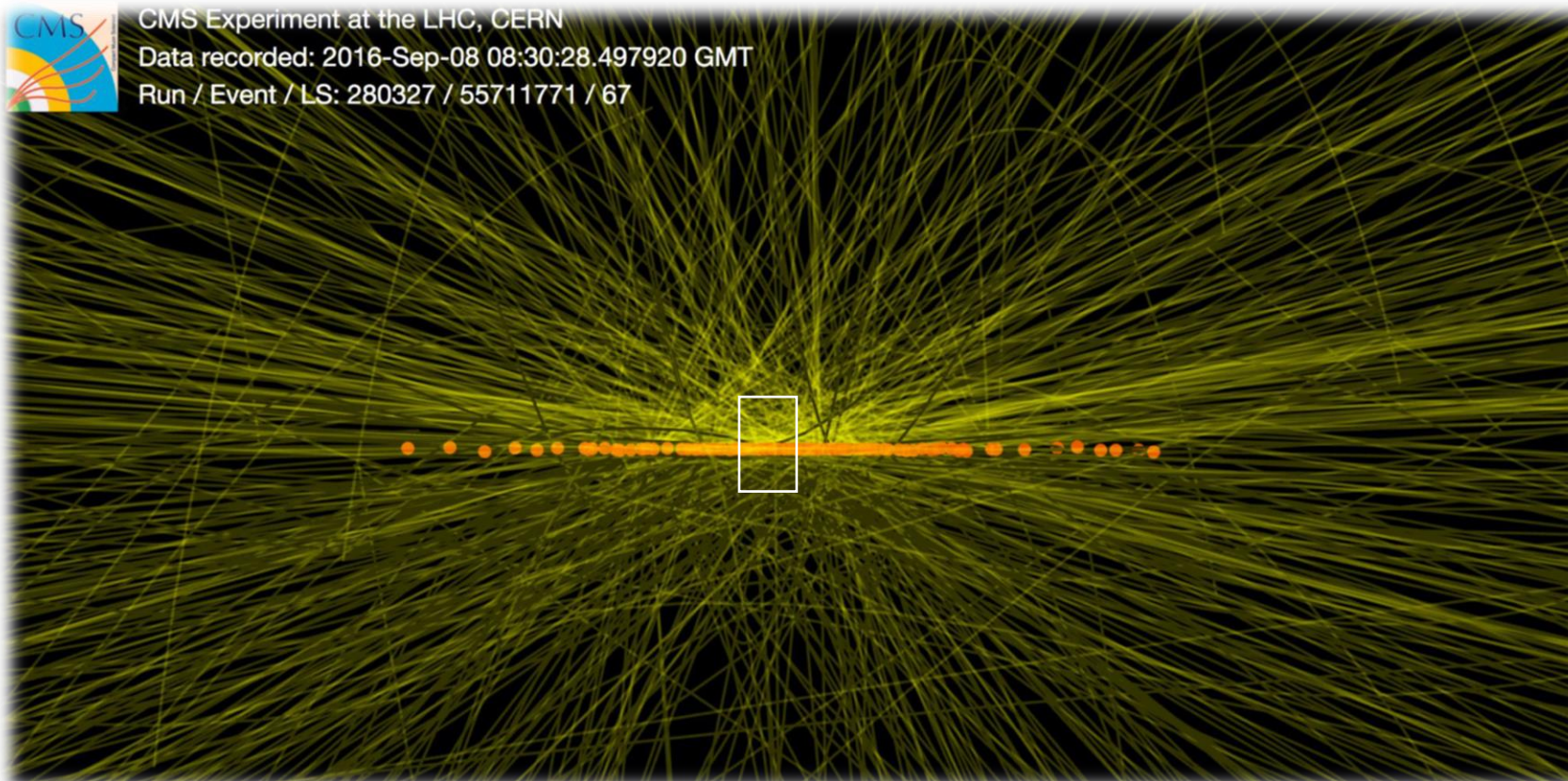
Increasing the luminosity also the number of events increases

At HL-LHC will be 150-200 events per bunch crossing

Why the *time* is important ?

Pileup at collider experiments

- At each bunch crossing multiple collisions may happen (events)
- A primary vertex is associated to each event



[Collision events recorded by CMS in 2016 - CERN Document Server](#)

Event at CMS with 86 reconstructed vertices

Increasing the luminosity also the number of events increases

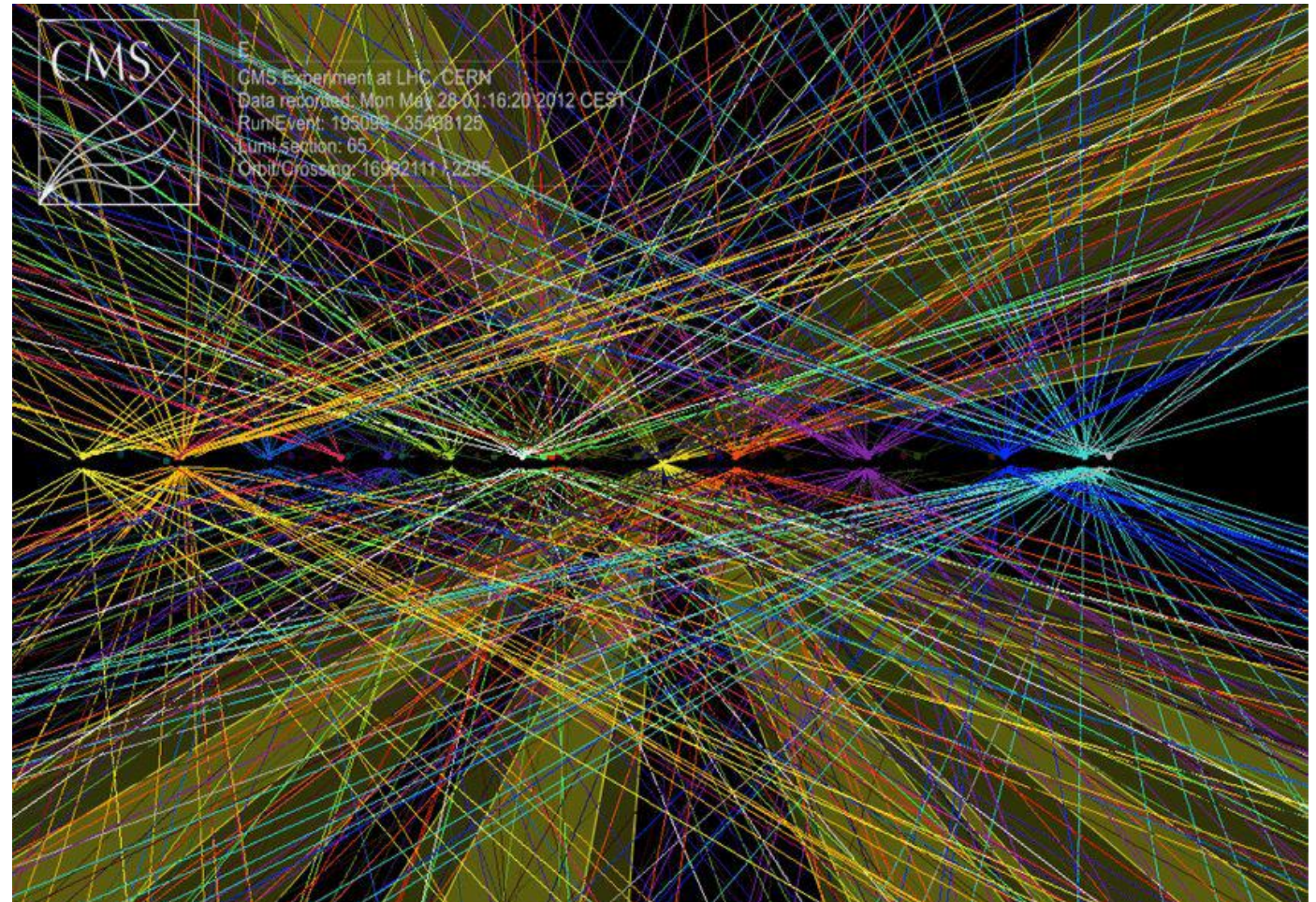
At HL-LHC will be 150-200 events per bunch crossing

Why the *time* is important ?

Pileup at collider experiments

- Event overlapping:
- Degradation in the reconstruction precision
- Loss of events
- Events do not happen at the same time

Event at CMS with ~50 vertices

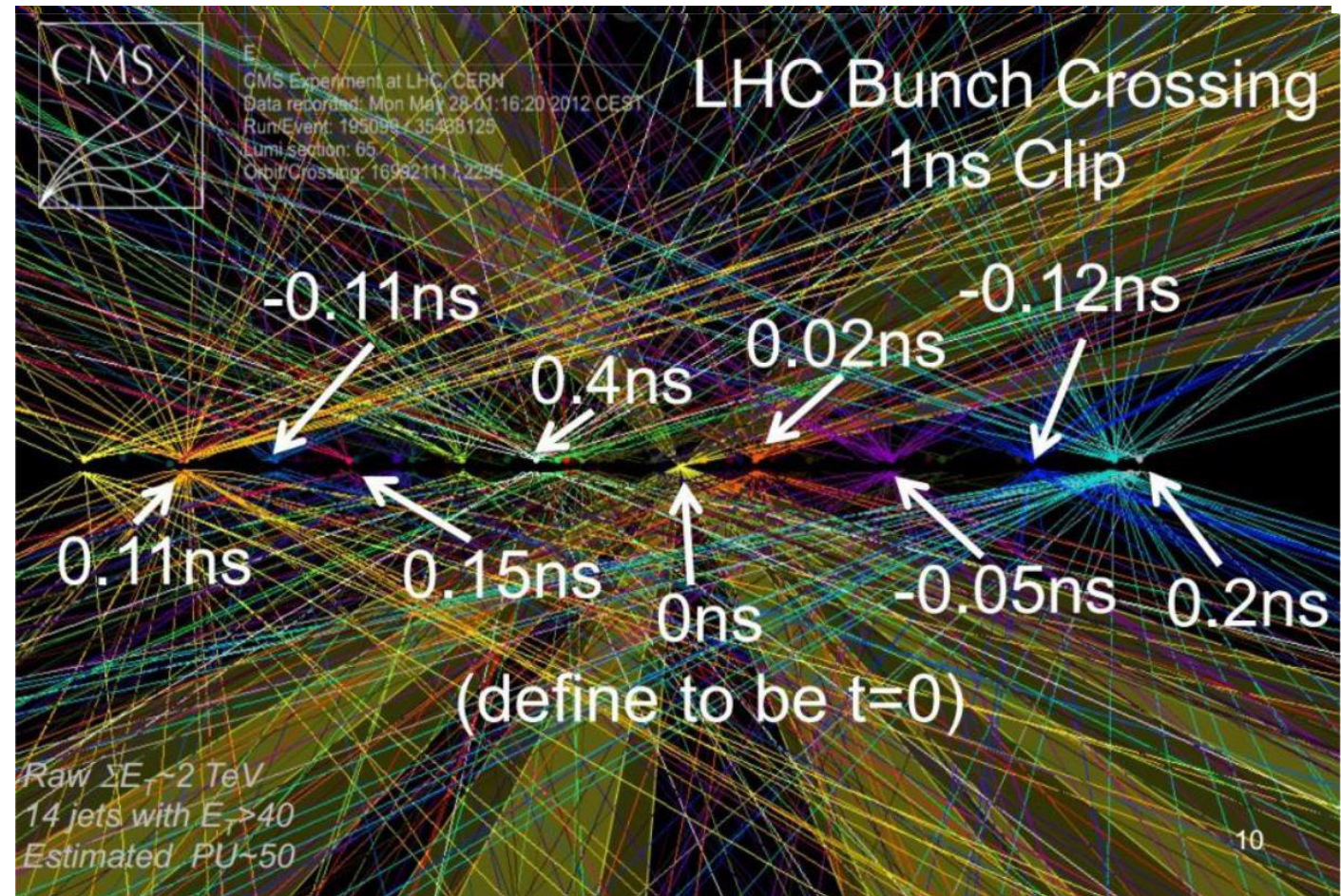


Why the *time* is important ?

Pileup at collider experiments

- Event Overlapping:
- degradation in the reconstruction precision
- Loss of events
- Events do not happen at the same time

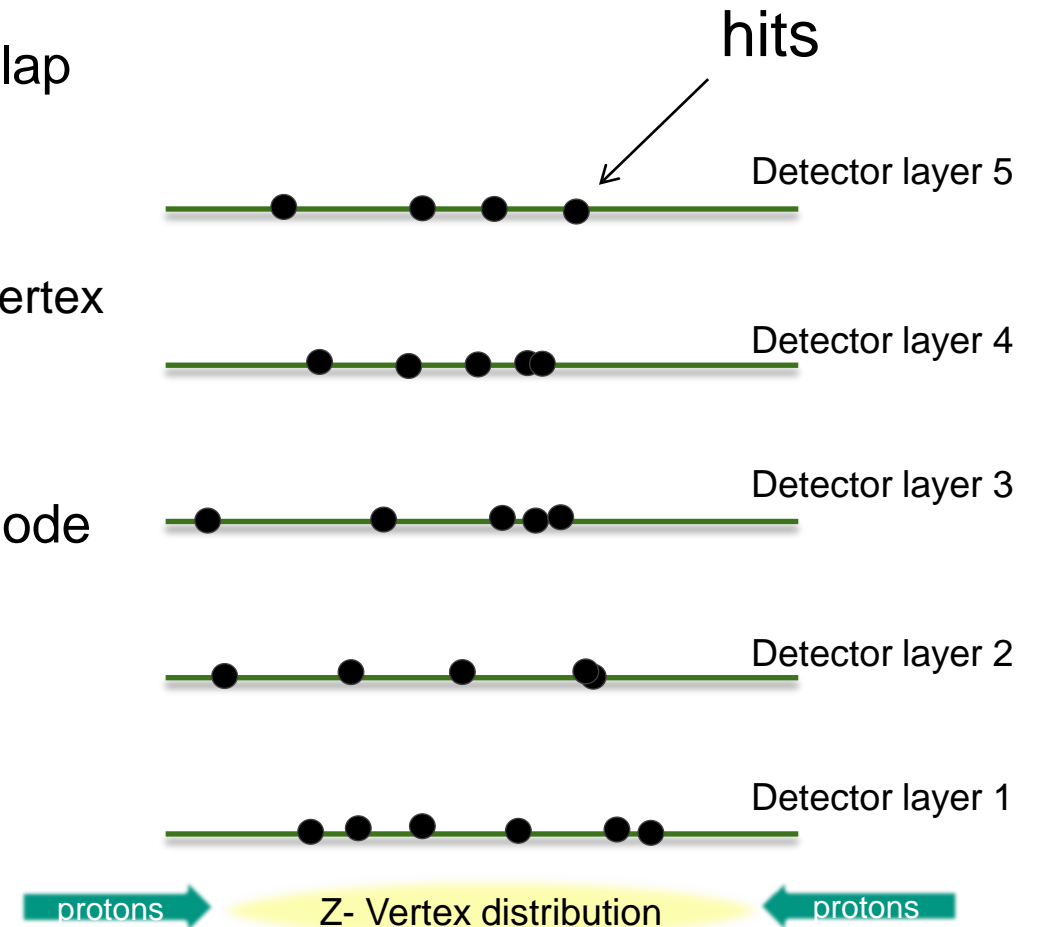
Event at CMS with ~50 vertices



Why the *time* is important ?

Pileup at collider experiments

- The spatial density is so high that the vertices will overlap
 - This overlap causes:
 - degradation in the reconstruction precision of primary vertex
 - Loss of events
 - Computational power for track reconstruction explode exponentially
- The only spatial position (3D) is not sufficient for the corrected event reconstruction



BUT ... *events do not happen at the same time*

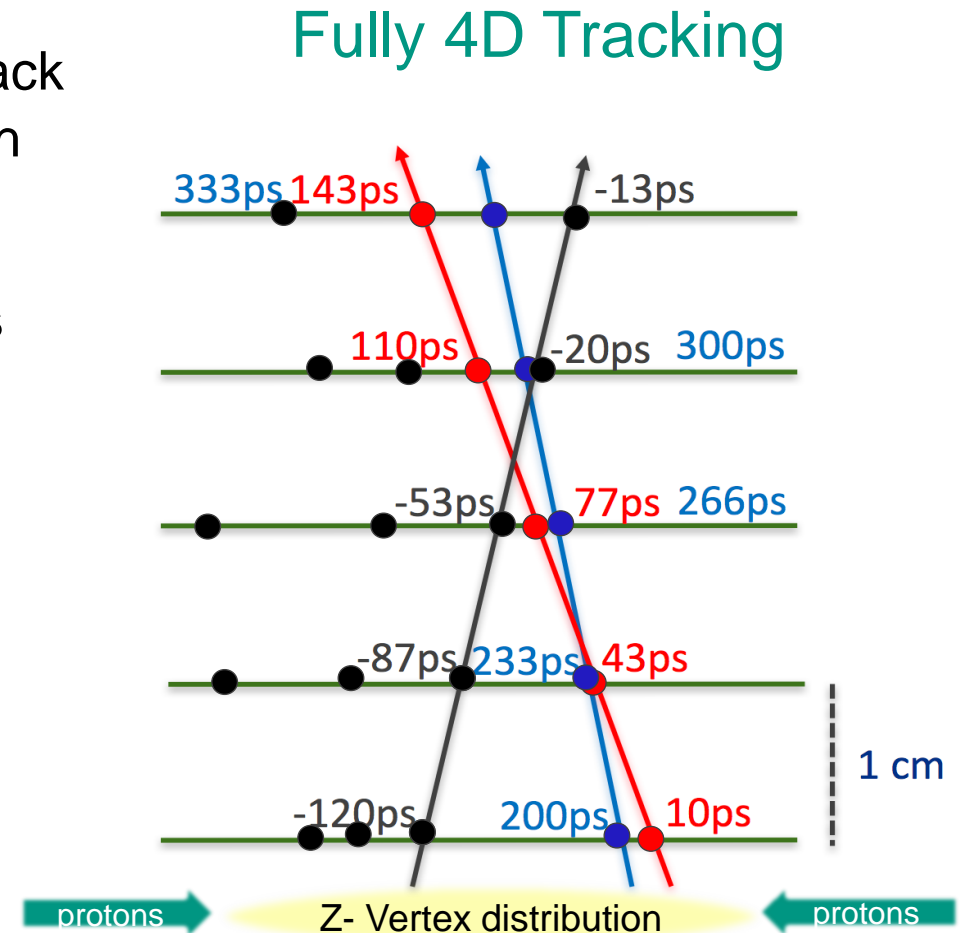
Why the *time* is important ?

Pileup at collider experiments

- Assigning a time with a resolution of ~ 30 ps to each track is possible to divide a bunch crossing in 5 groups, each with fewer events
- A tracker composed by all layer with timing capabilities associates a time to each hit
 - Drawback in terms of power and cooling requirements, readout circuits, and costs
- Considering only time compatible hits during track reconstruction reduces the possible hits combinations.



With timing information is possible to group time compatible hits (same color)



Why the *time* is important ?

Pileup at collider experiments

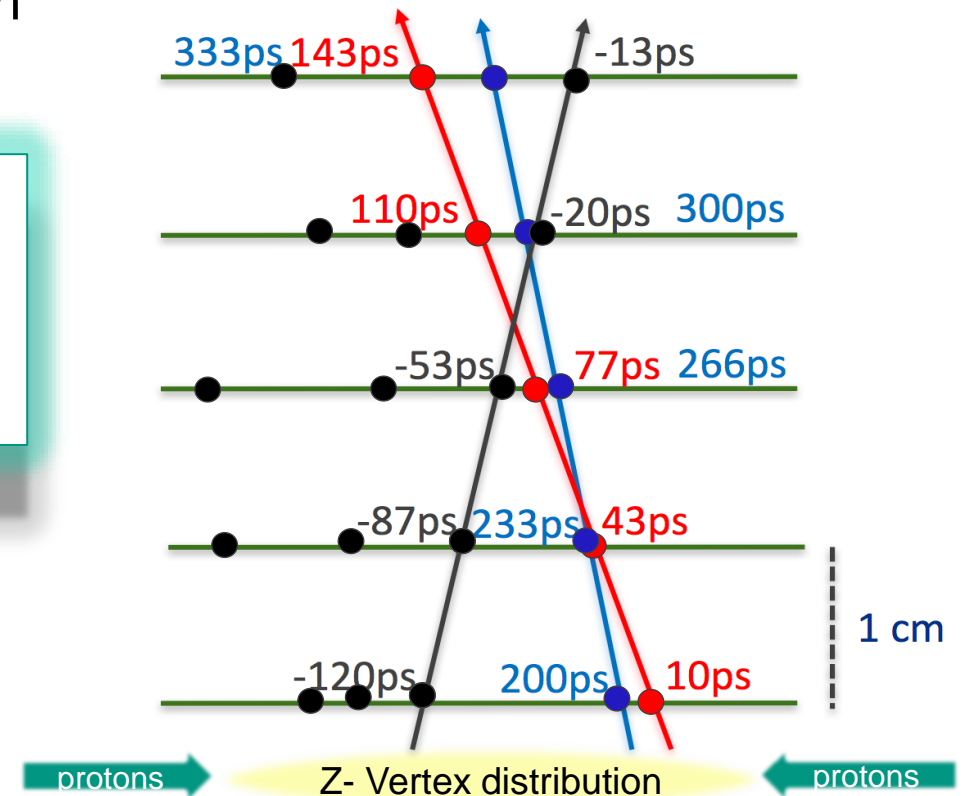
- Assigning a time with a resolution of ~ 30 ps to each track is possible to divide a bunch crossing in 5 groups, each with fewer events

The timestamp or time of arrival (ToA) of the particle as it passes through the detector is a key characteristic

- Considering only time compatible hits during track reconstruction reduces the possible hits combinations.

➔ With timing information is possible to group time compatible hits (same color)

Fully 4D Tracking



Why the time is important in future Photon Sciences Detector ?



Fast ADC

Jitter-clean
PLL (120 MHz)

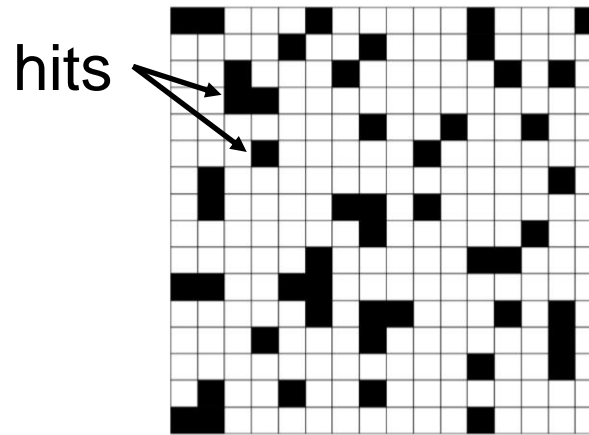
R

R

Difference between HEP and Photon Sciences

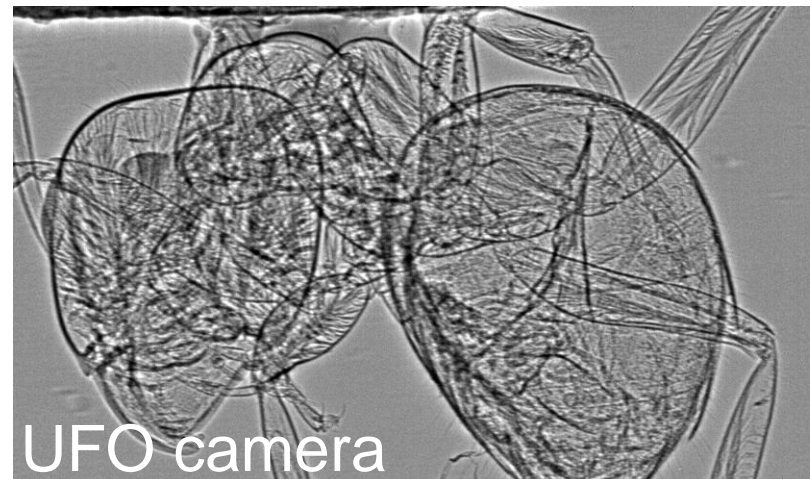
Similar detector technologies, but with different key parameters

■ High Energy Physics



- Spares readout architecture
- Zero suppression
- Time-of-arrival (**ToA**)
- Hit-rate and granularity depends on the luminosity $O(10\mu\text{m})$

■ Photon Sciences

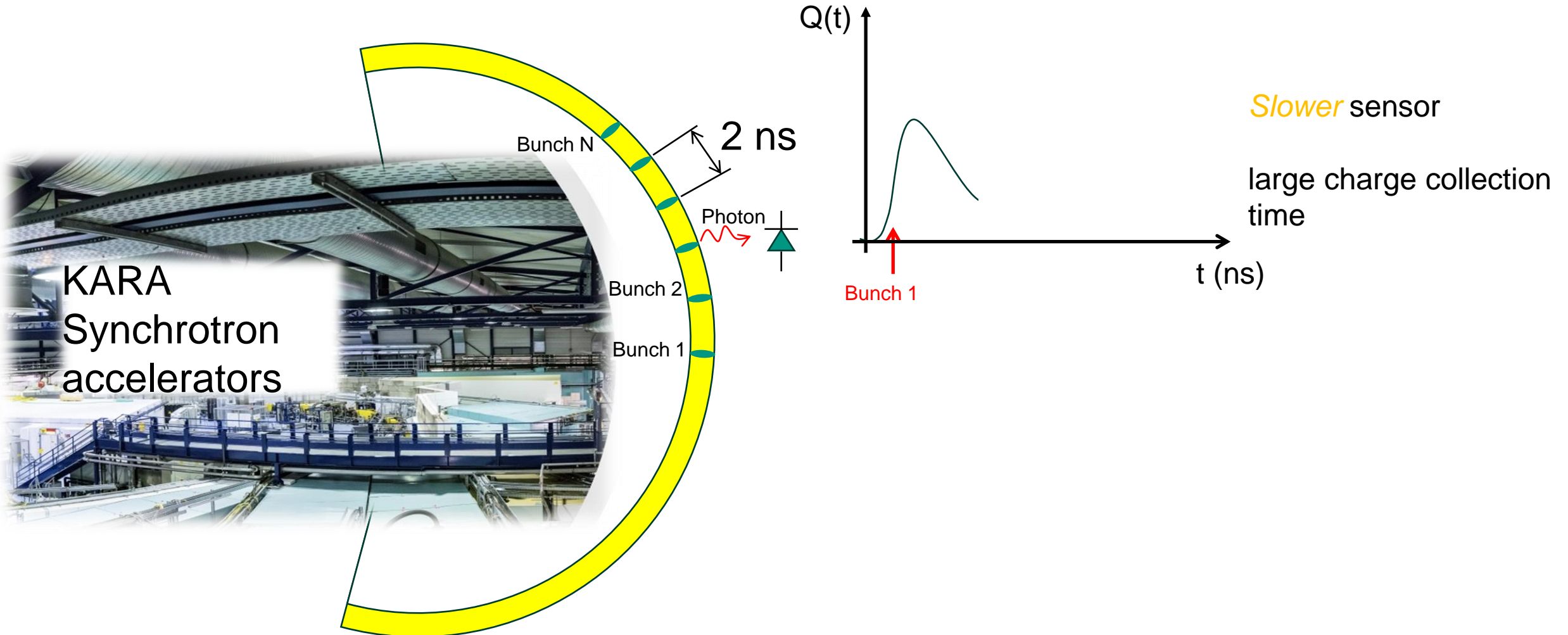


- Full occupancy readout
- No suppression
- Distance between frames (**framerate**)
- Extreme-granularity $O(\mu\text{m})$

M. Caselle, DOI: 10.1109/TNS.2013.2252528

Why the *time* is important ?

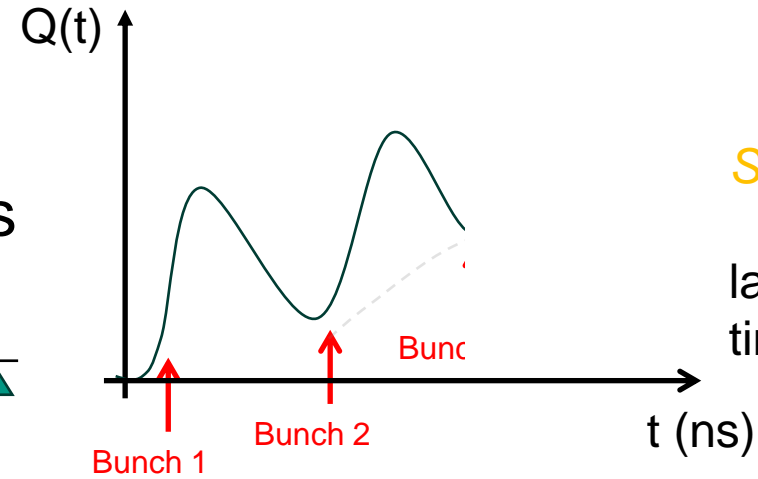
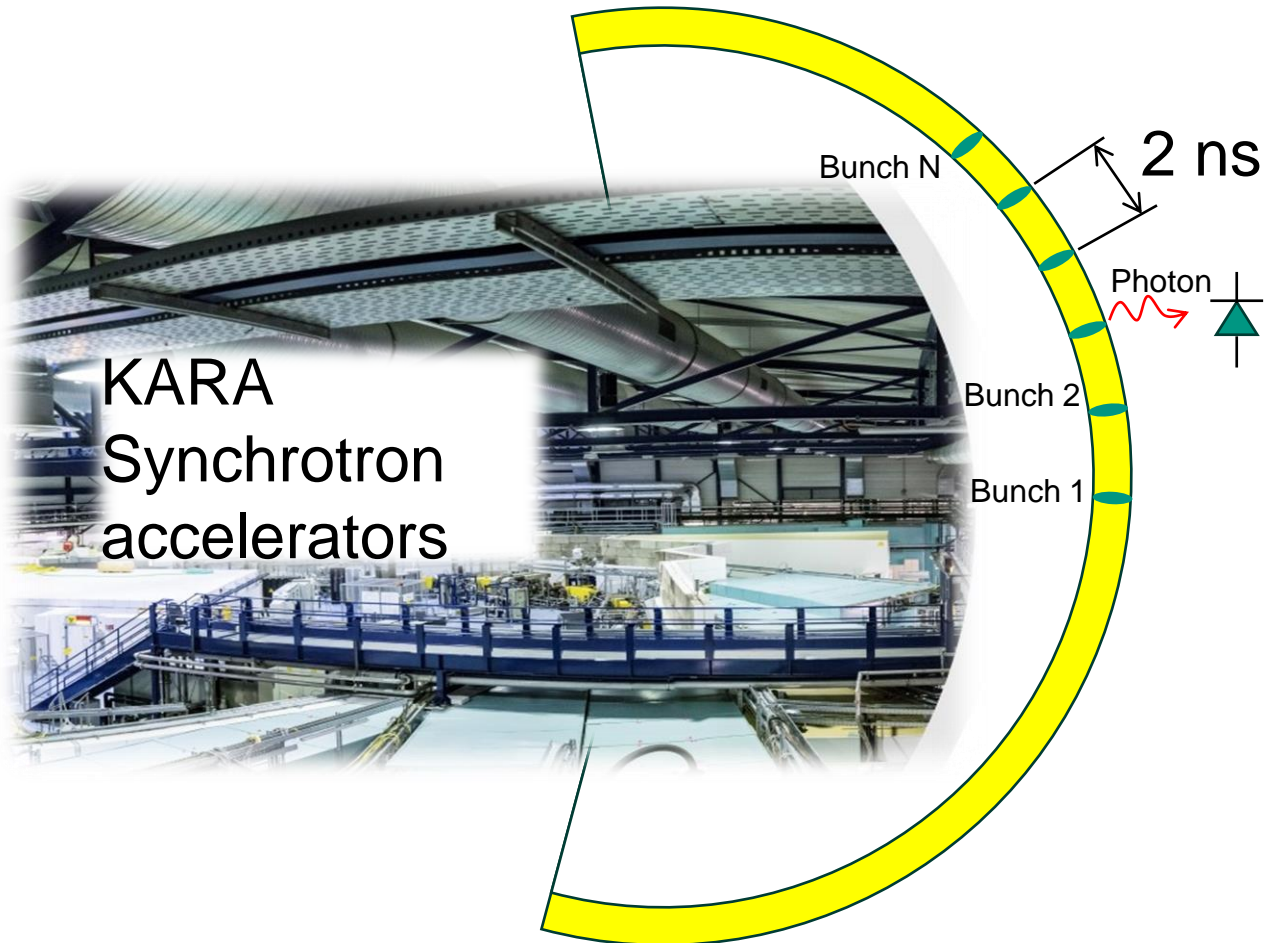
The total time required for collection charges is the critical property



KARA
Synchrotron
accelerators

Why the *time* is important ?

The total time required for collection charges is the critical property



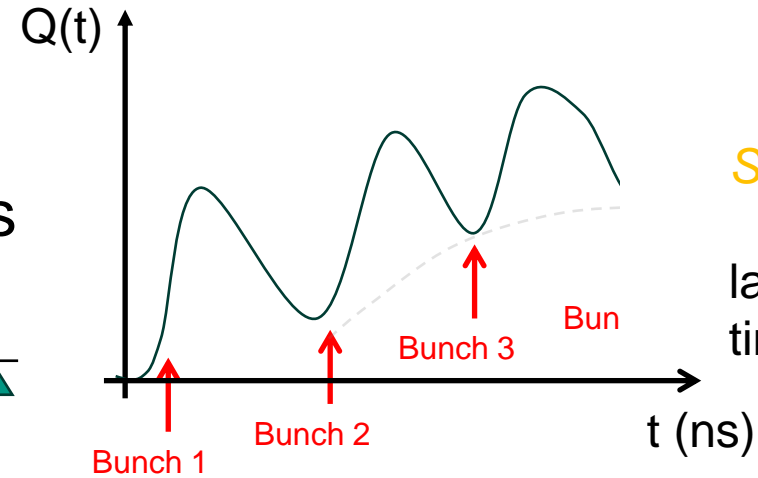
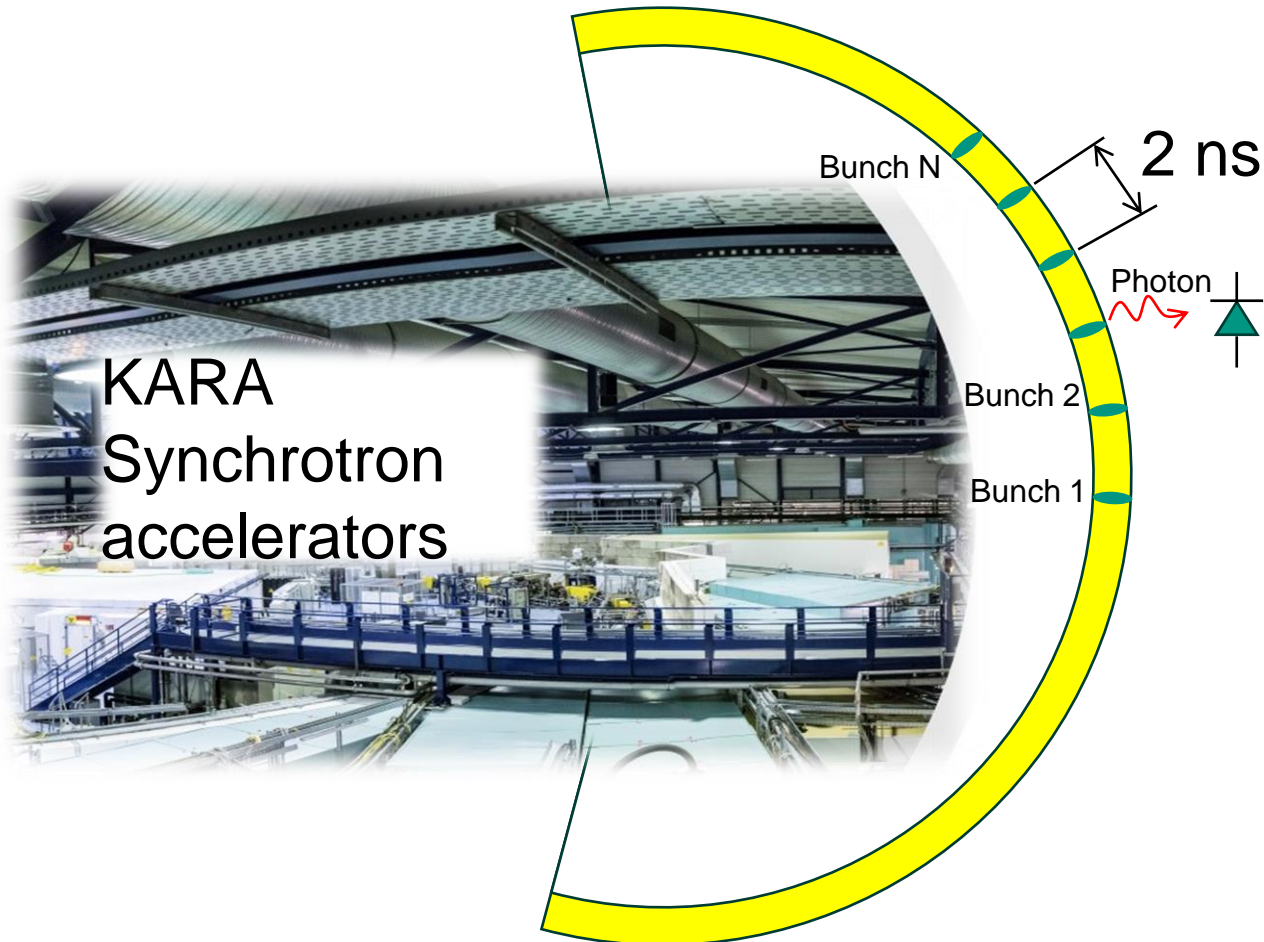
Slower sensor

large charge collection
time

KARA
Synchrotron
accelerators

Why the *time* is important ?

The total time required for collection charges is the critical property



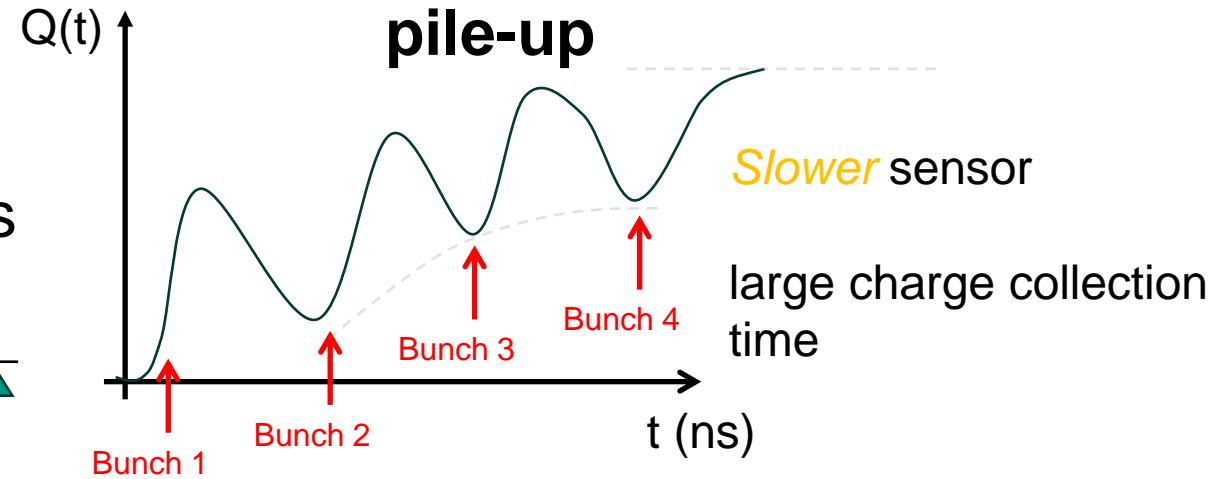
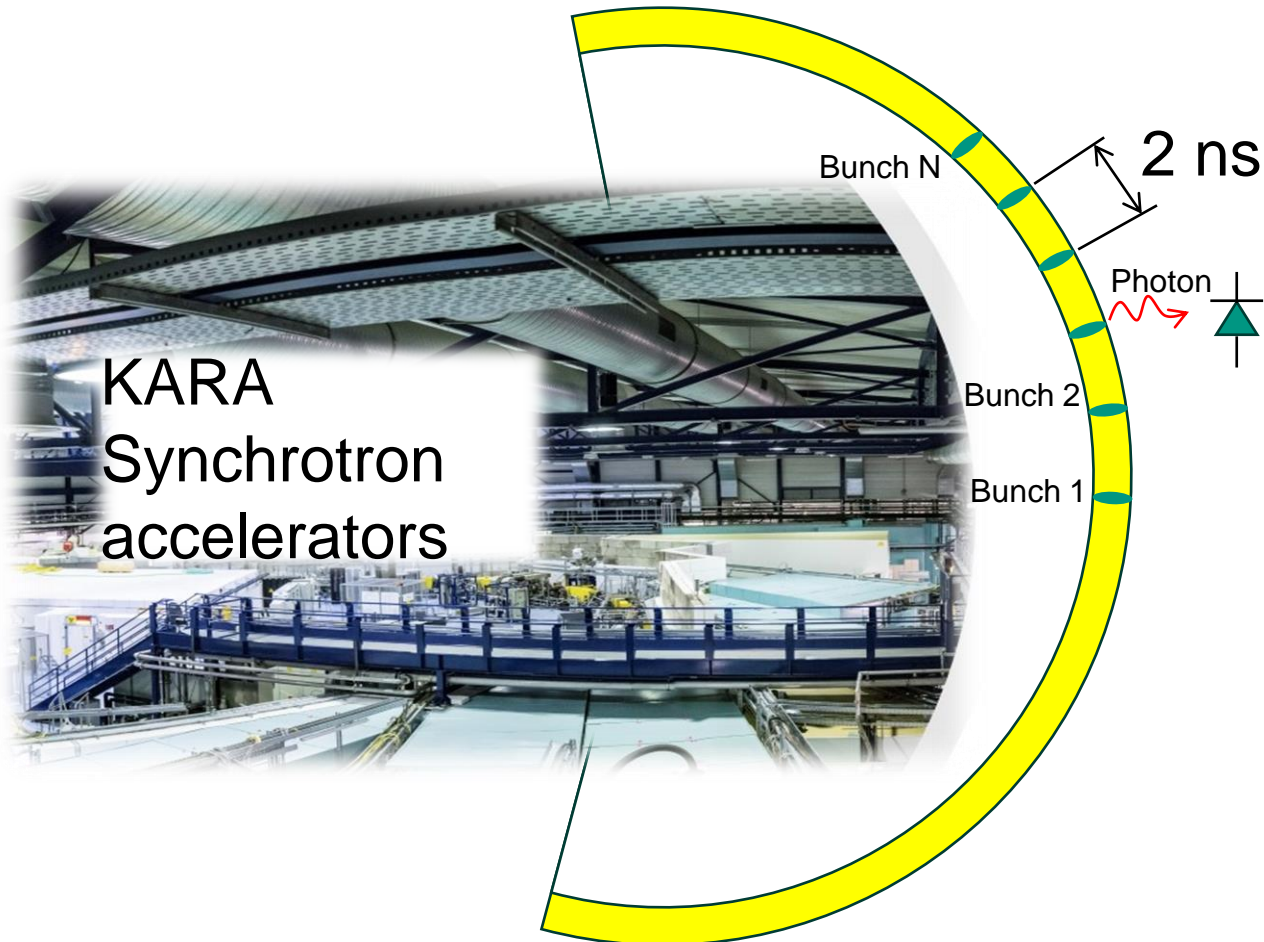
Slower sensor

large charge collection time

KARA
Synchrotron
accelerators

Why the *time* is important ?

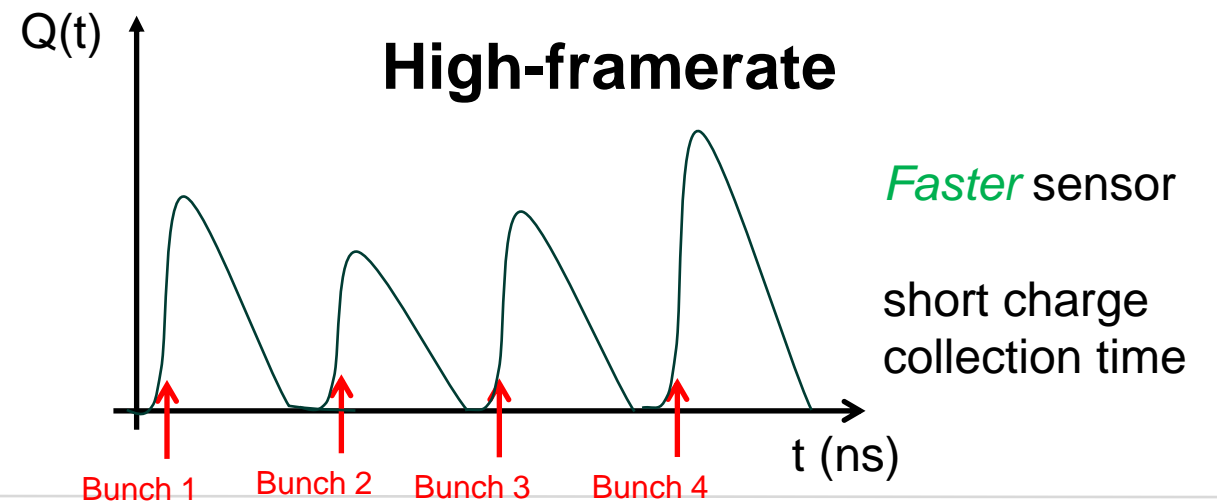
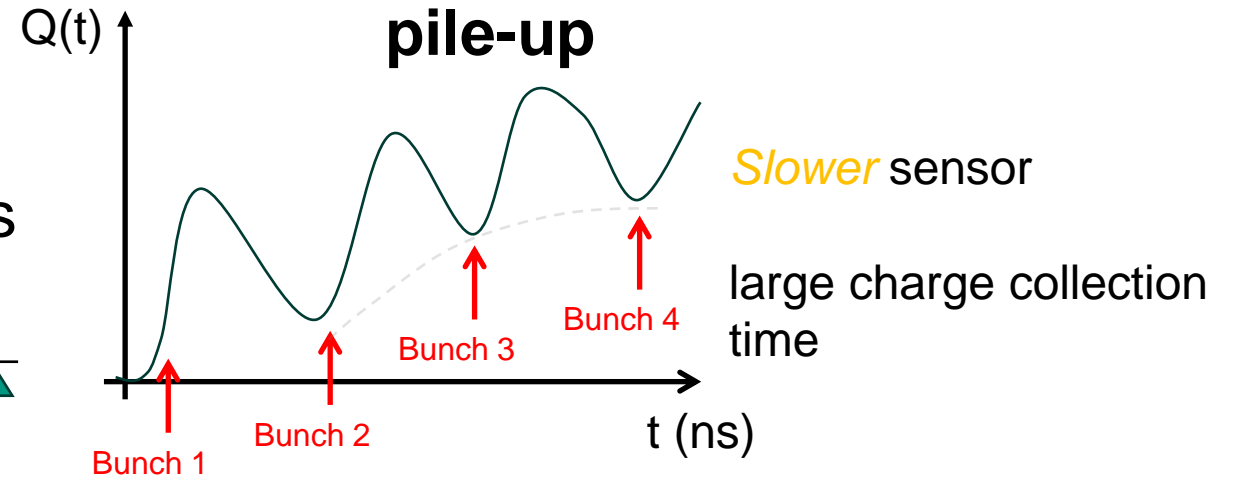
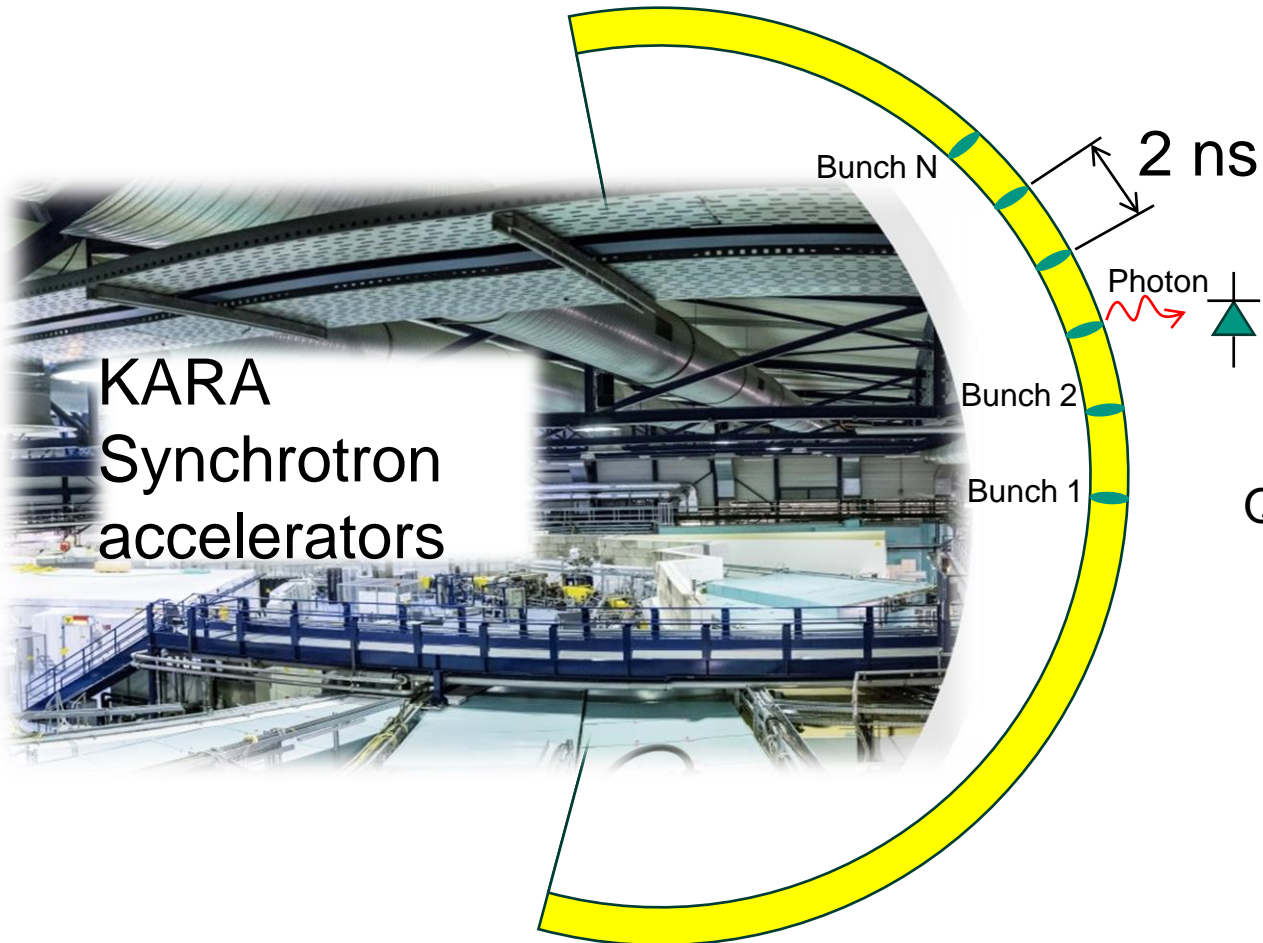
The total time required for collection charges is the critical property



KARA
Synchrotron
accelerators

Why the *time* is important ?

The total time required for collection charges is the critical property

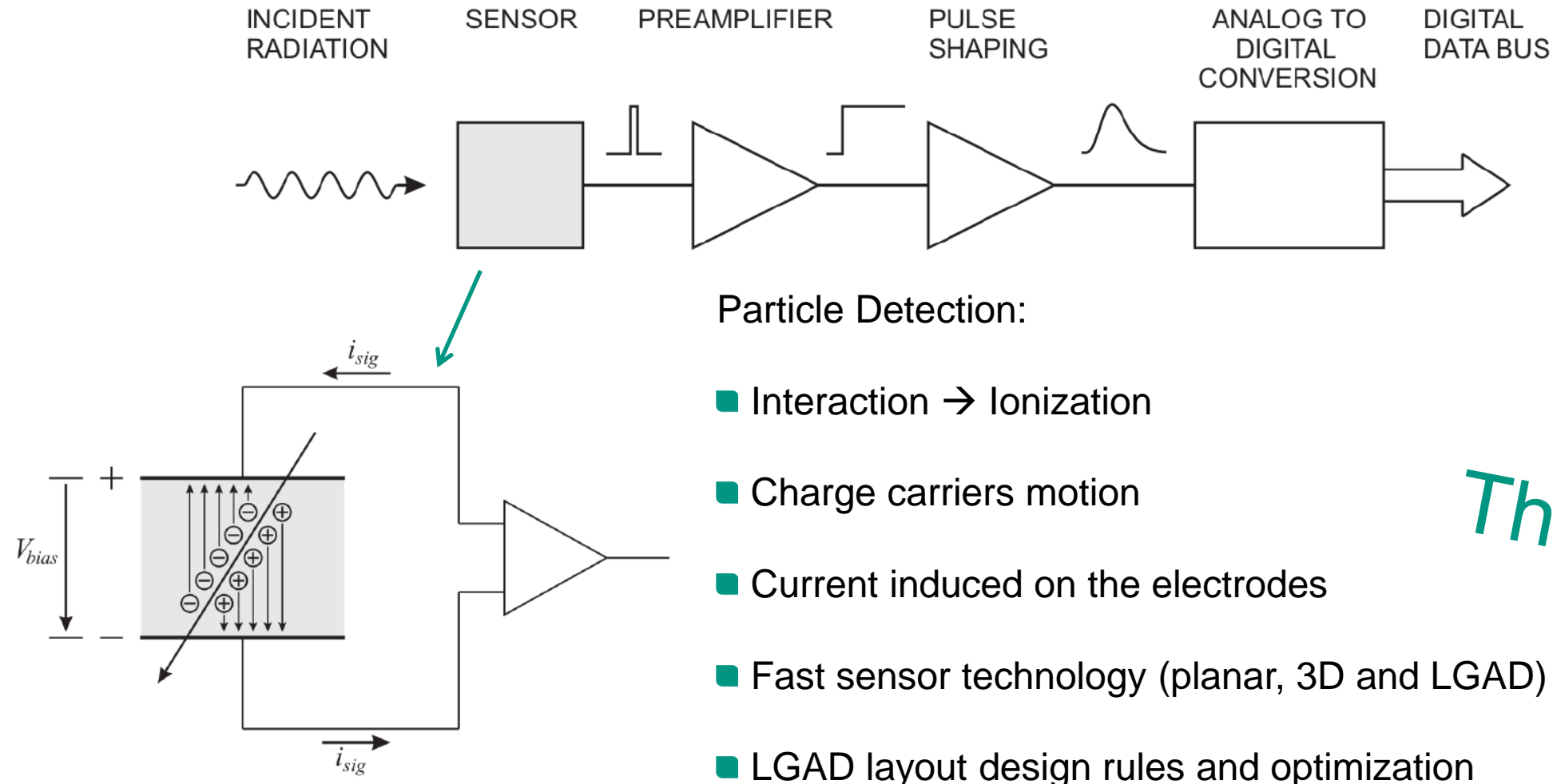


Is it feasible to develop a novel sensor technology that meets the requirements of both High-Energy Physics (higher time resolution) and Photon Sciences (faster data collection)?

What is the time resolution of standard silicon sensors?

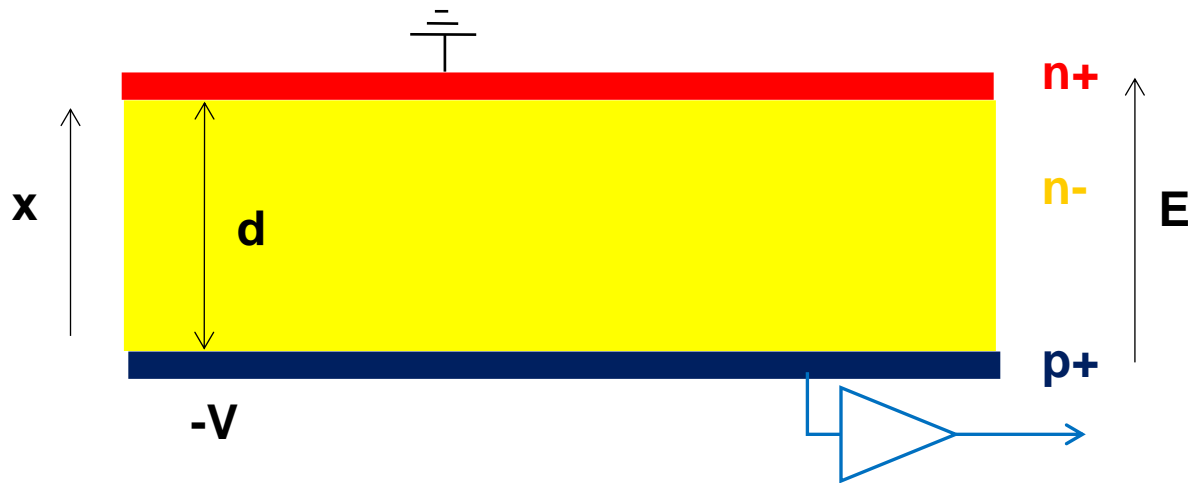
Sensor and readout chain

Introduction



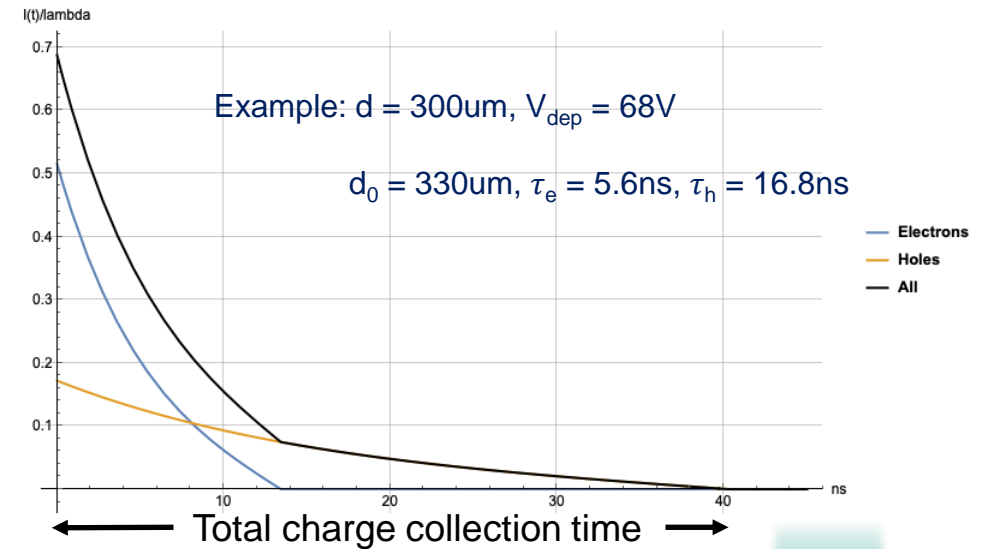
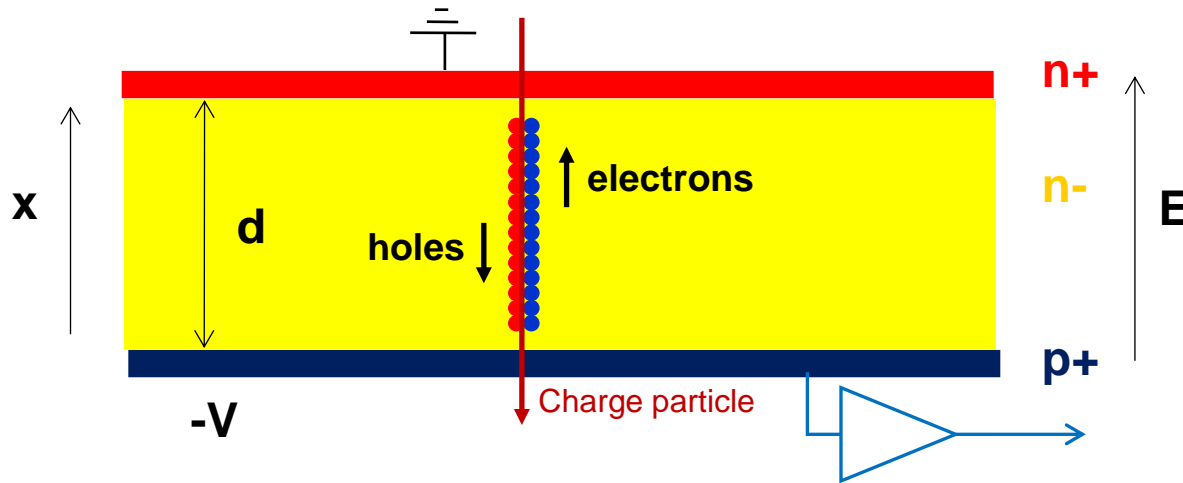
Intrinsic time resolution

'Large' silicon pad detector



Intrinsic time resolution

'Large' silicon pad detector



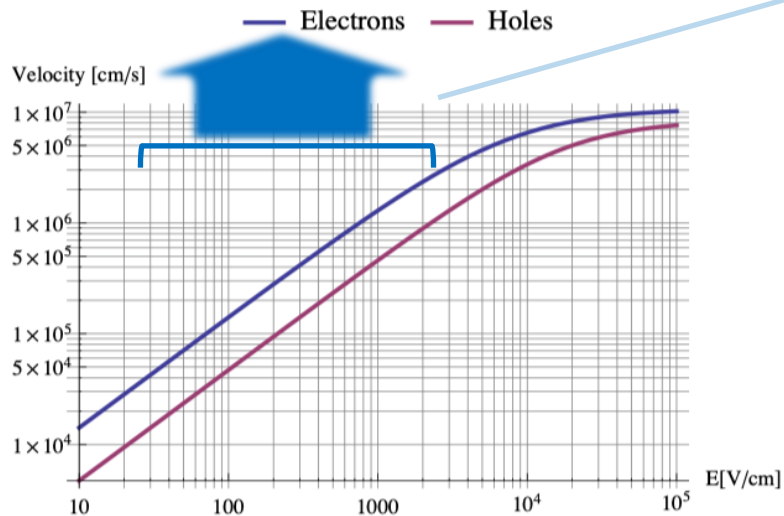
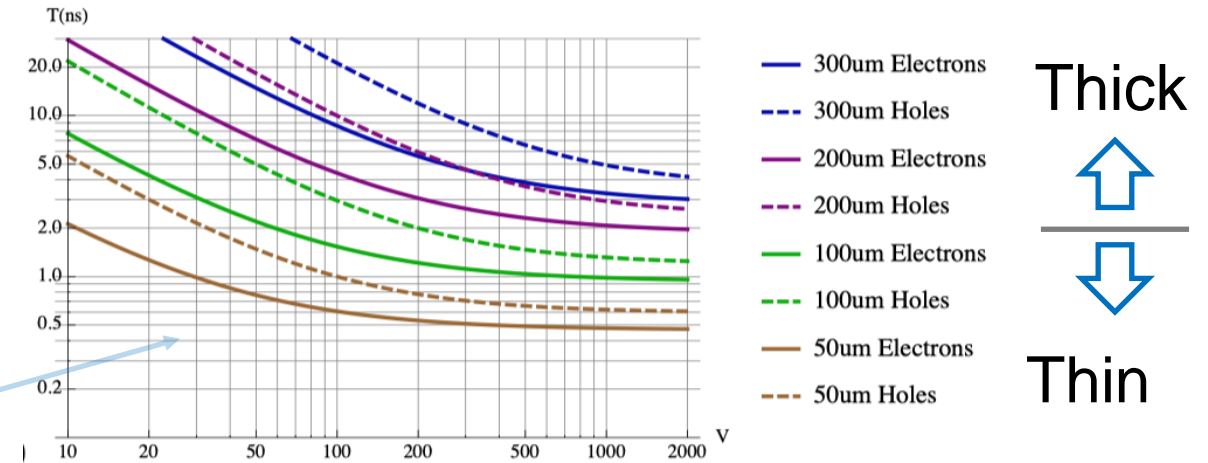
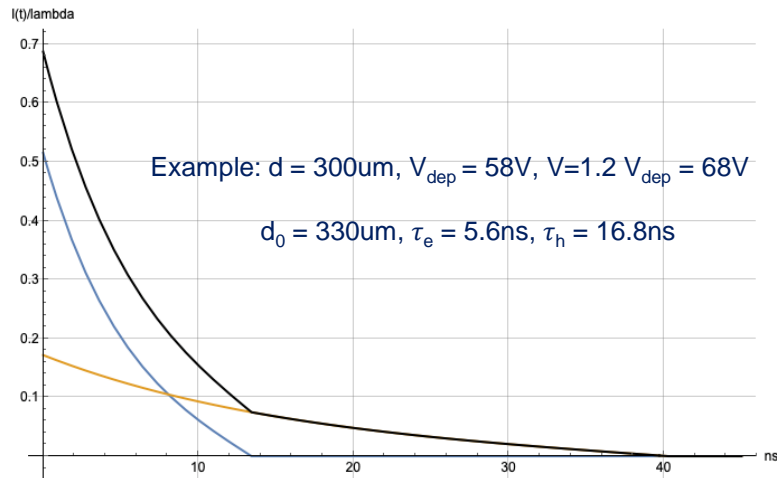
- In silicon sensors the signal edge is instantaneous (i.e. sub ps level)
 - Acceleration of electrons to 10^7cm/s in vacuum is 0.14 ps
 - Passage of the particle through a $50\mu\text{m}$ sensor takes 0.16 ps
- The intrinsic time resolution of a silicon sensor is infinite (sub ps)

Total drift time of electrons and holes in the silicon sensor is **different**

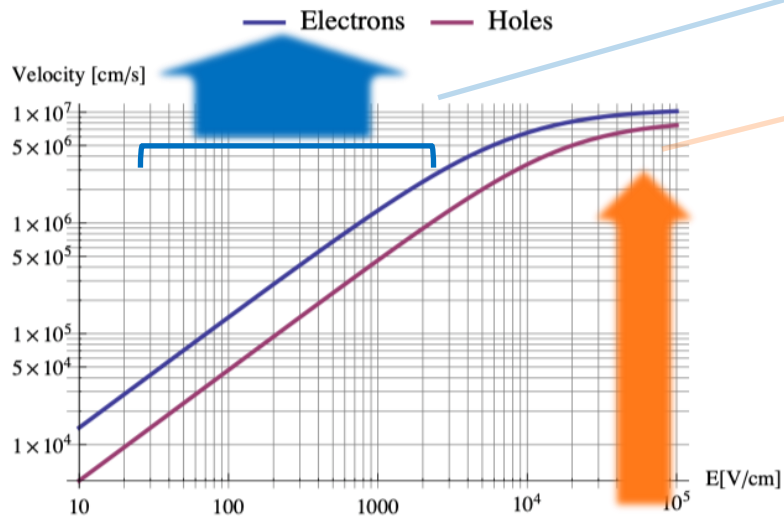
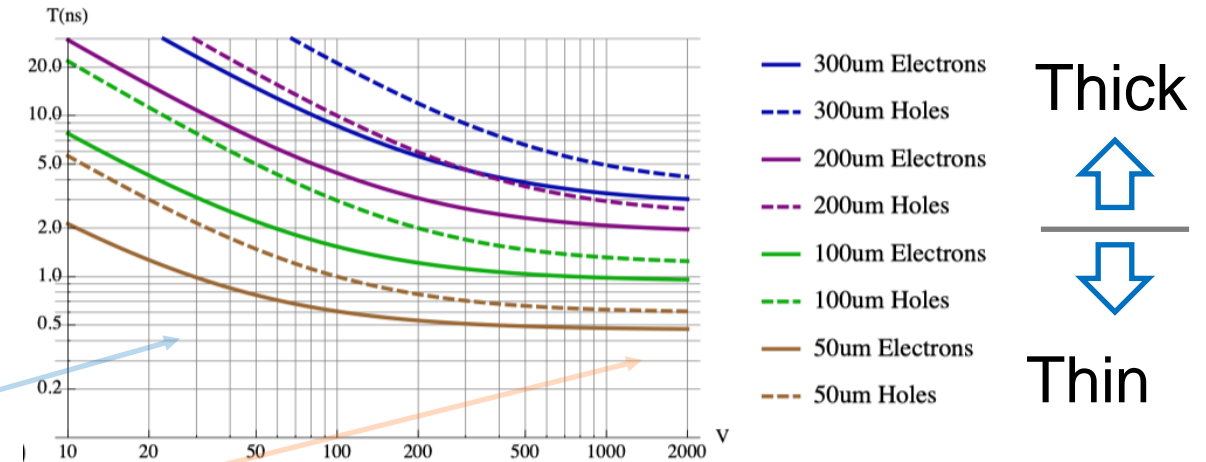
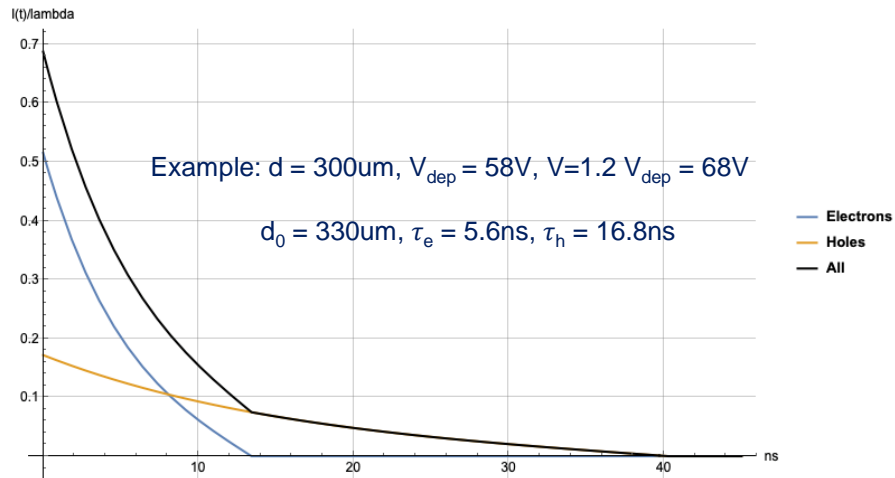
➔ The time resolution in a planar silicon sensor without gain is a question of **signal/noise** and specifically the **Landau fluctuations**

How to address or manage this drift time difference?

Total drift time of electrons and holes in the silicon sensor

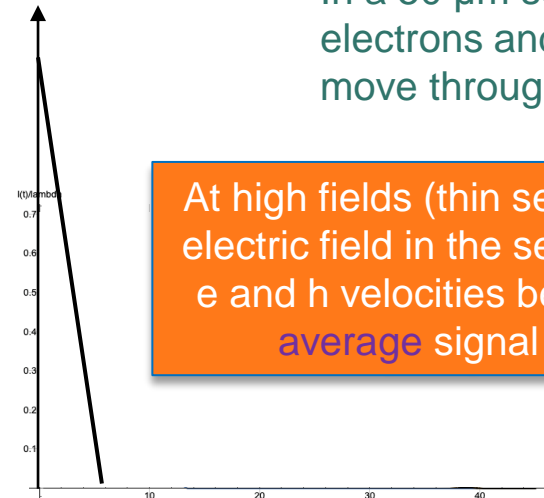


Total drift time of electrons and holes in the silicon sensor



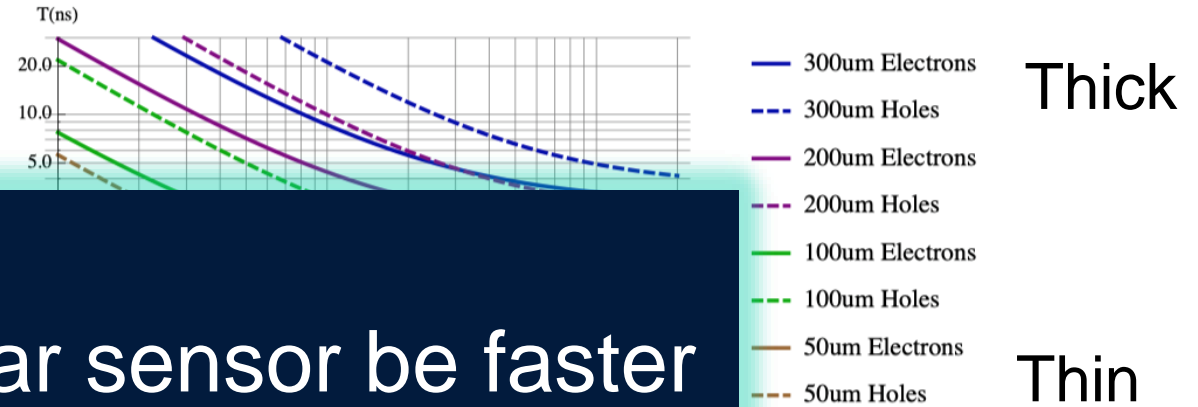
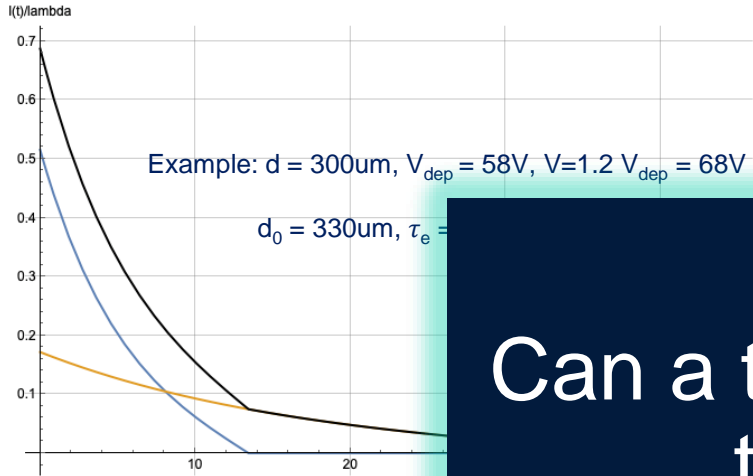
In a 50 μm sensor at very high voltage the electrons and holes take around **500 ps** to move through the sensor.

At high fields (thin sensors, large voltage), the electric field in the sensor is close to constant, e and h velocities become saturated and the **average** signal becomes a triangle.



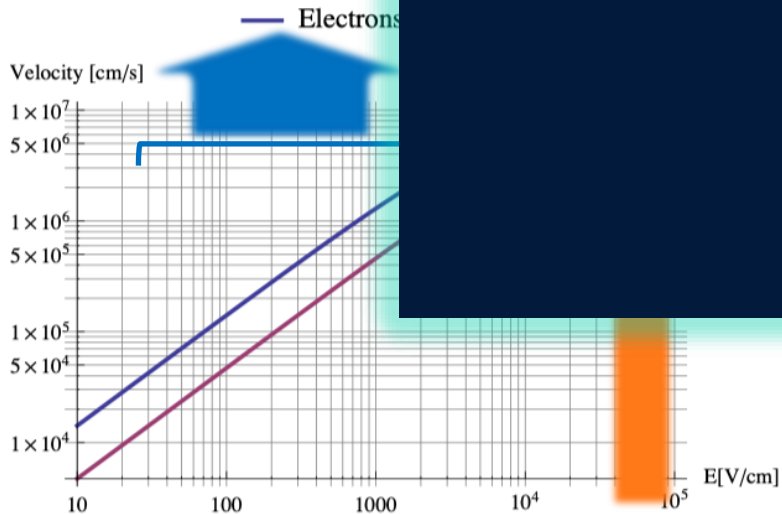
At high electric fields, the drift-velocity saturates around $10^7 \text{ cm/s} = 0.1 \mu\text{m/ps}$ for both, electrons and holes.

Total drift time of electrons and holes in the silicon sensor



Can a thinned planar sensor be faster than other sensor types?

YES

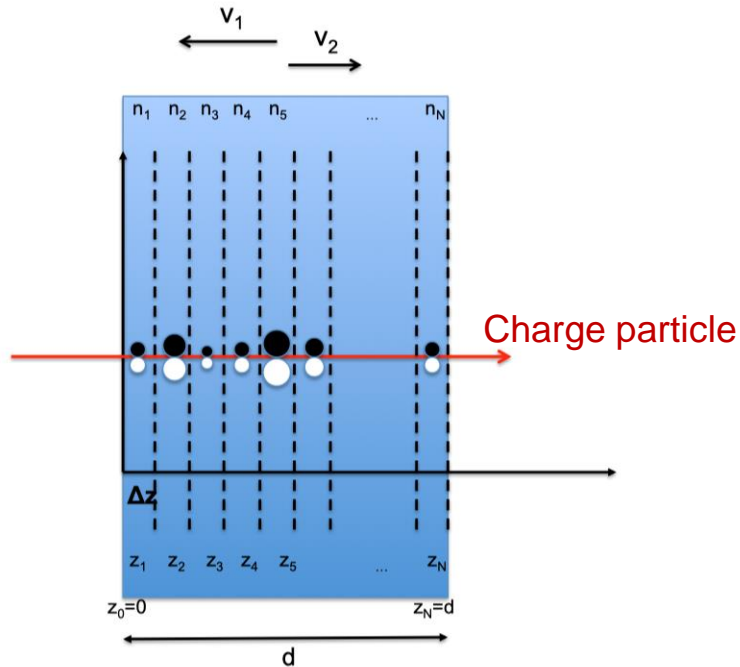


At very high voltage the μ and ν take around 500 ps to sensor.
 At very high voltage (large voltage), the μ and ν become close to constant, and μ and ν velocities become saturated and the average signal becomes a triangle.

At high electric fields, the drift-velocity saturates around $10^7 \text{ cm/s} = 0.1 \mu\text{m/ps}$ for both, electrons and holes.

Energy deposit in silicon

Landau distribution → Non-Uniform Energy deposition

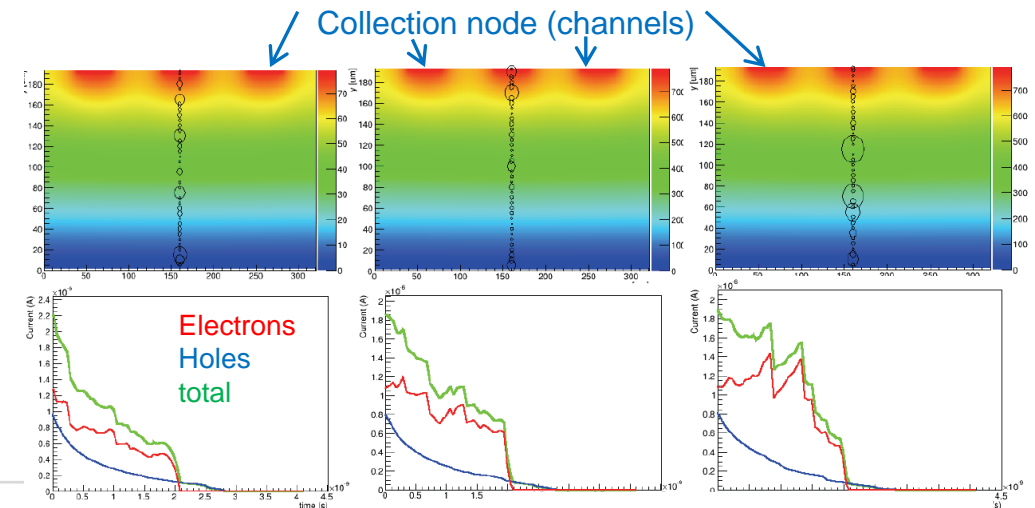
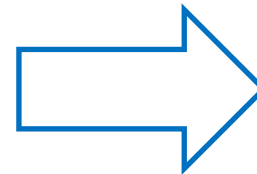


- A high energy particle passing the sensor will experience *primary interactions*, with an average distance of around $\lambda=0.21\mu\text{m}$. In each interaction there is a probability $p_{clu}(n)$ to produce a cluster of n electrons. The probability $p(n, \Delta z)$ have n e-h pairs in Δz is therefore

$$p(n, \Delta z)dn = \left(1 - \frac{\Delta z}{\lambda}\right) \delta(n)dn + \frac{\Delta z}{\lambda} p_{clu}(n)dn$$

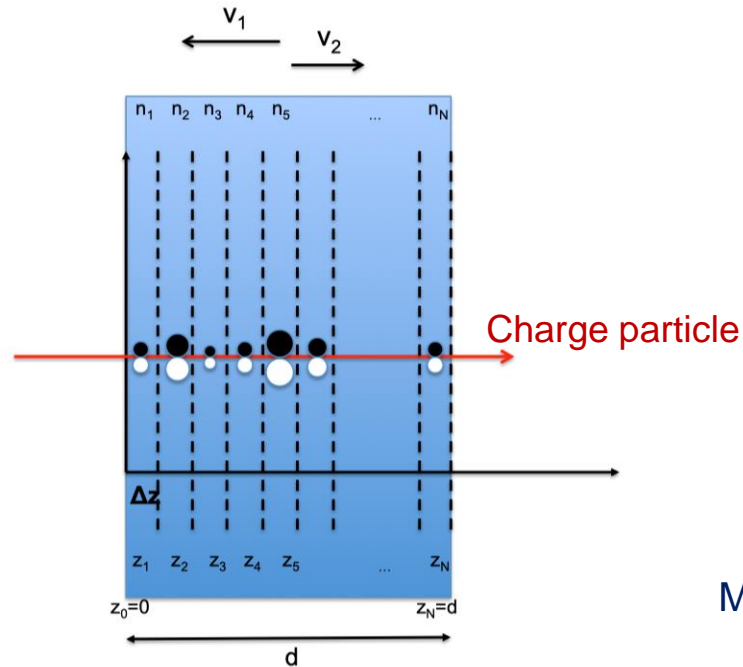
- Landau Fluctuations cause two major effects:
 - Amplitude variations, that can be corrected with time walk compensation (→ next lecture)

- For a given amplitude, the charge deposition is non uniform. These are 3 examples of this effect:



Energy deposit in silicon

Landau distribution → Non-Uniform Energy deposition



- A high energy particle passing the sensor will experience *primary interactions*, with an average distance of around $\lambda=0.21\mu\text{m}$. In each interaction there is a probability $p_{clu}(n)$ to produce a cluster of n electrons. The probability $p(n, \Delta z)$ have n e-h pairs in Δz is therefore

$$p(n, \Delta z)dn = \left(1 - \frac{\Delta z}{\lambda}\right) \delta(n)dn + \frac{\Delta z}{\lambda} p_{clu}(n)dn$$

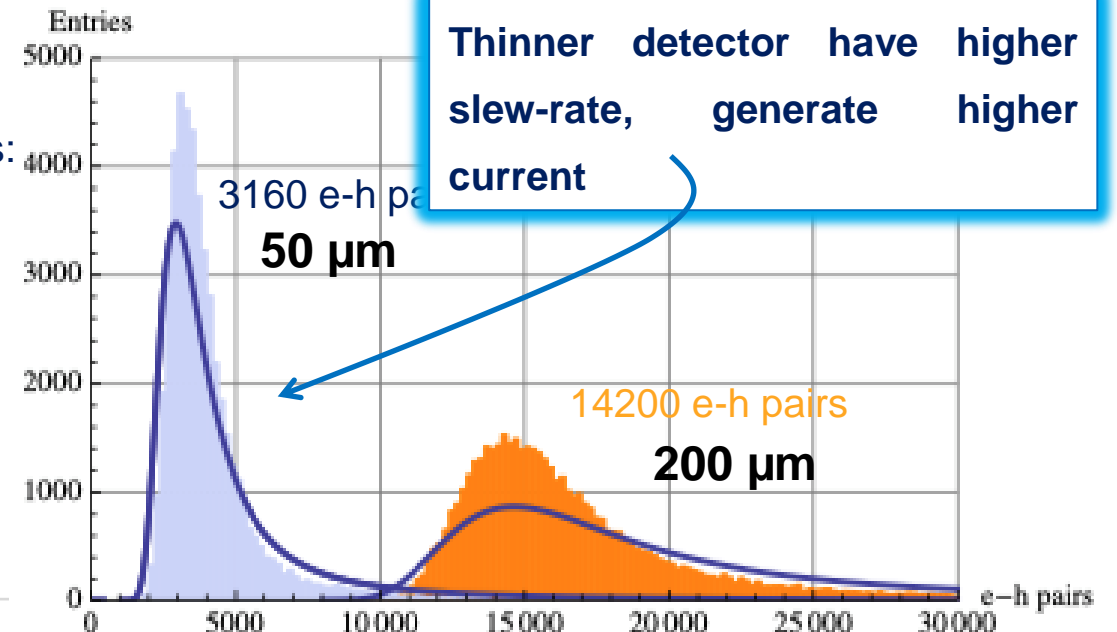
- No-Landau: ~ 80 e-h/ μm
- Thin: 63 e-h/ μm
- Thick: 71 e-h/ μm

Most probable number of e-h pairs:

$$n_{MP} \approx \frac{2.50 d}{\lambda} \left(0.2 + \log \frac{d}{\lambda}\right)$$

Full width of half maximum

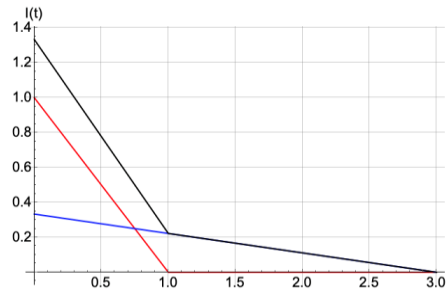
$$\frac{\Delta n_{FWHM}}{n_{MP}} \approx \frac{4.02}{0.2 + \log d/\lambda}$$



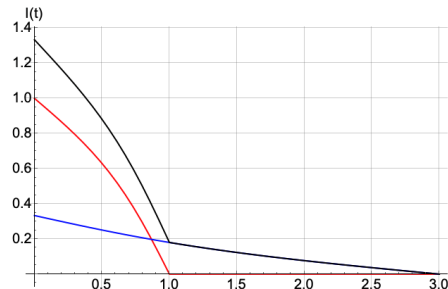
Weighting field of a pixel in a planar geometry

From large-pitch to small-pitch sensors

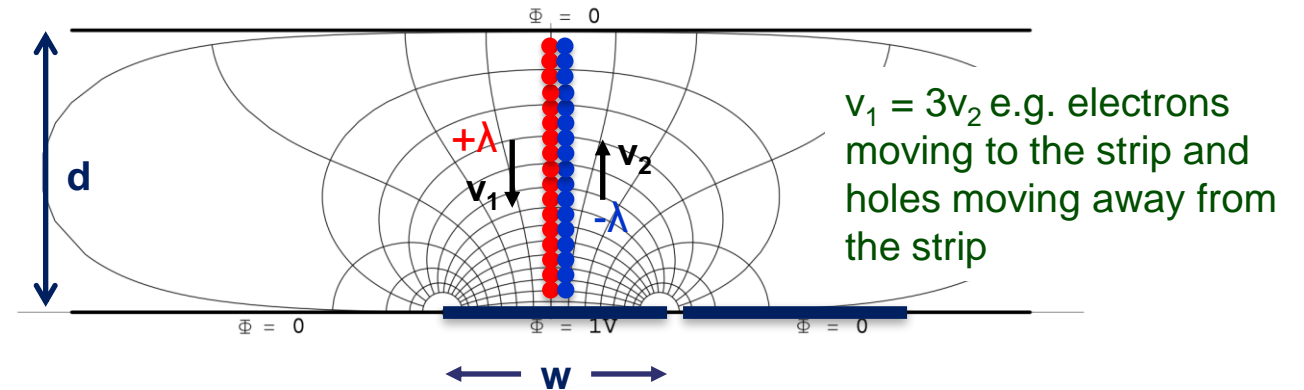
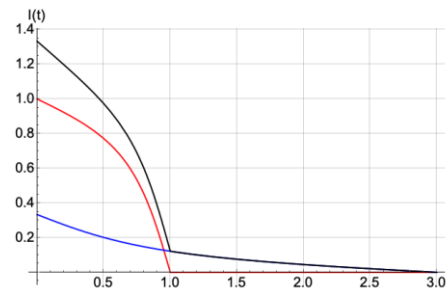
$w \gg d$



$w = d$



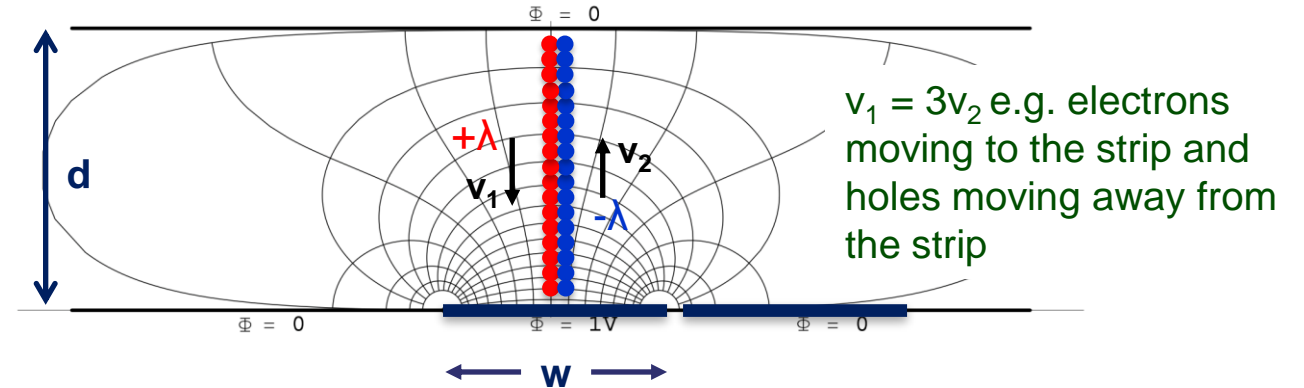
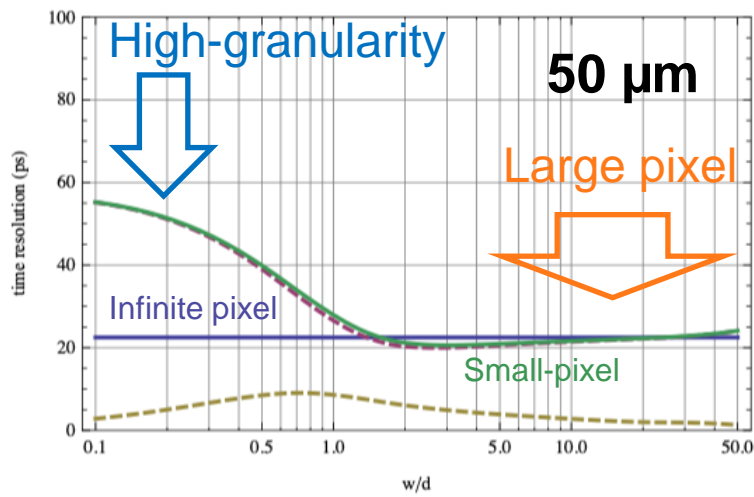
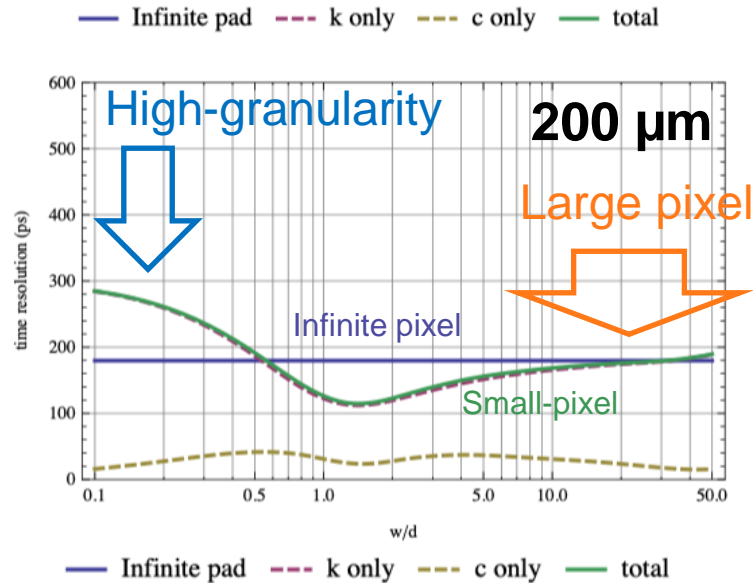
$w = d/2$



- Different positions of the particle inside the pixel will lead to different pulse-shapes
- This is also called the '**weighting field effect**'
- Weighting field, represents the coupling of a charge to the read-out electrode
- This weighting field effect is strongly correlated with the Landau fluctuations

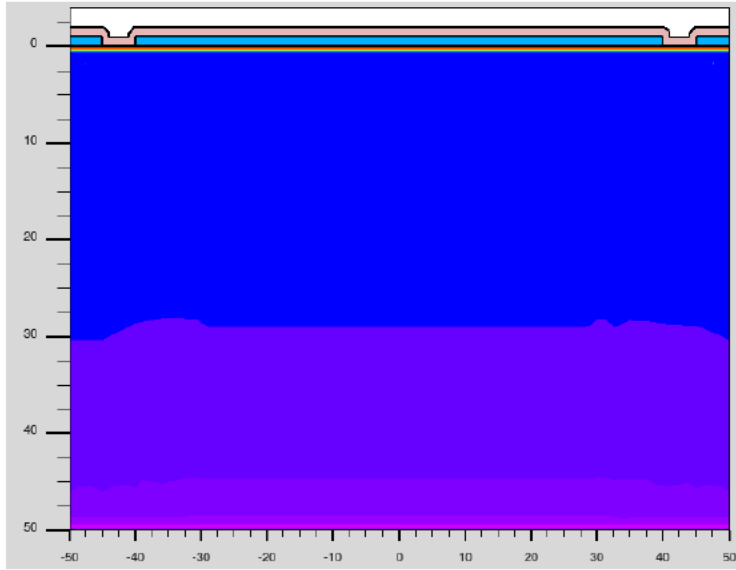
Weighting field of a pixel in a planar geometry

From large-pitch to small-pitch sensors

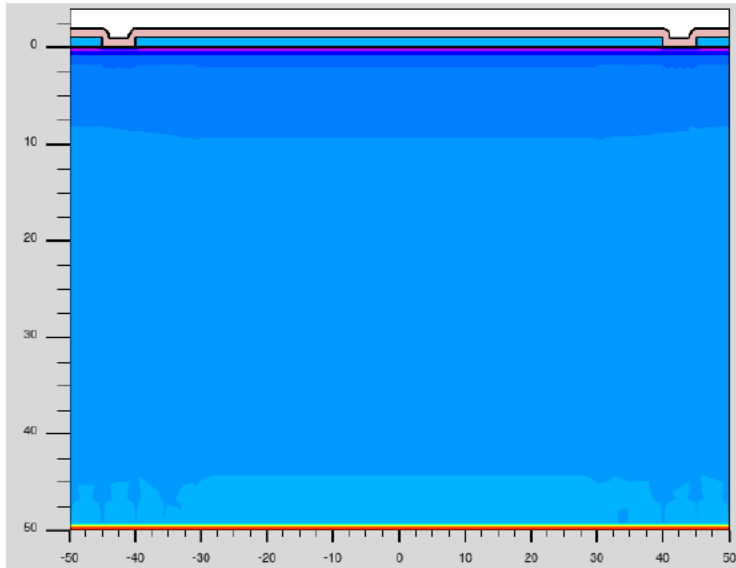


- Because electrons and holes have different velocities, it makes a significant difference whether the electrons or the holes move to the pixel
- For higher fields (*thinner sensors*) this difference will decrease
- The dependence on the different parameters is complex
- **These fluctuations can dominate the time resolution !**

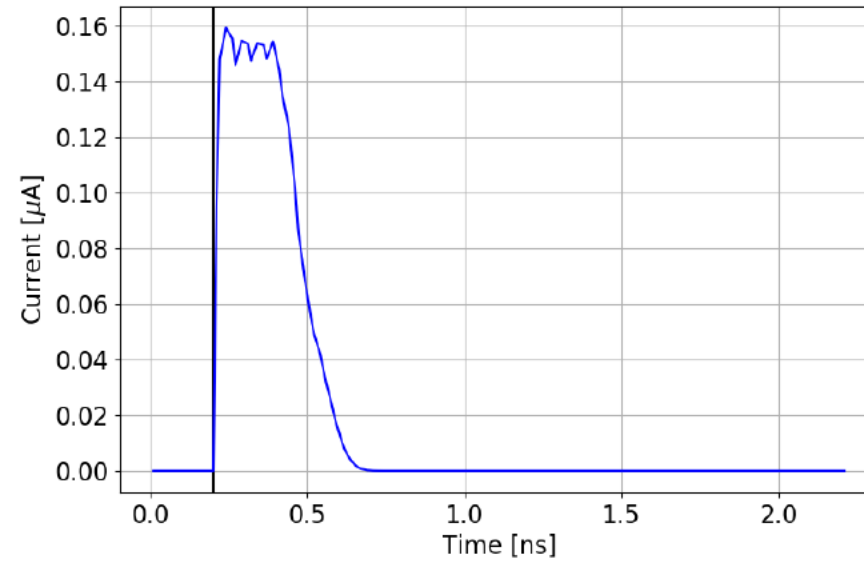
Time 0.20 ns
PIN e⁻



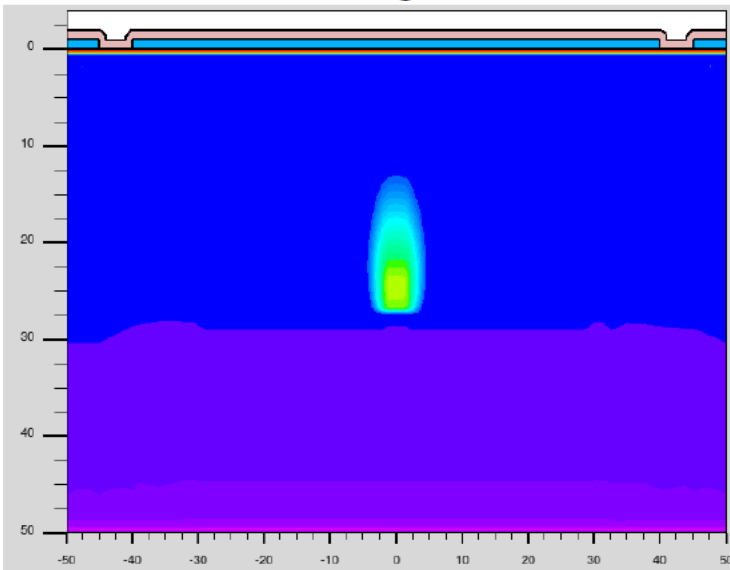
PIN h⁺



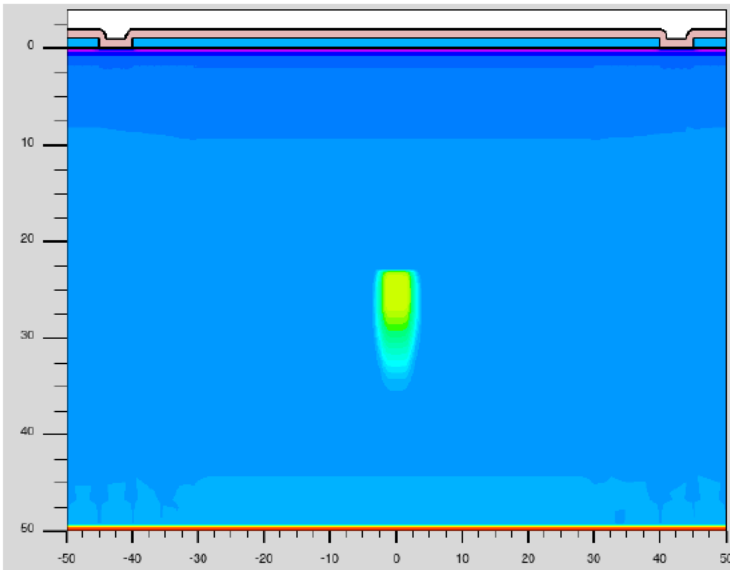
Waveform



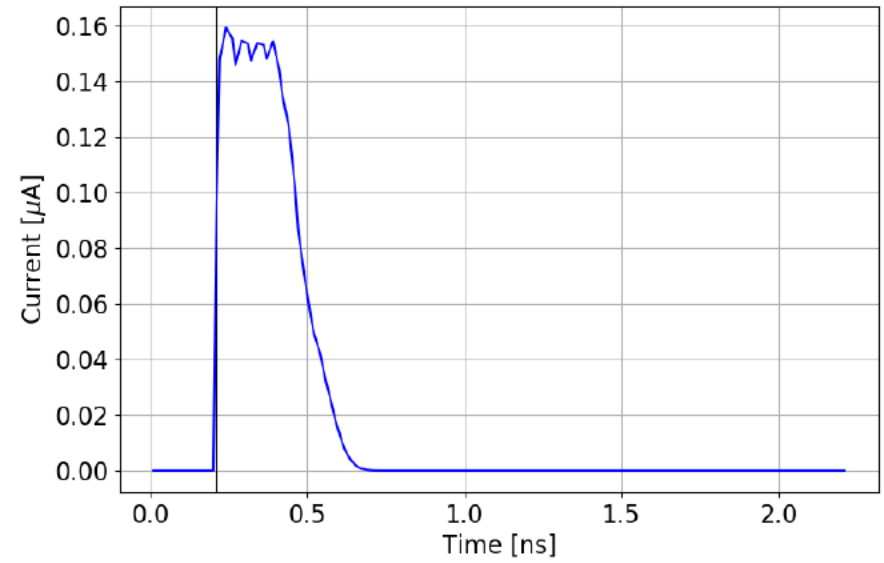
Time 0.21 ns
PIN e⁻



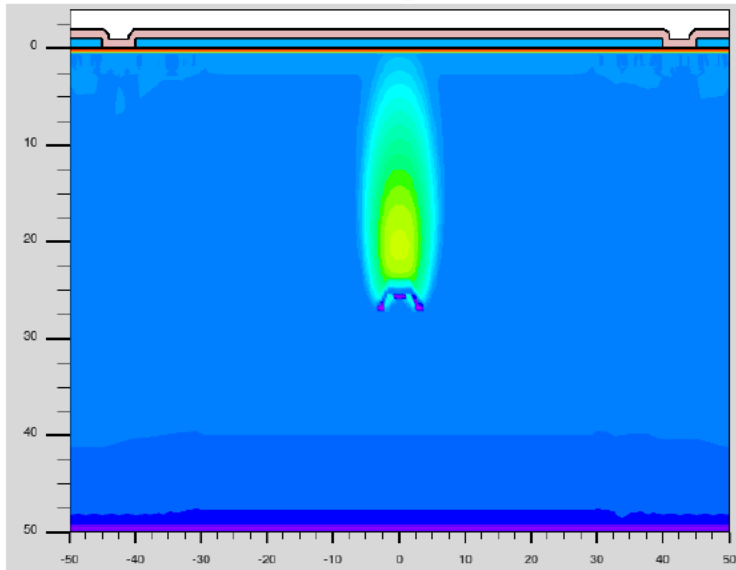
PIN h⁺



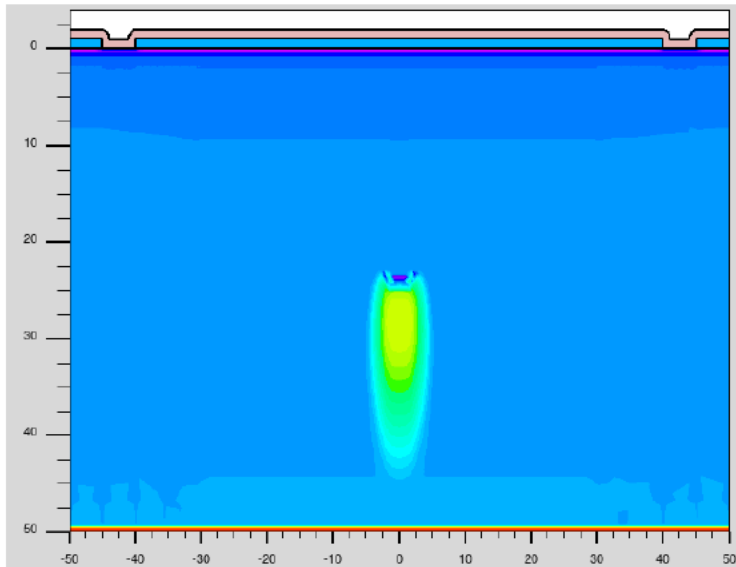
Waveform



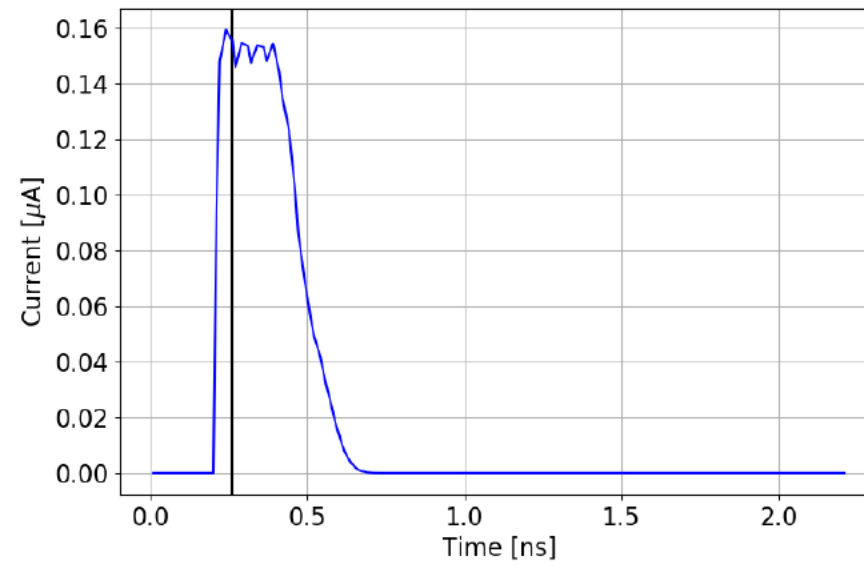
Time 0.26 ns
PIN e⁻



PIN h⁺

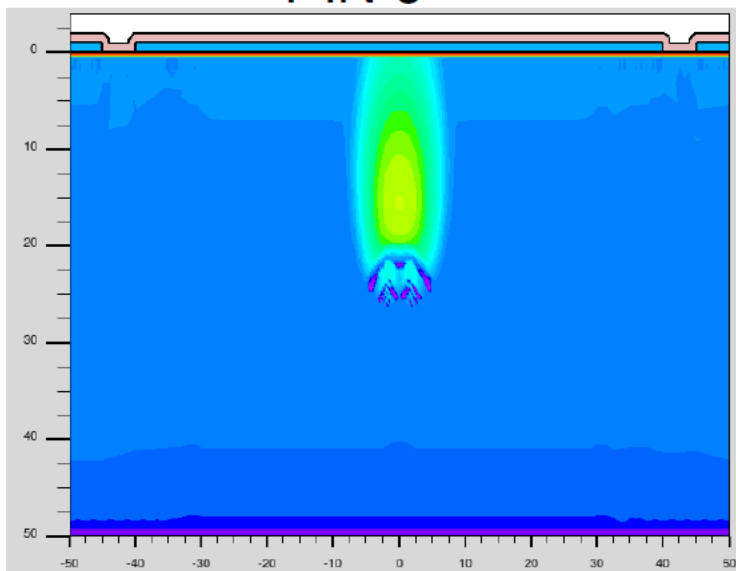


Waveform

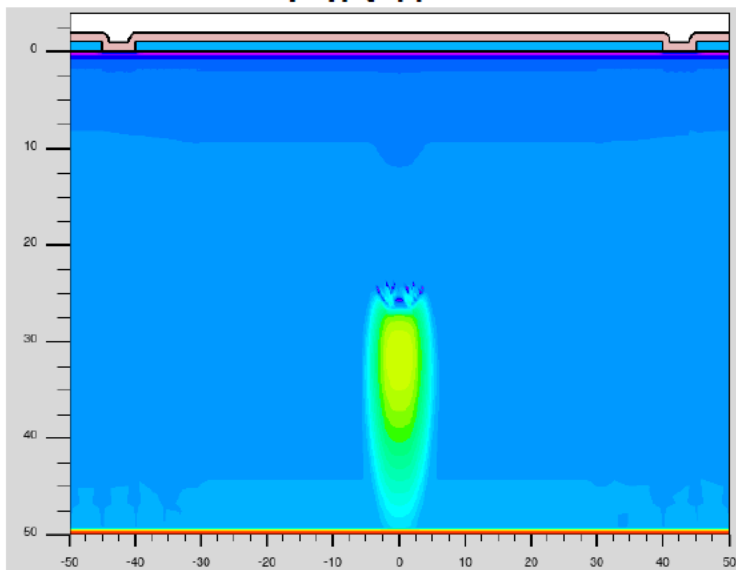


Courtesy: M. Centis Vignali (FBK)

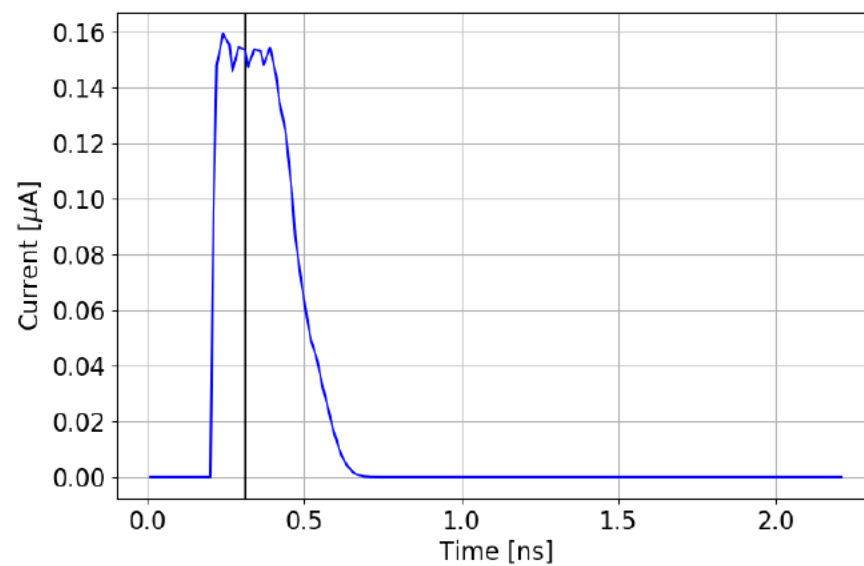
Time 0.31 ns
PIN e⁻



PIN h⁺

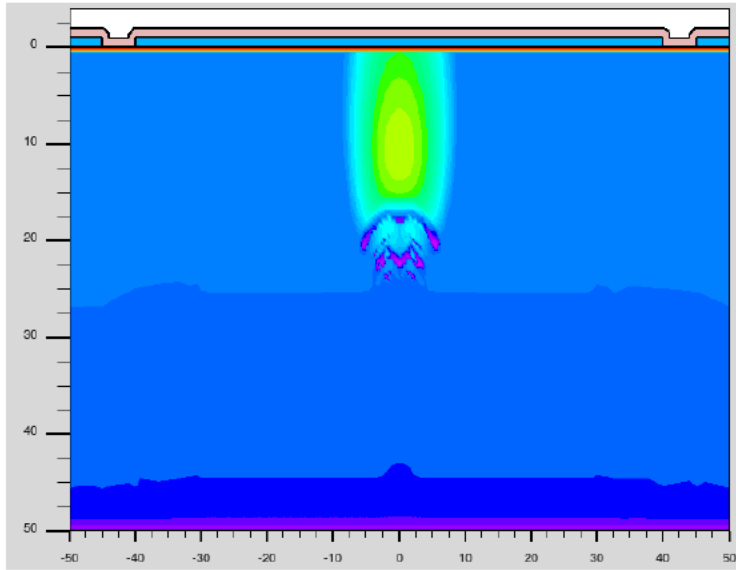


Waveform

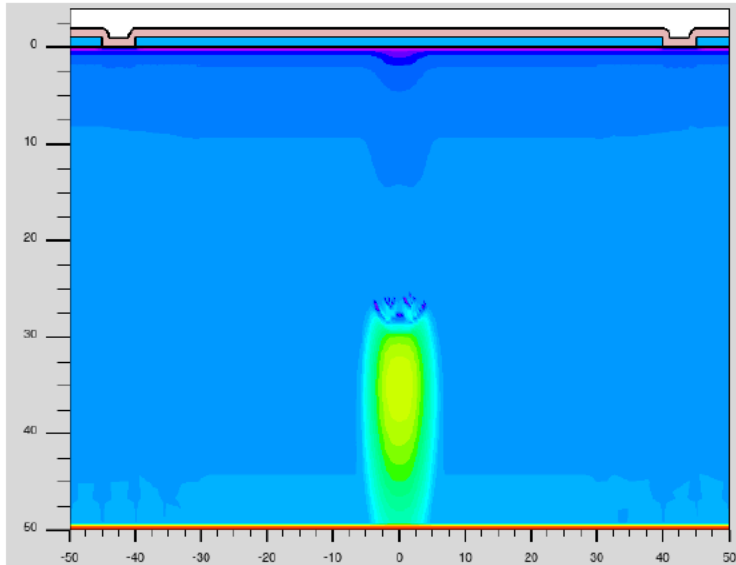


Courtesy: M. Centis Vignali (FBK)

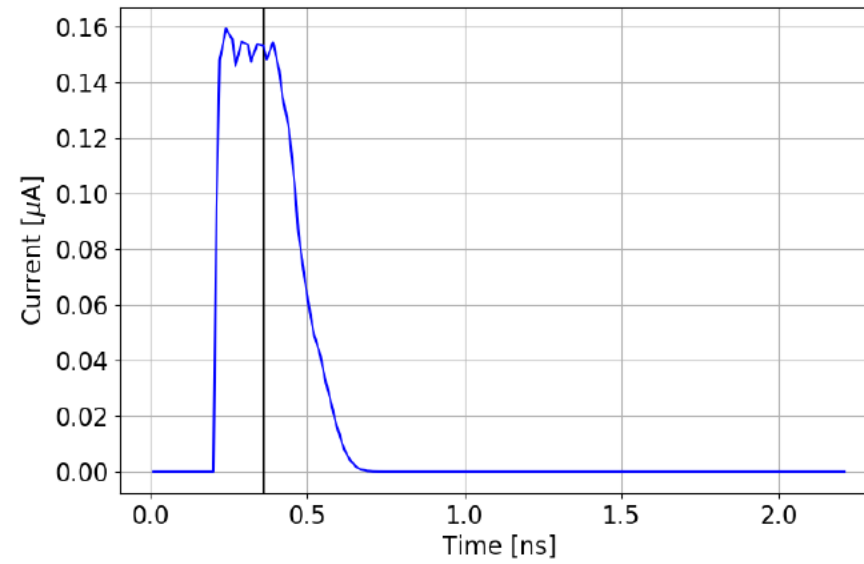
Time 0.36 ns
PIN e⁻



PIN h⁺

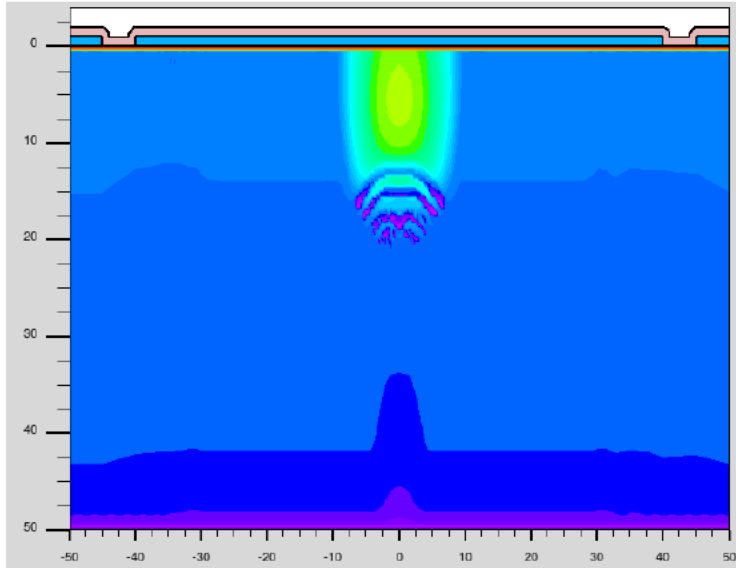


Waveform

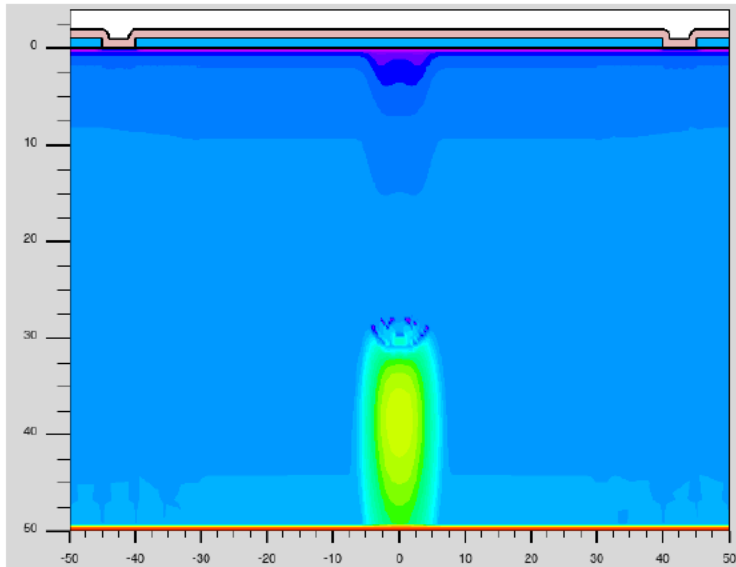


Courtesy: M. Centis Vignali (FBK)

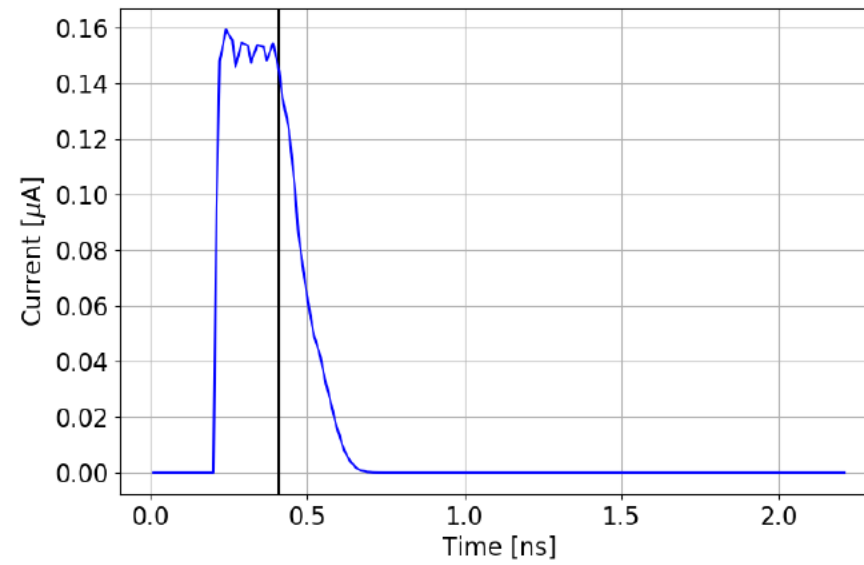
Time 0.41 ns
PIN e⁻



PIN h⁺

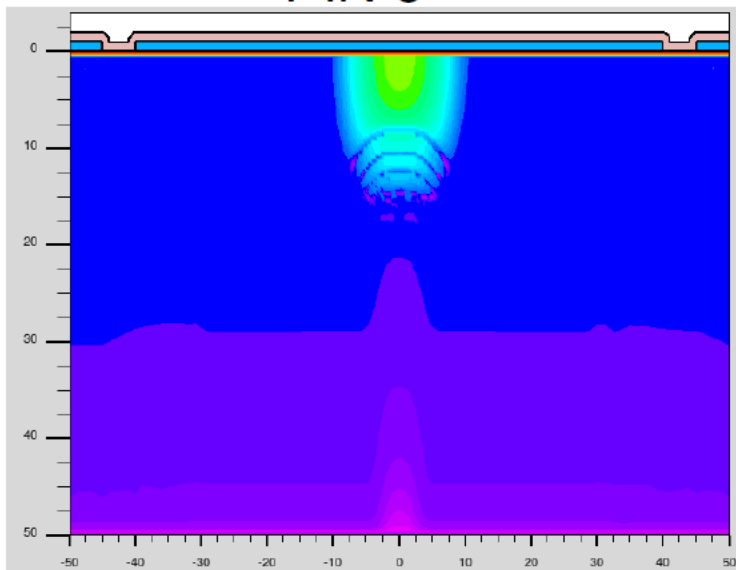


Waveform

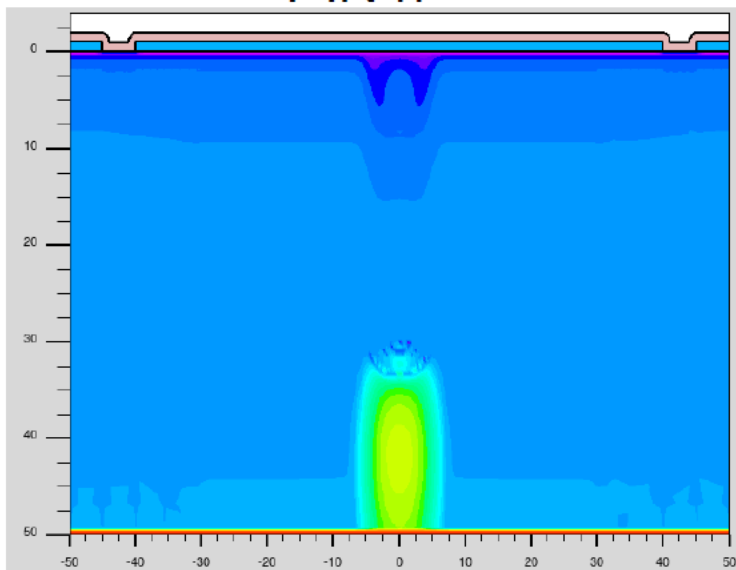


Courtesy: M. Centis Vignali (FBK)

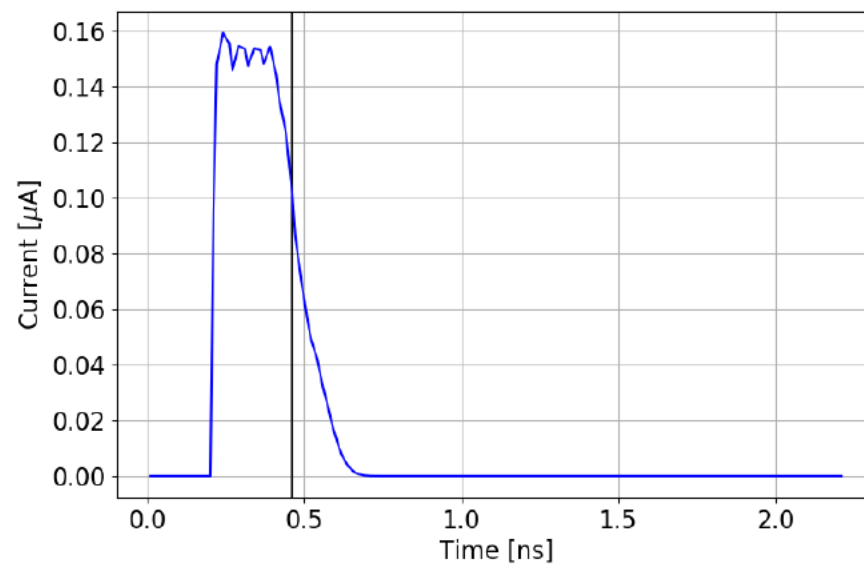
Time 0.46 ns
PIN e⁻



PIN h⁺

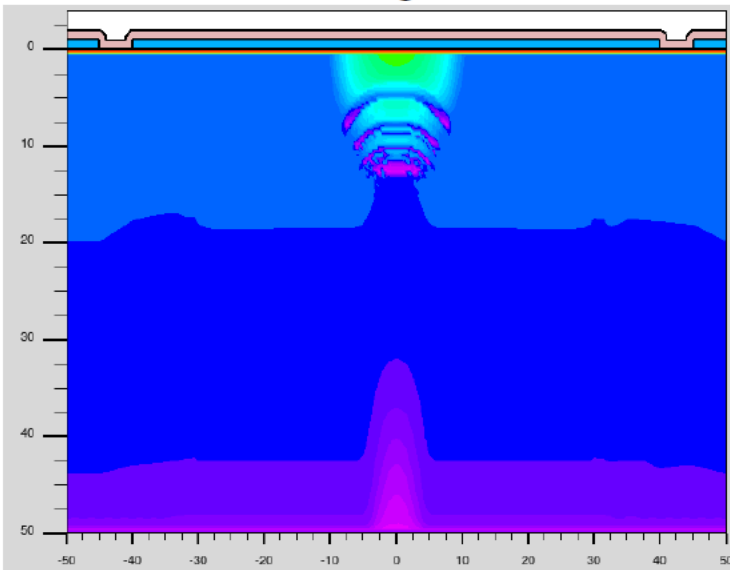


Waveform

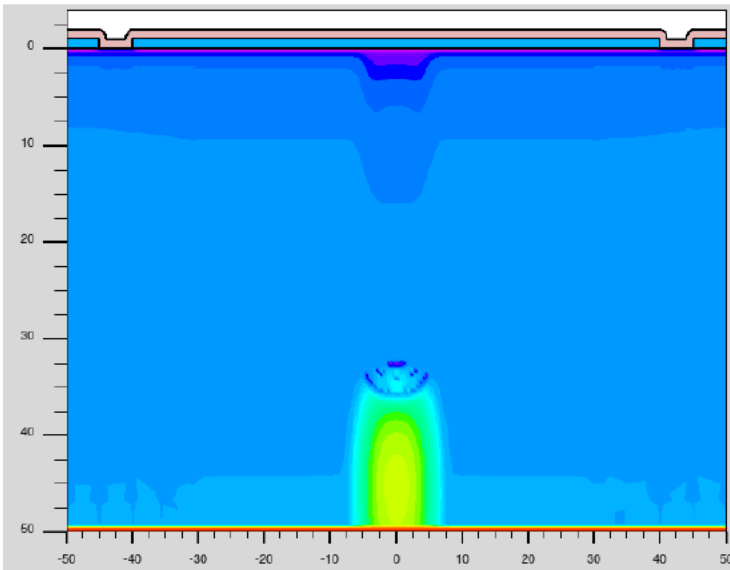


Courtesy: M. Centis Vignali (FBK)

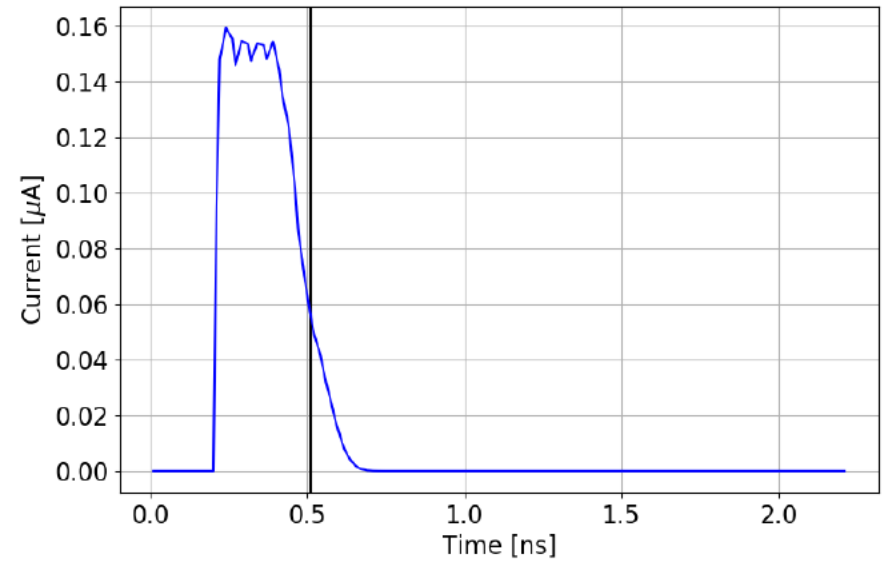
Time 0.51 ns
PIN e⁻



PIN h⁺

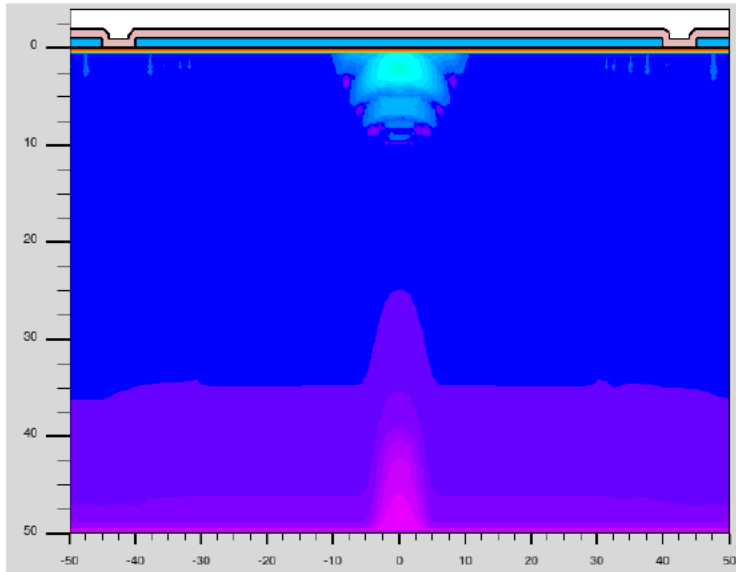


Waveform

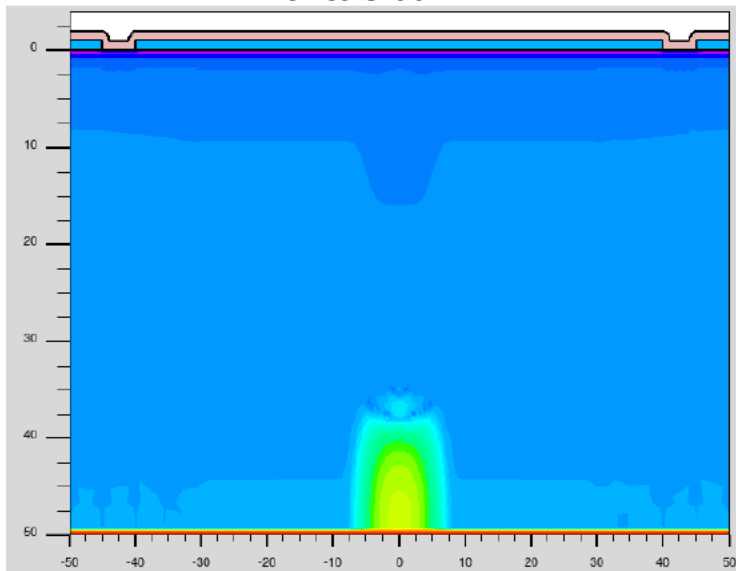


Courtesy: M. Centis Vignali (FBK)

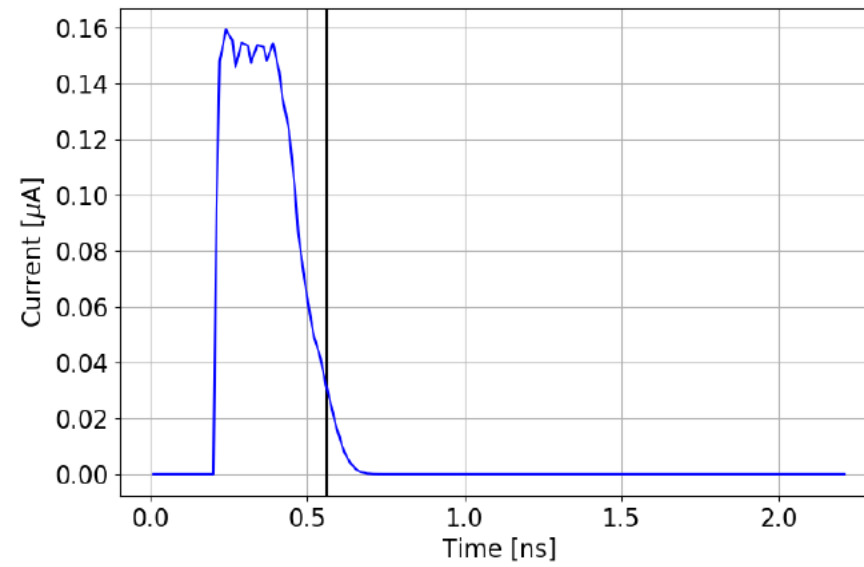
Time 0.56 ns
PIN e⁻



PIN h⁺

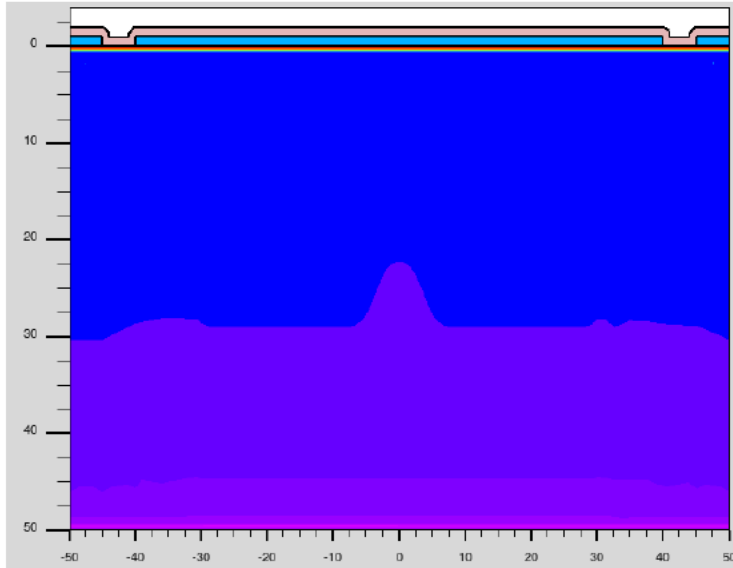


Waveform

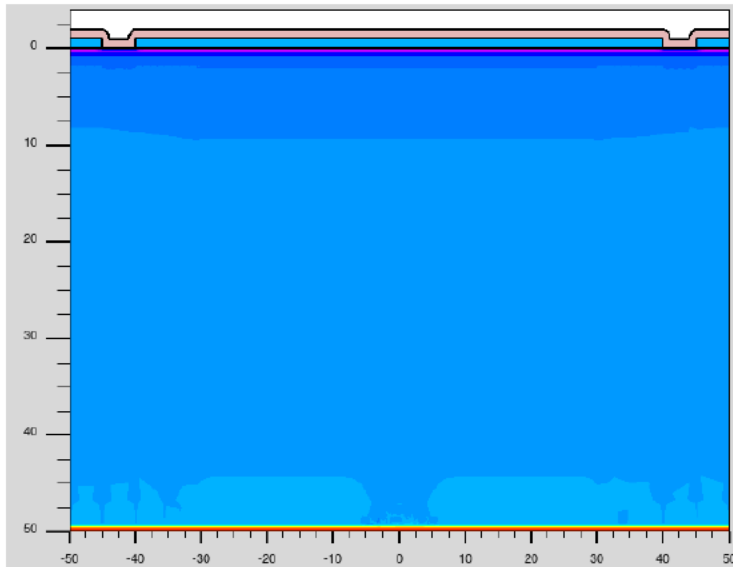


Courtesy: M. Centis Vignali (FBK)

Time 0.81 ns
PIN e⁻

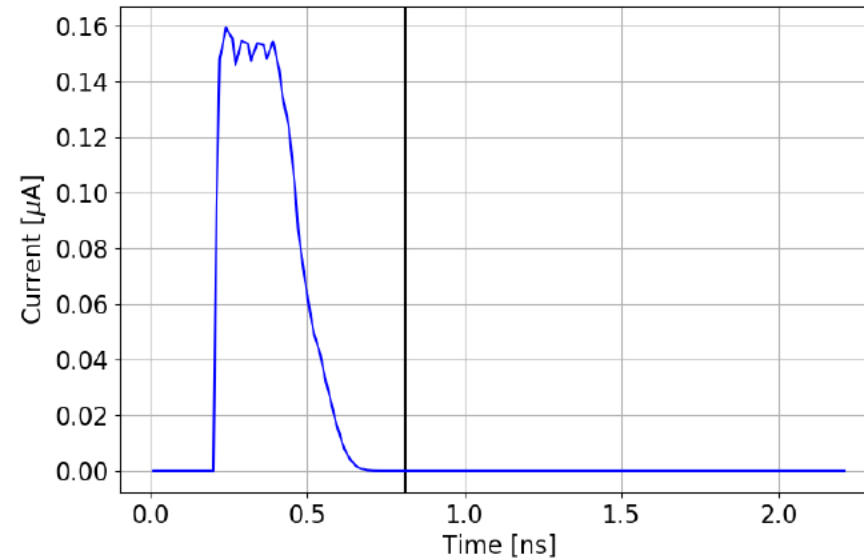


PIN h⁺



- Simulations clearly demonstrate that thinner planar silicon sensors are significantly faster compared to other types of silicon sensors

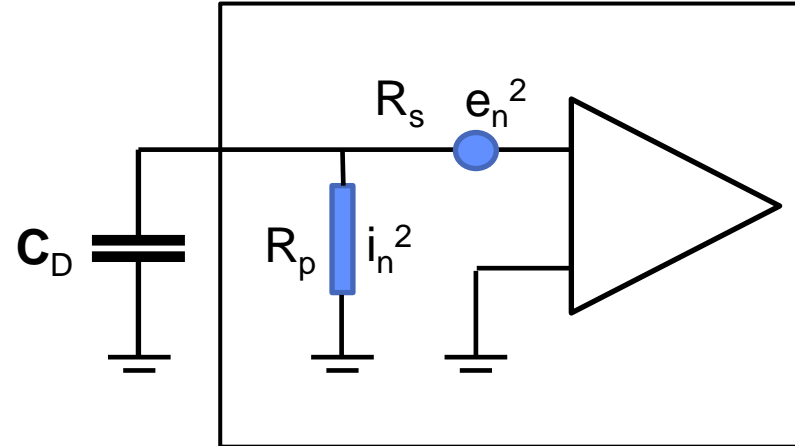
Waveform



- The key question remains *why have only a few groups pursued the development of such sensors for timing applications*

Intrinsic time resolution

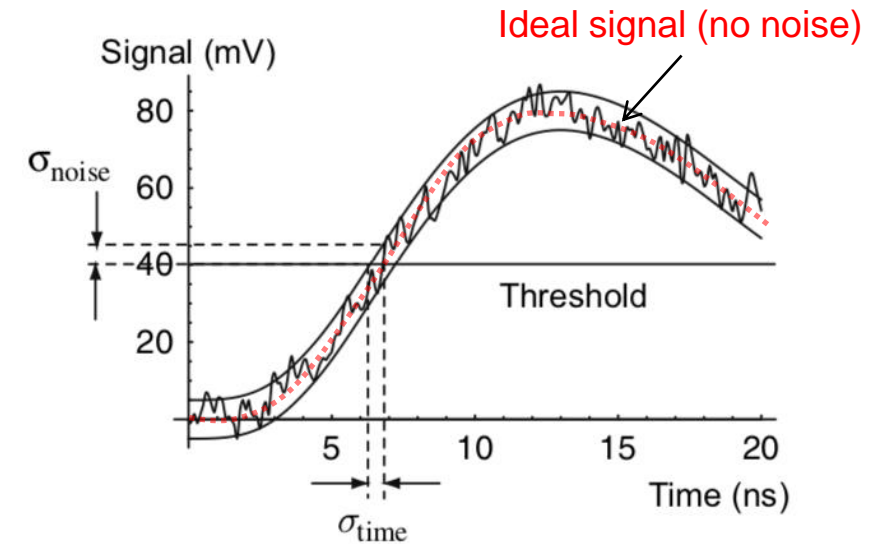
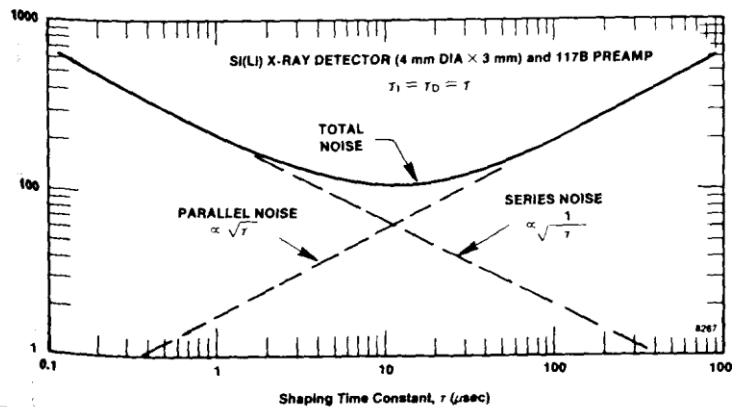
'Noise'



- For a sensor that is represented by a capacitance, the noise is determined by the amplifier only. The amplifier noise can be characterized by the parallel and series noise power spectrum
- In case the parallel and series noise power spectra are 'white' we can formulate this as noise resistance R_s and R_p

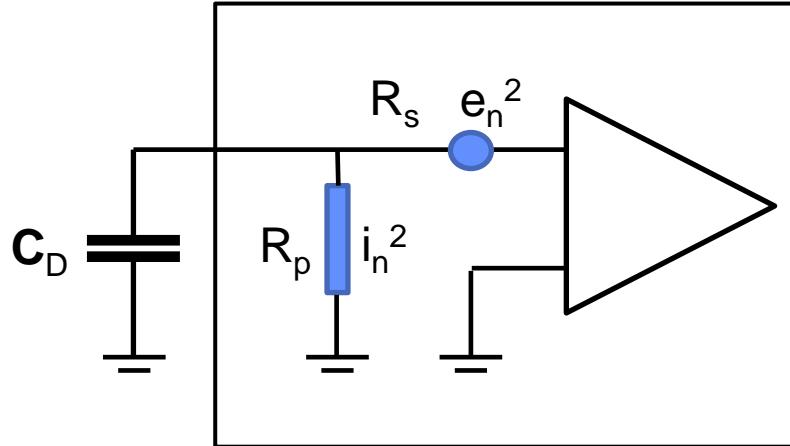
$$\sigma_{time} = \frac{\sigma_{noise}}{k} \quad k \propto \frac{dV}{dt}$$

→ Large signal
→ Short signal rise time



Intrinsic time resolution

‘Noise’

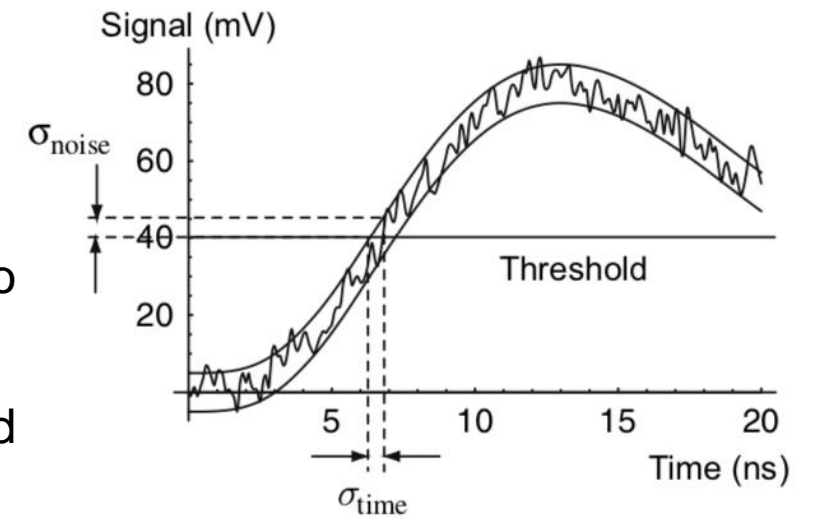


- For a sensor that is represented by a capacitance, the noise is determined by the amplifier only. The amplifier noise can be characterized by the parallel and series noise power spectrum
- In case the parallel and series noise power spectra are ‘white’ we can formulate this as noise resistance R_s and R_p

$$\sigma_{time} = \frac{\sigma_{noise}}{k} \quad k \propto \frac{dV}{dt} \begin{matrix} \rightarrow \text{Large signal} \\ \rightarrow \text{Short signal rise time} \end{matrix}$$

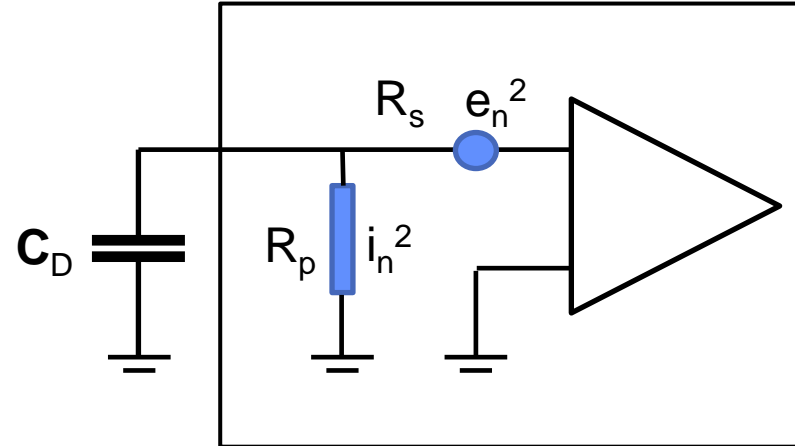
- In a planar thinned sensor, the collected signal is small, leaving two options:

- Amplify the signal at the preamplifier by increasing power and complexity of the preamplifier



Intrinsic time resolution

‘Noise’



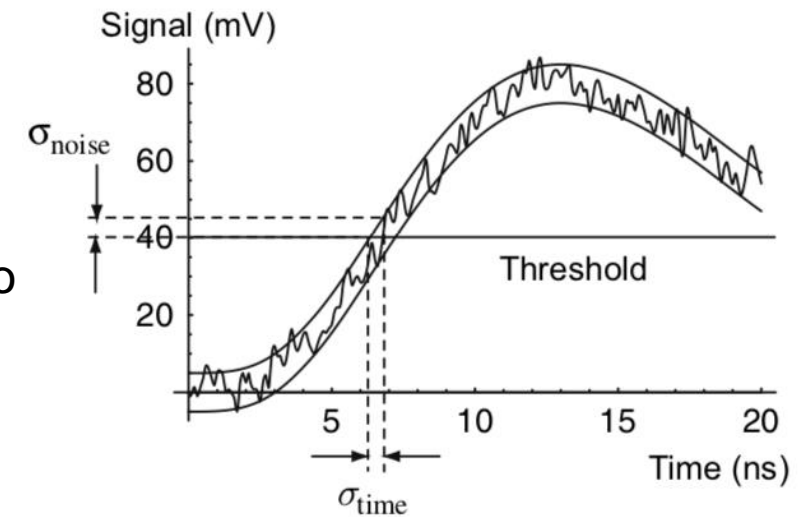
- For a sensor that is represented by a capacitance, the noise is determined by the amplifier only. The amplifier noise can be characterized by the parallel and series noise power spectrum
- In case the parallel and series noise power spectra are ‘white’ we can formulate this as noise resistance R_s and R_p

$$\sigma_{time} = \frac{\sigma_{noise}}{k} \quad k \propto \frac{dV}{dt}$$

→ Large signal
→ Short signal rise time

- In a planar thinned sensor, the collected signal is small, leaving two options:

- Amplify the signal at the preamplifier by increasing power
- Integrate a gain layer into the sensor



→ **LGAD (Low Gain Avalanche Diode)**

Time resolution of 'standard' silicon sensors

Summary

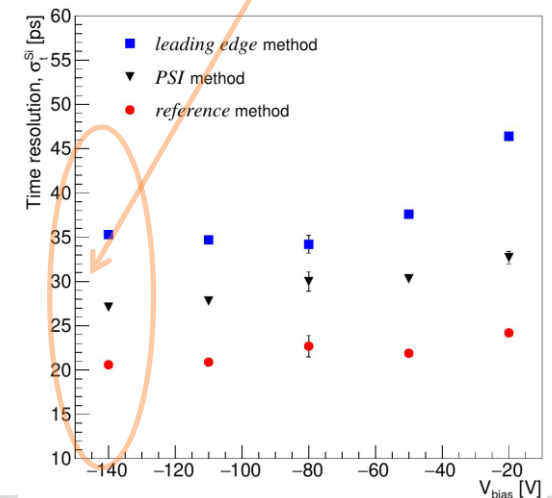
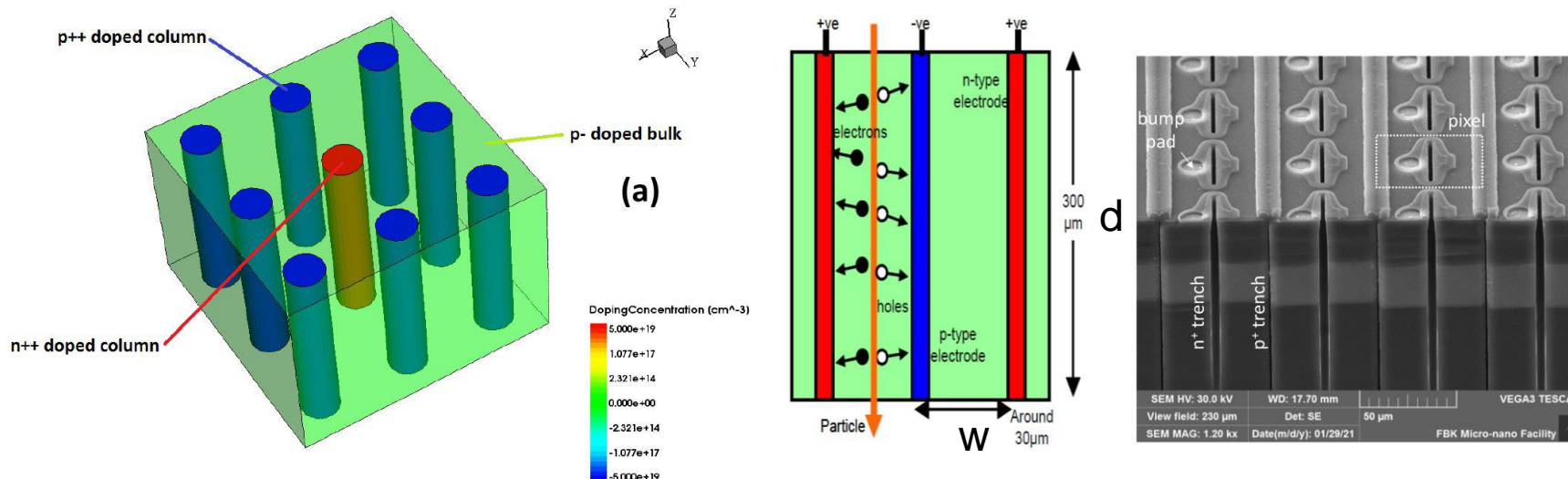
- Good time resolution demands **thin sensors**
- Thin sensors give small charge and large capacitance i.e. **unfavourable S/N and k/N**.
- Capacitance can be reduced by **making the pixels small**
- If the pixel size is in the same order as the sensor thickness, **the weighting field fluctuations start to dominate** ... and there will be many channels ...
- ... between a rock and a hard place ...
 - ***Turn the by sensor 90 degrees and realise a parallel plate geometry in 3D !***
 - ***Sensors with internal gain to overcome the noise limit (like gas detectors !)***

3D silicon detectors

TimeSPOT 3D trench-type silicon pixels (INFN, Uni. PD, Uni. TO, ...)

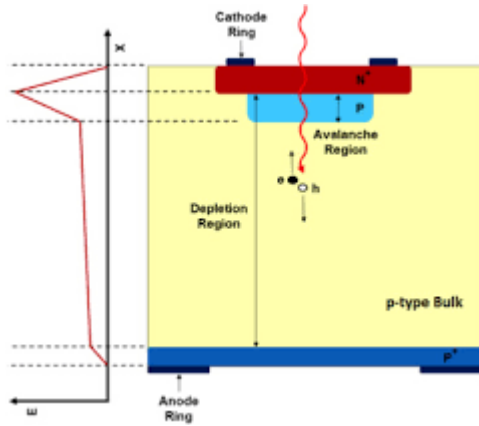
- In 1997 a new architecture was proposed: a 3D array of electrodes that penetrate into the detector bulk.
- 2011: study about timing performance (my last beam test at CERN-SPS)
- 2017: first studies for the realization of a real sensor optimized for timing measurements.
- Sensor thickness (d) and electrodes distance (w) are now uncorrelated.
- The current is enhanced respect to a plain sensor because is now proportional to d/w .

High time resolution with a significantly low V_{bias}

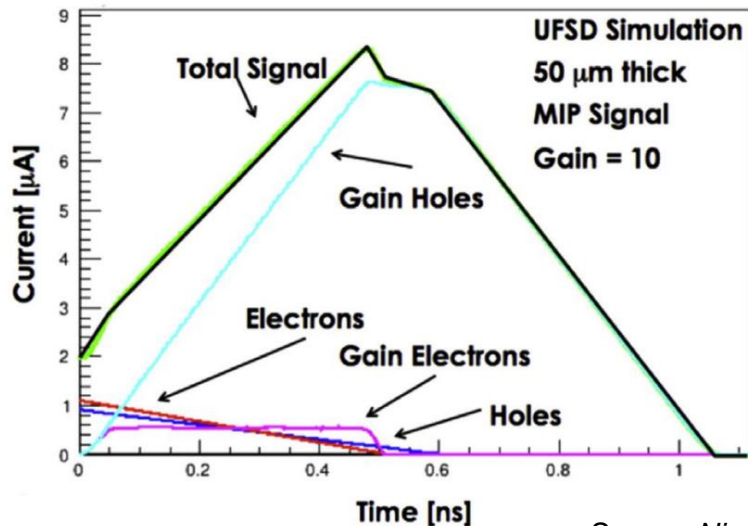


Low Gain Avalanche Diode

First generation of LGAD device



- The high field region is implemented by doping and related 'space-charge' in the volume
- Electrons will produce an avalanche in this high field region
- The sensor is operated in a region where there is electron multiplication but not yet hole multiplication
- This allows to have thin sensors (high field, short signal) but still have enough signal charge to overcome the limitation from noise
- Noise level like normal sensor, therefore **SNR → very high**

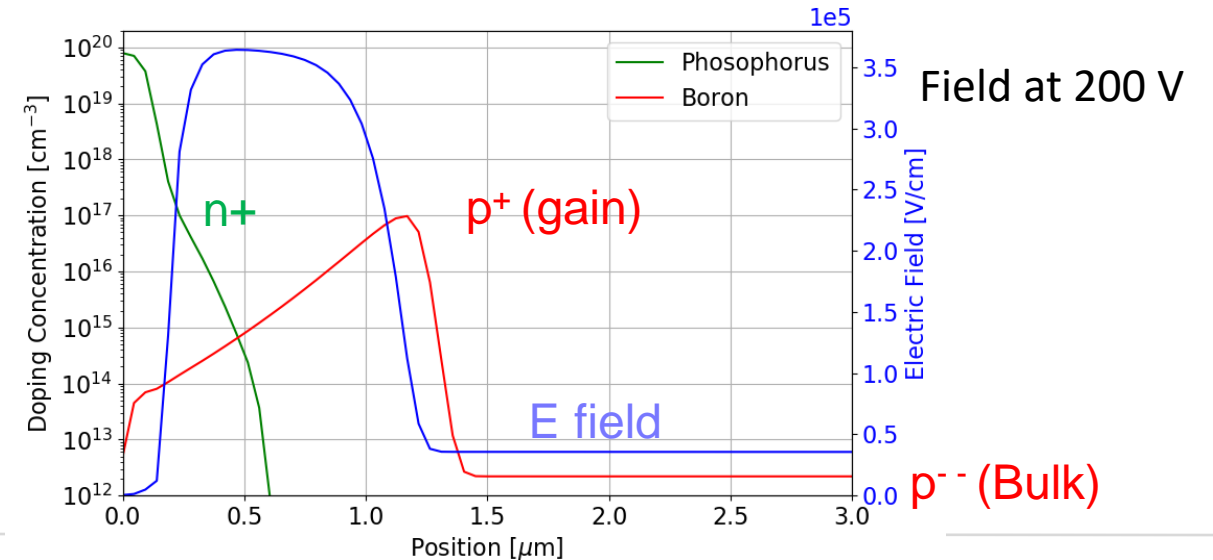
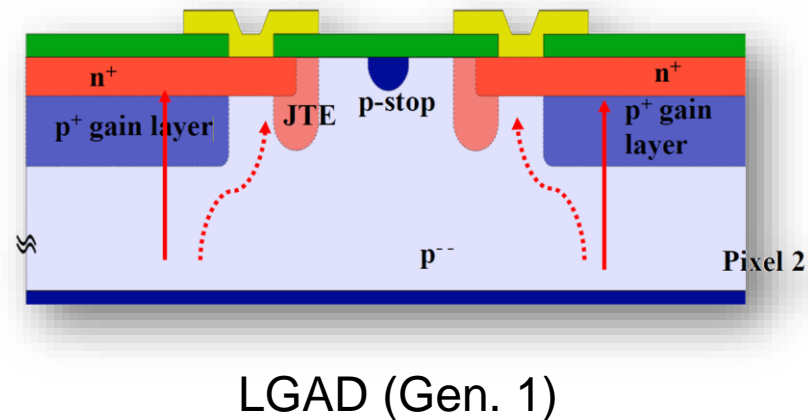
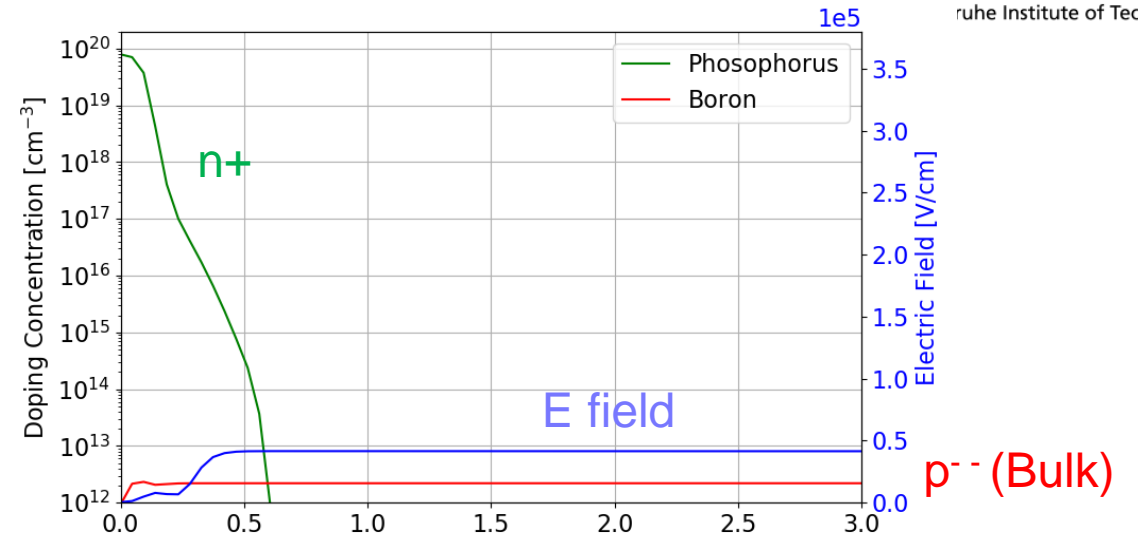
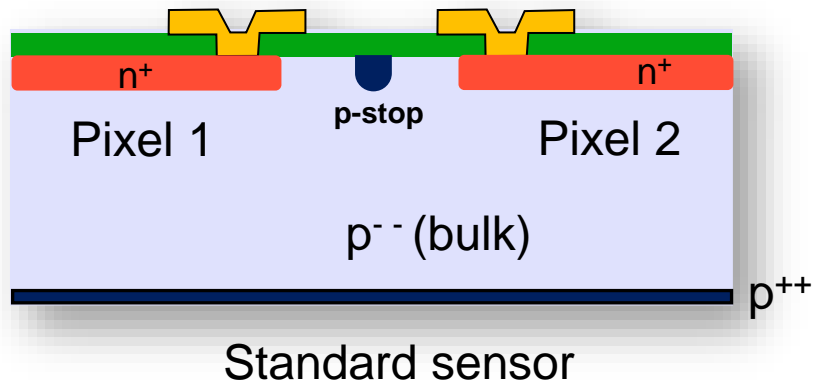


Source: *Nicolo Cartiglia (INFN-To)*

- **Charge Collection and Energy Proportionality:** In LGAD sensors, the total charge collected is proportional to the energy deposited by the particle in the sensor, making them suitable for dE/dx measurements. LGADs enable 5D sensing (space, time, and energy)
- **Comparison with SiPM/SPAD (Single Photon Avalanche Diode):** In SiPMs/SPADs, both electrons and holes are multiplied with very high gain. However, the use of quenching circuits disrupts the proportionality between the total charge collected and the particle's ionization energy, limiting their suitability for energy-resolved measurements

Low Gain Avalanche Diode

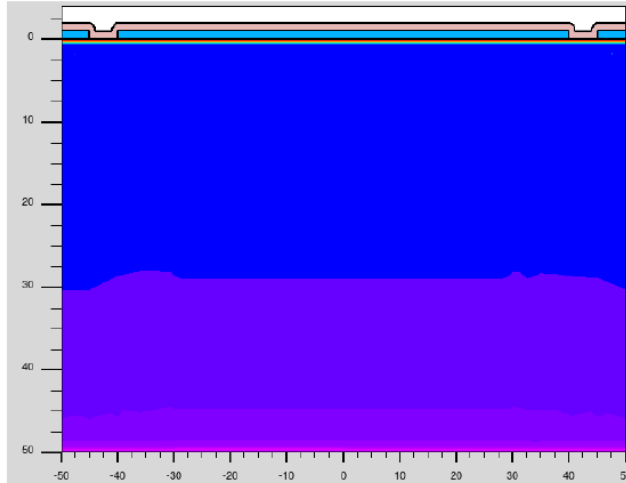
Idea goes back to the 1960ies



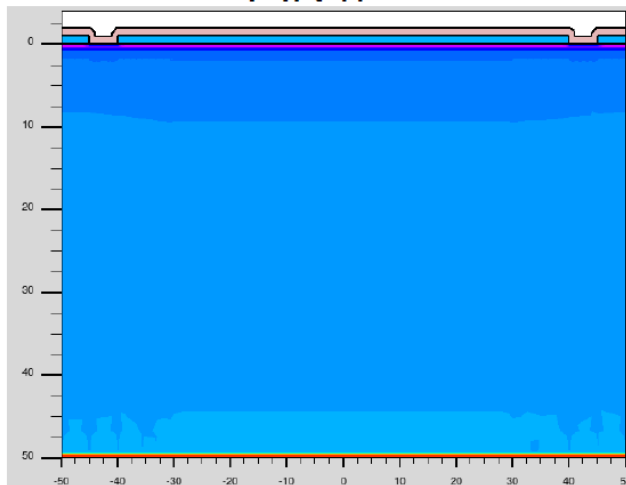
Thin sensor (PIN) vs LGAD

Bottom charge injection

Time 0.20 ns
PIN e⁻

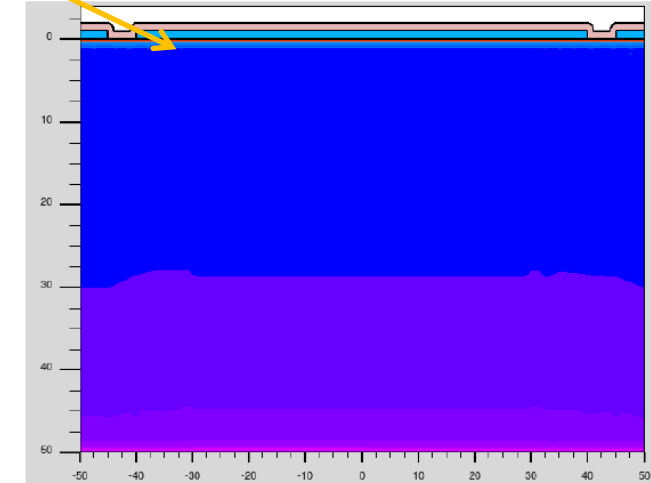


PIN h⁺

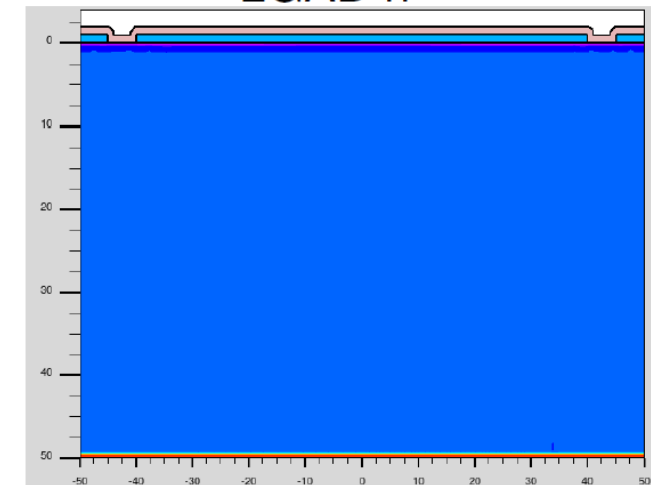


Gain layer

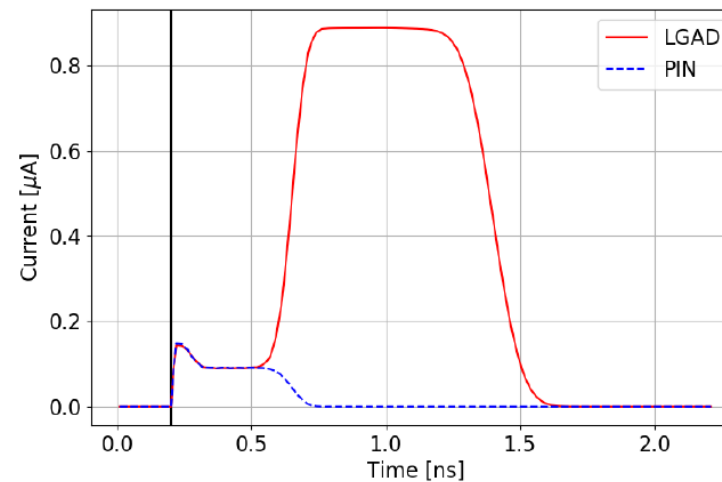
LGAD e⁻



LGAD h⁺



Waveforms

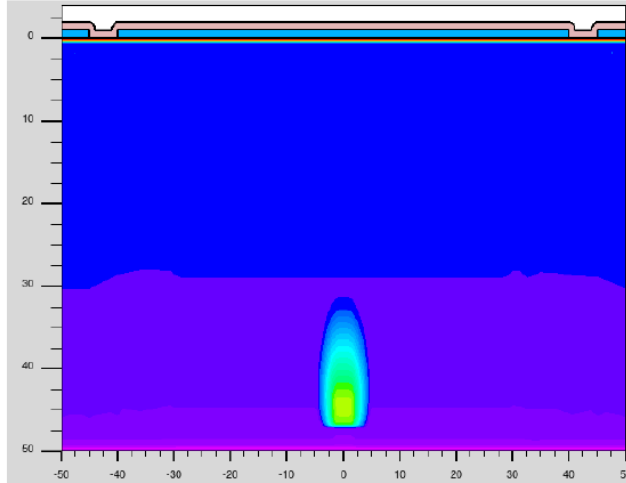


Courtesy: M. Centis Vignali (FBK)

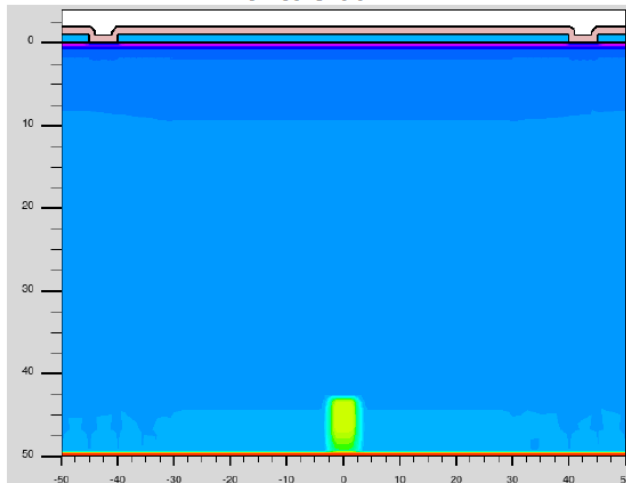
Thin sensor (PIN) vs LGAD

Bottom charge injection

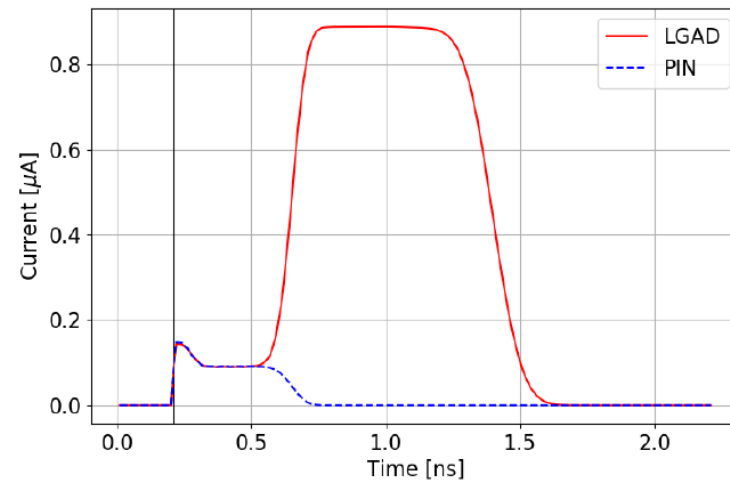
Time 0.21 ns
PIN e^-



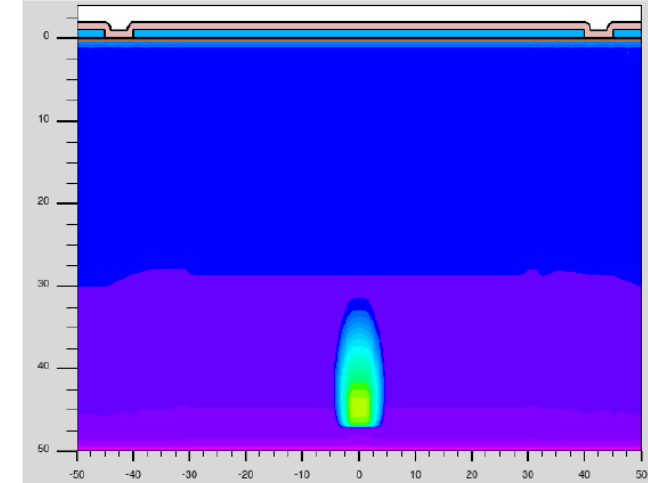
PIN h^+



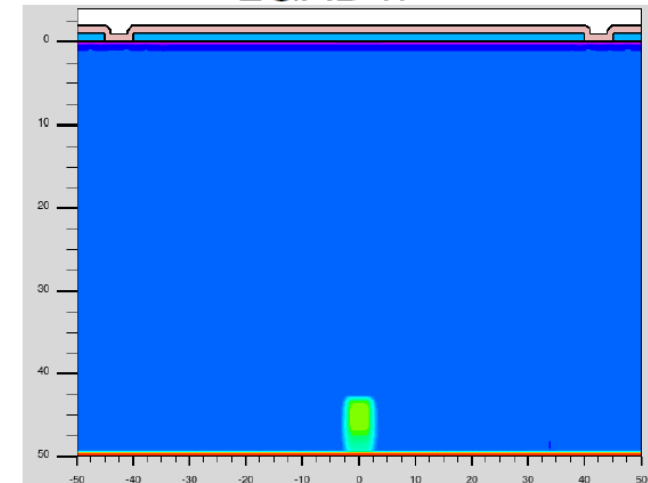
Waveforms



LGAD e^-



LGAD h^+

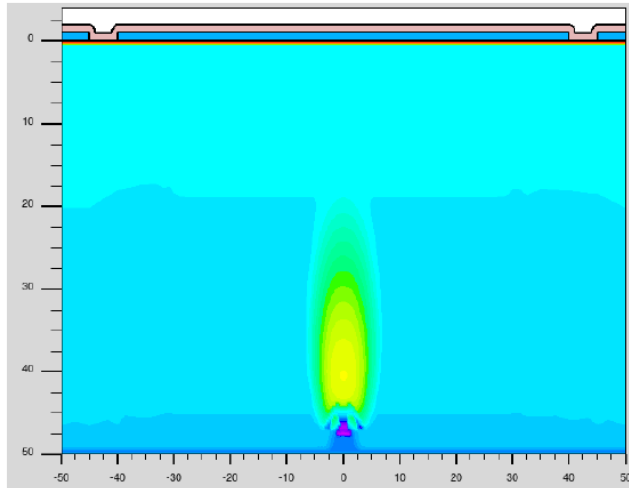


Courtesy: M. Centis Vignali (FBK)

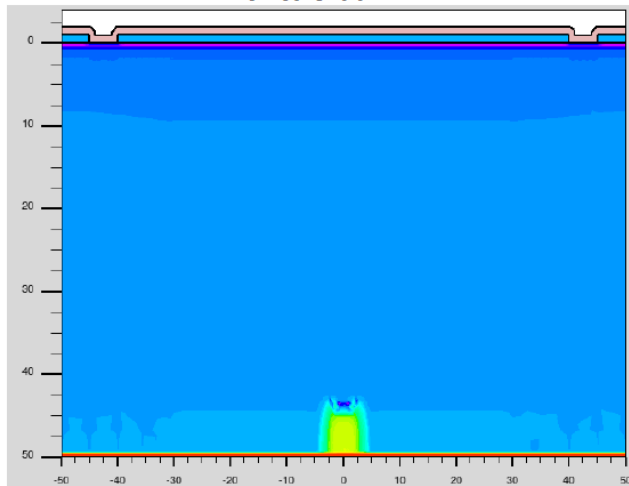
Thin sensor (PIN) vs LGAD

Bottom charge injection

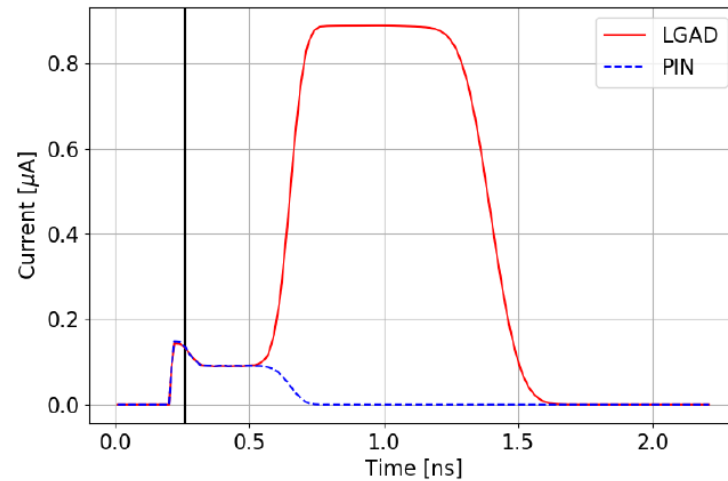
Time 0.26 ns
PIN e^-



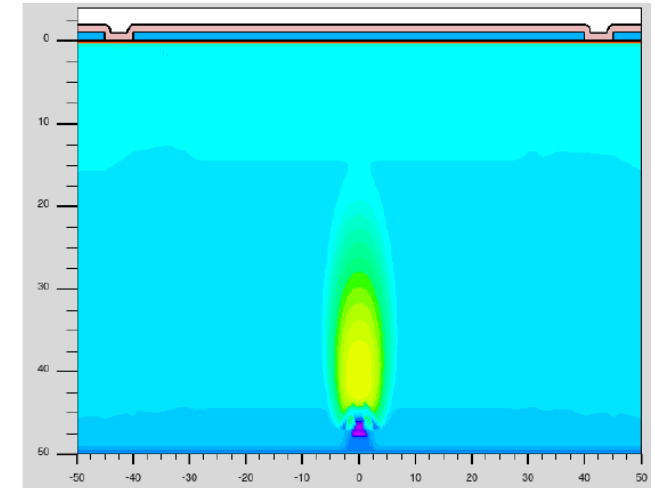
PIN h^+



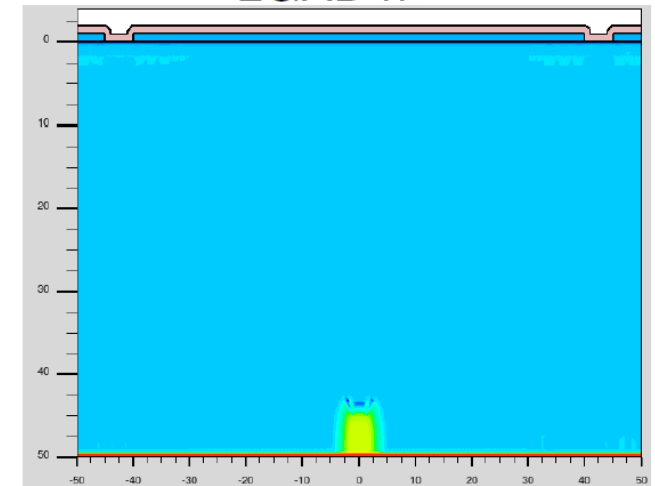
Waveforms



LGAD e^-



LGAD h^+

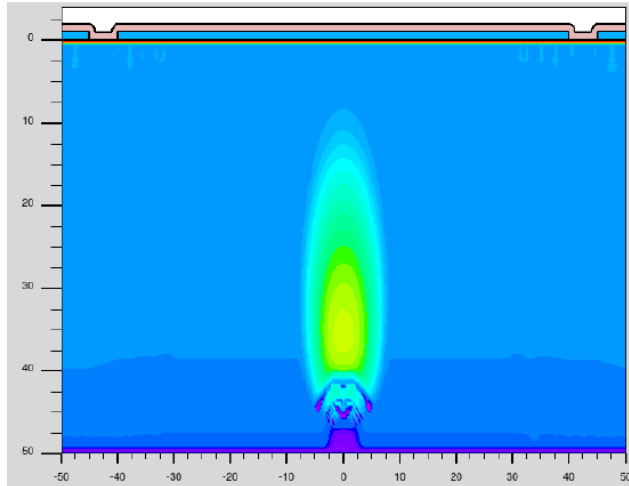


Courtesy: M. Centis Vignali (FBK)

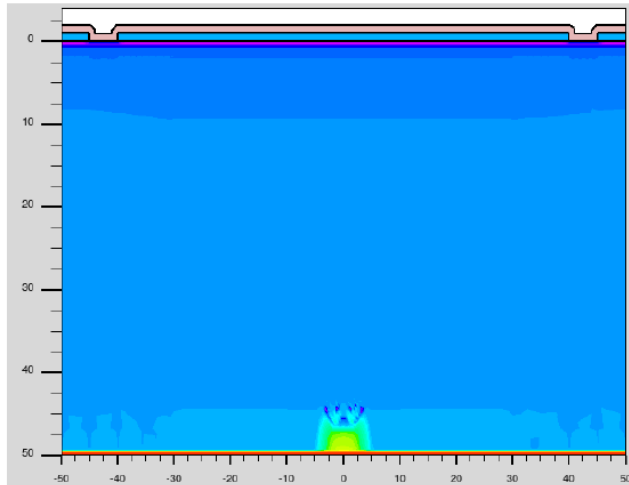
Thin sensor (PIN) vs LGAD

Bottom charge injection

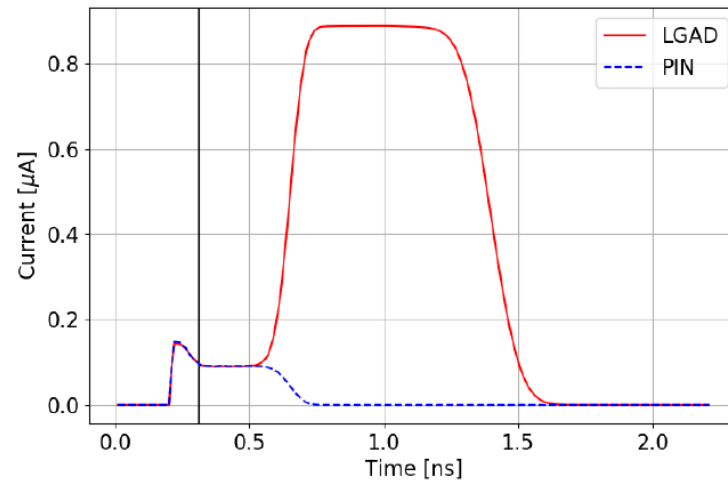
Time 0.31 ns
PIN e^-



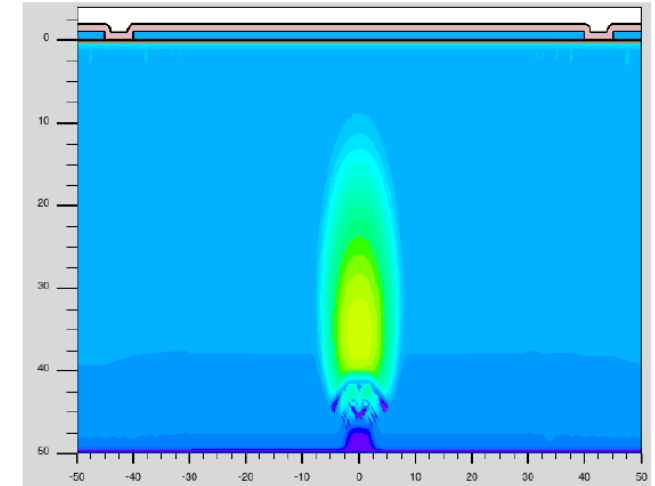
PIN h^+



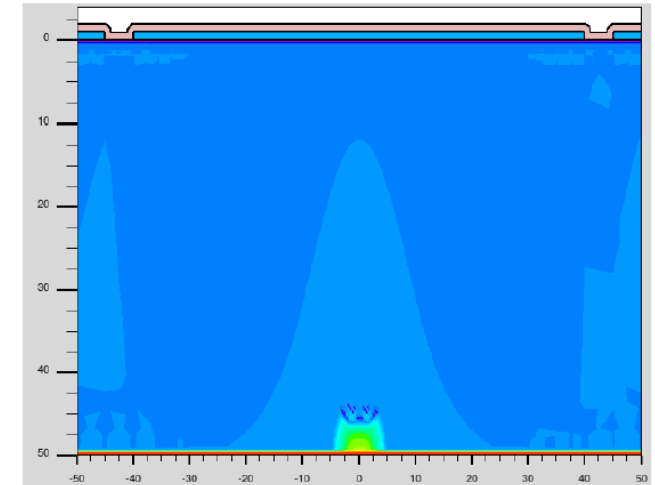
Waveforms



LGAD e^-



LGAD h^+

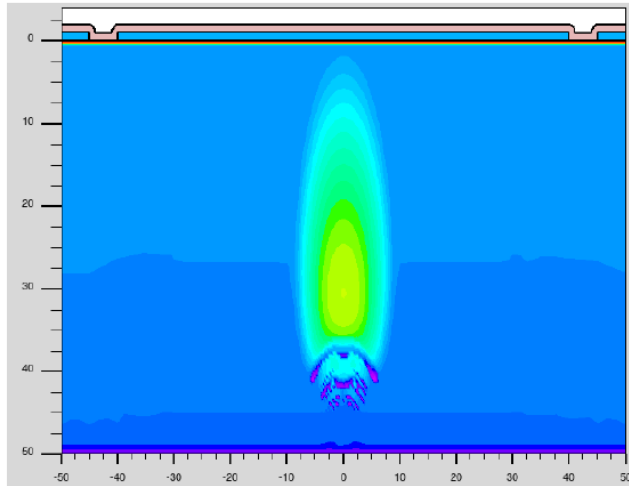


Courtesy: M. Centis Vignali (FBK)

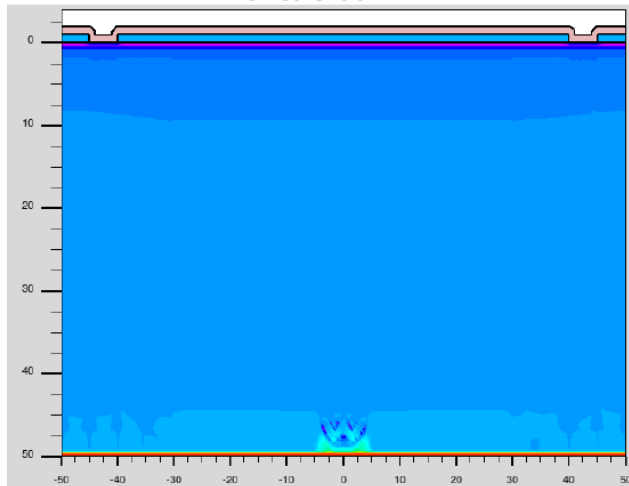
Thin sensor (PIN) vs LGAD

Bottom charge injection

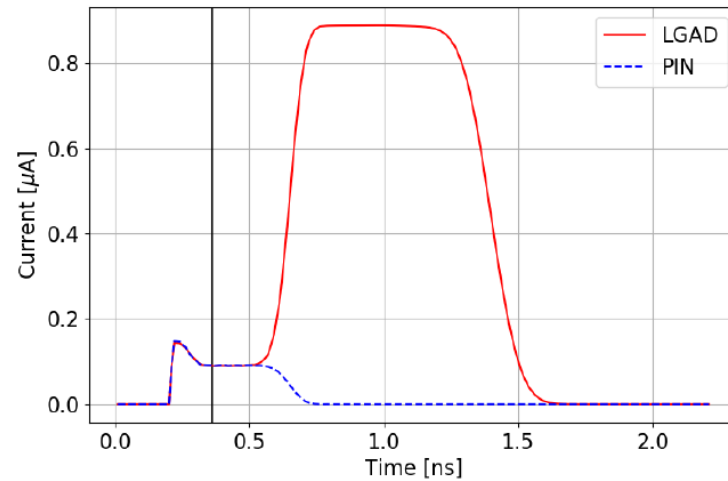
Time 0.36 ns
PIN e^-



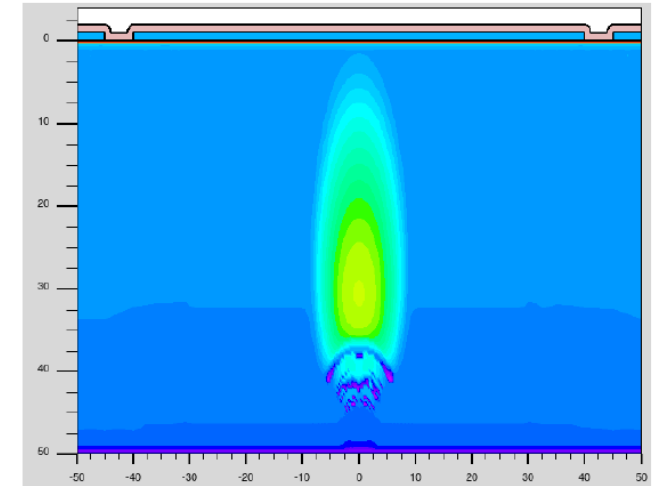
PIN h^+



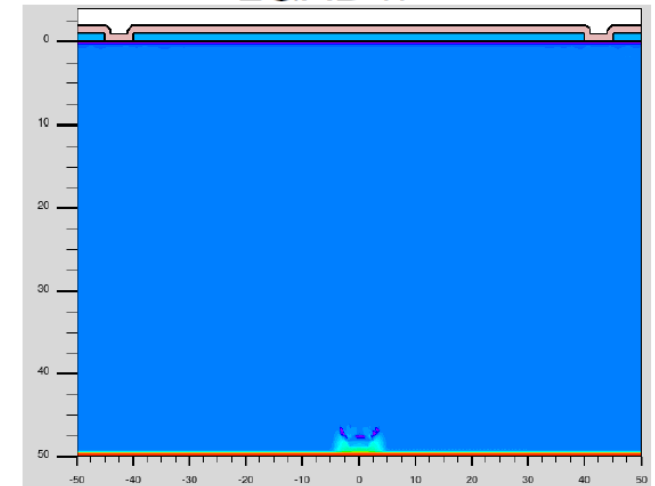
Waveforms



LGAD e^-



LGAD h^+

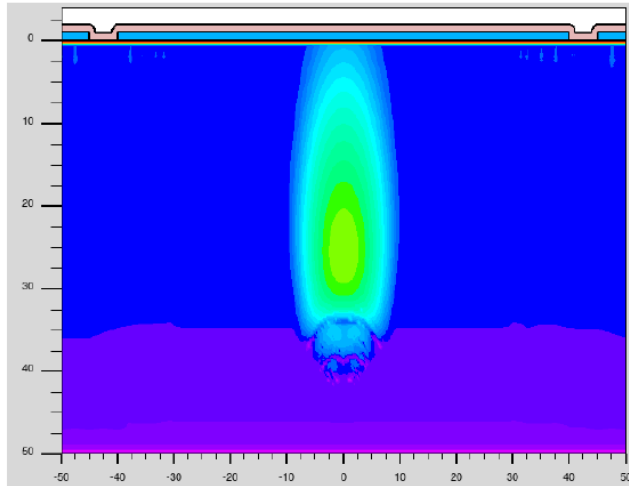


Courtesy: M. Centis Vignali (FBK)

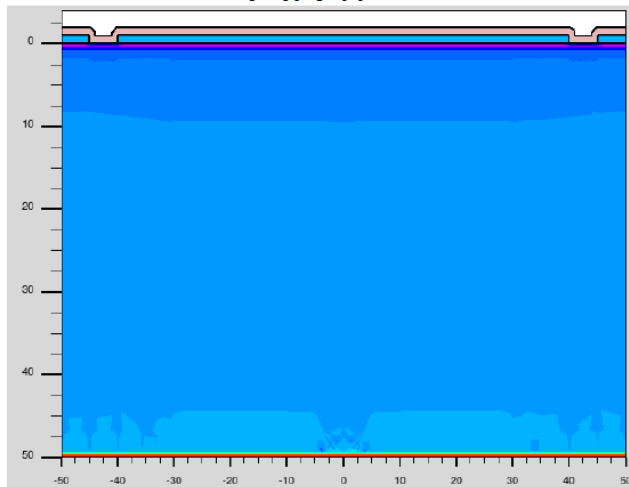
Thin sensor (PIN) vs LGAD

Bottom charge injection

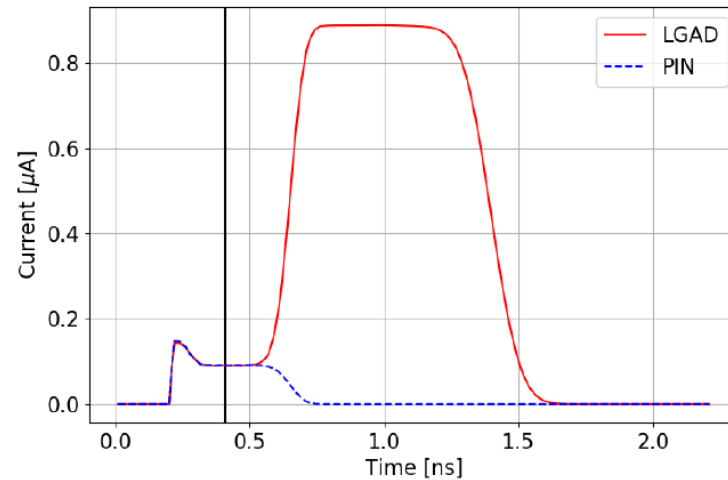
Time 0.41 ns
PIN e^-



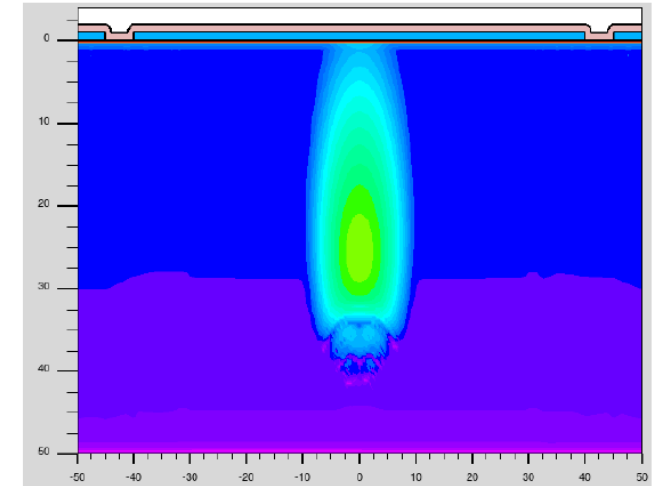
PIN h^+



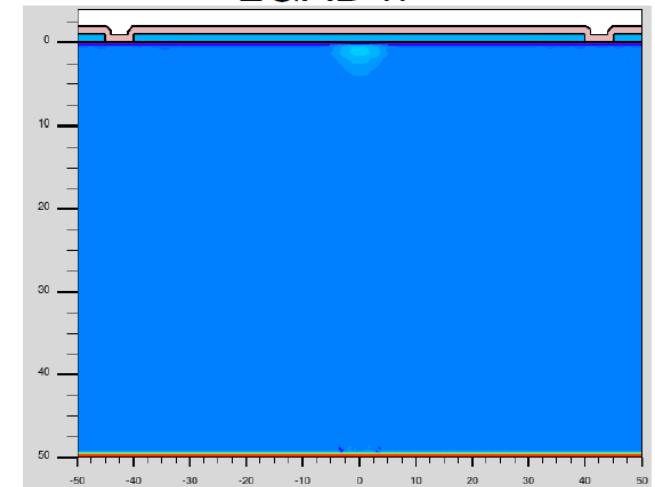
Waveforms



LGAD e^-



LGAD h^+



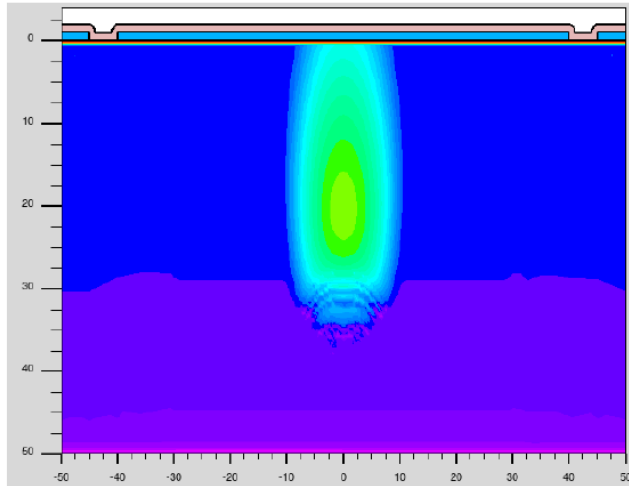
Courtesy: M. Centis Vignali (FBK)

Thin sensor (PIN) vs LGAD

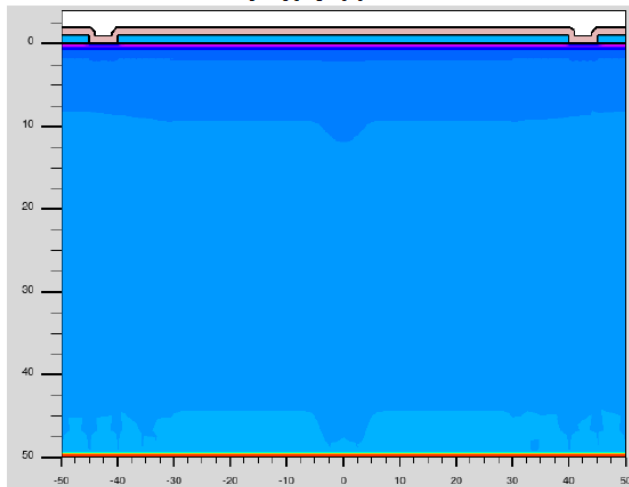
Bottom charge injection

Time 0.46 ns

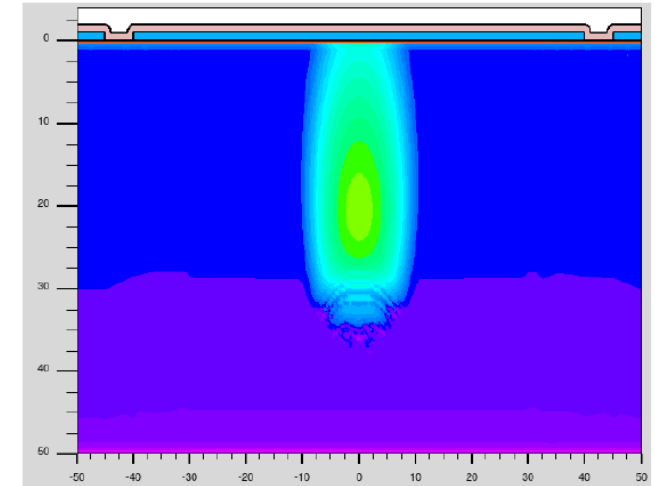
PIN e^-



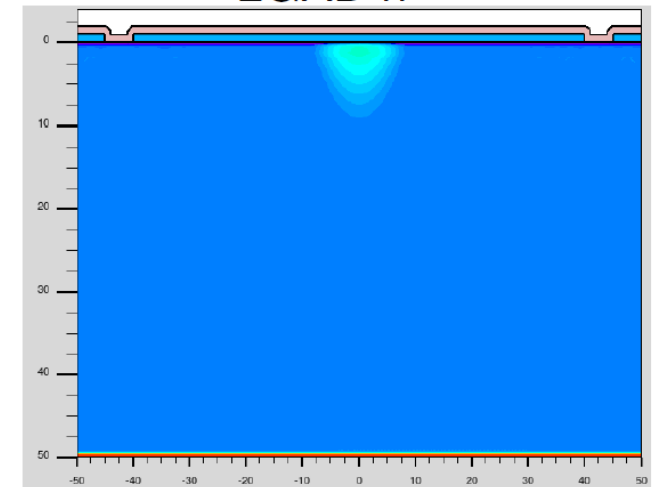
PIN h^+



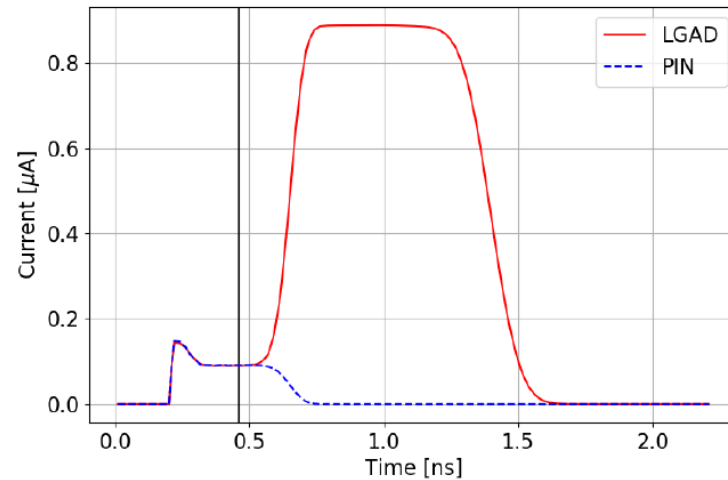
LGAD e^-



LGAD h^+



Waveforms

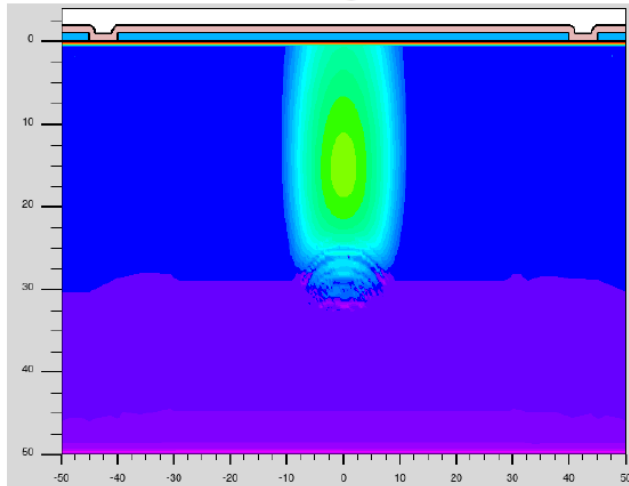


Courtesy: M. Centis Vignali (FBK)

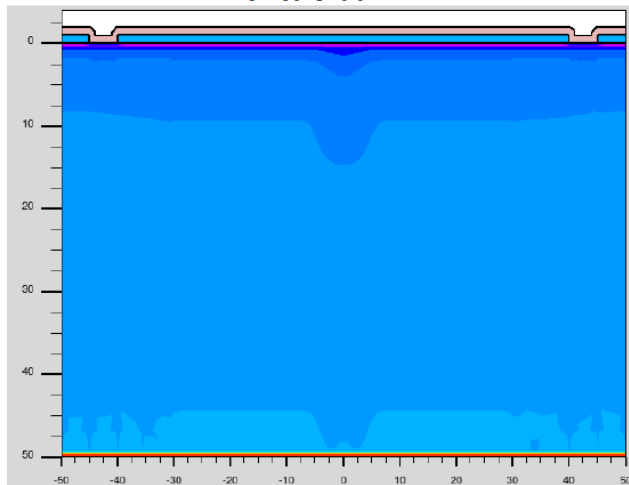
Thin sensor (PIN) vs LGAD

Bottom charge injection

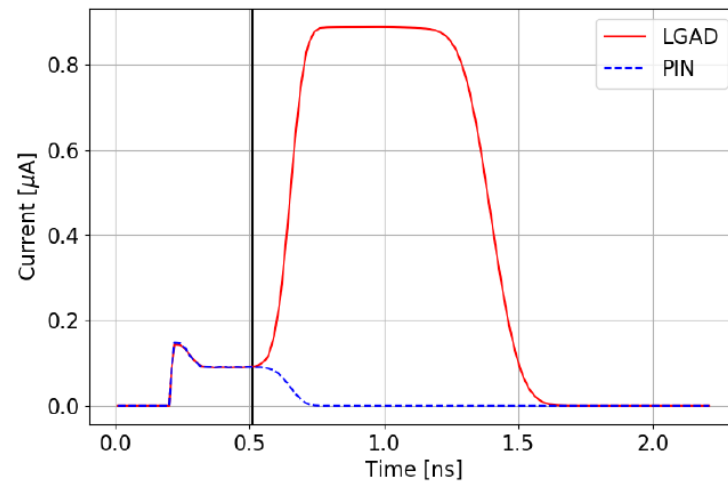
Time 0.51 ns
PIN e^-



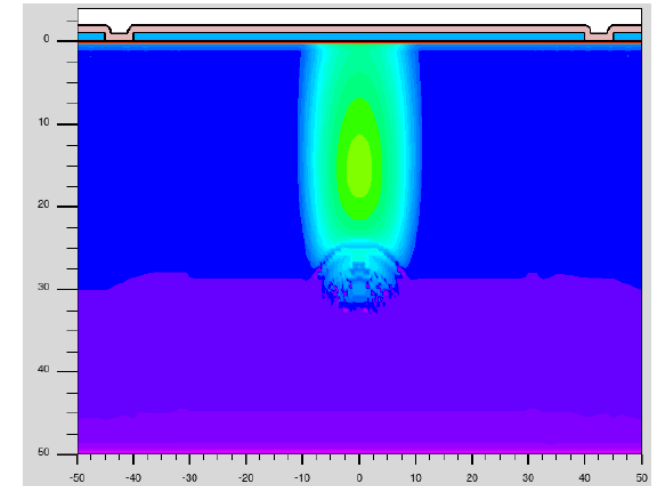
PIN h^+



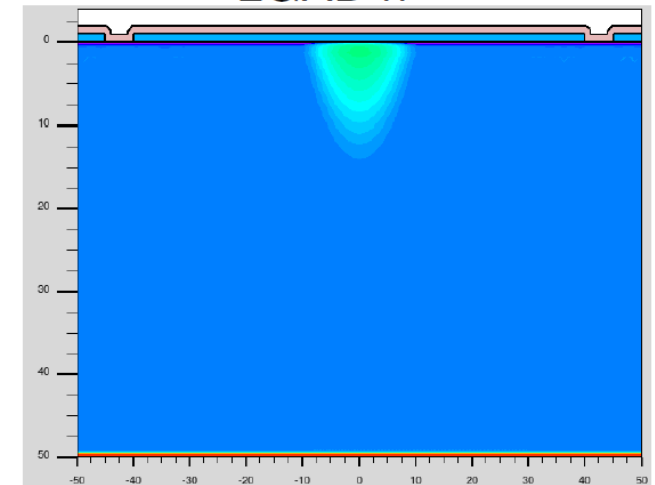
Waveforms



LGAD e^-



LGAD h^+

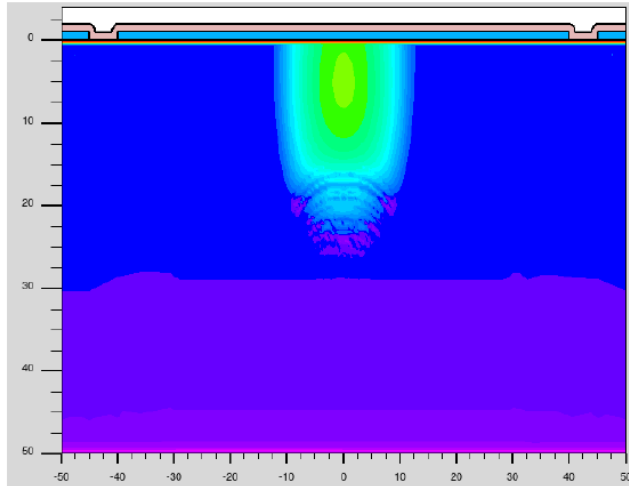


Courtesy: M. Centis Vignali (FBK)

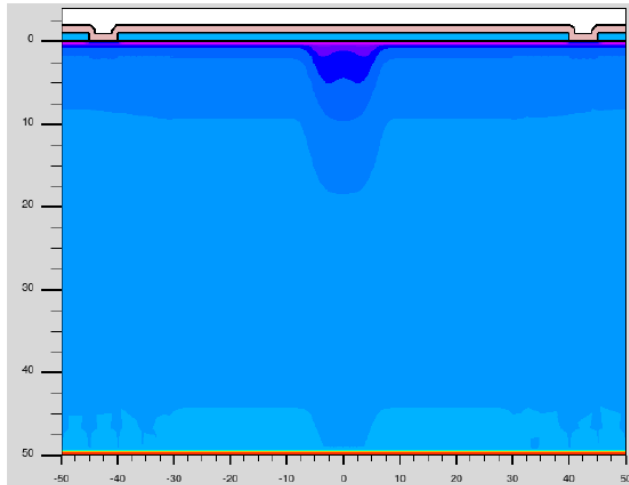
Thin sensor (PIN) vs LGAD

Bottom charge injection

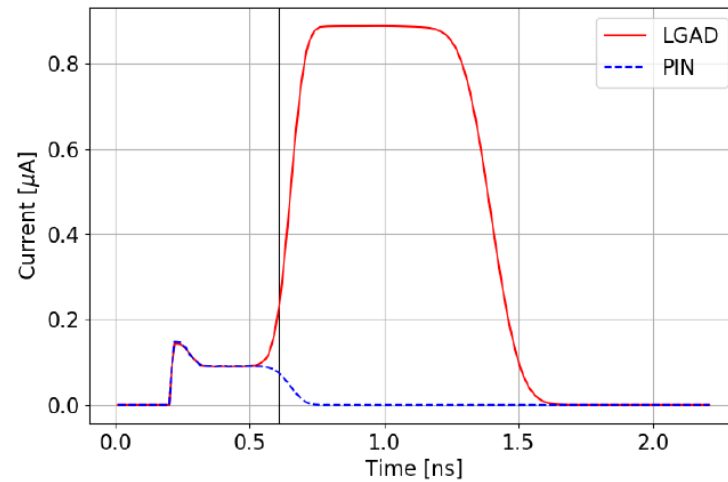
Time 0.61 ns
PIN e^-



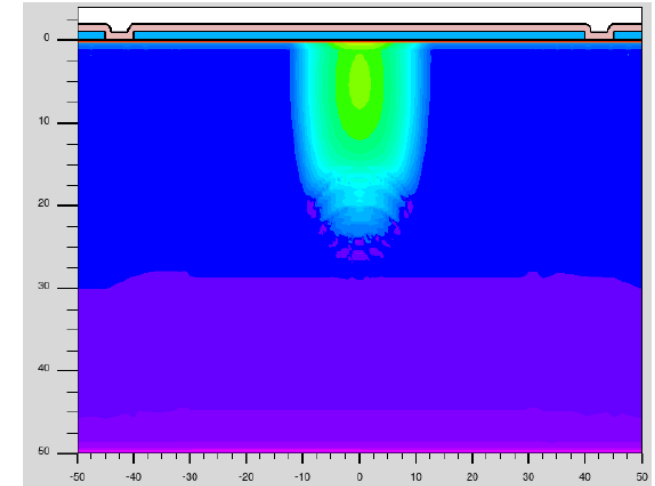
PIN h^+



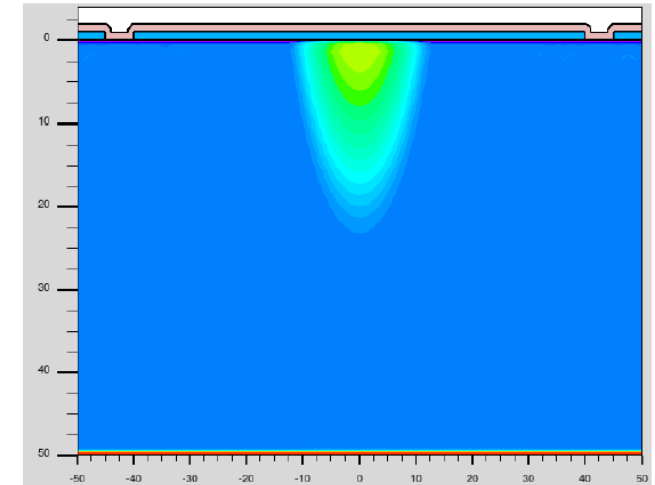
Waveforms



LGAD e^-



LGAD h^+



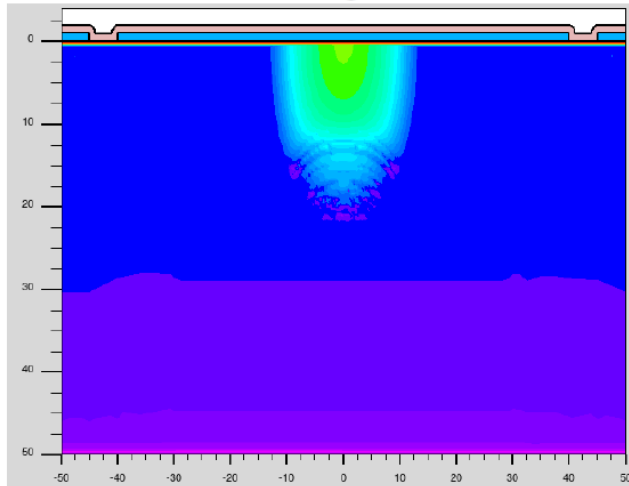
Courtesy: M. Centis Vignali (FBK)

Thin sensor (PIN) vs LGAD

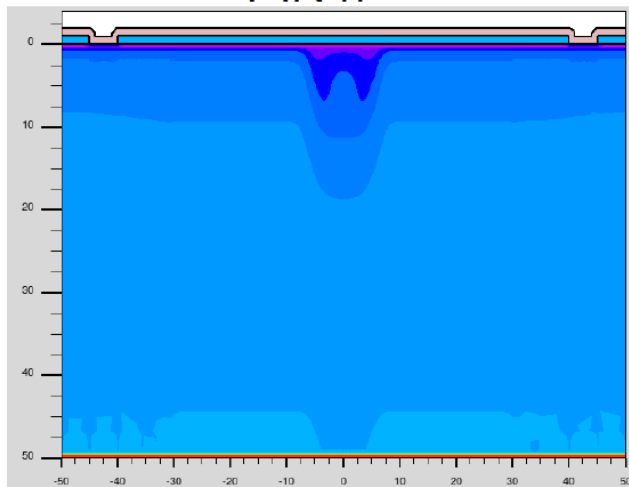
Bottom charge injection

Time 0.66 ns

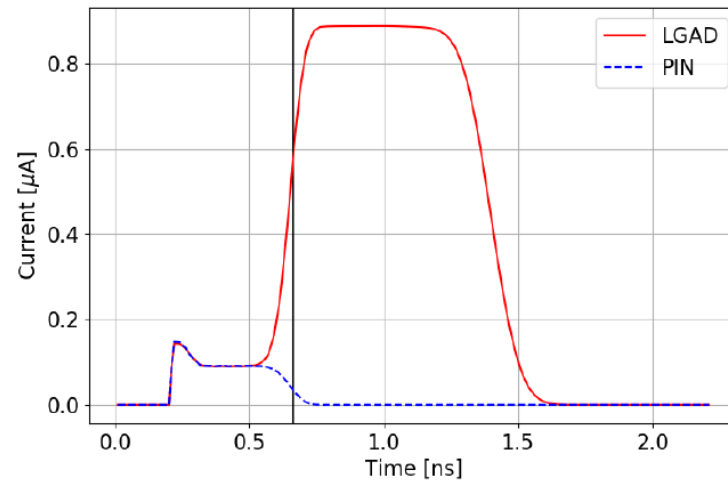
PIN e^-



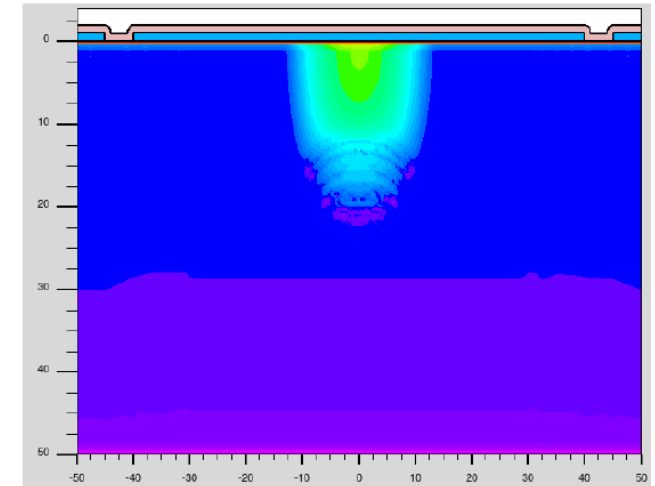
PIN h^+



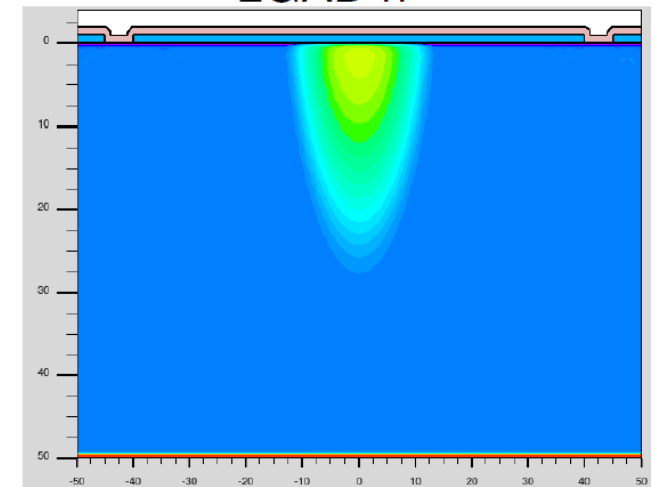
Waveforms



LGAD e^-



LGAD h^+



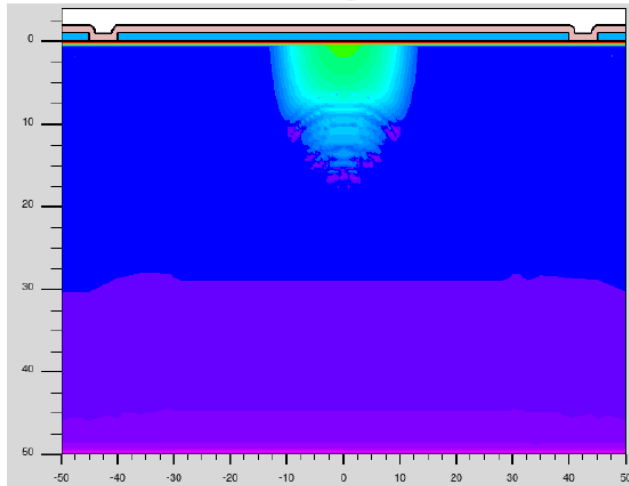
Courtesy: M. Centis Vignali (FBK)

Thin sensor (PIN) vs LGAD

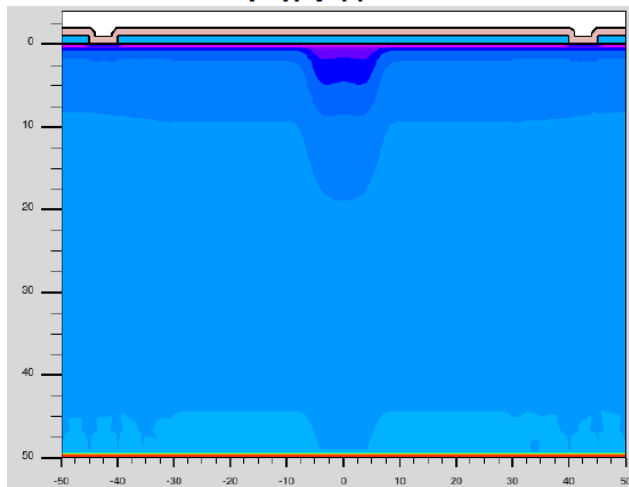
Bottom charge injection

Time 0.71 ns

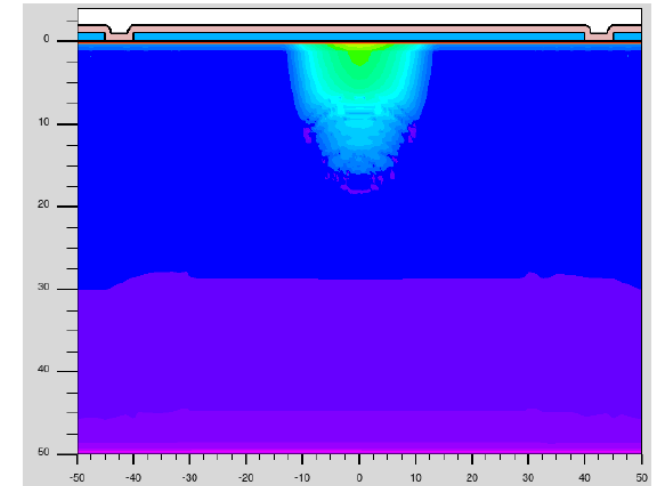
PIN e⁻



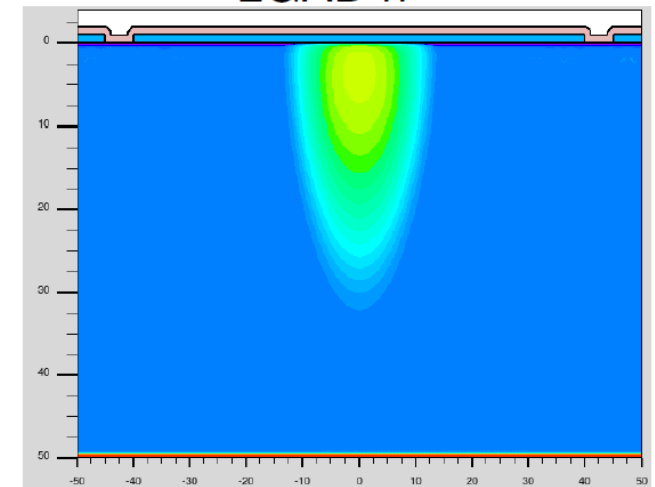
PIN h⁺



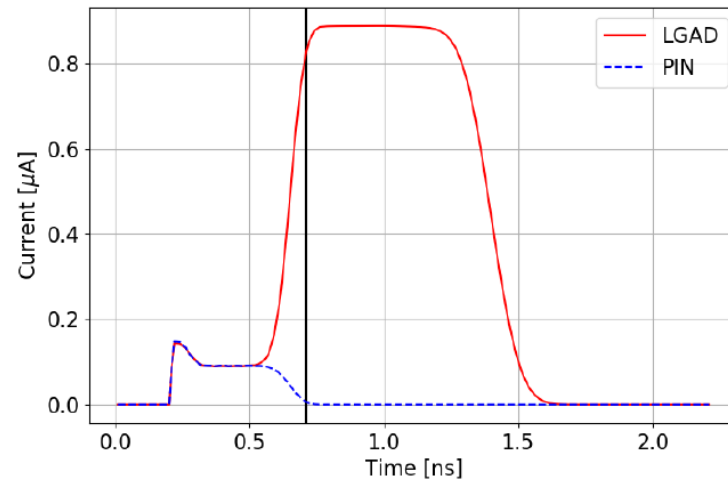
LGAD e⁻



LGAD h⁺



Waveforms



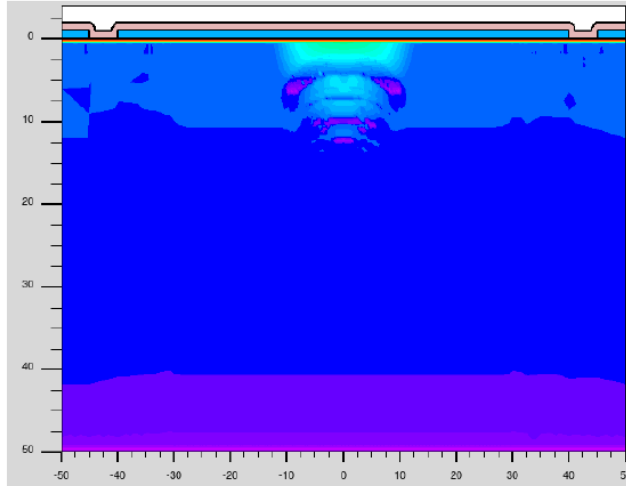
Courtesy: M. Centis Vignali (FBK)

Thin sensor (PIN) vs LGAD

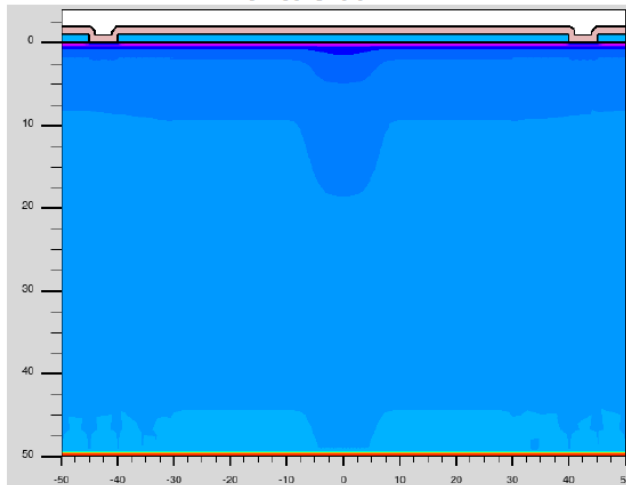
Bottom charge injection

Time 0.76 ns

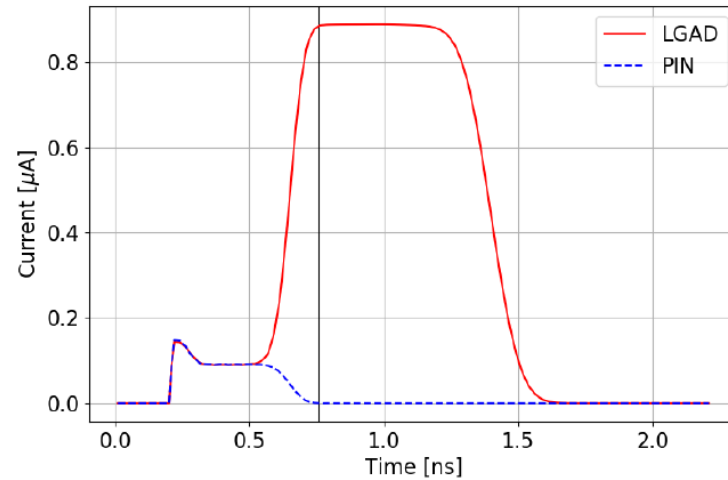
PIN e^-



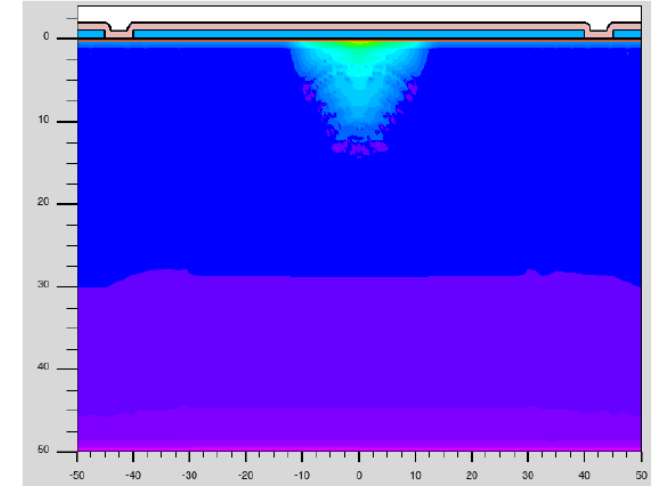
PIN h^+



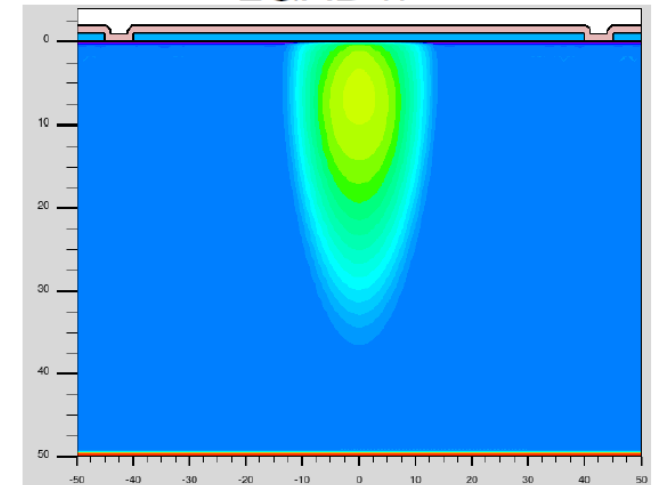
Waveforms



LGAD e^-



LGAD h^+

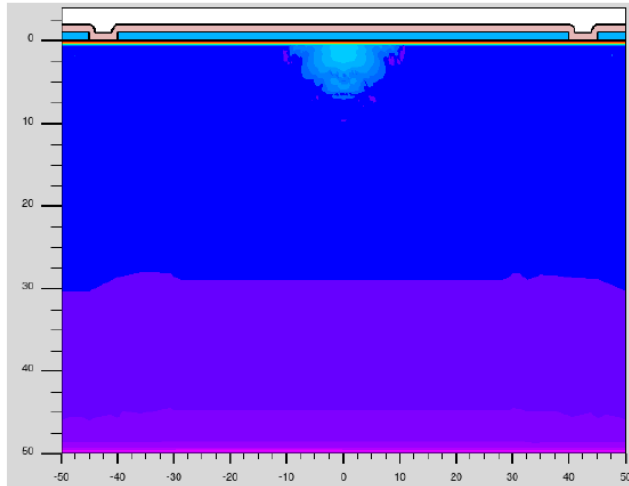


Courtesy: M. Centis Vignali (FBK)

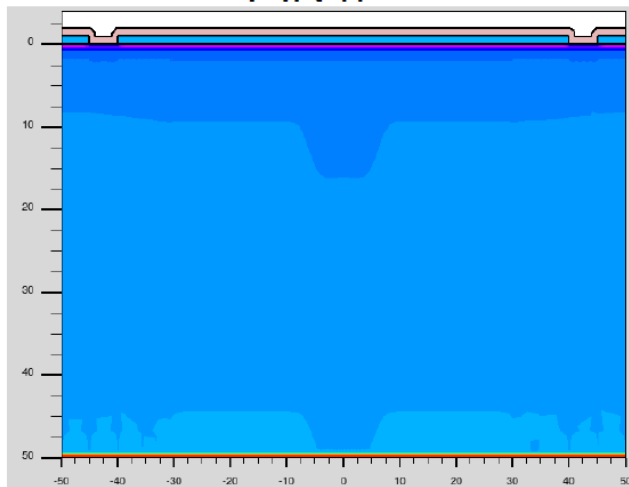
Thin sensor (PIN) vs LGAD

Bottom charge injection

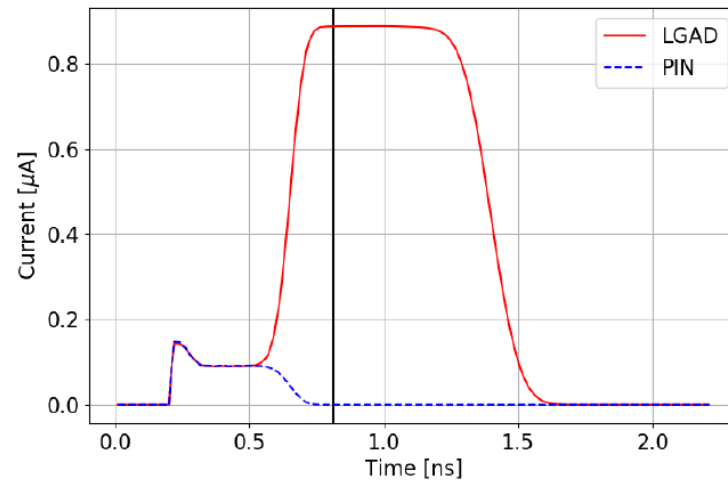
Time 0.81 ns
PIN e^-



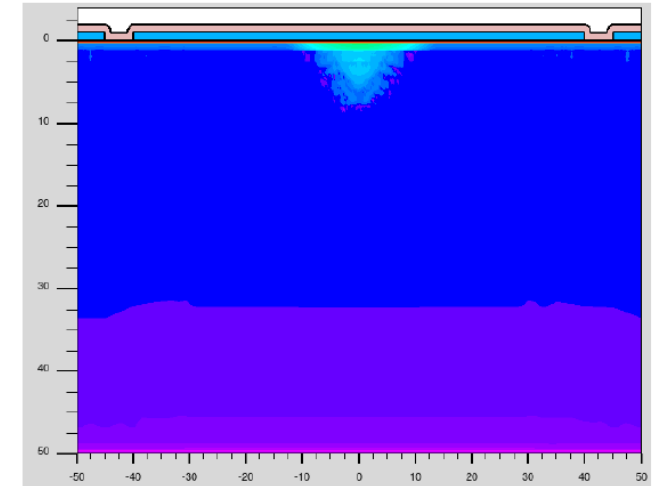
PIN h^+



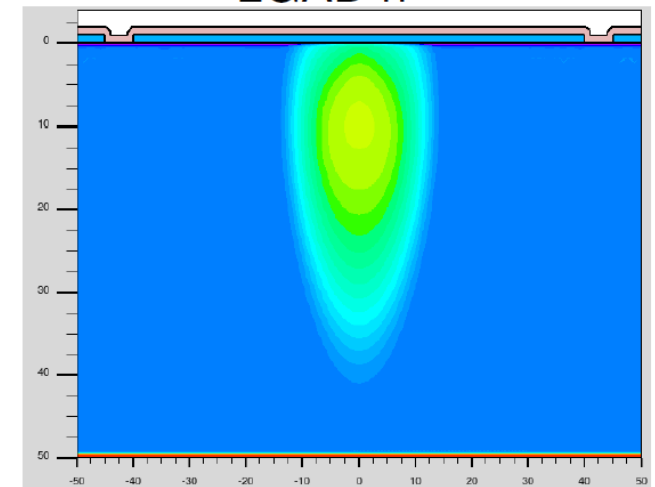
Waveforms



LGAD e^-



LGAD h^+



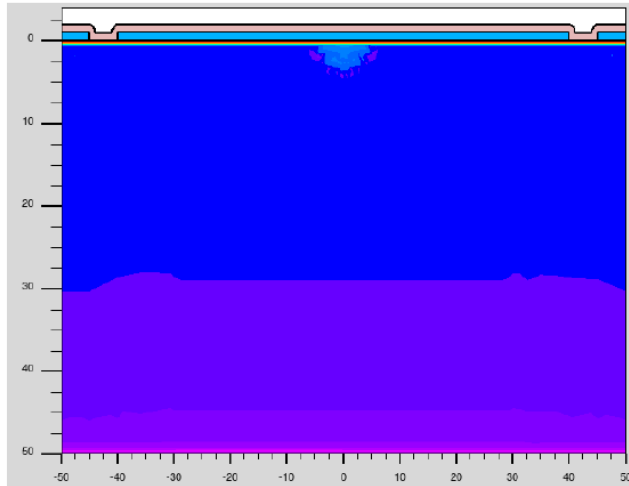
Courtesy: M. Centis Vignali (FBK)

Thin sensor (PIN) vs LGAD

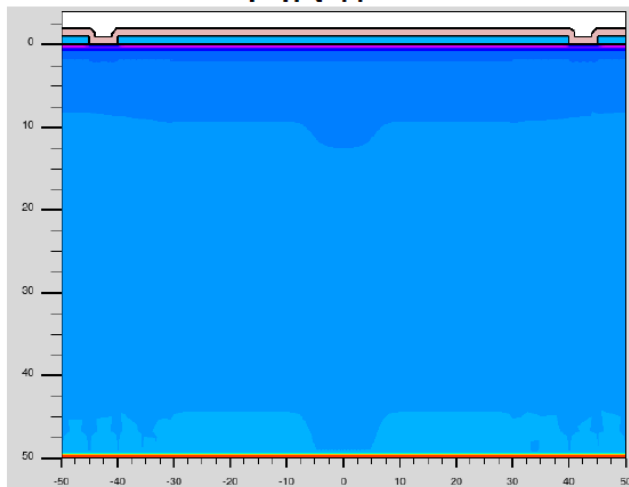
Bottom charge injection

Time 0.86 ns

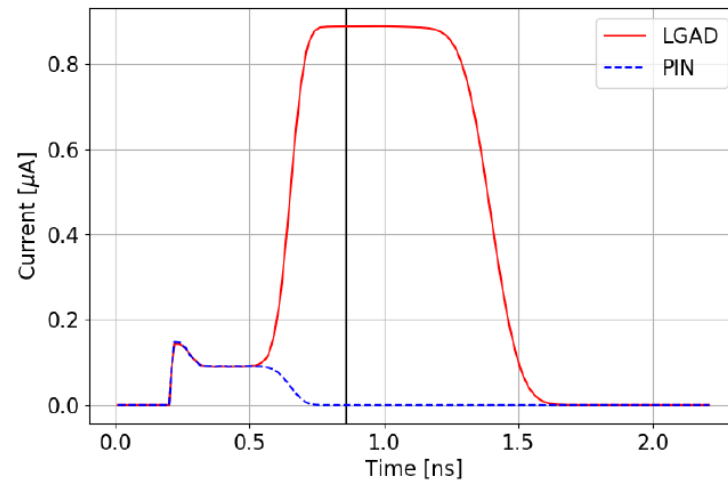
PIN e^-



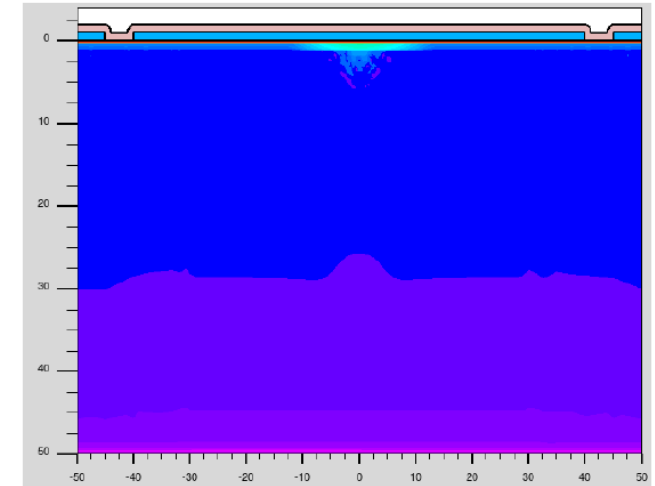
PIN h^+



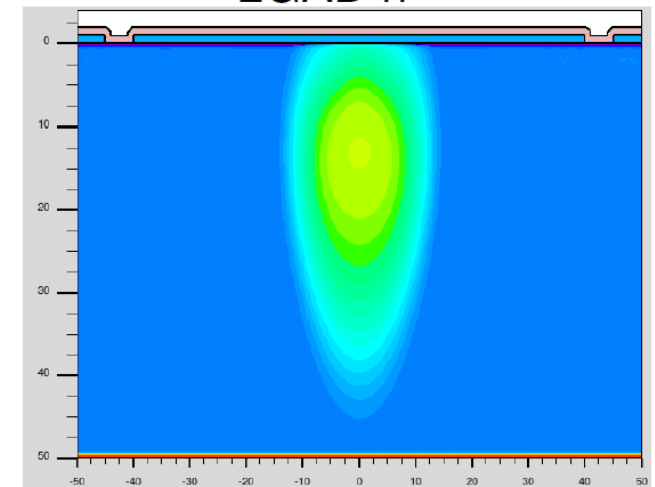
Waveforms



LGAD e^-



LGAD h^+

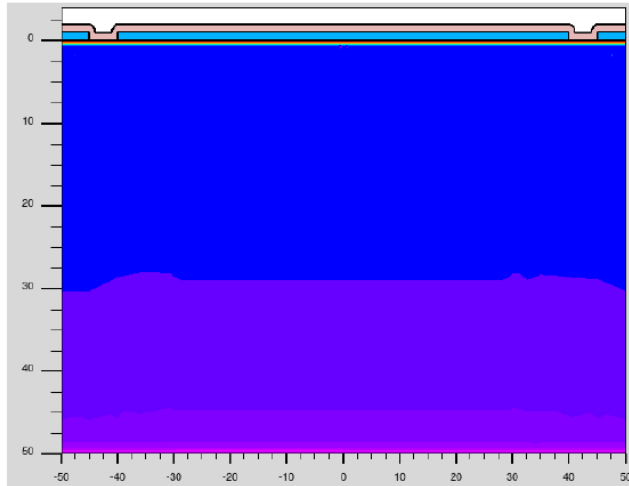


Courtesy: M. Centis Vignali (FBK)

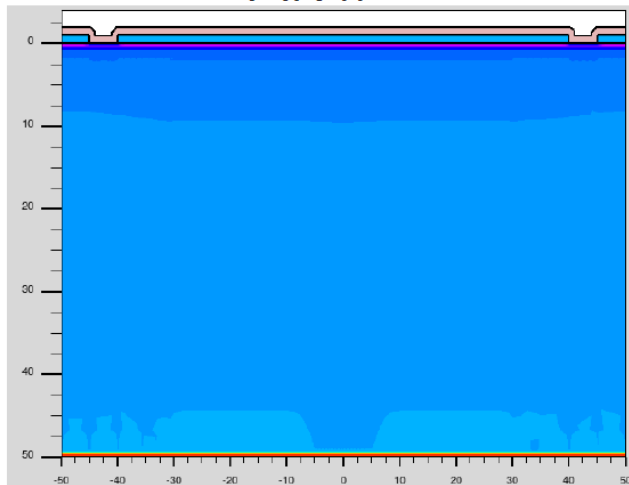
Thin sensor (PIN) vs LGAD

Bottom charge injection

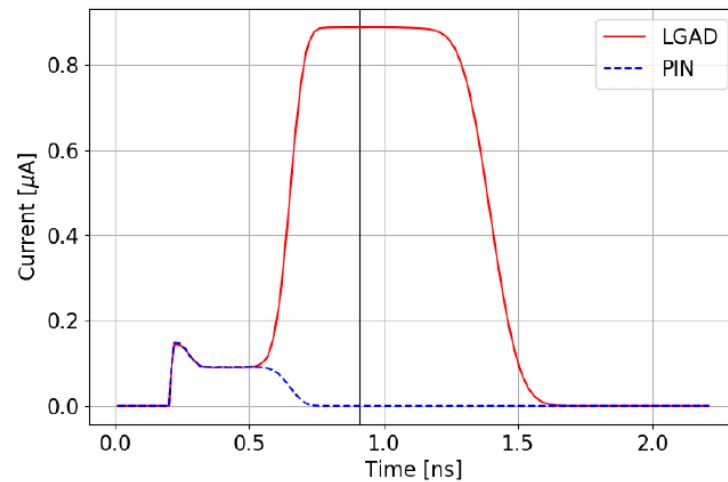
Time 0.91 ns
PIN e^-



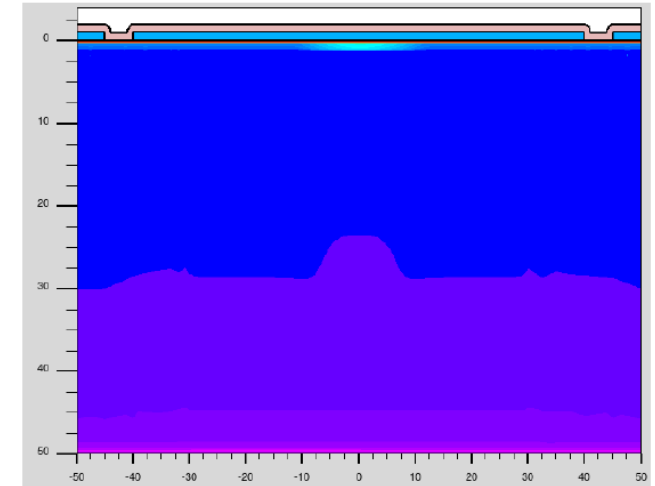
PIN h^+



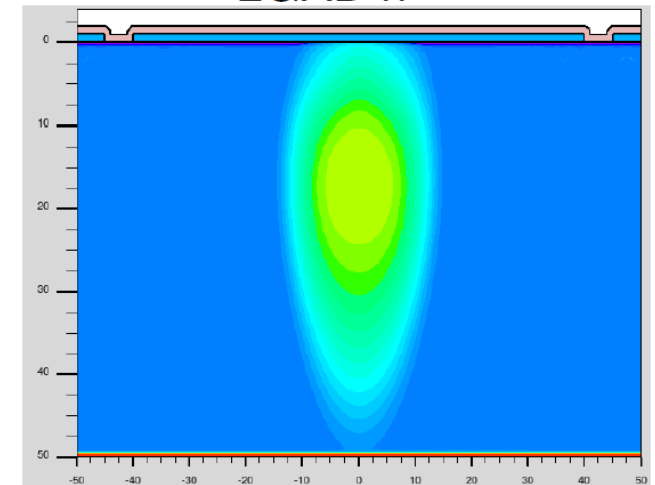
Waveforms



LGAD e^-



LGAD h^+

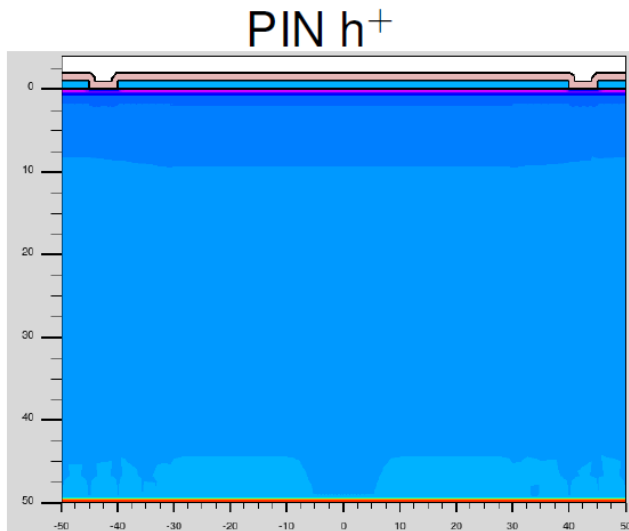
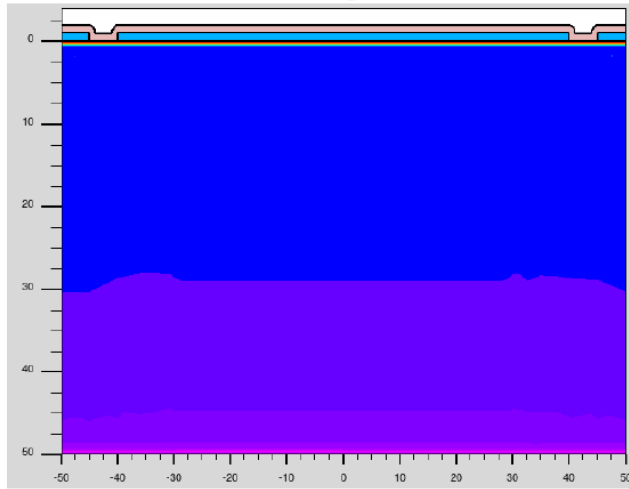


Courtesy: M. Centis Vignali (FBK)

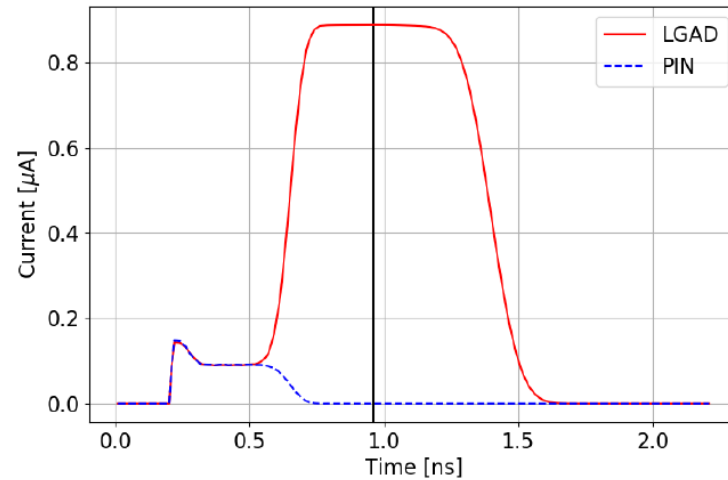
Thin sensor (PIN) vs LGAD

Bottom charge injection

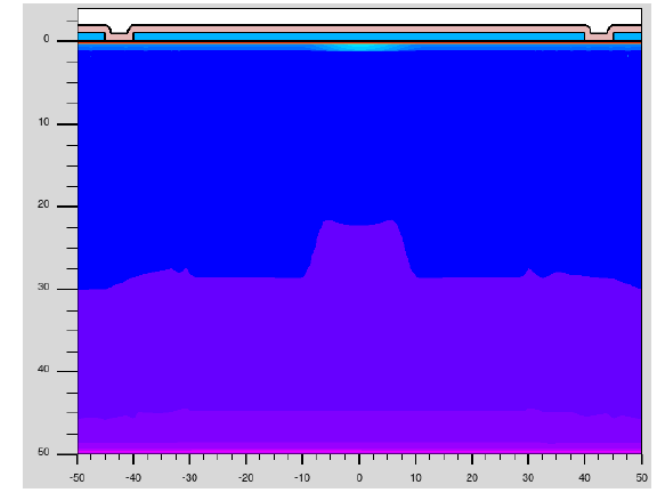
Time 0.96 ns
PIN e^-



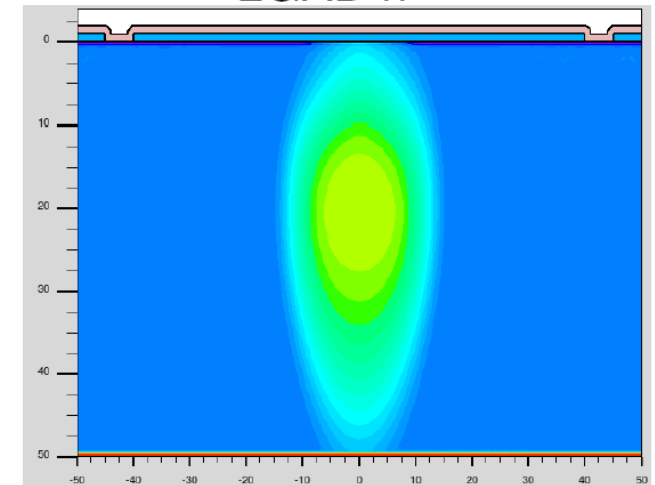
Waveforms



LGAD e^-



LGAD h^+

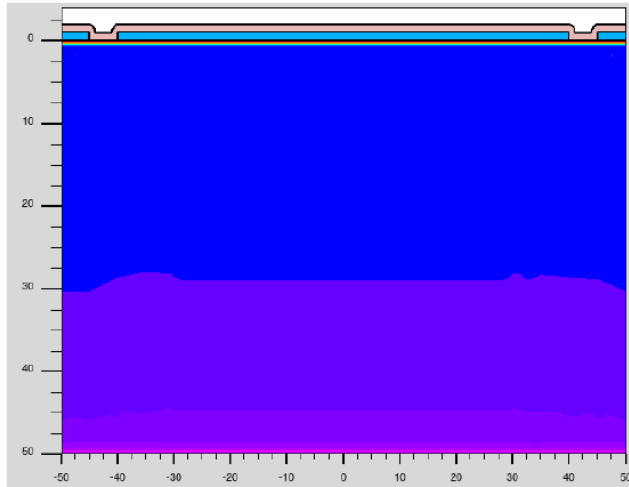


Courtesy: M. Centis Vignali (FBK)

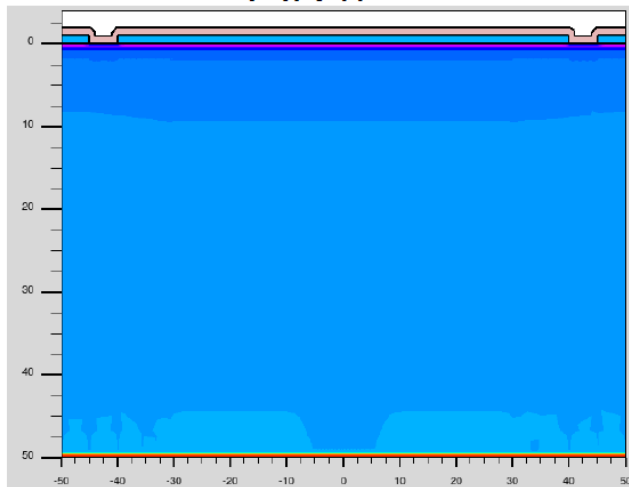
Thin sensor (PIN) vs LGAD

Bottom charge injection

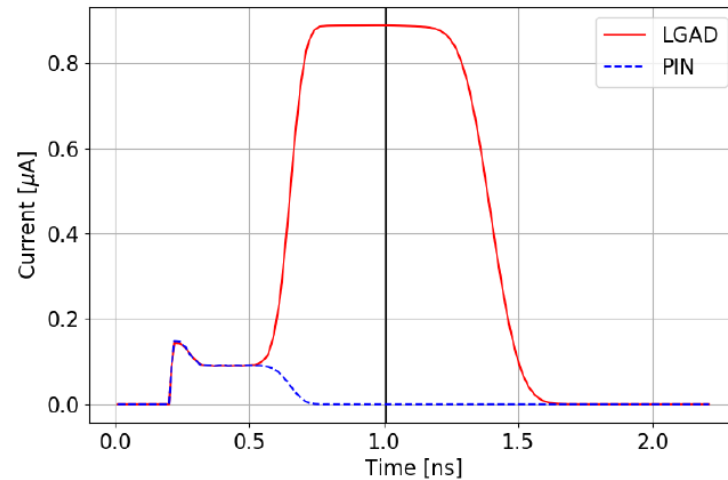
Time 1.01 ns
PIN e^-



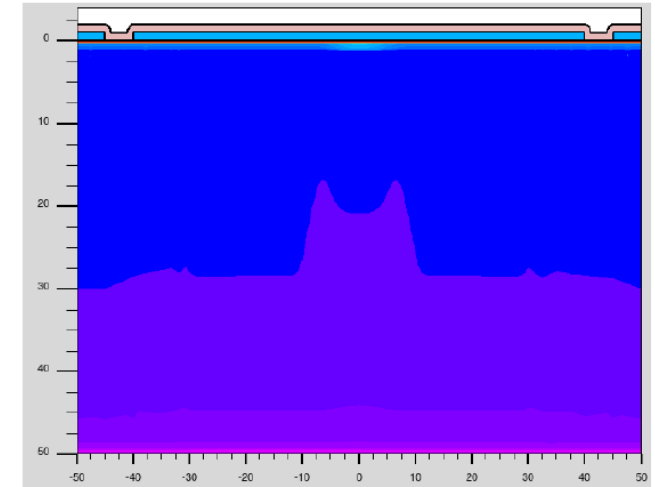
PIN h^+



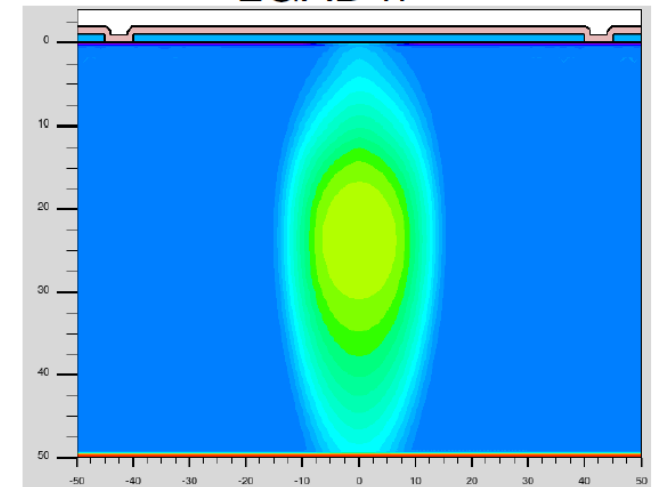
Waveforms



LGAD e^-



LGAD h^+

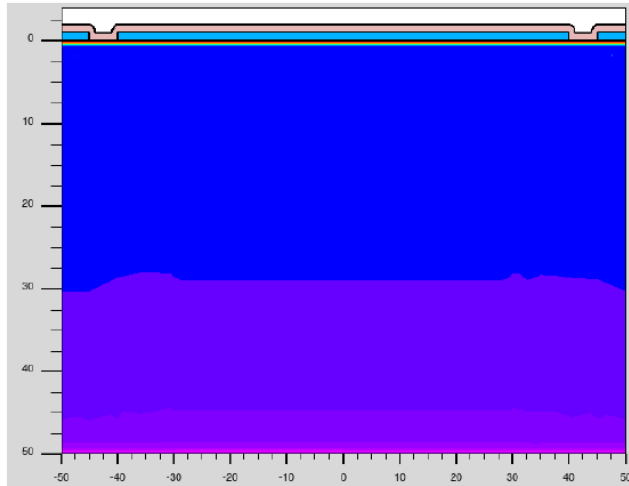


Courtesy: M. Centis Vignali (FBK)

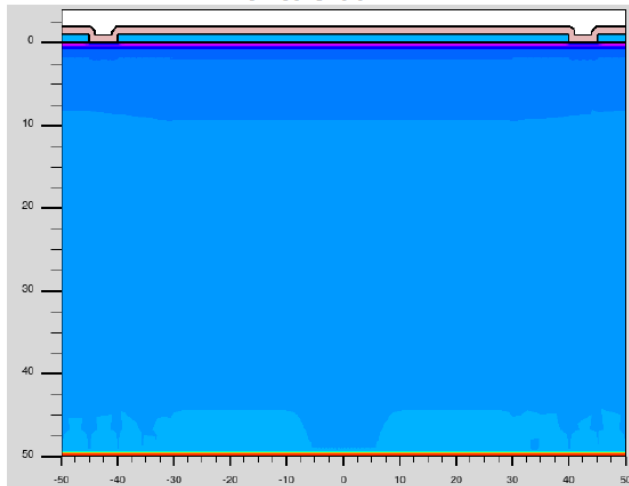
Thin sensor (PIN) vs LGAD

Bottom charge injection

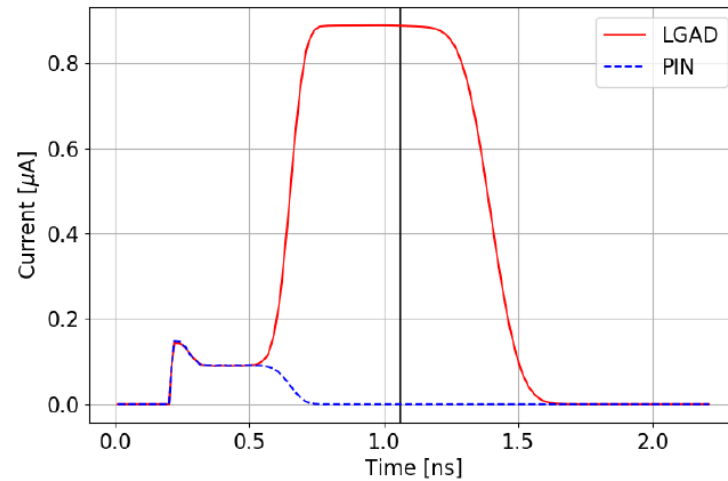
Time 1.06 ns
PIN e^-



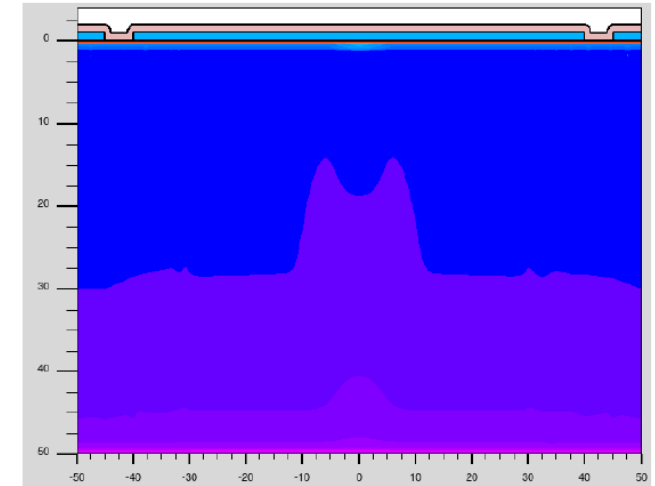
PIN h^+



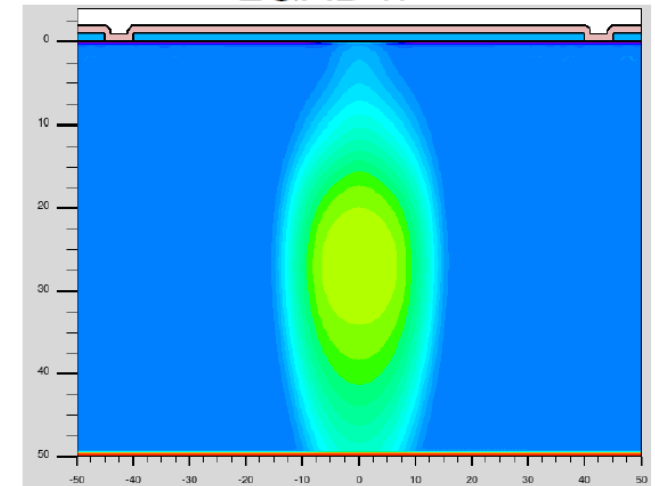
Waveforms



LGAD e^-



LGAD h^+



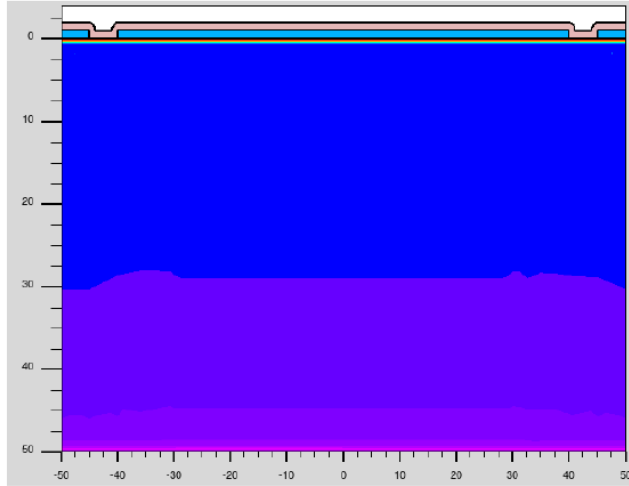
Courtesy: M. Centis Vignali (FBK)

Thin sensor (PIN) vs LGAD

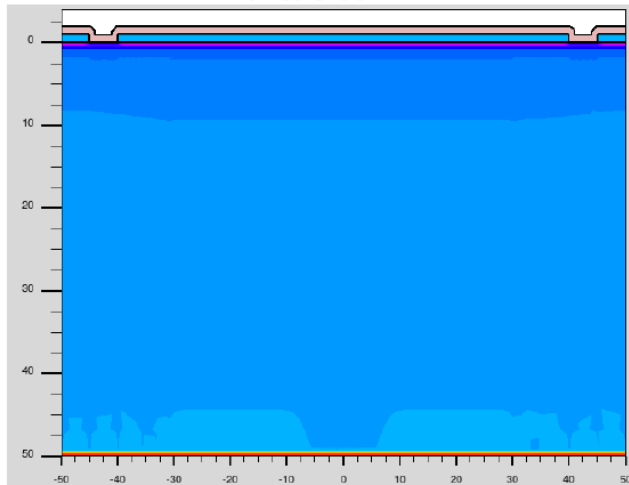
Bottom charge injection

Time 1.11 ns

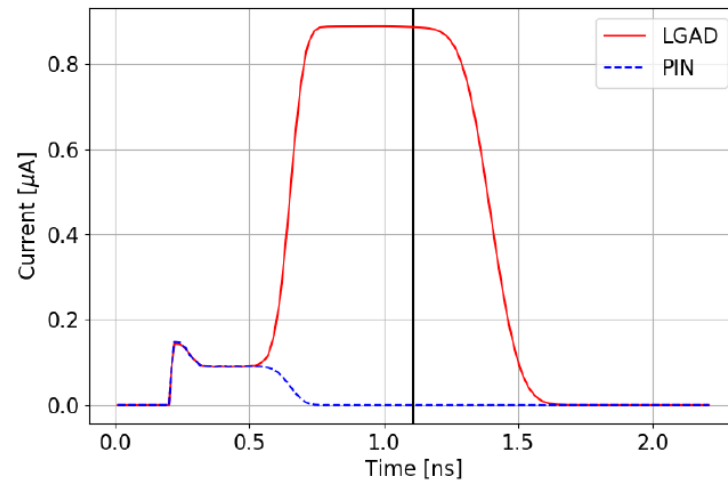
PIN e⁻



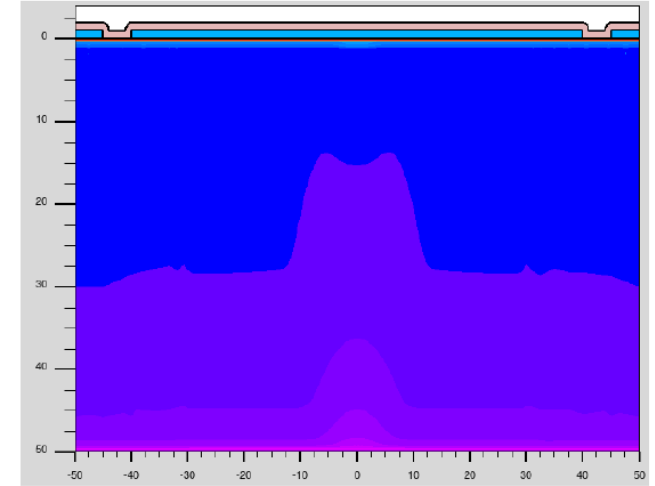
PIN h⁺



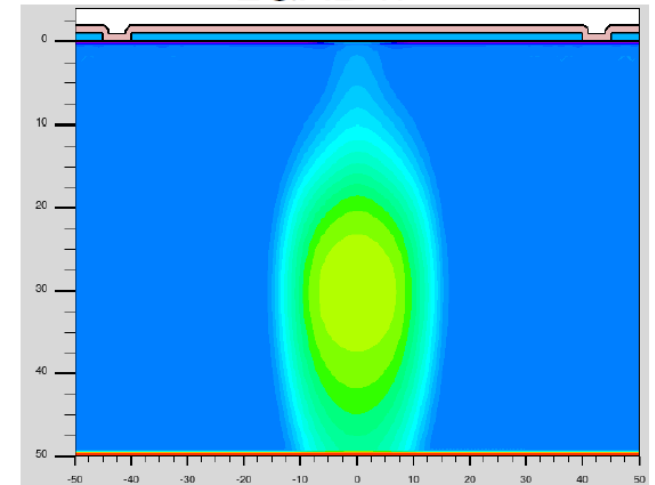
Waveforms



LGAD e⁻



LGAD h⁺



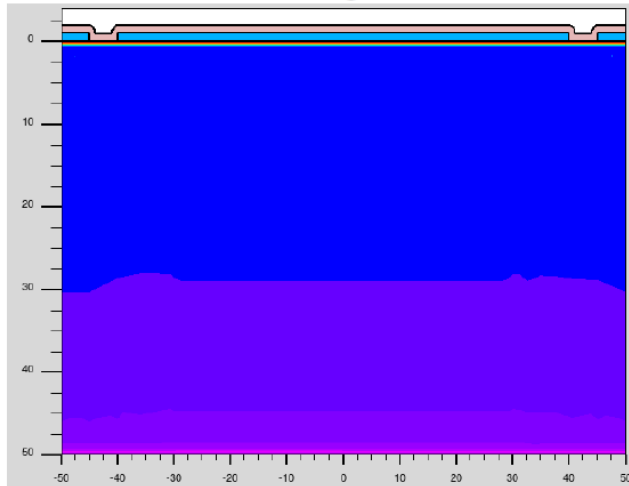
Courtesy: M. Centis Vignali (FBK)

Thin sensor (PIN) vs LGAD

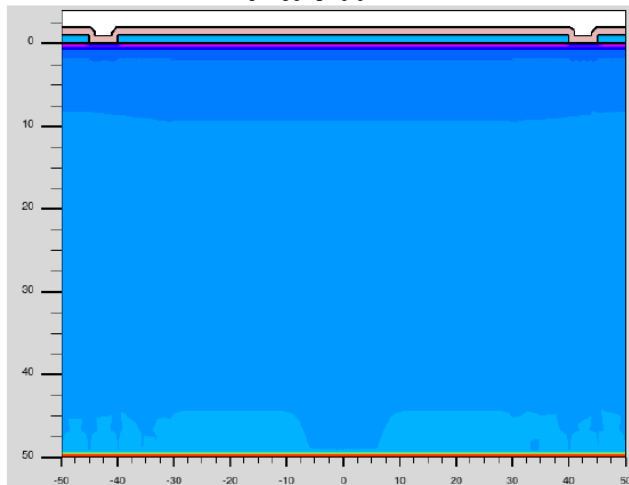
Bottom charge injection

Time 1.16 ns

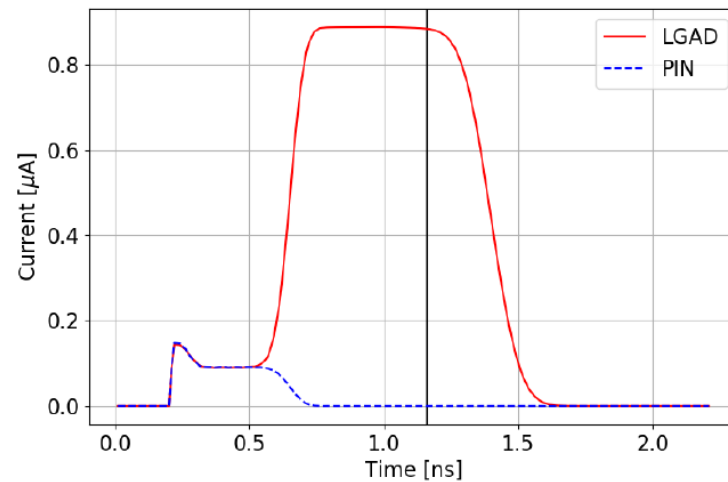
PIN e^-



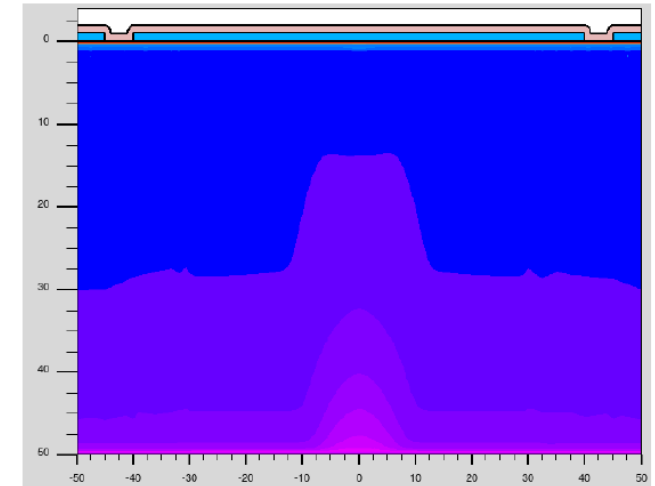
PIN h^+



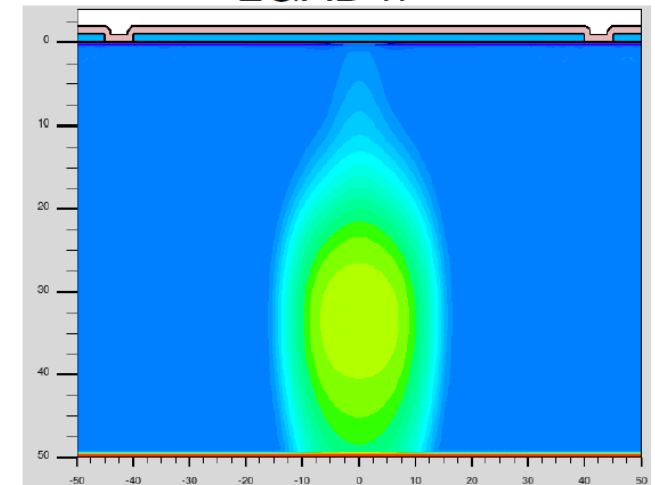
Waveforms



LGAD e^-



LGAD h^+

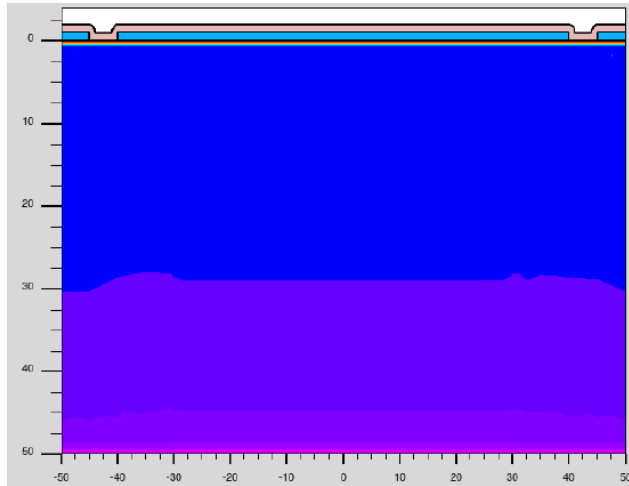


Courtesy: M. Centis Vignali (FBK)

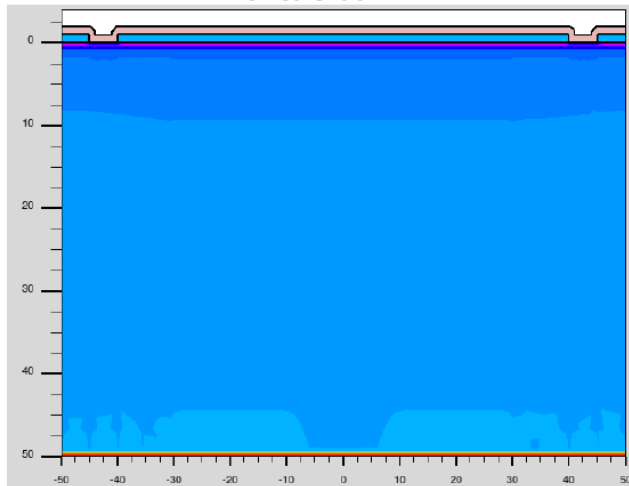
Thin sensor (PIN) vs LGAD

Bottom charge injection

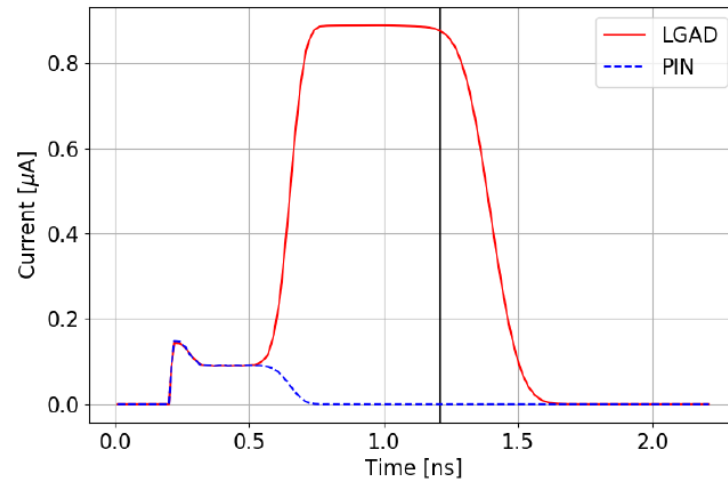
Time 1.21 ns
PIN e^-



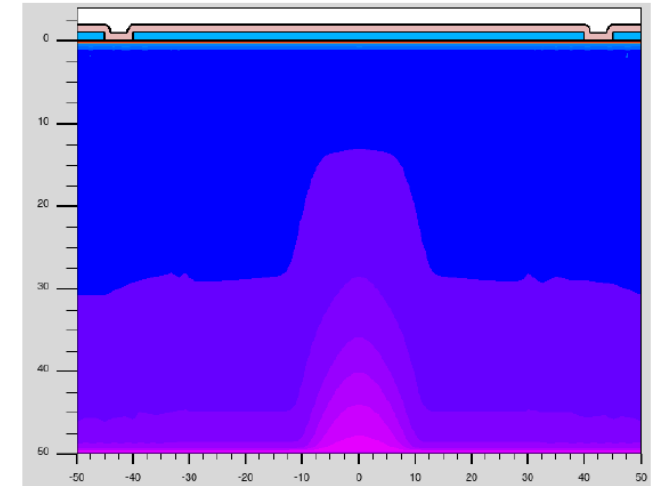
PIN h^+



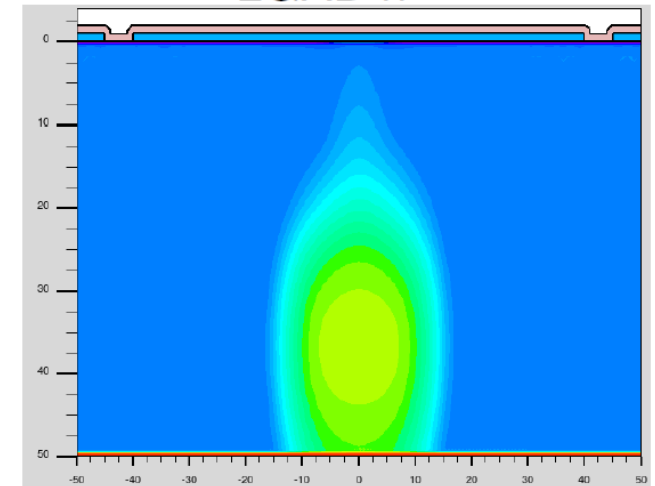
Waveforms



LGAD e^-



LGAD h^+



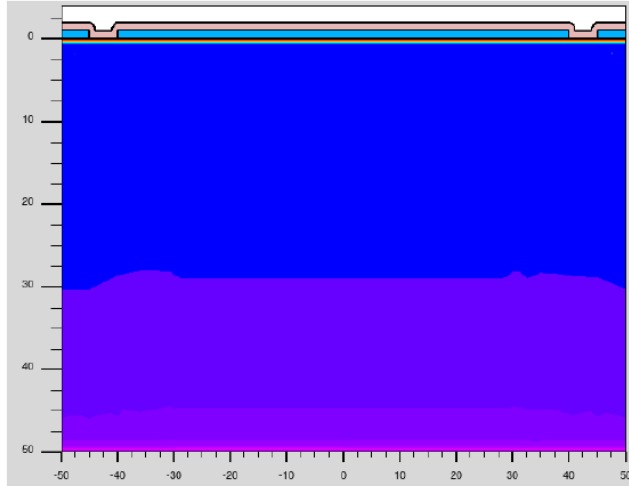
Courtesy: M. Centis Vignali (FBK)

Thin sensor (PIN) vs LGAD

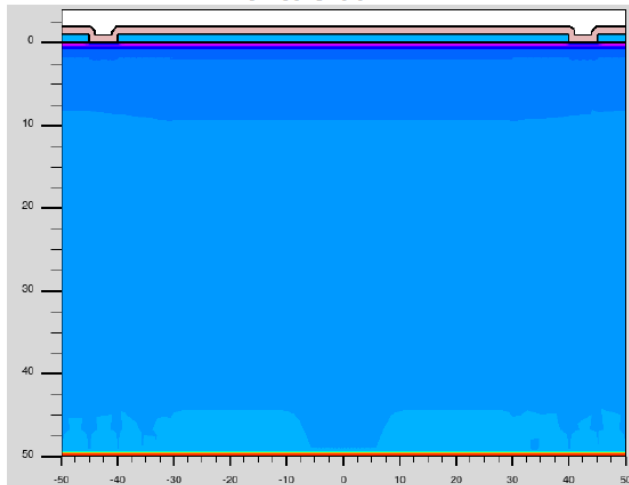
Bottom charge injection

Time 1.26 ns

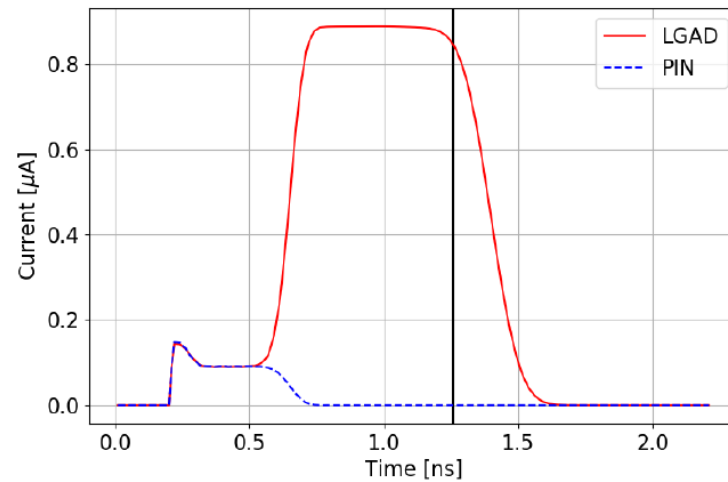
PIN e^-



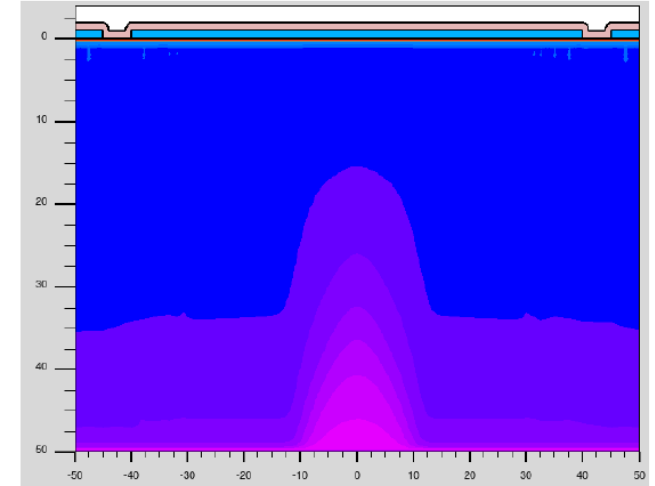
PIN h^+



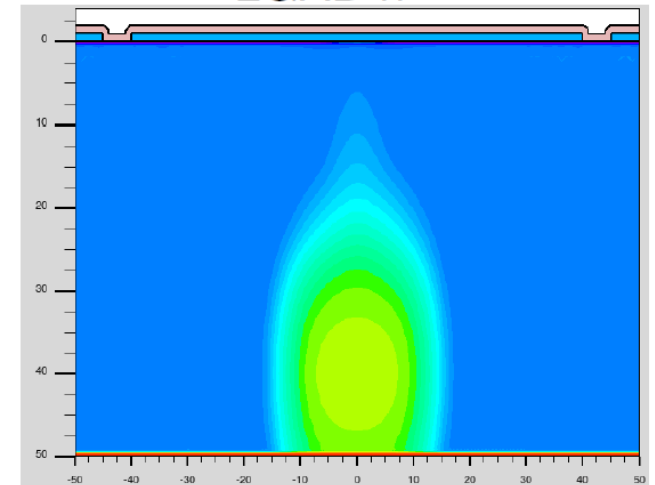
Waveforms



LGAD e^-



LGAD h^+

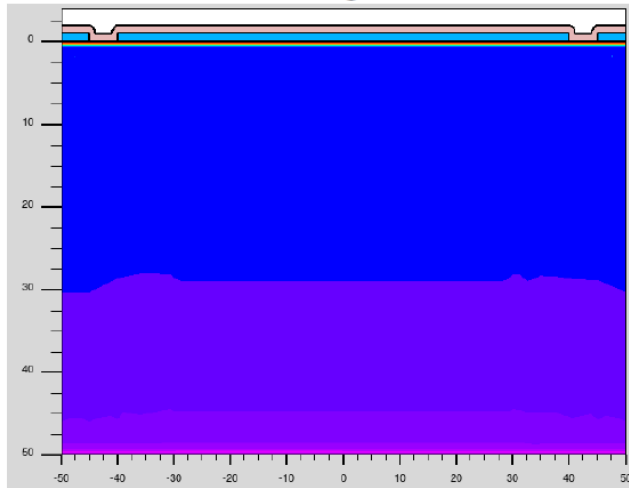


Courtesy: M. Centis Vignali (FBK)

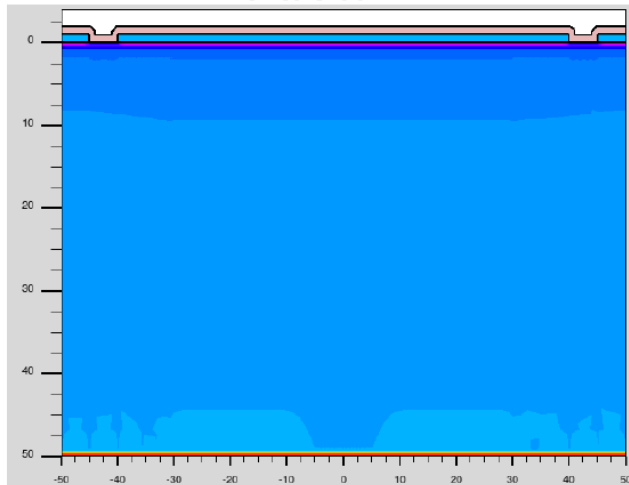
Thin sensor (PIN) vs LGAD

Bottom charge injection

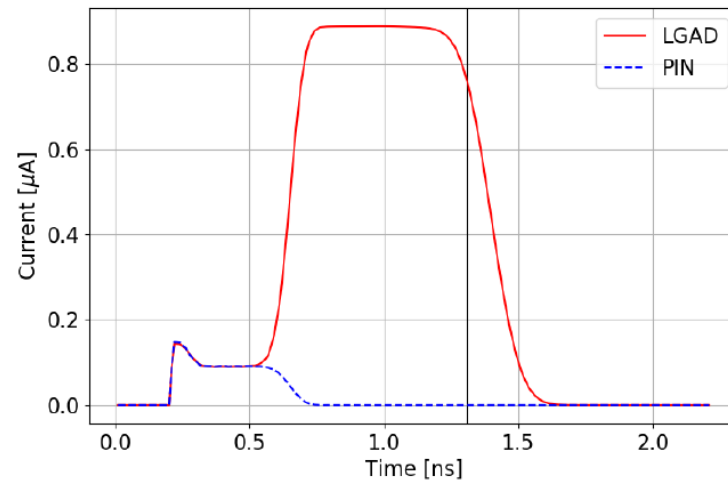
Time 1.31 ns
PIN e^-



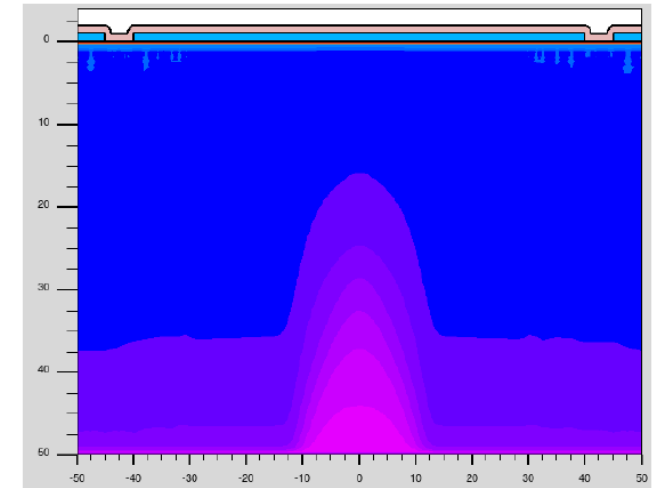
PIN h^+



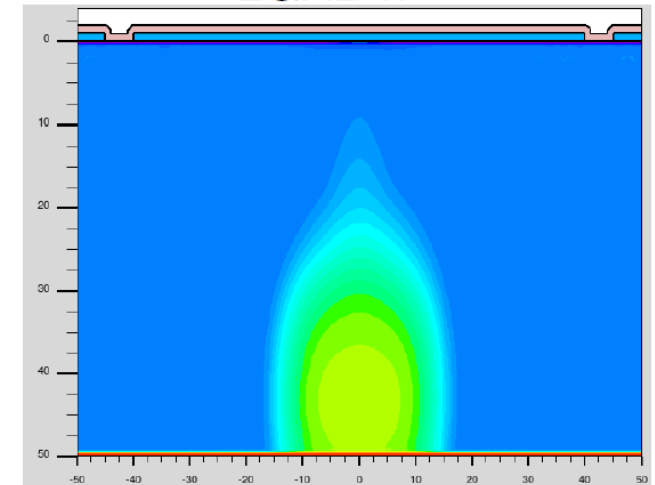
Waveforms



LGAD e^-



LGAD h^+



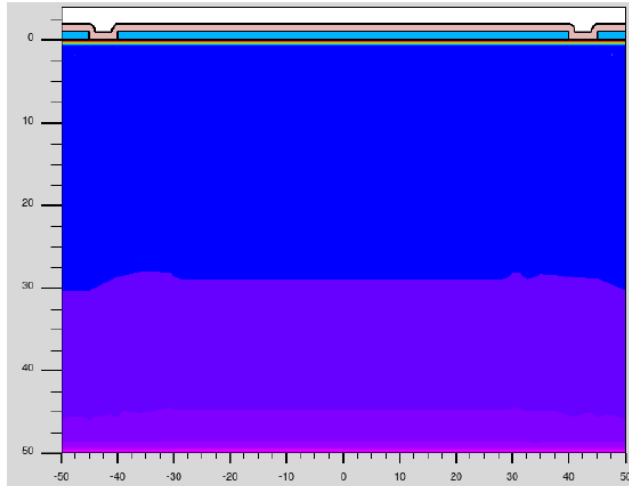
Courtesy: M. Centis Vignali (FBK)

Thin sensor (PIN) vs LGAD

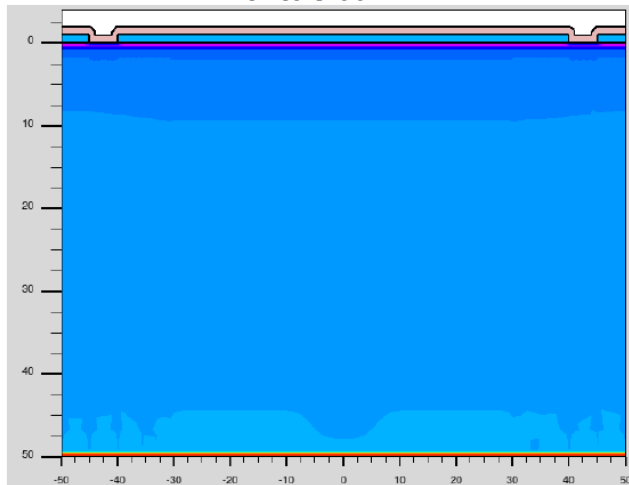
Bottom charge injection

Time 1.36 ns

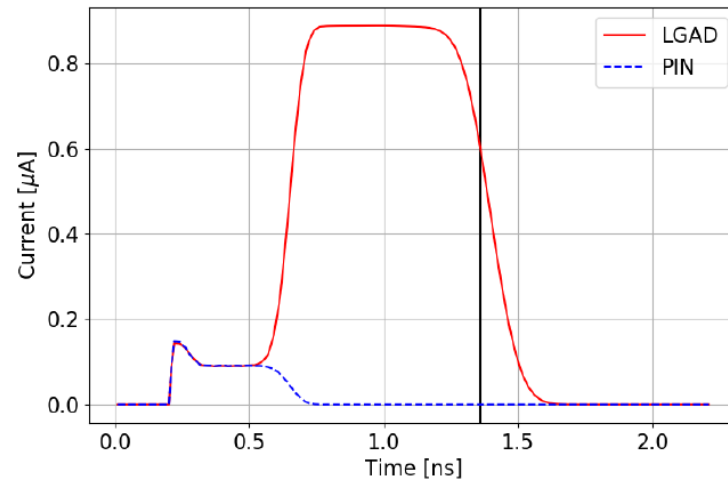
PIN e⁻



PIN h⁺

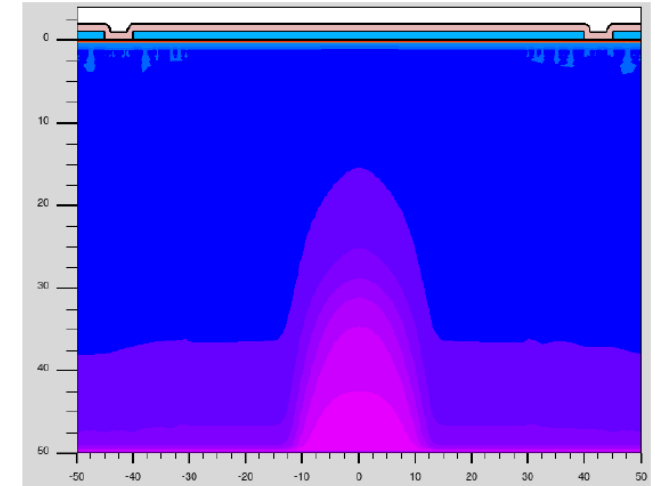


Waveforms

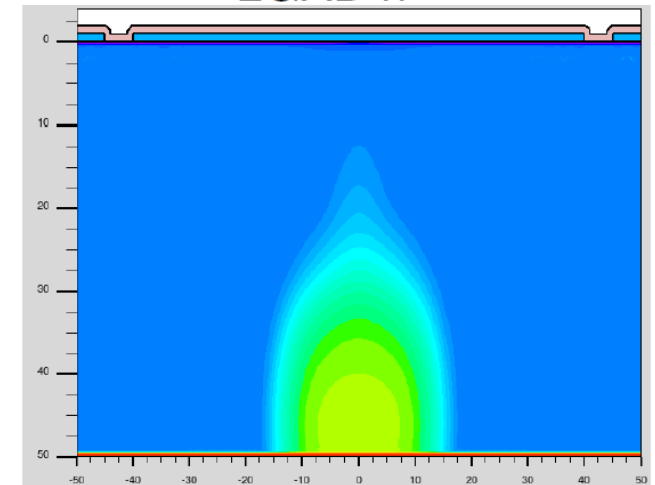


Courtesy: M. Centis Vignali (FBK)

LGAD e⁻



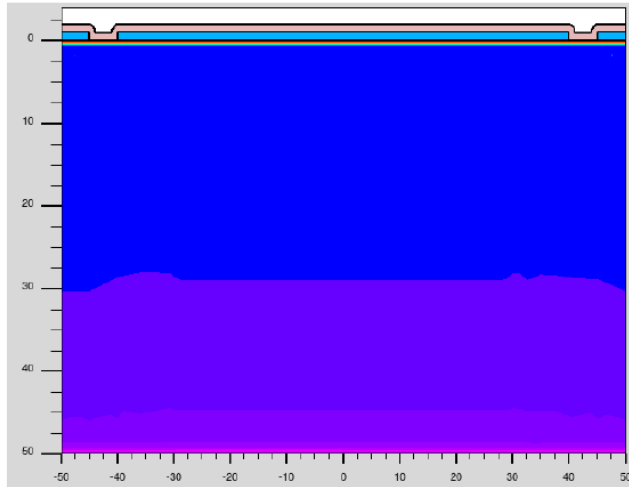
LGAD h⁺



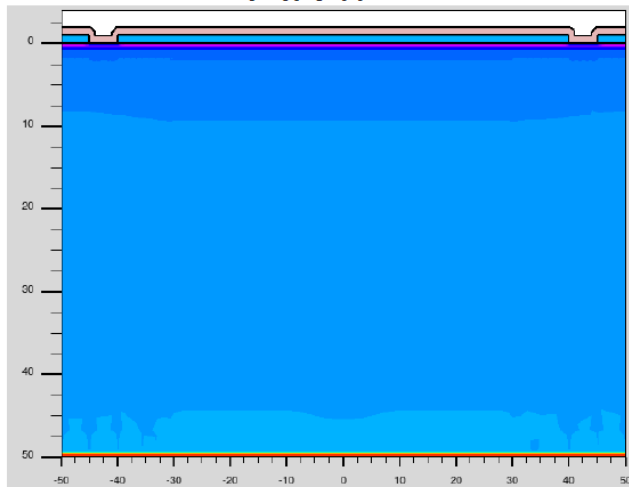
Thin sensor (PIN) vs LGAD

Bottom charge injection

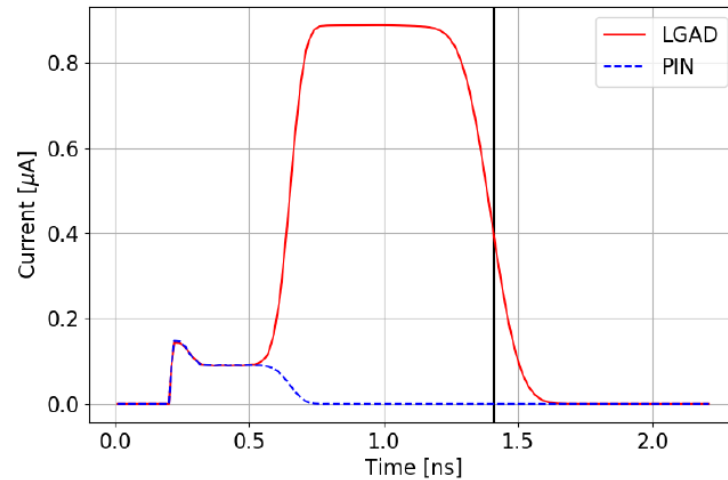
Time 1.41 ns
PIN e^-



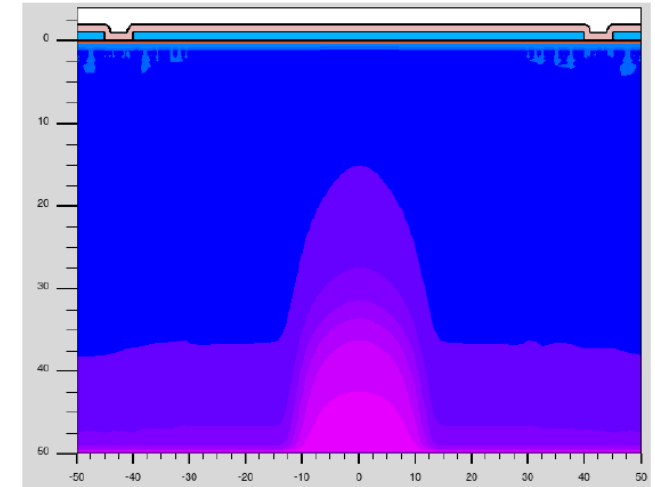
PIN h^+



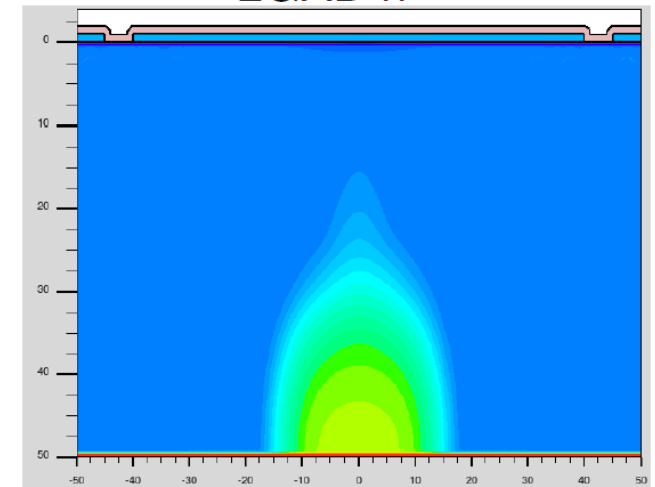
Waveforms



LGAD e^-



LGAD h^+

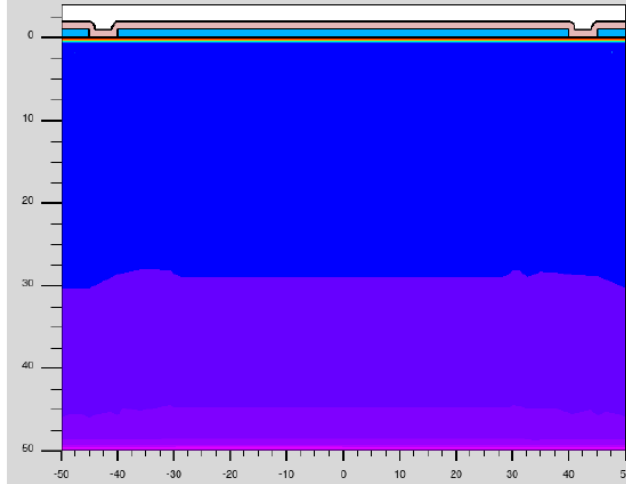


Courtesy: M. Centis Vignali (FBK)

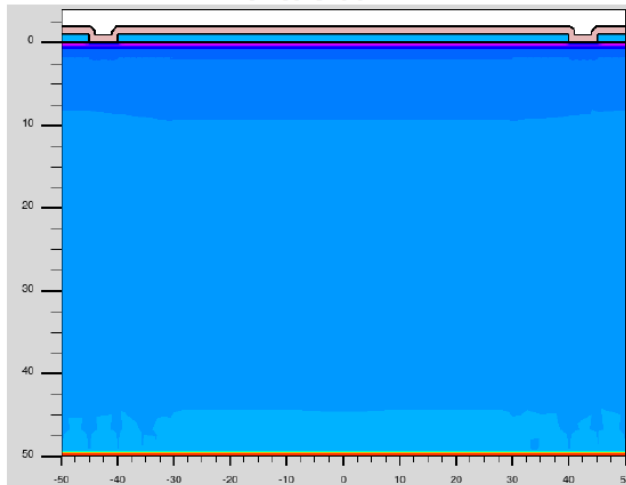
Thin sensor (PIN) vs LGAD

Bottom charge injection

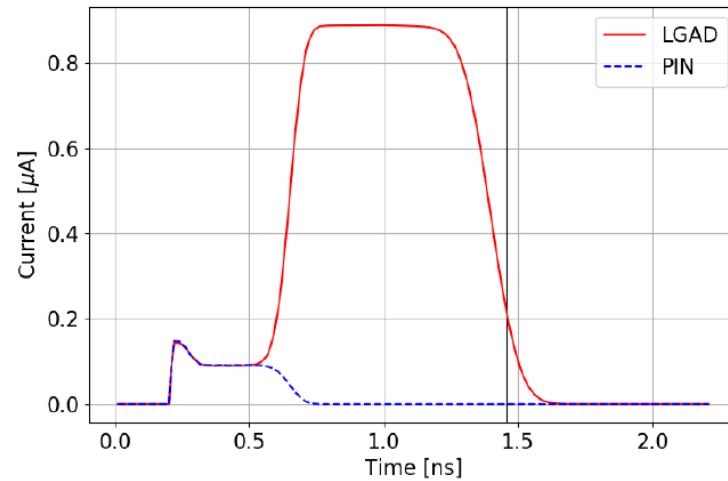
Time 1.46 ns
PIN e^-



PIN h^+

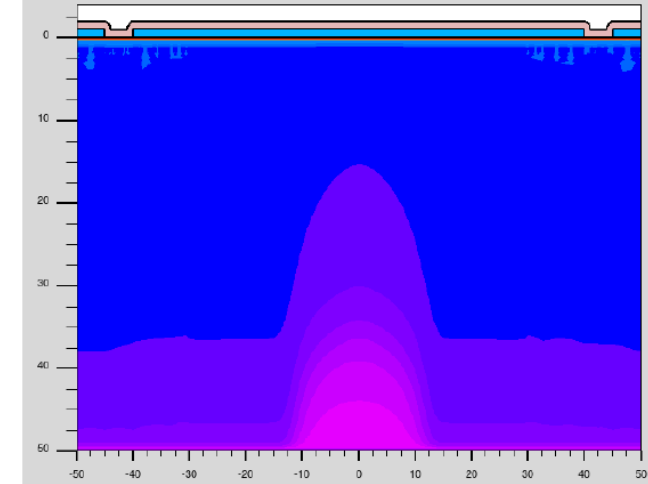


Waveforms

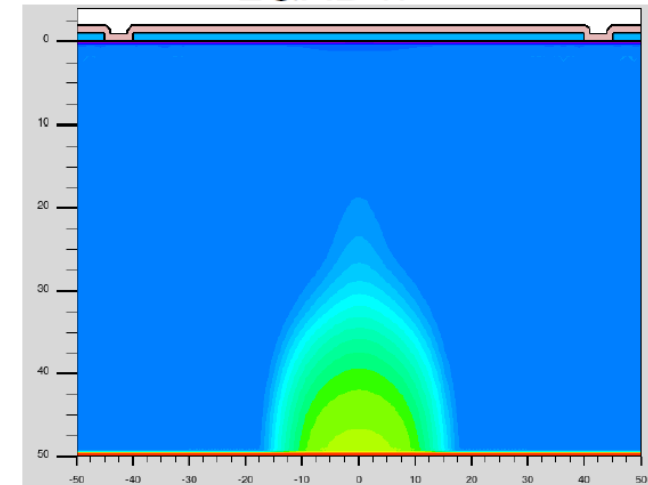


Courtesy: M. Centis Vignali (FBK)

LGAD e^-



LGAD h^+

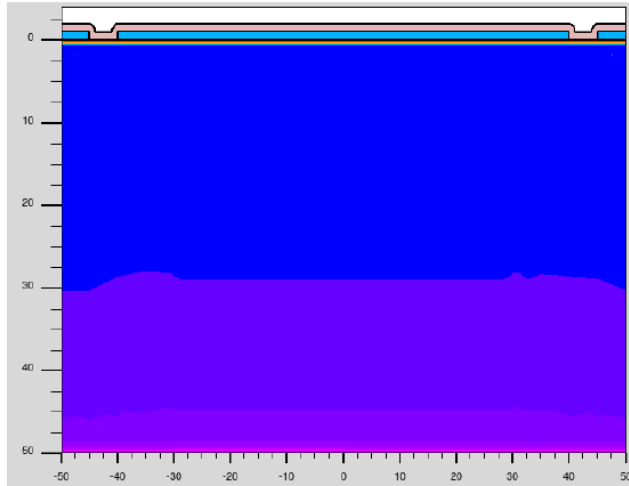


Thin sensor (PIN) vs LGAD

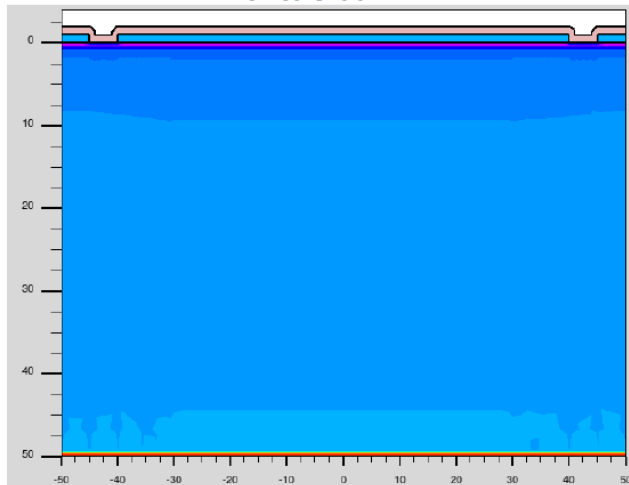
Bottom charge injection

Time 1.51 ns

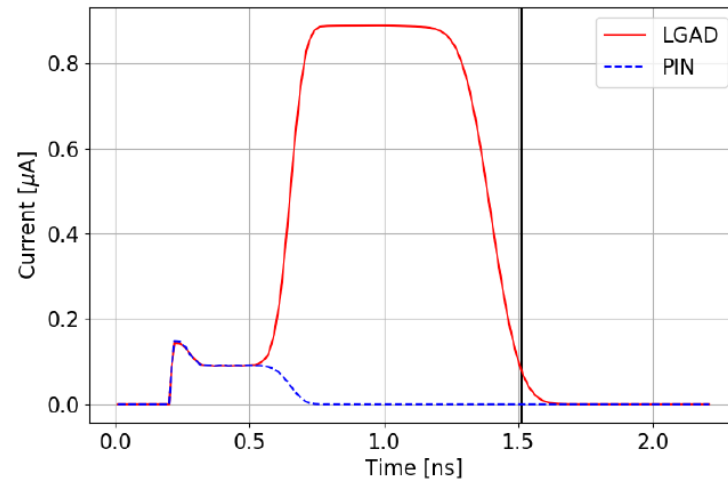
PIN e⁻



PIN h⁺

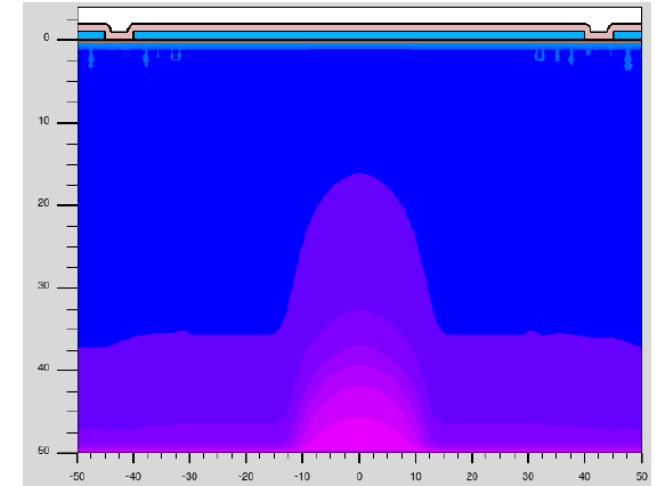


Waveforms

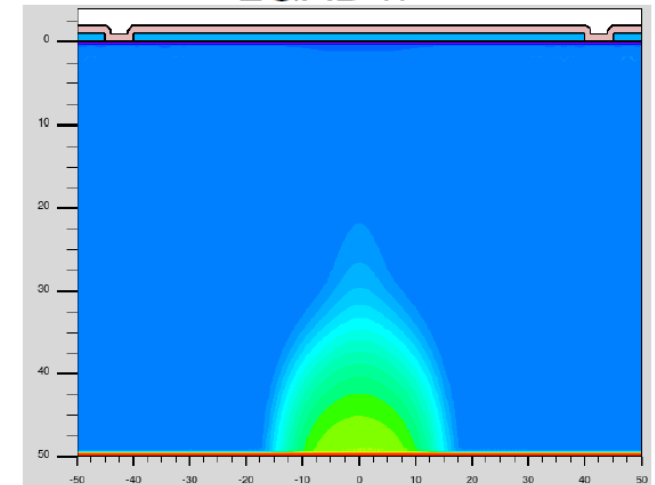


Courtesy: M. Centis Vignali (FBK)

LGAD e⁻



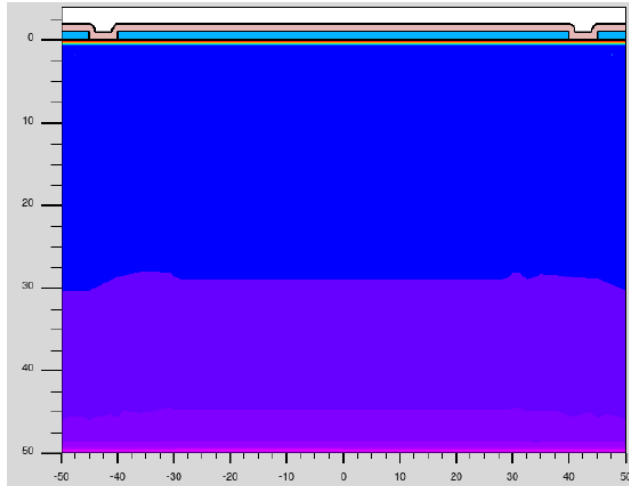
LGAD h⁺



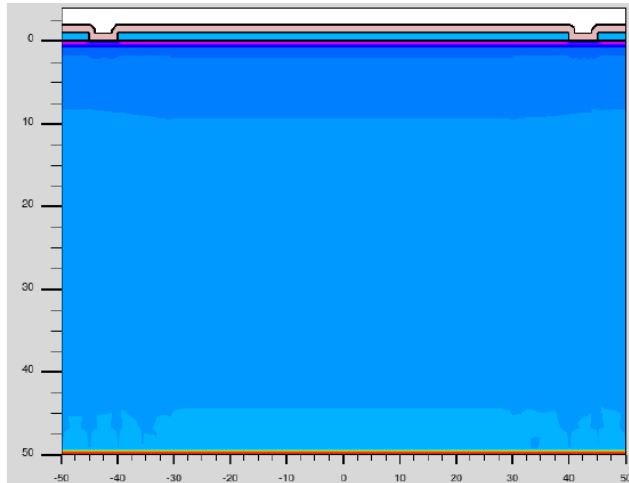
Thin sensor (PIN) vs LGAD

Bottom charge injection

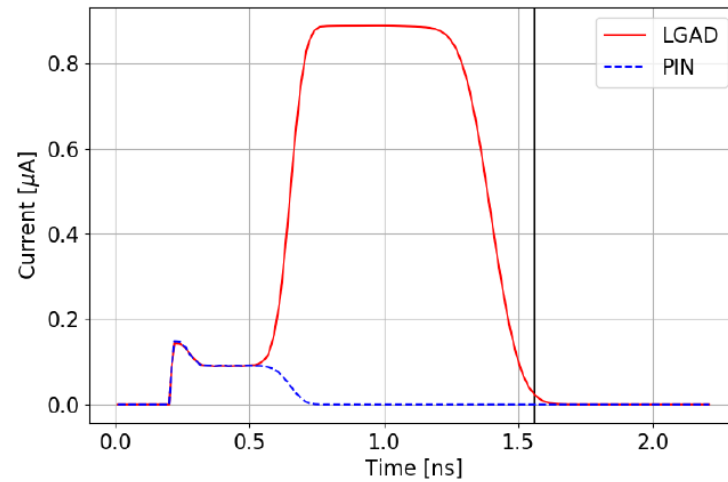
Time 1.56 ns
PIN e⁻



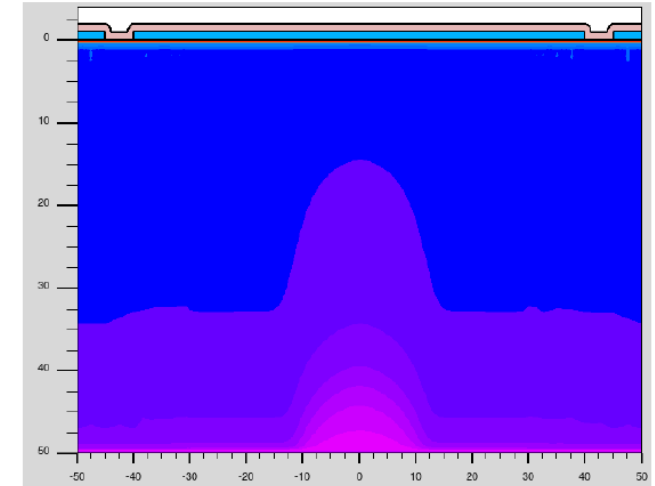
PIN h⁺



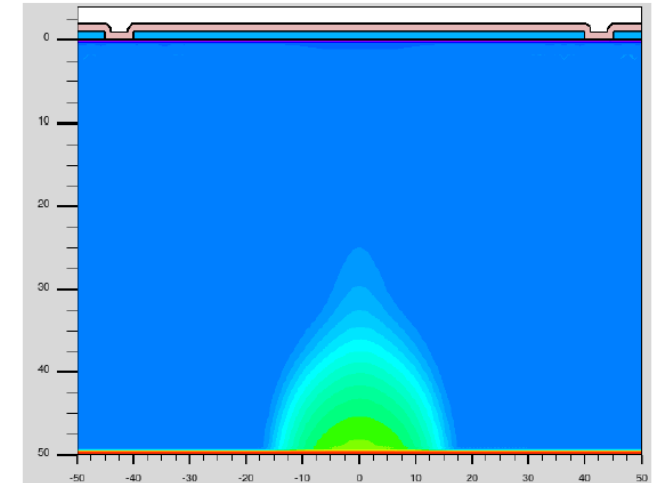
Waveforms



LGAD e⁻



LGAD h⁺

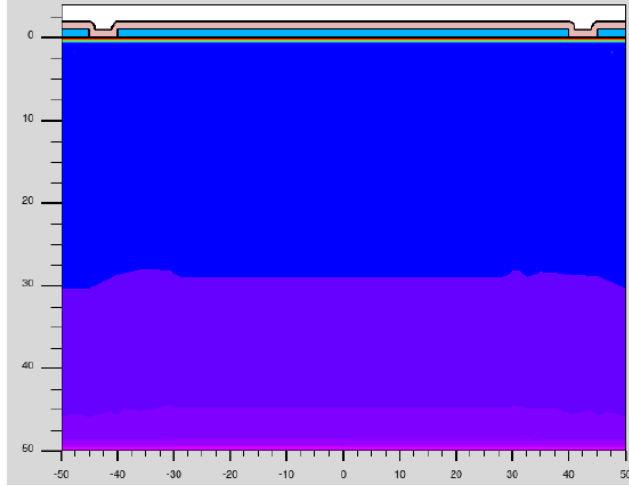


Courtesy: M. Centis Vignali (FBK)

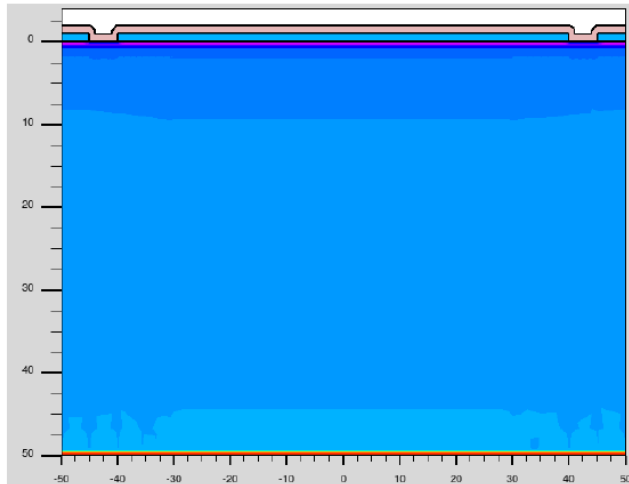
Thin sensor (PIN) vs LGAD

Bottom charge injection

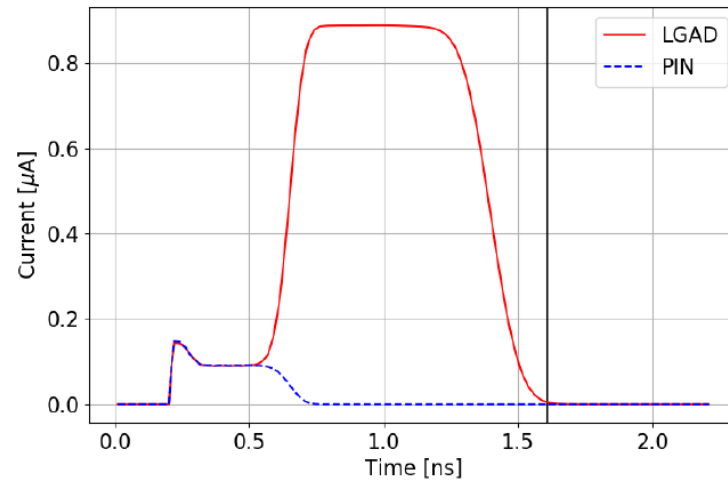
Time 1.61 ns
PIN e^-



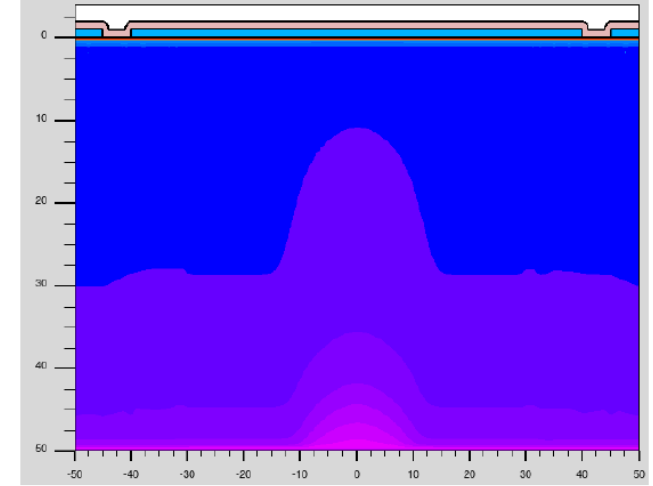
PIN h^+



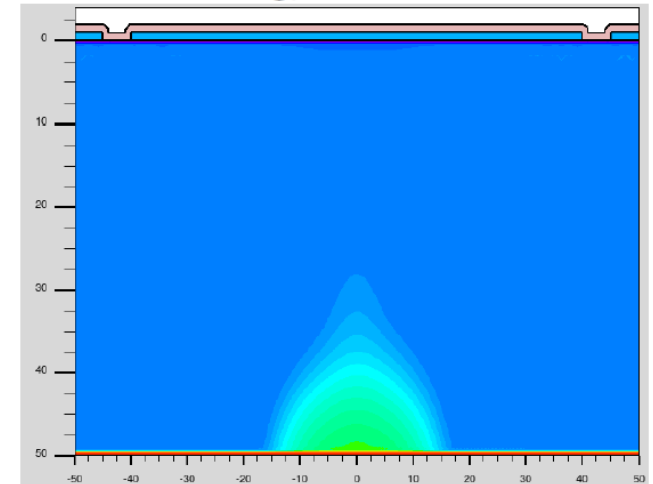
Waveforms



LGAD e^-



LGAD h^+

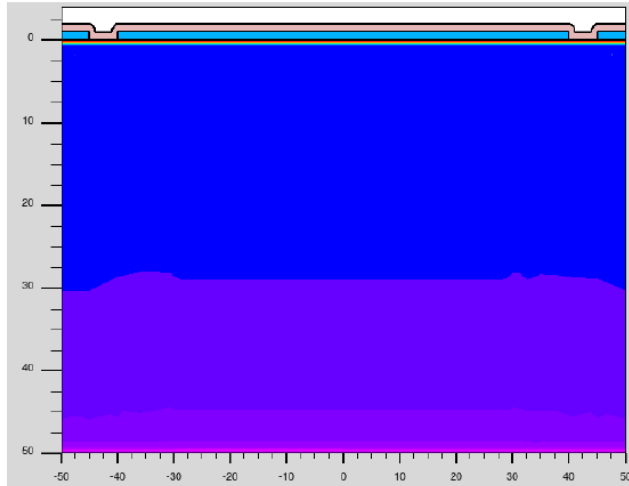


Courtesy: M. Centis Vignali (FBK)

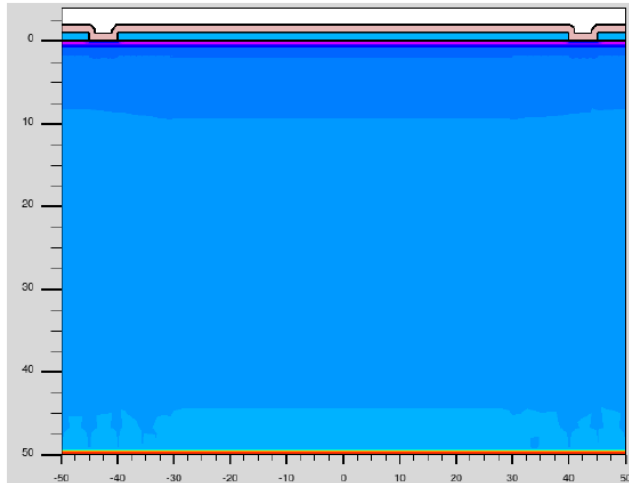
Thin sensor (PIN) vs LGAD

Bottom charge injection

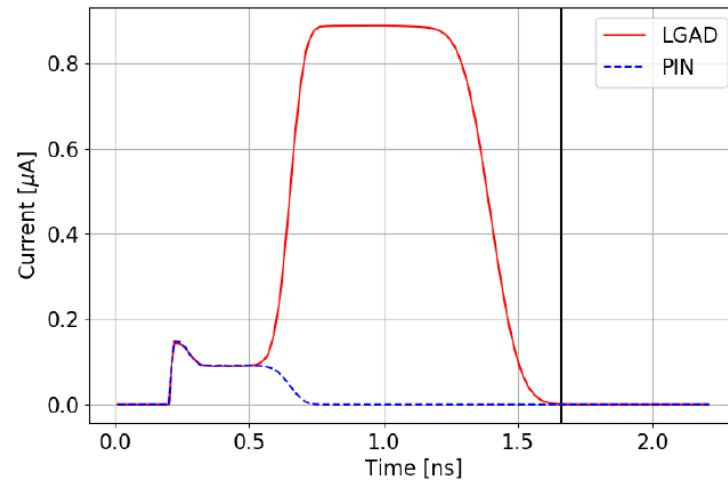
Time 1.66 ns
PIN e^-



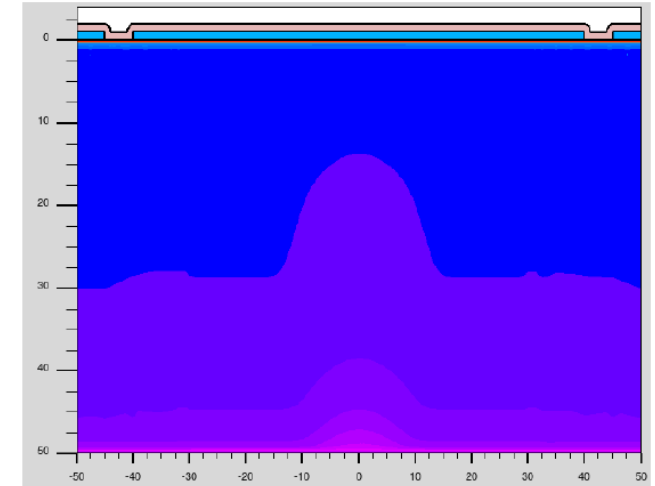
PIN h^+



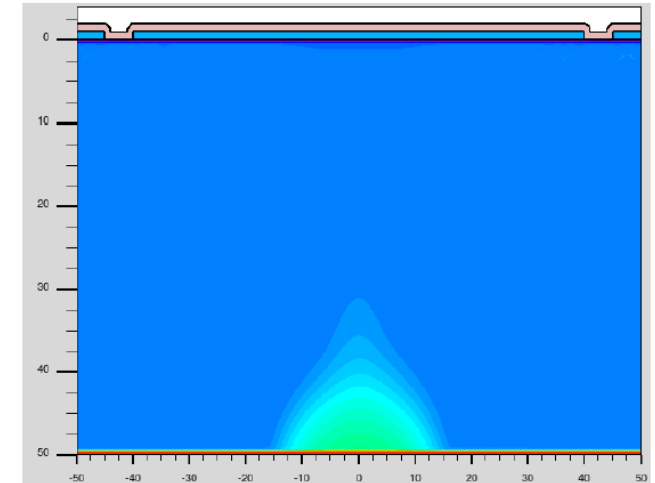
Waveforms



LGAD e^-



LGAD h^+



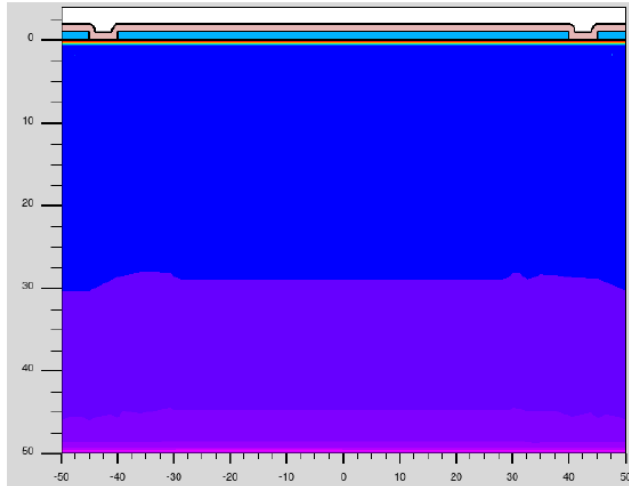
Courtesy: M. Centis Vignali (FBK)

Thin sensor (PIN) vs LGAD

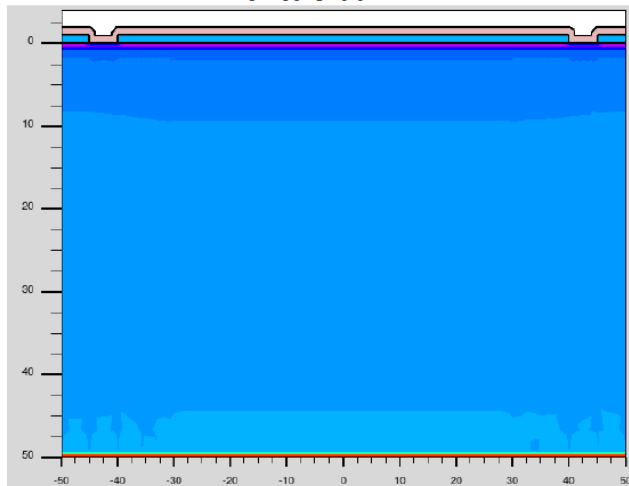
Bottom charge injection

Time 1.71 ns

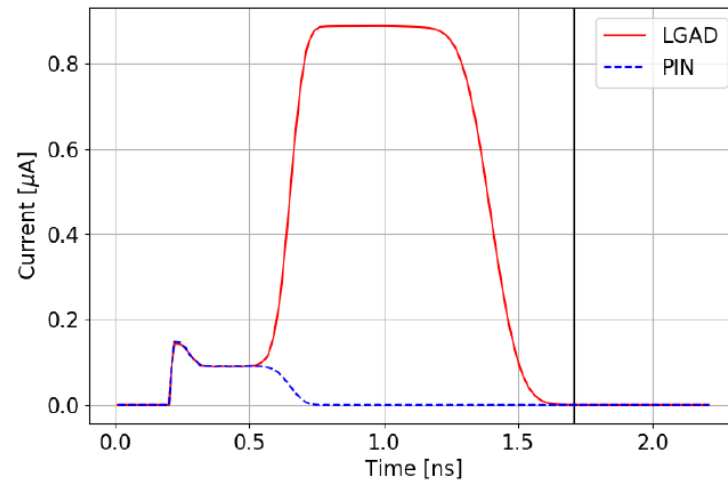
PIN e⁻



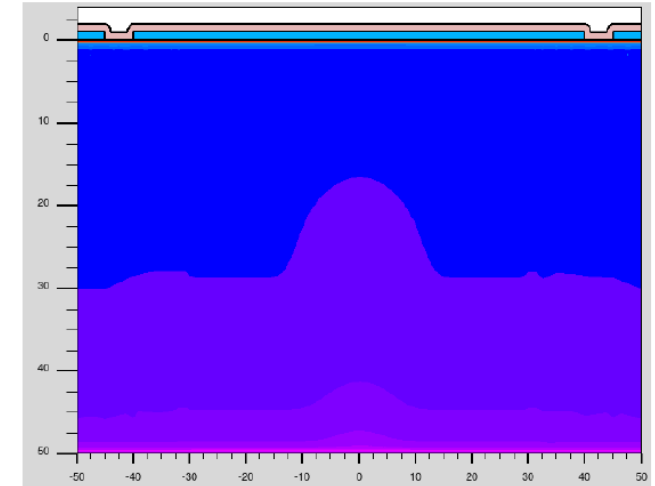
PIN h⁺



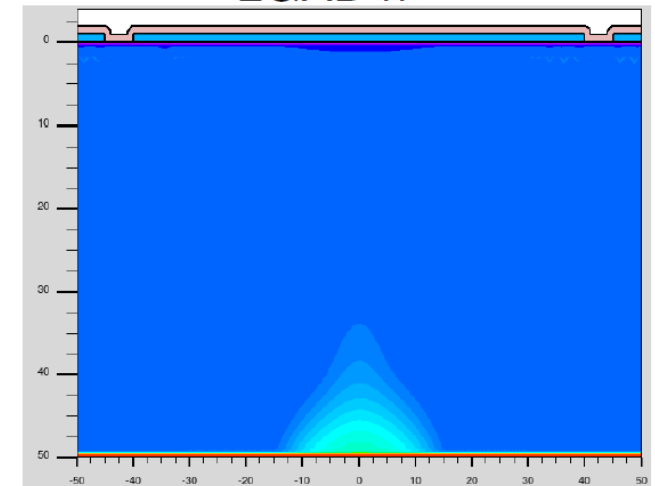
Waveforms



LGAD e⁻



LGAD h⁺



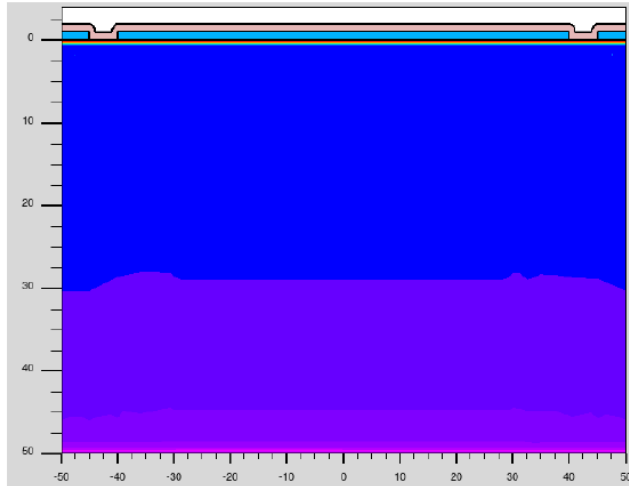
Courtesy: M. Centis Vignali (FBK)

Thin sensor (PIN) vs LGAD

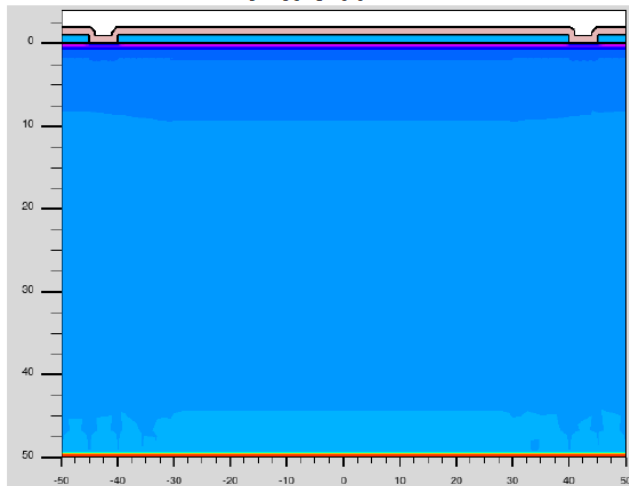
Bottom charge injection

Time 1.76 ns

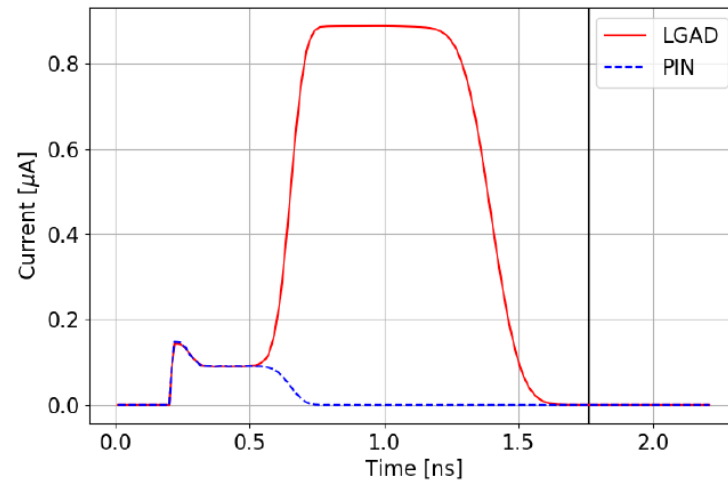
PIN e^-



PIN h^+

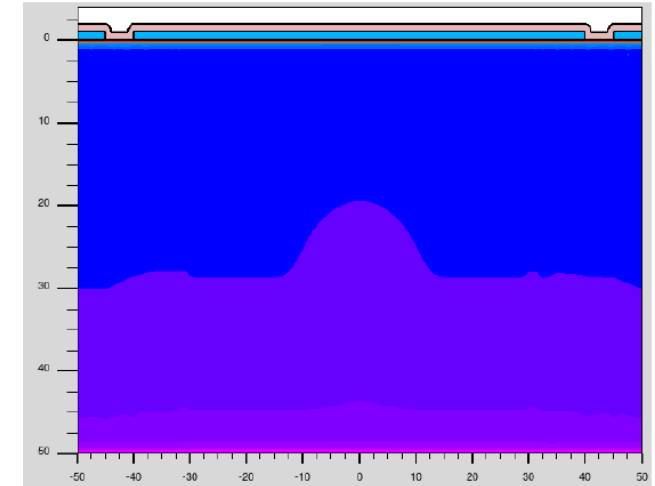


Waveforms

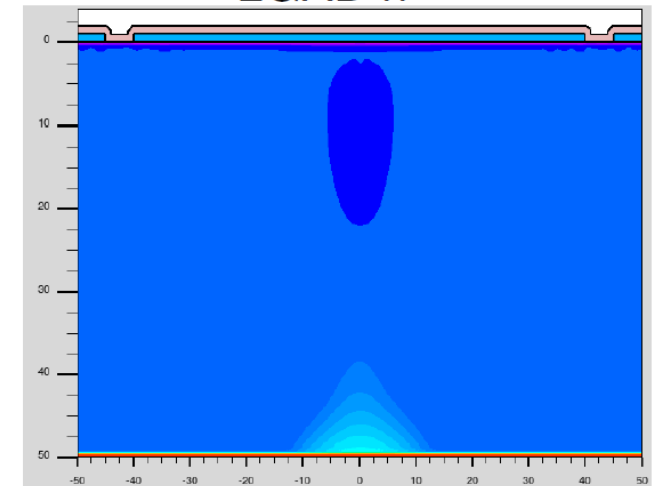


Courtesy: M. Centis Vignali (FBK)

LGAD e^-



LGAD h^+

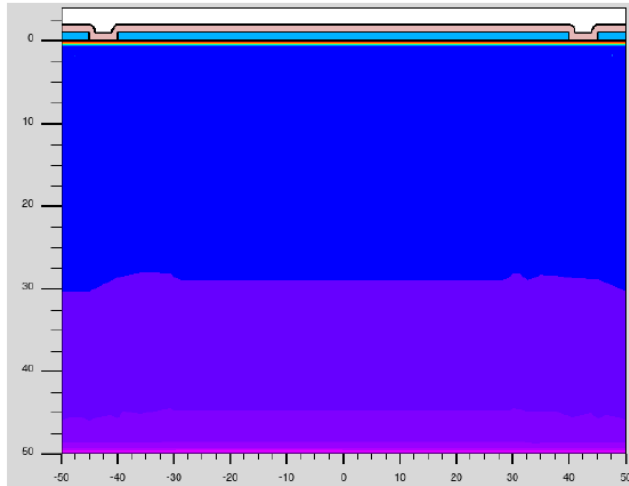


Thin sensor (PIN) vs LGAD

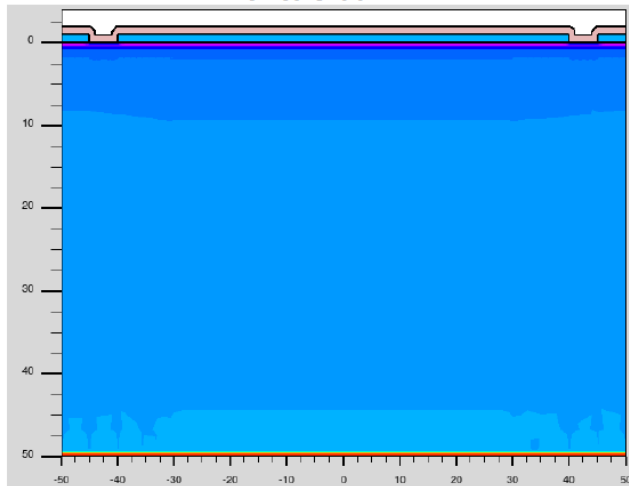
Bottom charge injection

Time 1.81 ns

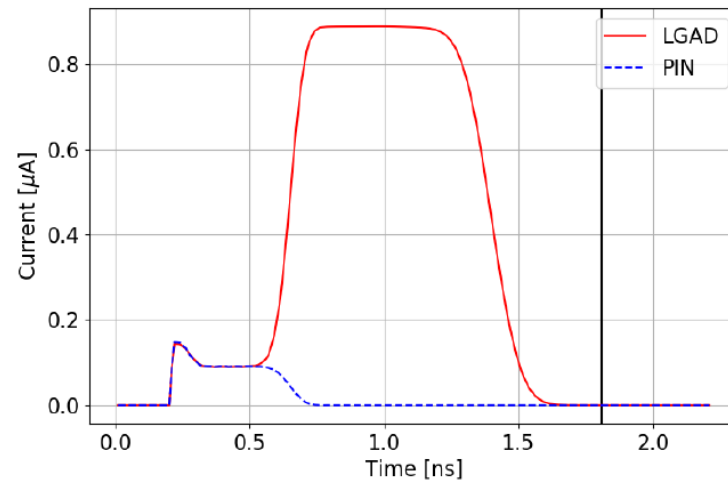
PIN e^-



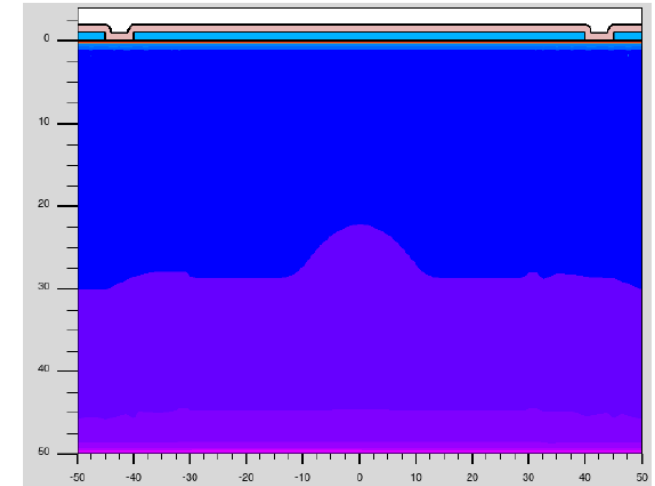
PIN h^+



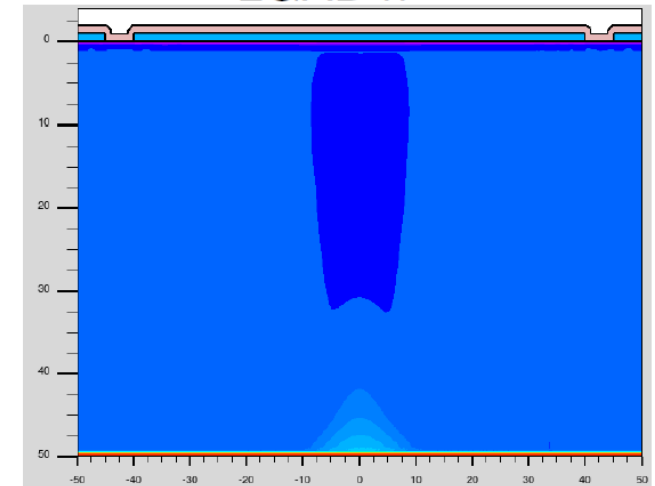
Waveforms



LGAD e^-



LGAD h^+



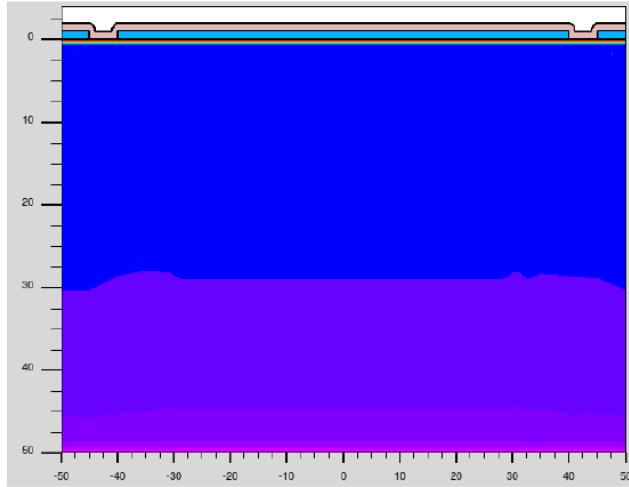
Courtesy: M. Centis Vignali (FBK)

Thin sensor (PIN) vs LGAD

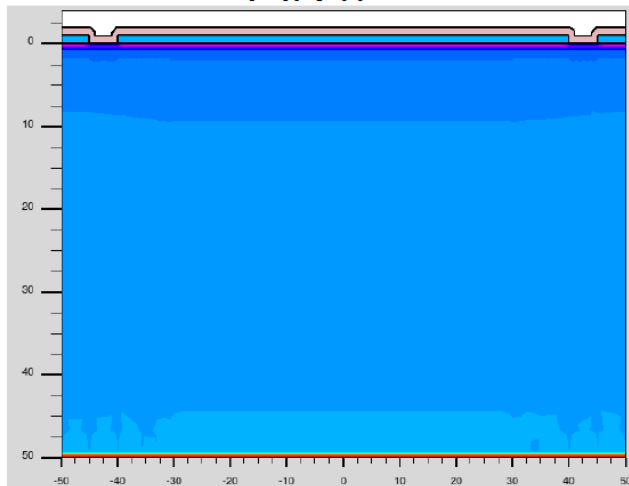
Bottom charge injection

Time 1.86 ns

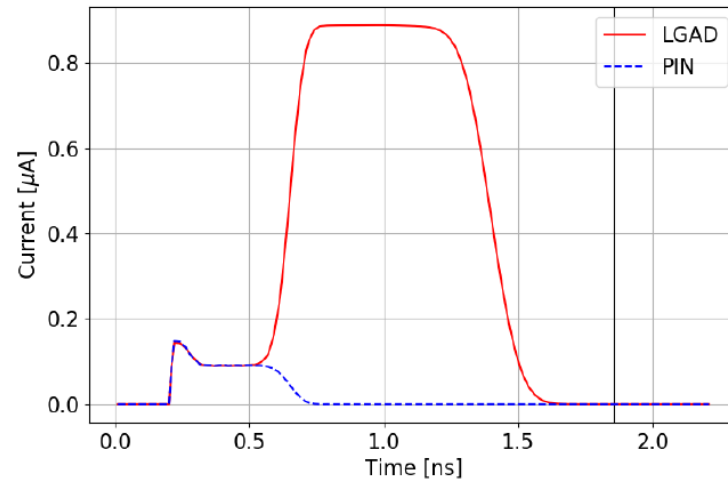
PIN e^-



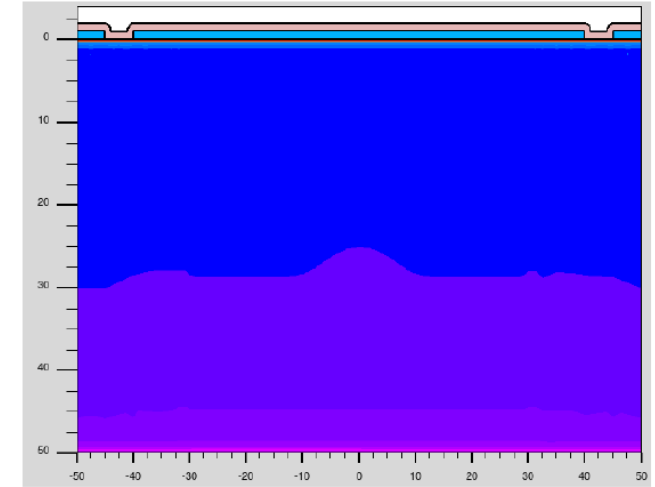
PIN h^+



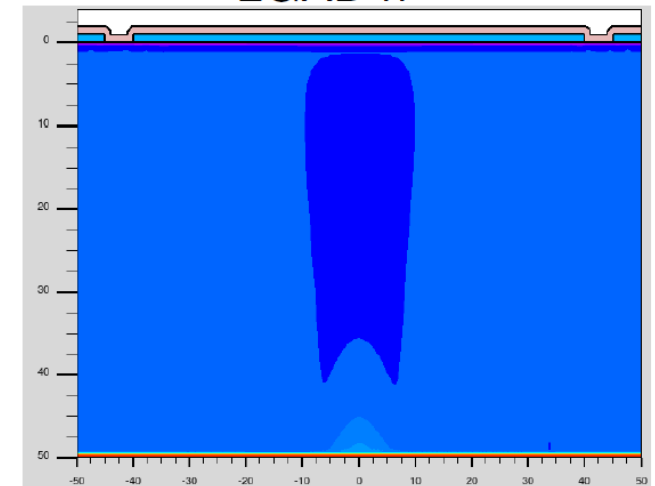
Waveforms



LGAD e^-



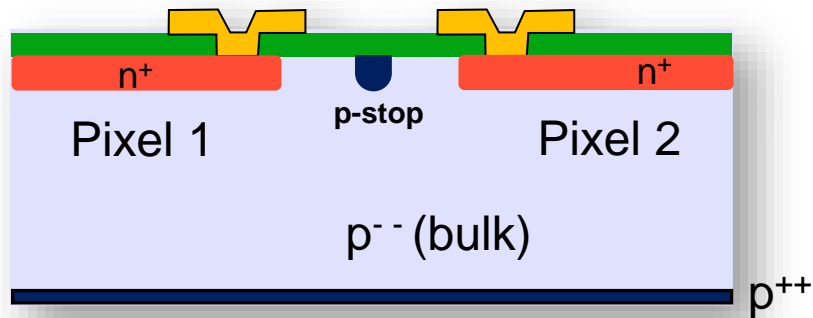
LGAD h^+



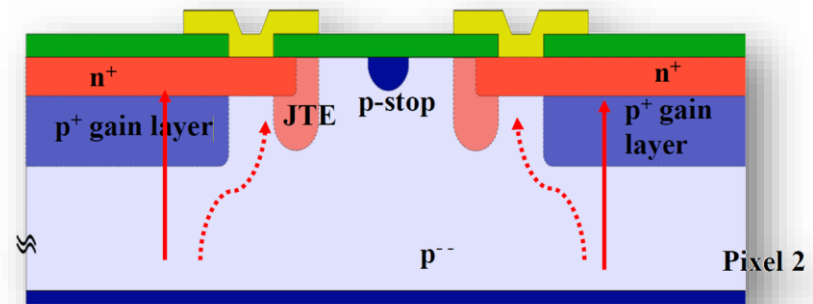
Courtesy: M. Centis Vignali (FBK)

Thin sensor (PIN) vs LGAD

Summary



Standard sensor



LGAD (Gen. 1)

- Thinner standard sensor (< 50μm) operating with an internal E field close to saturation is **extremely fast**
- Both Weighting field, Landau limitation are **reduced**
- e⁻ and h⁺ velocities become **saturated**
- Collected signal **is small**, therefore the slew rate k very low $k \propto \frac{dV}{dt}$
- The time resolution is **poor**

$$\sigma_{time} = \frac{\sigma_{noise}}{k}$$

Small signal (pointing to dV)

k small (pointing to k)

- Thinner standard sensor (< 50μm) operating with an internal E field close to saturation is **fast**
- Both Weighting field, Landau limitation are **reduced**
- e⁻ and h⁺ velocities become **saturated**
- Collected signal **higher thanks to the internal gain**, therefore the slew rate k high
- The final time resolution is **very high**

$$\sigma_{time} = \frac{\sigma_{noise}}{k}$$

k very high (pointing to k)

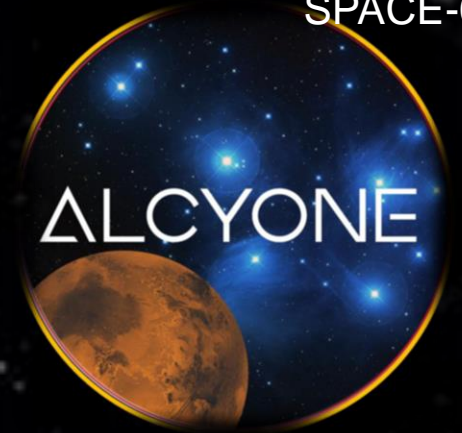
Lattice dynamics

Active site structures in proteins and
batteries with

Nuclear Resonance Scattering

BMBF ^{57}Fe

Bring to light an unknown world of
beam physics



High-time resolution detection
for novel Nuclear Resonance
experiments

High-resolution dosimeter for
space experiments

Novel strategies for high- granularity LGAD sensors



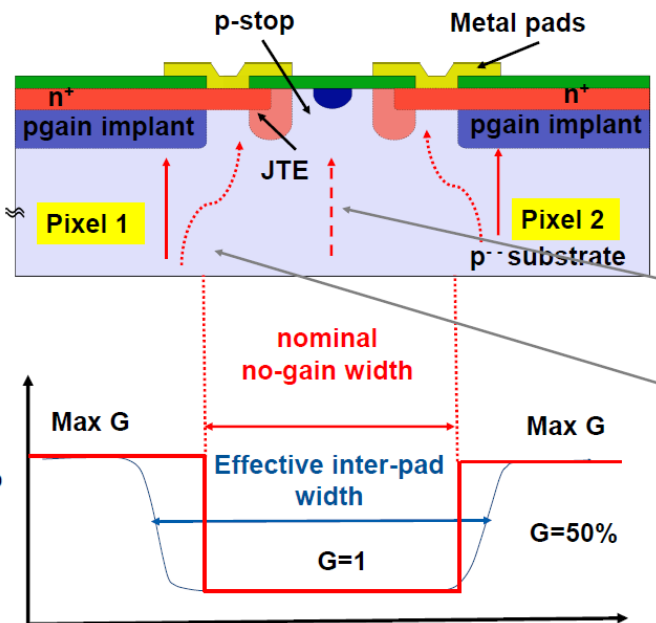
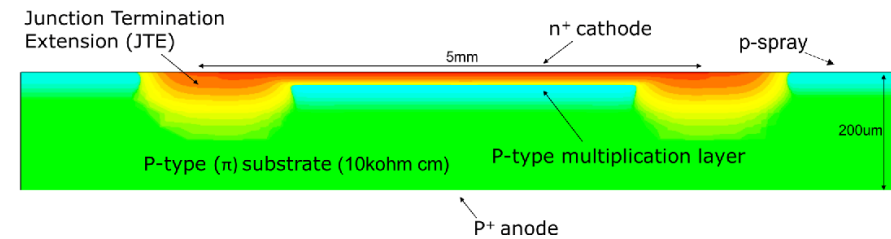
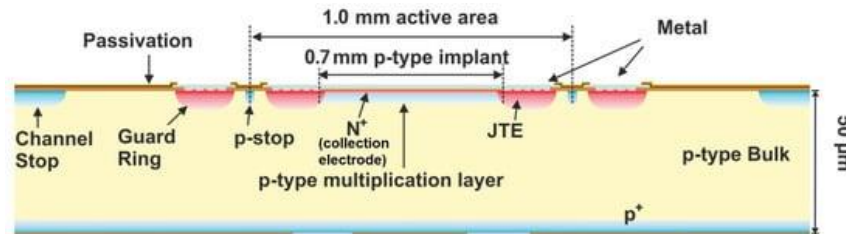
New funding opportunities
Novel research fields



Low Gain Avalanche Diode

First generation of LGAD device

- In the first generation of LGAD sensors, the Junction Termination Extension (JTE) was essential to prevent premature breakdown caused by the high lateral electric field in the gain layer diffusion



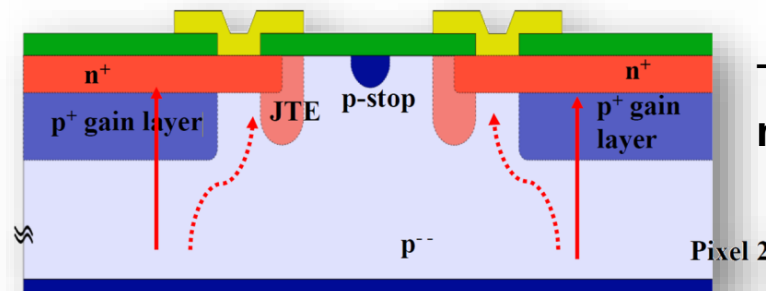
- Inter pixel region hosts the isolation and termination structures:
 - P stop
 - Junction Termination Extension (JTE)
- The pixel border is a dead region.** The carriers generated in this area are not multiplied
- Some carriers, even if generated below the nominal gain layer, are collected by the deeper JTE and does not pass through the gain layer → these carriers are multiplied with reduced gain
- The P stop and JTE structure significantly limit the granularity**

Trench-Isolated LGAD technology

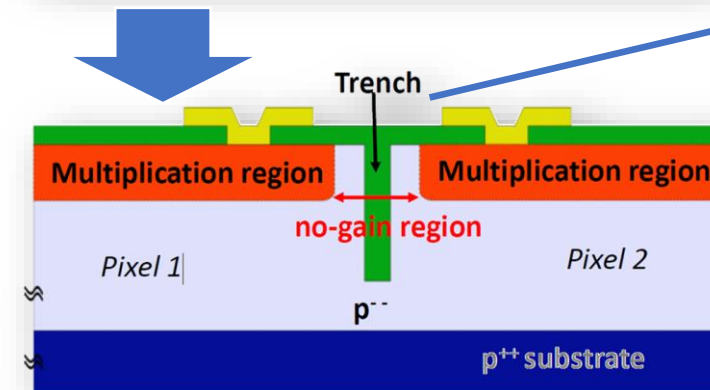
Developed within the RD50 collaboration (2019/2020)



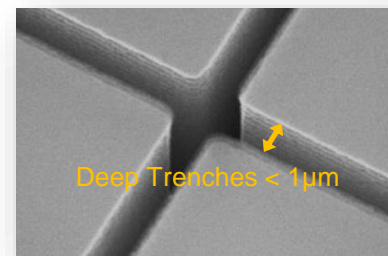
- The project aims to develop a new LGAD sensor for timing applications, featuring fine pixel segmentation, high gain uniformity and high fill-factor



Traditional LGAD structure
no-gain region of $\sim 30 \mu\text{m}$



Trench isolated LGAD structure
no-gain region of $\sim \text{few } \mu\text{m}$



SEM picture of a STI,
width of $< 1 \mu\text{m}$

- JTE and p-stop are replaced by a single trench
- Trenches act as a drift/diffusion barrier for electrons and isolate the pixels
- Filled with Silicon Oxide

RD50 Project Proposal	
Development of Segmented LGAD with small pixels and high Fill-Factor (High Density LGAD, HD-LGAD)	
Contact Person:	Giovanni Paternoster Fondazione Bruno Kessler, Trento, Italy Via Sommarive, 18, Trento, Italy Tel. +390461314462 paternoster@fbk.eu
Involved Institutes:	<ol style="list-style-type: none"> 1. Fondazione Bruno Kessler (Giovanni Paternoster, Maurizio) 2. INFN Torino (Nicolo Cartiglia) 3. KIT (Michele Caselle, Alexander Dierlamm) 4. University of Zurich (Ben Kilminster) 5. Paul Scherrer Institut (Tilman Rohe, Anna Bergamaschi) 6. Institut "Jozef Stefan" (Gregor Kramberger) 7. University of Birmingham (Phil Allport) 8. UC Santa Cruz (Hartmut Sadrozinski)
Total Project Costs	69.000 €
Request to RD50	25.000 €

- KIT mission: design of microstrip sensors and provide a set of *layout design rules* for this technology

Layout option of TI-LGAD technology (I)

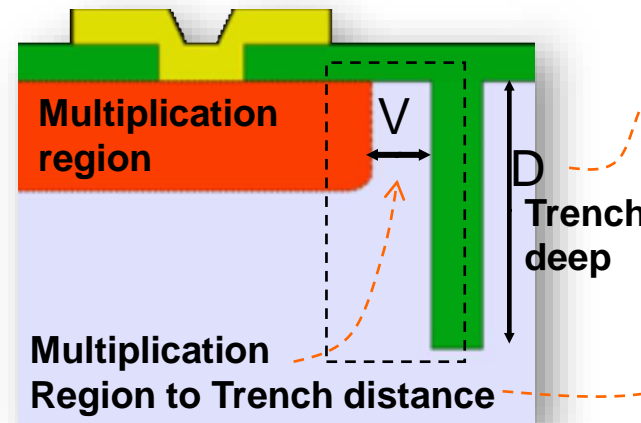
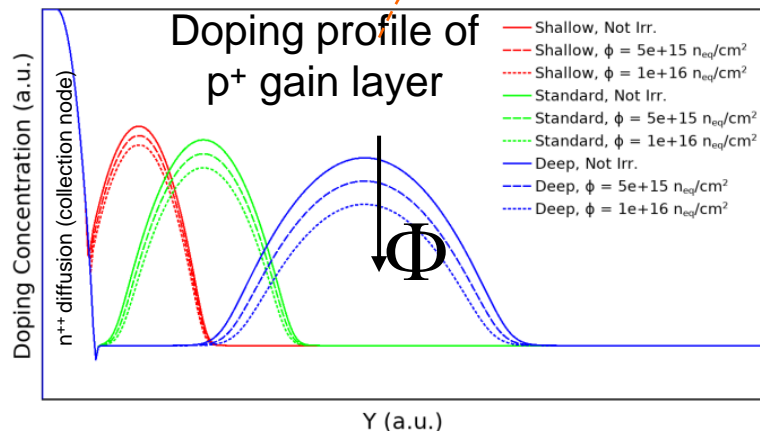
Large area, fast 4D tracking system based on TI-LGAD sensors



- In order to grant access to these distinguished detector technologies, it is imperative that we thoroughly examine and characterize various layout and geometrical optimizations. This includes a comprehensive study of the doping profile and shape

Doping profile:

- Shallow, Standard and Deep



- Trench deep: $D1 < D2 < D3$

- The multiplication region to trench distance:

- Aggressive layout: $V1 < 1 \mu\text{m}$
- $V2 < 3 \mu\text{m}$, $V3 < 4 \mu\text{m}$
- Conservative layout: $V4 < 5 \mu\text{m}$

Trade-off between “smaller gain-loss region” and conservative “E-field conditions”

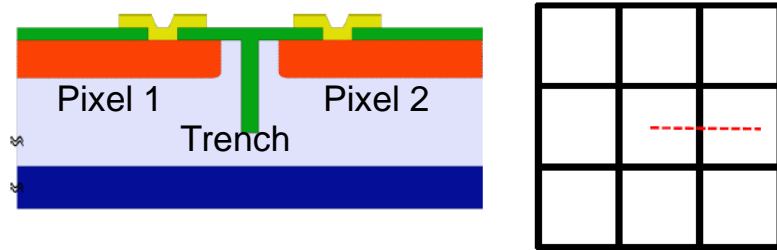
Layout option of TI-LGAD technology (II)

Large area, fast 4D tracking system based on TI-LGAD sensors

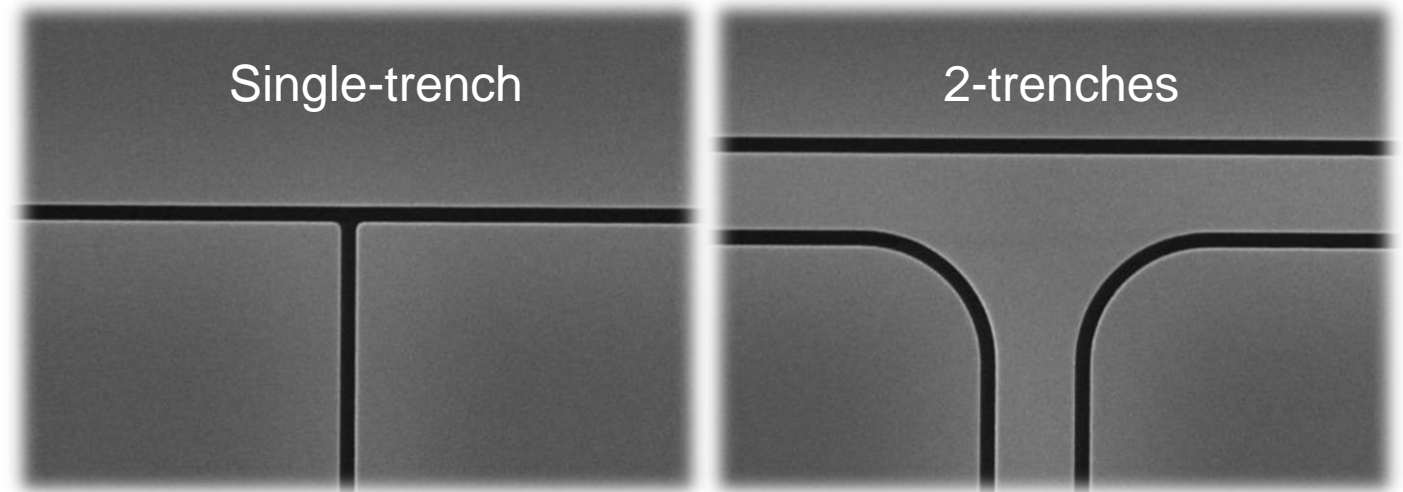
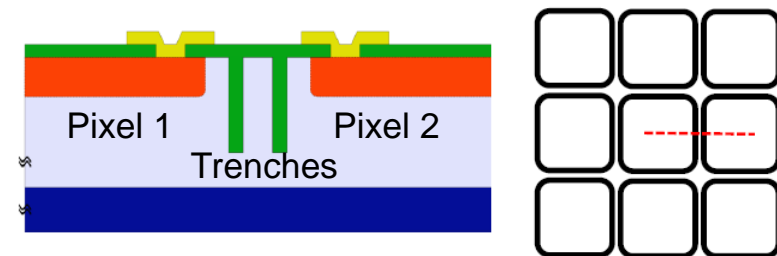


- Number of trenches between channels/pixels. By simulation is expected that 2-trenches version has wider no-gain region but very conservative E-field conditions

- Single-trench isolation layout (trench grid)



- 2-trenches isolation layout



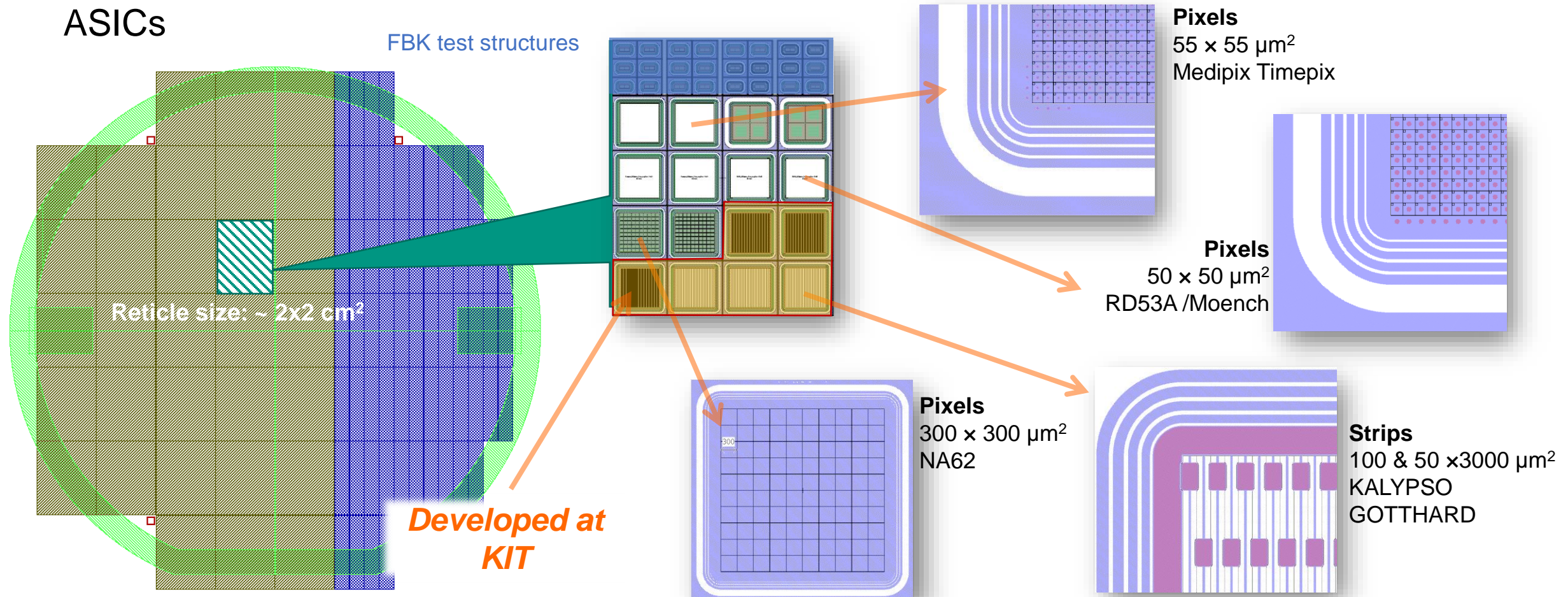
SEM images after trench etching

Layout	Nominal no-gain width
1 Trench	~ 4 μm
2 Trenches	~ 6 μm

TI-RD50 Batch – Wafer Layout

Design and production of TI-LGAD prototypes

- Many different small pixels sensors have been included, compatible with many different ASICs

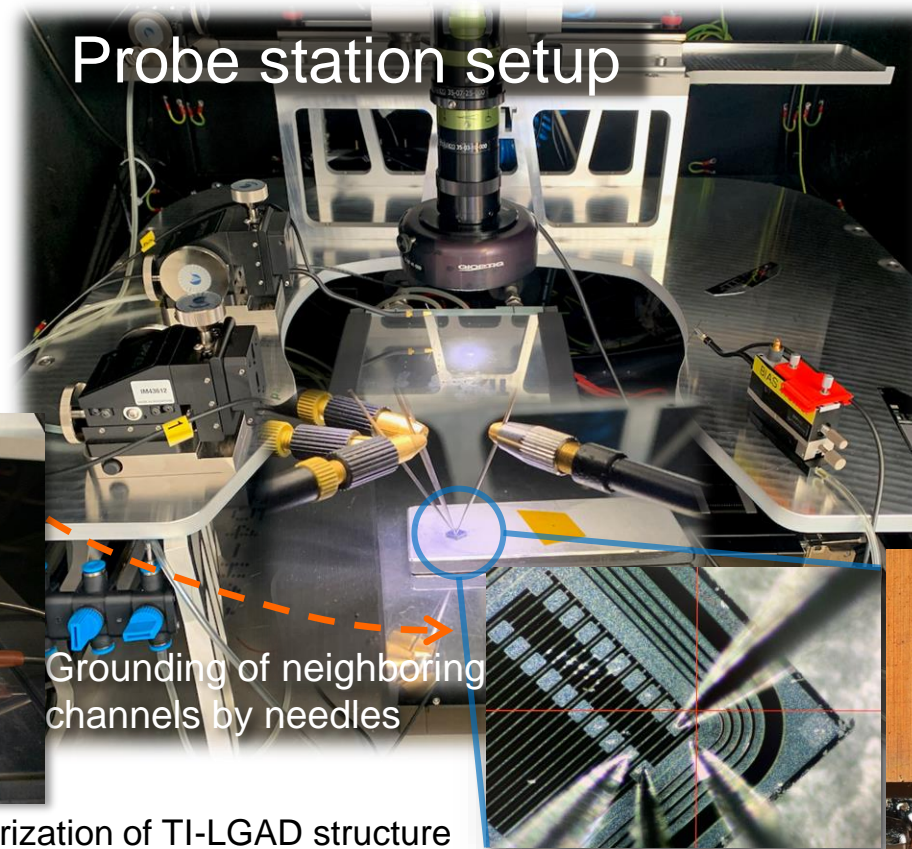
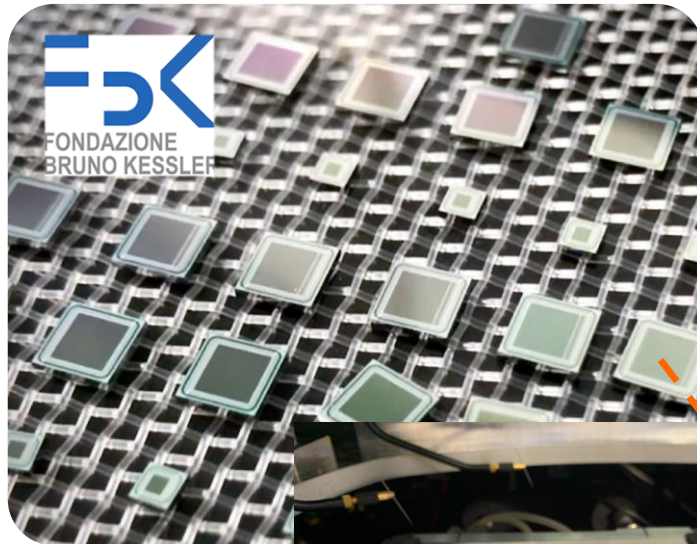


TI-LGAD sensor characterization at KIT

Probe-station setup for I-V and C-V measurements

- The LGAD sensors have been received and an intensive testing and characterization campaign was conducted

Thanks to Alexander Dierlamm

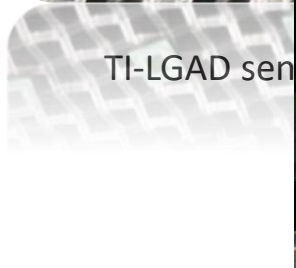


Picoammeter
KEITHLEY 6485

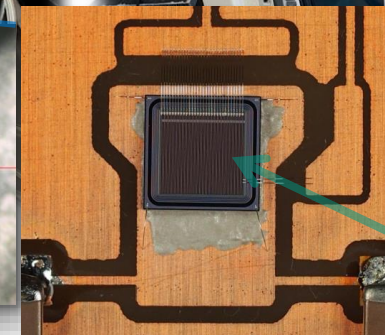
LRC par. analyzer
Keysight E4980AL LC

Voltage source
KEITHLEY 2410 1100V

KIT-ETP



Grounding of neighboring channels by needles

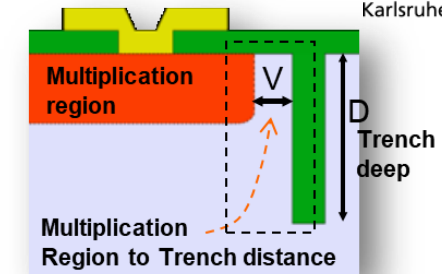


Probe station test setup suitable for the characterization of TI-LGAD structure

TI-LGAD sensor characterization

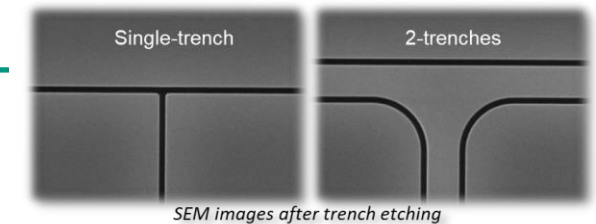
Performed on the test structures designed at KIT

- I-V characterization
- C-V characterization
- Gain characterization & uniformity across pixels
- Interpix measurements (no-gain region)
- Time characterization & uniformity
- Long-time stability

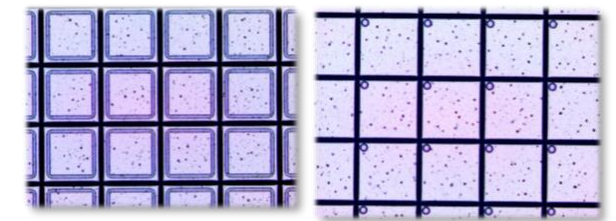


Trench deep: $D1 < D2 < D3$

Trench distance: $V1 < V2 < V3 < v4$



Two structures: **single-trench** and **2-trenches**



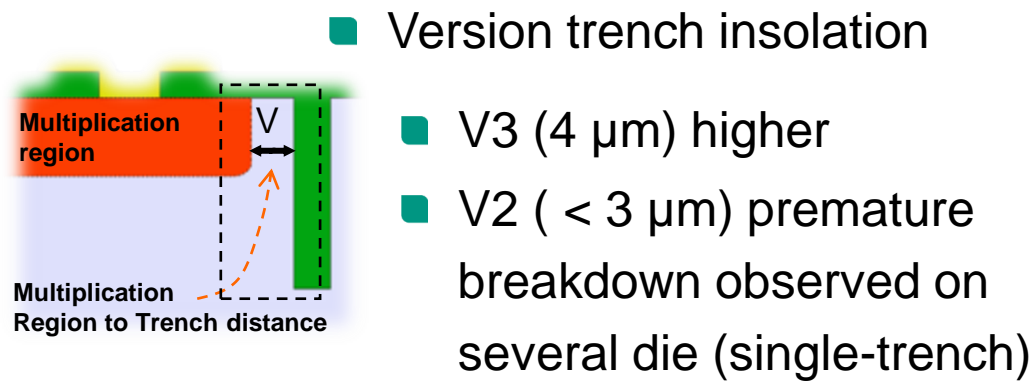
Contact M1: **Ring** or **single** contact

Reference: Johannes Deutsch, Master thesis: "Development and characterization of novel LGAD sensors for the next generation of detectors", Feb. 1st (2022)

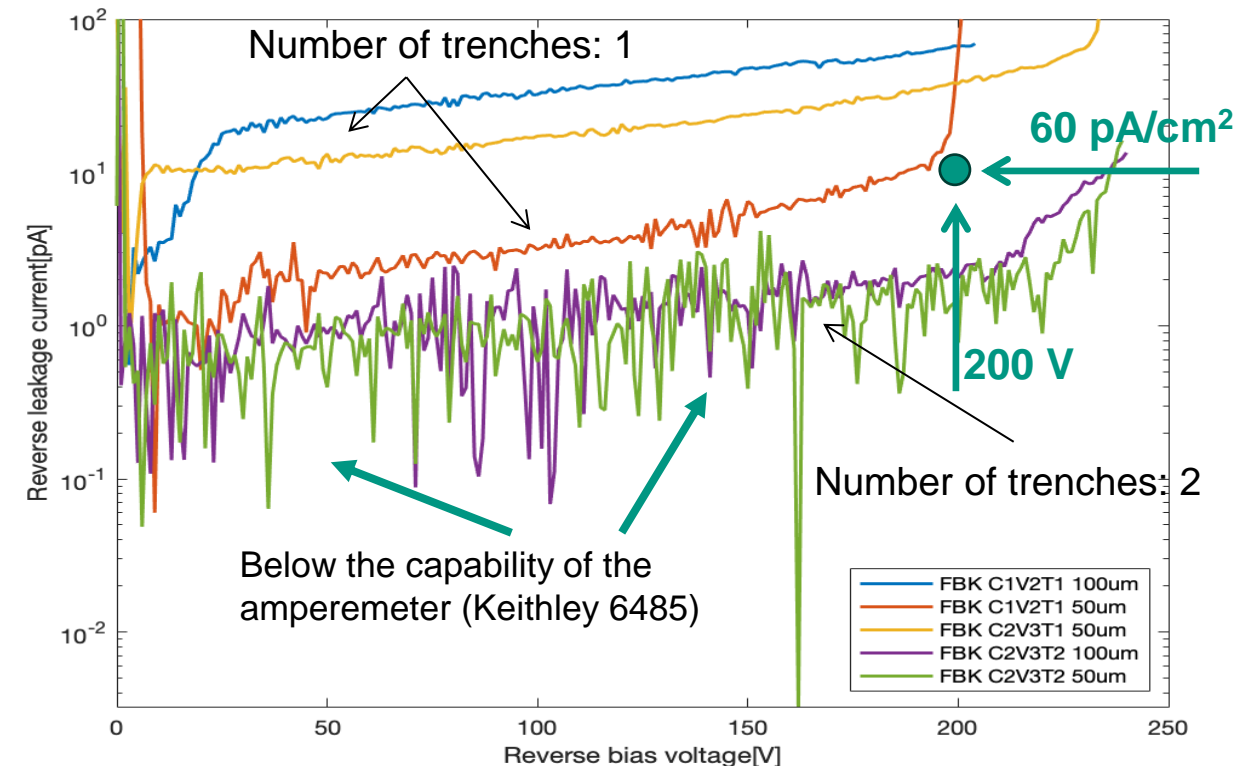
TI-LGAD parametric characterization (I)

Comparison of the I-V characteristics across different layout options

- Both single and double trenches work perfectly, extremely low leakage currents $O(\text{pA})$, the measurement is consistent with the leakage current observed in standard pixels
- Avalanche breakdown $> 200 \text{ V}$



- 2-trenches (T2) show a higher breakdown combined to very low leakage current



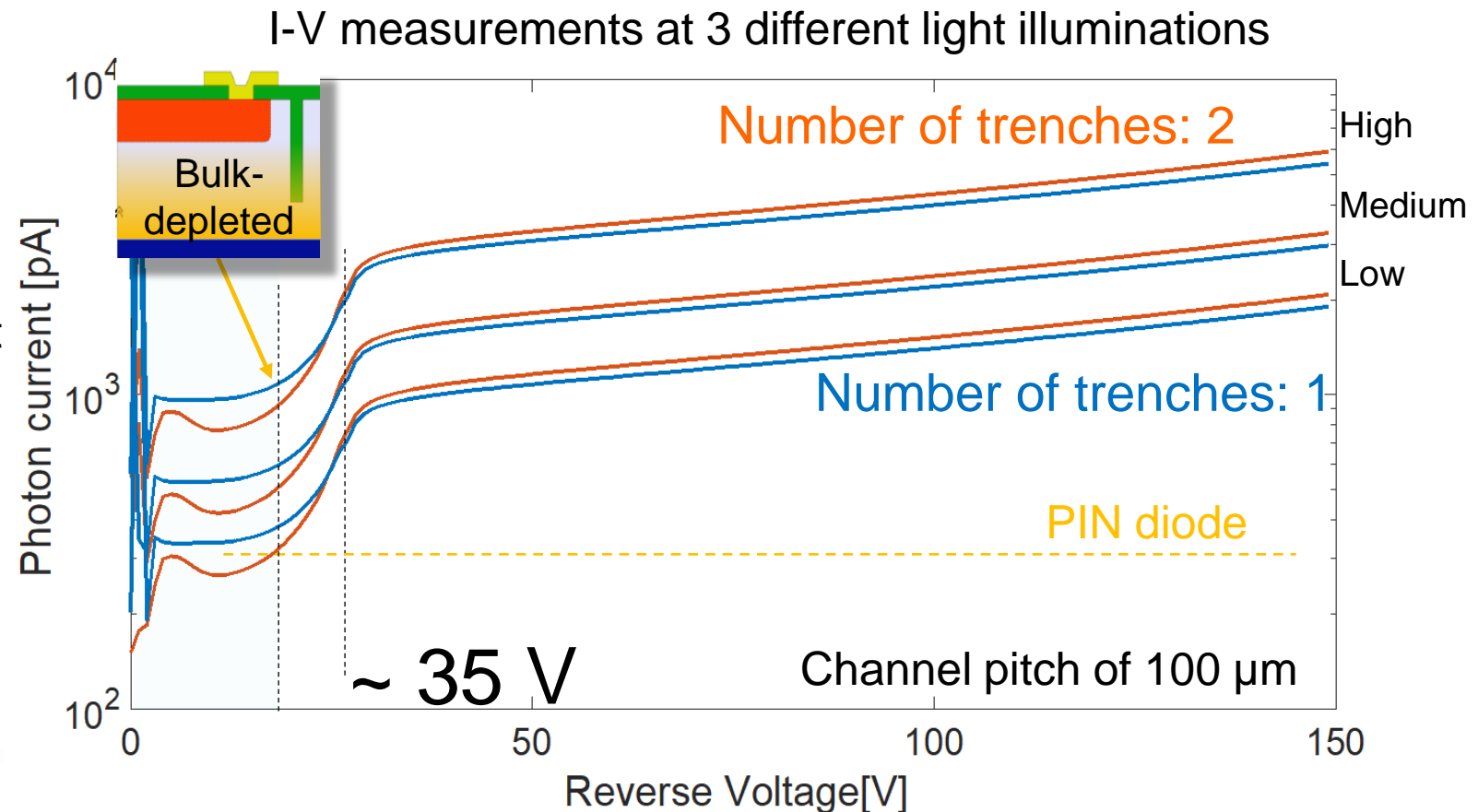
The trench version V3 and 2-trenches (T2) is considered to be the best combination

TI-LGAD gain characterization (II)

Gain characterization based on illuminated sensor

- Preliminary gain characterization, the gain obtained is a pessimistic value due to the metal layer on the microstrip and the not focused light source
- Same behavior for both 100 and 50 μm channel pitch
- T2 shows high signal compared to T1, which is a strong indication that the *effective gain-loss width* is reduced compared to T1

Layout	Nominal no-gain width
1 Trench	$\sim 4 \mu\text{m}$
2 Trenches	$\sim 6 \mu\text{m}$

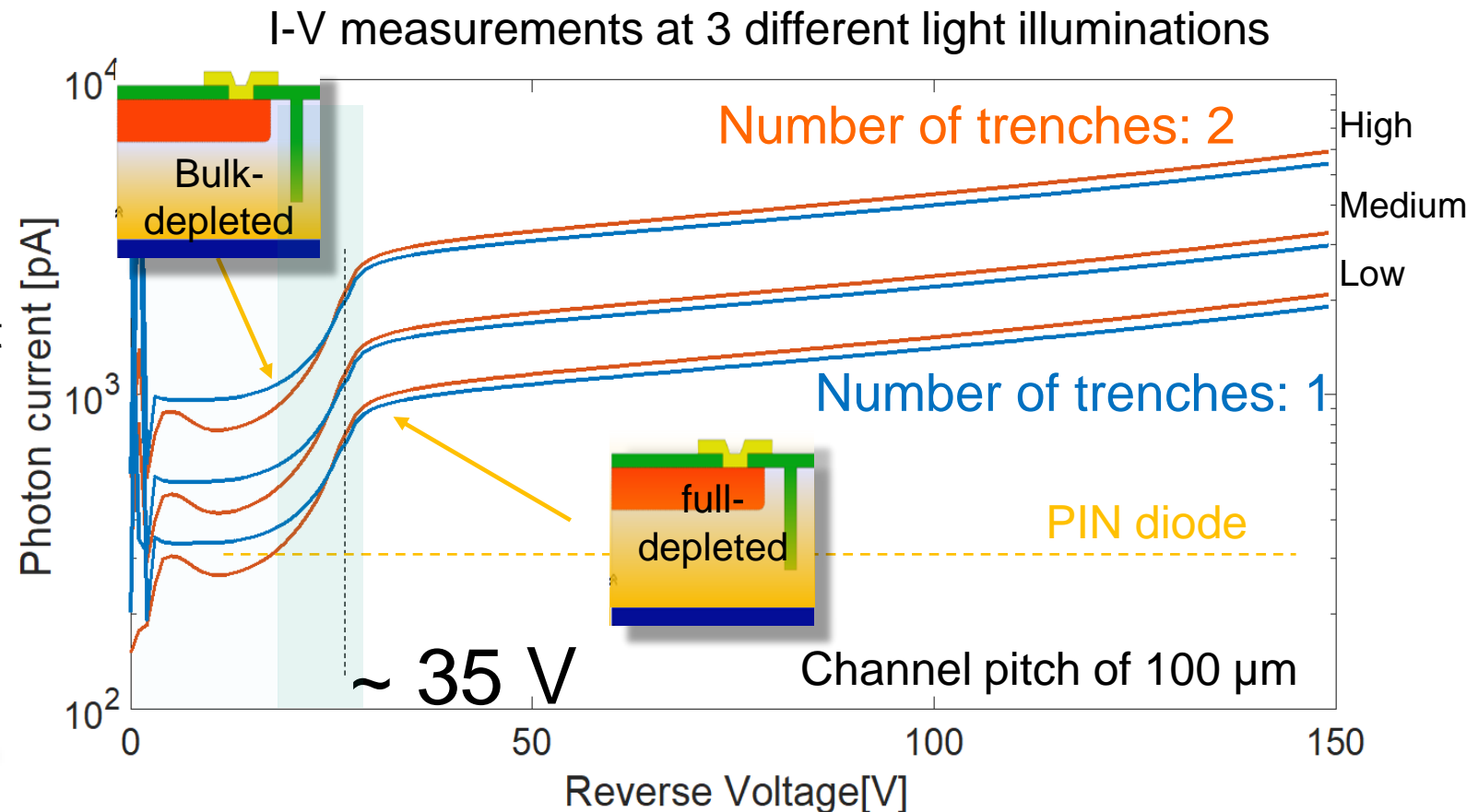


TI-LGAD gain characterization (II)

Gain characterization based on illuminated sensor

- Preliminary gain characterization, the gain obtained is a pessimistic value due to the metal layer on the microstrip and the not focused light source
- Same behavior for both 100 and 50 μm channel pitch
- T2 shows high signal compared to T1, which is a strong indication that the *effective gain-loss width* is reduced compared to T1

Layout	Nominal no-gain width
1 Trench	$\sim 4 \mu\text{m}$
2 Trenches	$\sim 6 \mu\text{m}$

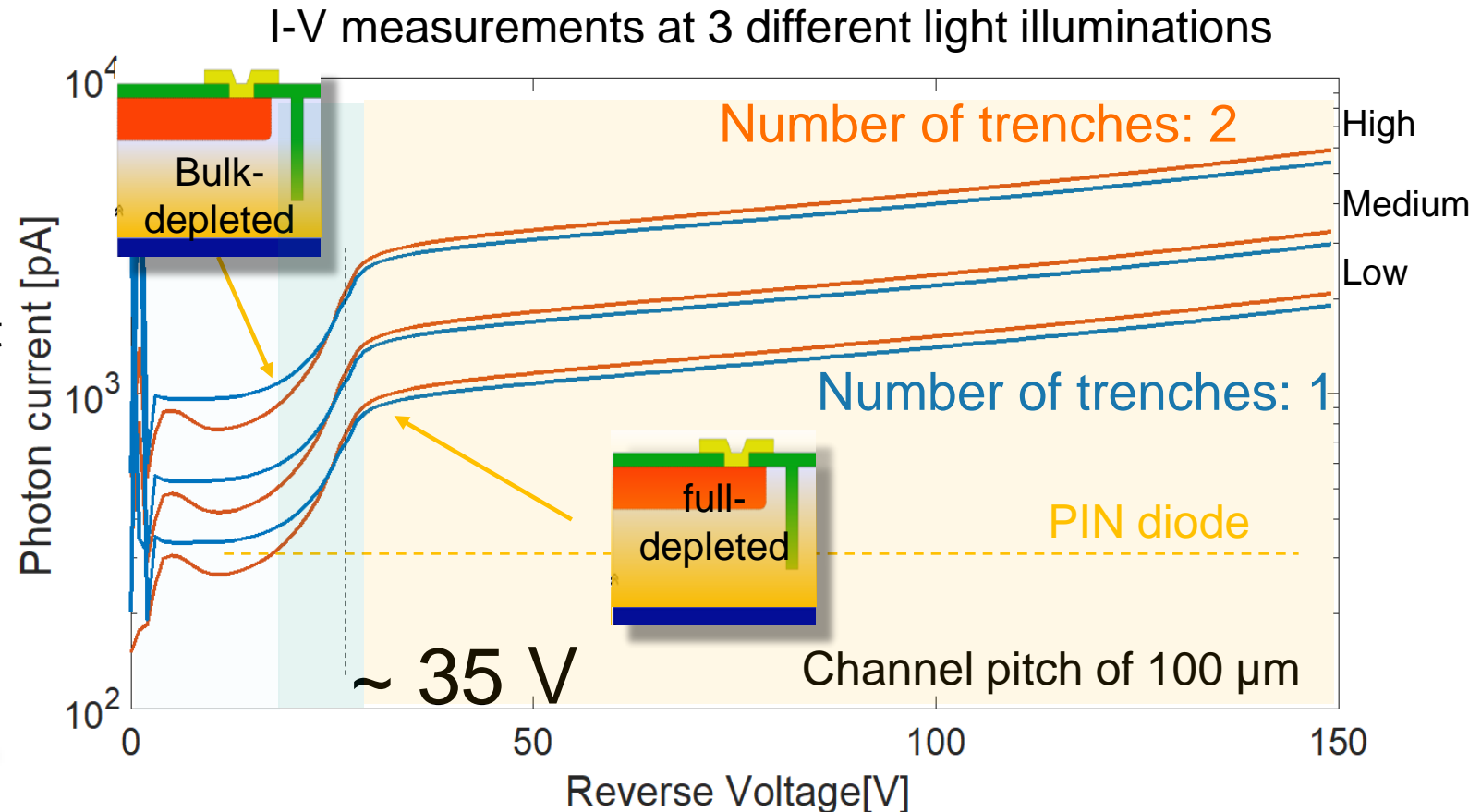


TI-LGAD gain characterization (II)

Gain characterization based on illuminated sensor

- Preliminary gain characterization, the gain obtained is a pessimistic value due to the metal layer on the microstrip and the not focused light source
- Same behavior for both 100 and 50 μm channel pitch
- T2 shows high signal compared to T1, which is a strong indication that the *effective gain-loss width* is reduced compared to T1

Layout	Nominal no-gain width
1 Trench	$\sim 4 \mu\text{m}$
2 Trenches	$\sim 6 \mu\text{m}$



Transient Current Technique (TCT) setup

Precise time characterisation of fast sensors (planar, 3D and LGAD)

- To understand the irradiation effect by measuring depleted region
- *Shooting two lasers on the sensor pulses*

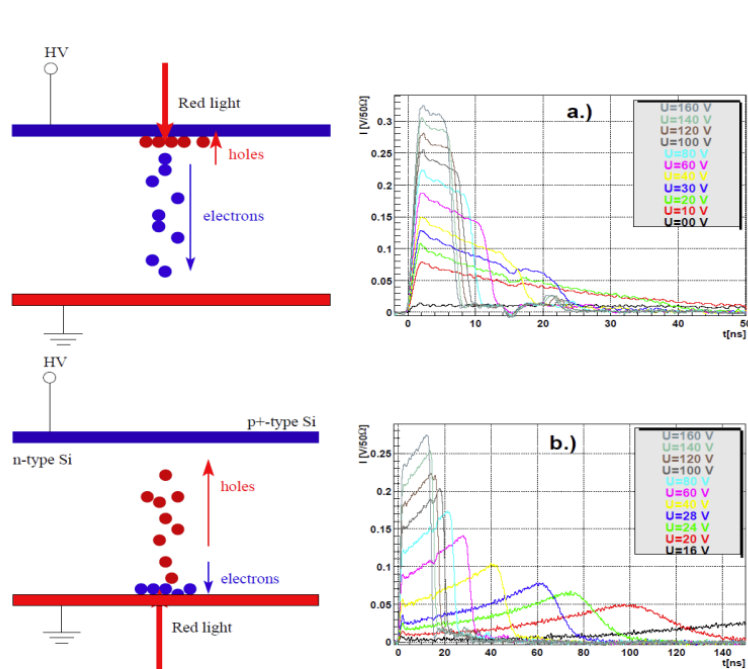
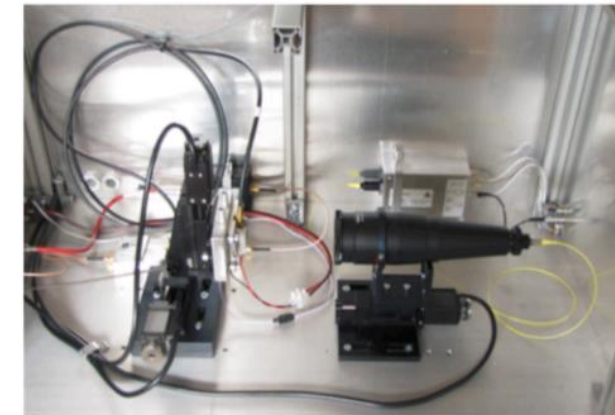
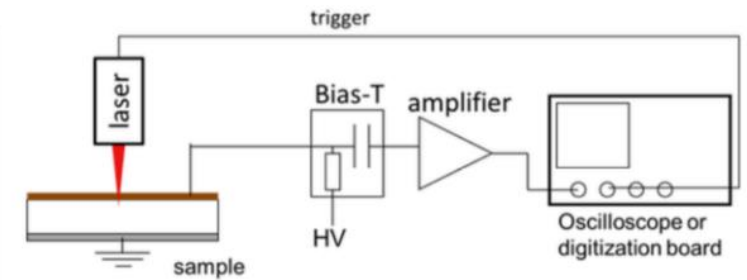
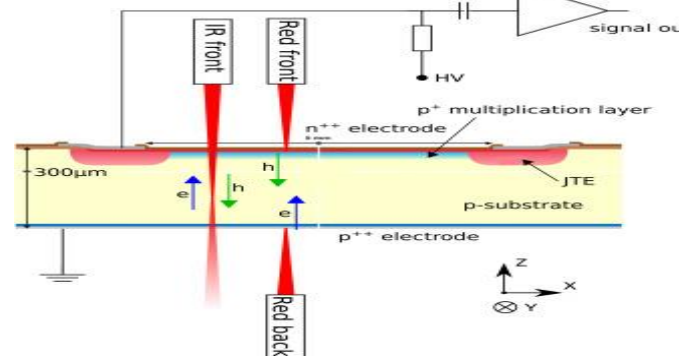
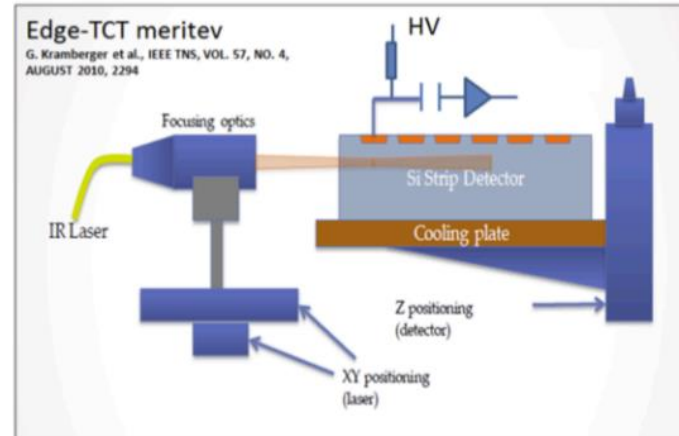


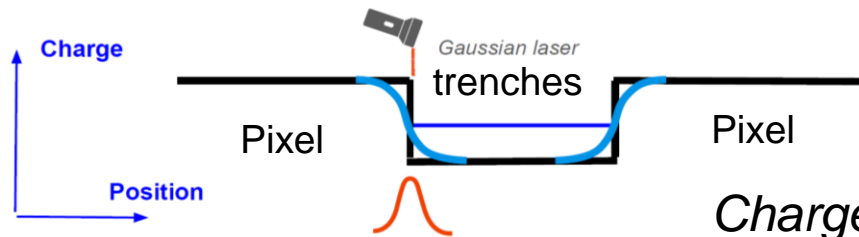
Figure 1: Schematic representation of e-h pair generation when observing induced signals from electrons (a) and holes (b). Electrons are travelling from the high field region towards the small field region, while for holes it is the other way around.



TCT: interpixel measurements (I)

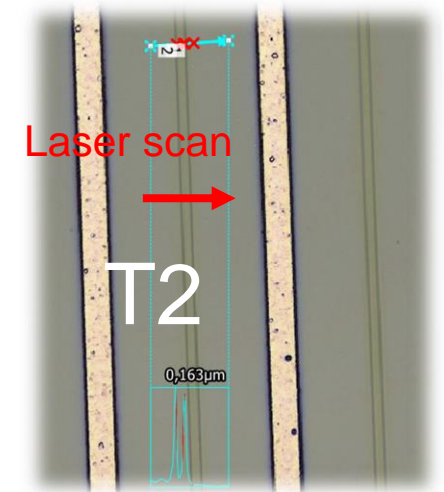
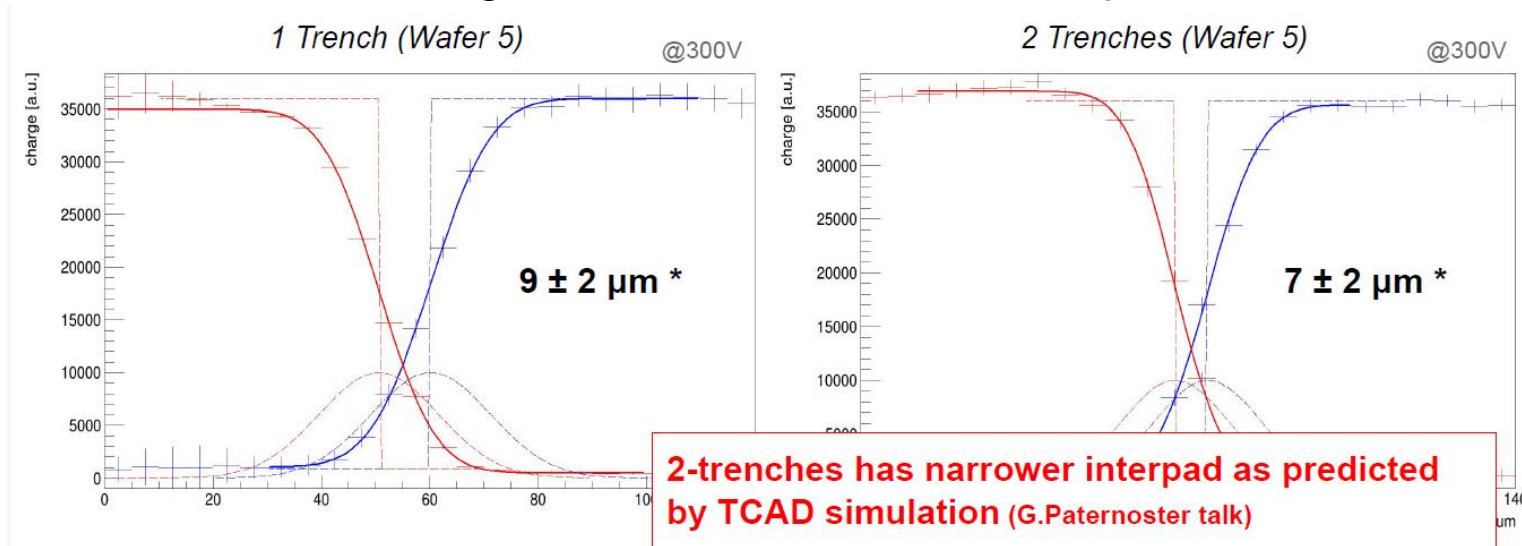
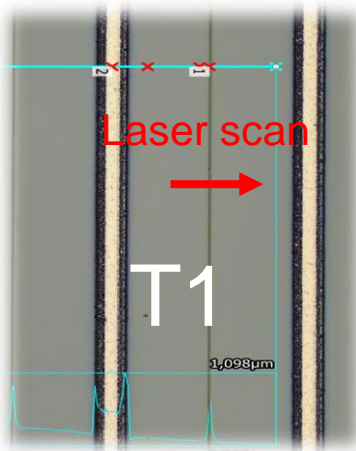
Characterisation of the no-gain region between channels

- The measurements were performed at KIT, INFN-TO and UZH. A scanning *Transient Current Technique* (TCT) setup was used based on infrared laser. Get the width by scanning two nearby channels → *charge vs position*



Laser pulses are split in two paths, one containing 20 extra meters of optic fiber, before being sent to the DUT. This produces two almost identical pulses of light with a fixed temporal separation of 100 ns and allows to study the time resolution of the DUT.

Charge collected as a function of position

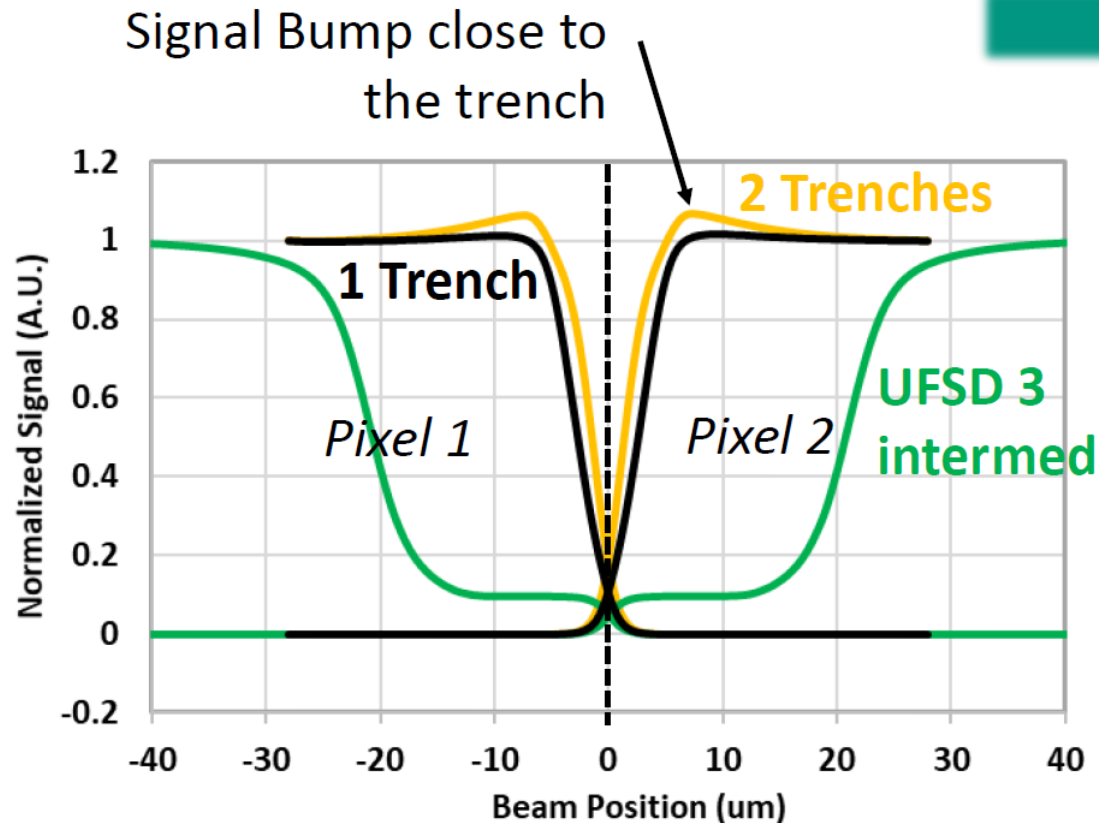


Source: **Siviero F., (INFN) -35th RD50 Workshop**

TCT: interpixel measurements (II)

Characterisation of the no-gain region between channels

■ TI-LGAD Design & Simulations



Source: **G. Paternoster**, (FBK) -35th RD50 Workshop

Even if T2 Layout has larger nominal no-gain region the effective gain-loss width is less wrt T1 layout

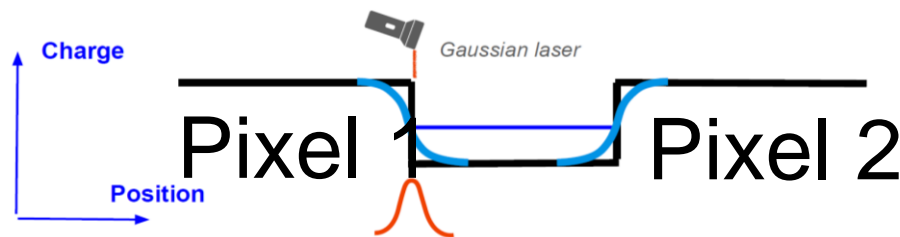
T2 layout shows increased signals at the border (high local E-field)

- Design optimization: trade-off between **minimization of the gain-loss region** and **reduction of E-field at the border**
- High local E-field could potentially trigger an premature breakdown *as observed at KIT*, which could be solved by DJ-LGAD structure

TCT: time resolution and uniformity (III)

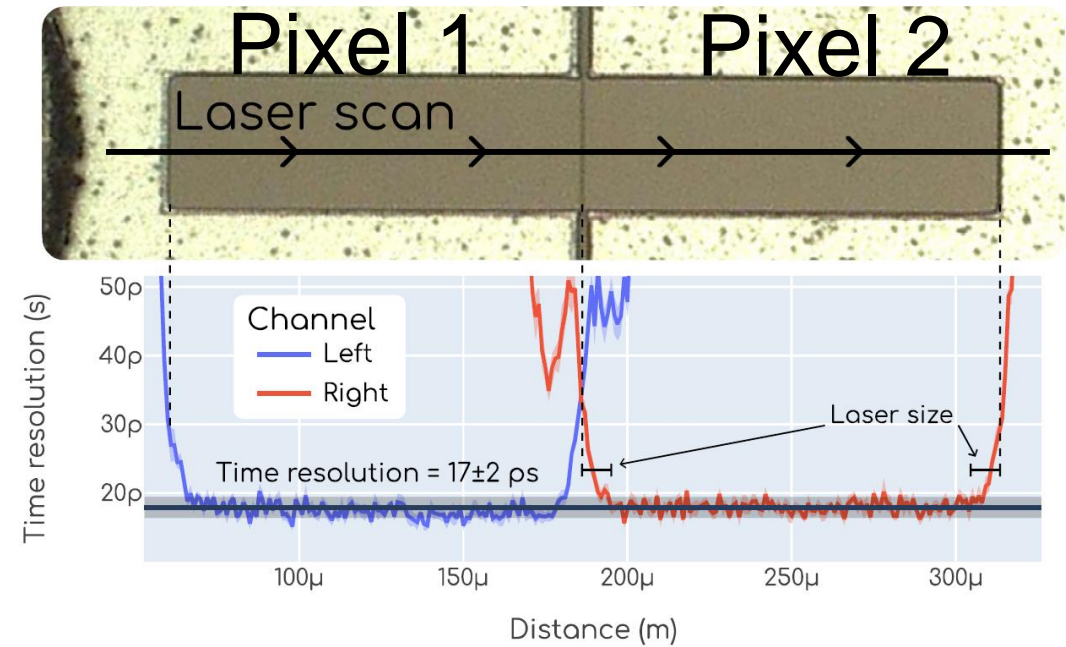
Characterisation of the uniformity of the time resolution along the pixels

- The measurements were performed at INFN-TO and UZH. A scanning *Transient Current Technique* (TCT) setup was used based on infrared laser.



Laser pulses are split in two paths, one containing 20 extra meters of optic fiber, before being sent to the DUT. This produces two almost identical pulses of light with a fixed temporal separation of 100 ns and allows to study the time resolution of the DUT.

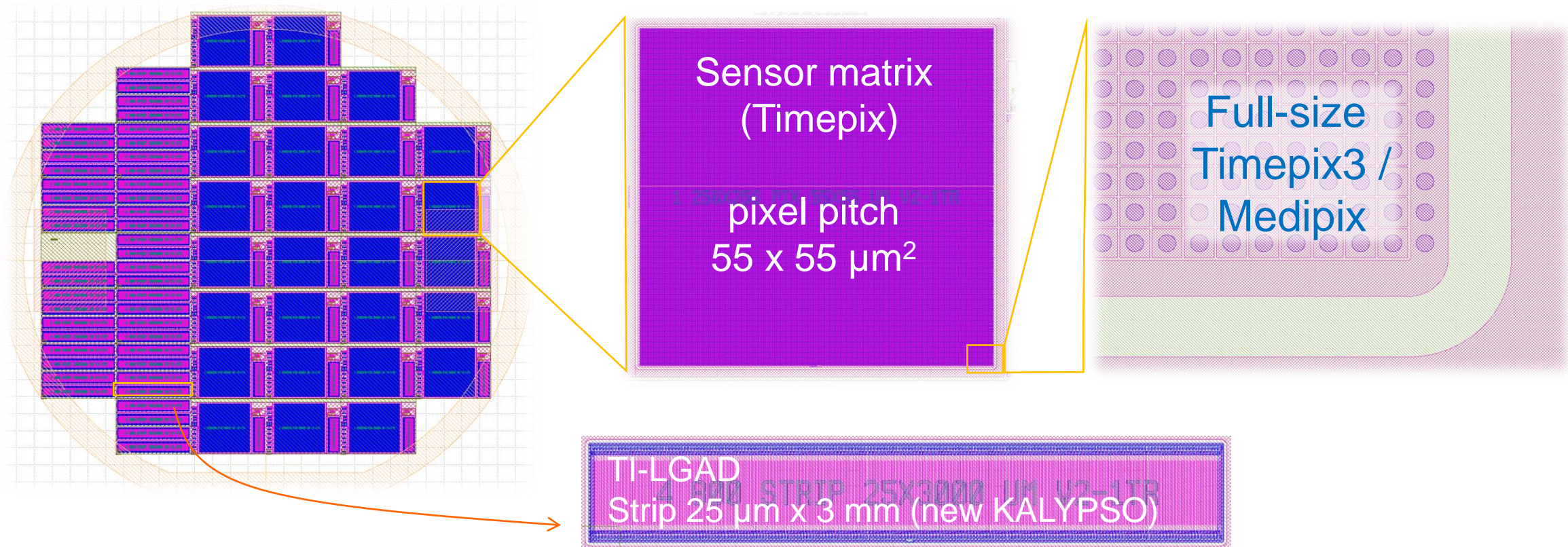
- Measurement performed at University of Zurich
- Time resolution of 17 ± 2 ps measured
- Impressive uniformity of the time resolution along the pixels



Reference: Matias Senger, "A Comprehensive Characterization of the TI-LGAD Technology", doi.org/10.3390/s23136225

Towards to manufacturing of full-reticle sensors

First institute in the world to submit an engineering run for the production of TI-LGAD sensors



Technology: Trench-Isolated LGAD
under production at FBK

- Spatial resolution $< 55/\sqrt{12} = 16 \mu\text{m}$, expected time resolution $< 18 \text{ ps}$

Towards to manufacturing of full-reticle sensors

TI-LGAD for HEP and photon sciences applications

Split table TI-LGAD under production
Delivery: March/April 2025

Wafer	Thickness	Gain Dose	Trench depth	Trench process
1	110	1.02	D2	P2
2	110	1.02	D2	P2
3	110	1.04	D2	P2
4	110	1.04	D2	P2
5	110	1.02	D3	P2
6	110	1.02	D3	P2
7	110	1.04	D3	P2
8	150	1.04	D3	P2
9	150	1.02	D4	P2
10	150	1.02	D4	P2
11	150	1.02	D4	P3
12	150	1.02	D4	P3
13	150	1.02	D4	P4
14	150	1.04	D4	P4
15	275	1.04	D3	P2
16	275	1.04	D3	P2
17	275	1.04	D4	P3
18	275	1.04	D4	P3
19	55	1.02	D2	P2
20	55	1.02	D2	P2

} TI-LGAD for HEP, high time and spatial resolution to fulfil DTS-2 milestone

Towards to manufacturing of full-reticle sensors

TI-LGAD for HEP and photon sciences applications

Wafer	Thickness	Gain Dose	Trench depth	Trench process
1	110	1.02	D2	P2
2	110	1.02	D2	P2
3	110	1.04	D2	P2
4	110	1.04	D2	P2
5	110	1.02	D3	P2
6	110	1.02	D3	P2
7	110	1.04	D3	P2
8	150	1.04	D3	P2
9	150	1.02	D4	P2
10	150	1.02	D4	P2
11	150	1.02	D4	P3
12	150	1.02	D4	P3
13	150	1.02	D4	P4
14	150	1.04	D4	P4
15	275	1.04	D3	P2
16	275	1.04	D3	P2
17	275	1.04	D4	P3
18	275	1.04	D4	P3
19	55	1.02	D2	P2
20	55	1.02	D2	P2

Split table TI-LGAD under production

Delivery: March/April 2025

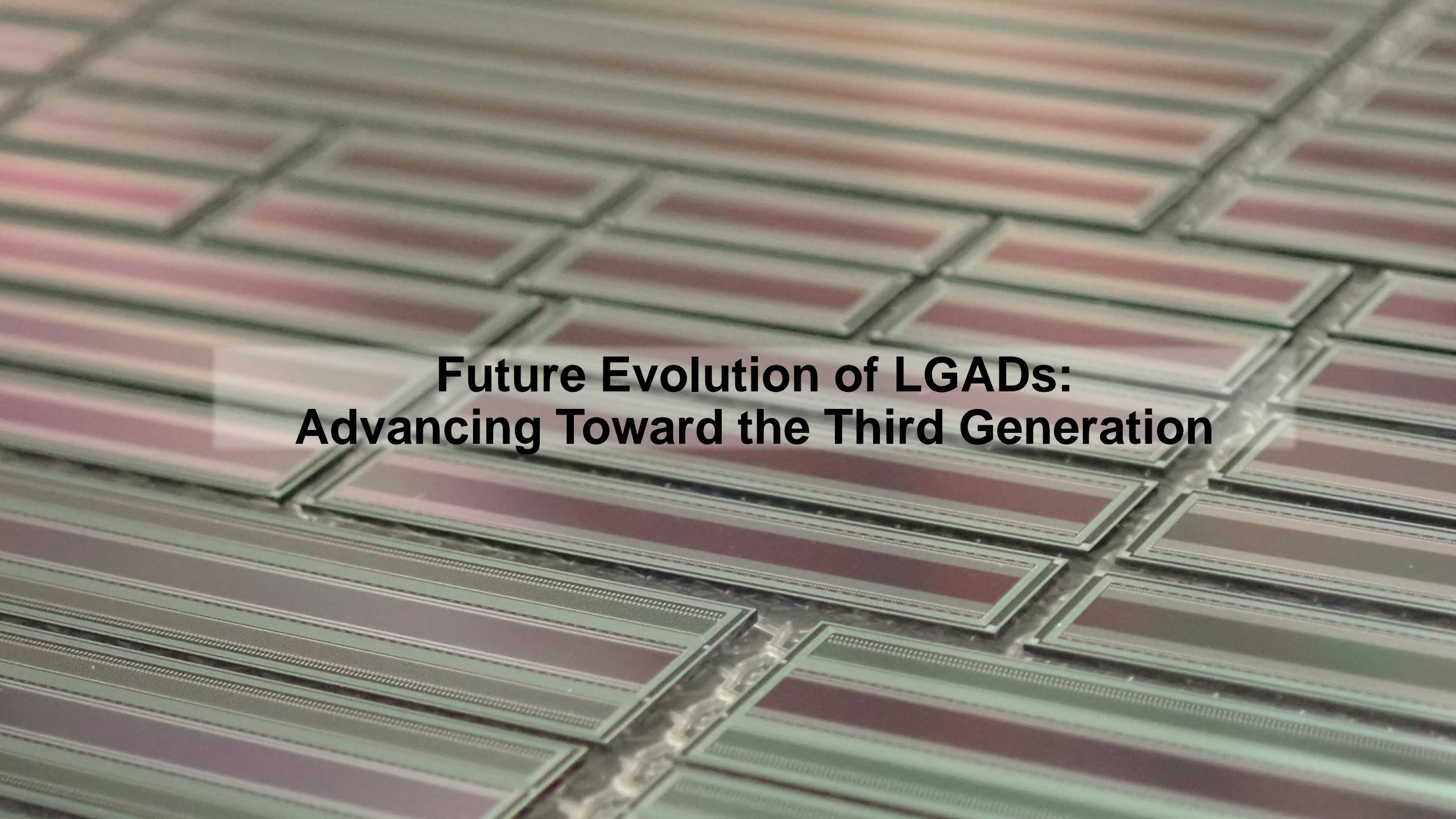


Advancing thick LGAD technology for photon science applications and beyond

...

Si thickness	Absorption (X-rays 6.4 KeV)	Expected time resolution
55 μm	74 %	< 20 ps
110 μm	94 %	c.a. 100 ps
150 μm	98 %	c.a. 180 ps
275 μm	close to 100 %	c.a. > 200 ps

TI-LGAD for HEP, high time and spatial resolution to fulfil DTS-2 milestone

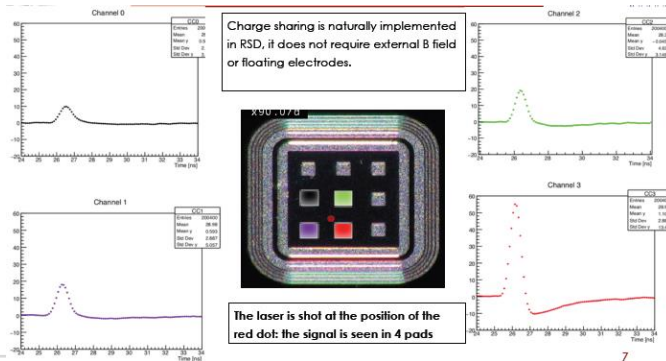
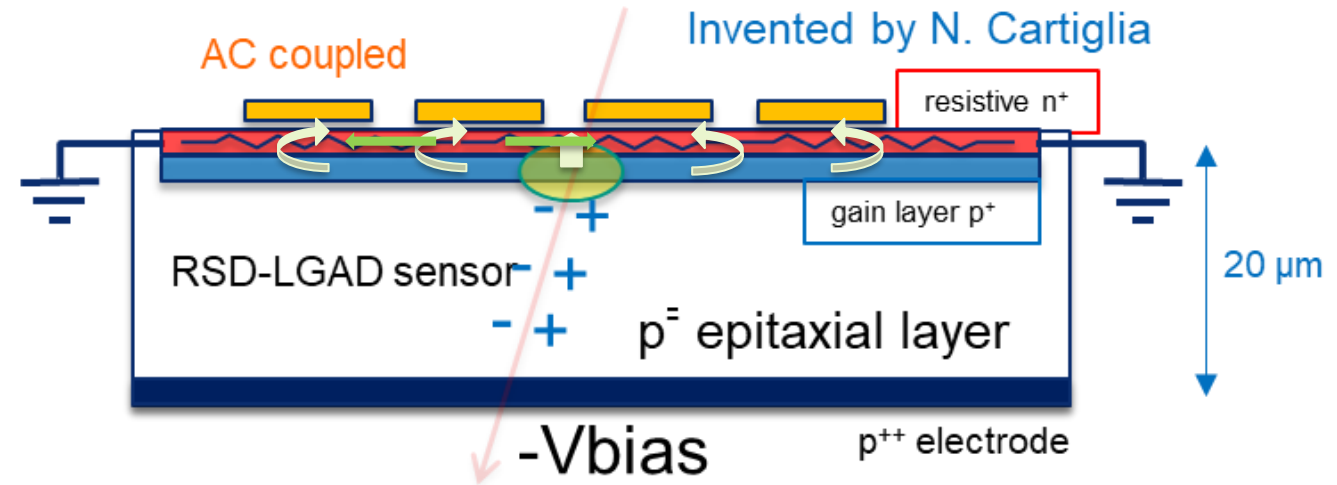


**Future Evolution of LGADs:
Advancing Toward the Third Generation**

AC-coupled LGAD

Development of a demonstrator based on resistive silicon detector (RSD or AC-LGAD) optimized for timing and position

- Uniform gain of > 20, signal up to 10 fC possible even with very thin detector (down to 20 μm)
- Noise similar to standard pixel → excellent S/N with very low thin sensor → low multiple scattering → high-precision
- Charges collected by a uniform n+ resistive layer and drifted by strong lateral electrical field → high charge sharing
- Signal collected by AC-coupled
- No pixel segmentation or diffusion regions → high radiation tolerance without p-stop/p-spray structures



- High spatial resolution up to x10 better of binary resolution $\sigma_x = \frac{pitch}{\sqrt{12}}$

Geometry	50-100	100-200	150-300	200-500
RSD spatial resolution, μm	4	5.5	5.9	15
Binary spatial resolution, μm	14.4	28.9	43.3	86.6

- ML algorithms implemented on the front-end for evaluating precise spatial and temporal information with high resolution/accuracy.

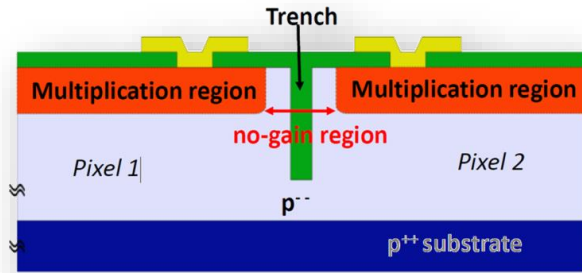


New generation of LGAD technology

Deep-Junction LGAD to achieve high granularity and radiation hardness



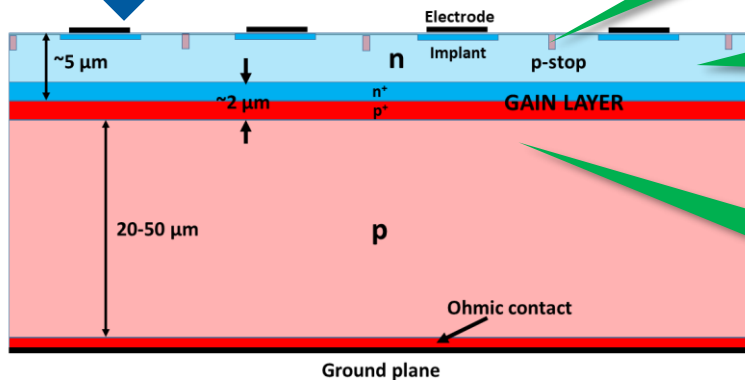
- Continuous deep-junction (DJ) gain layer → very uniform gain. Premature breakdown issues → removed
- Expected an improvement in the radiation-hardness, very-thin, very-fast, high-granularity, edgeless technology



Trench isolated LGAD structure

Pixel insulation based on p-stop or trenches → high-granularity

Technology evolution



n-type epi-layer → dramatically reduction of premature breakdown

Continuous gain-layer → very uniform

S.M. Mazza et al, Univ. of Santa Cruz (2022)

Deep-Junction LGAD to achieve high granularity and radiation hardness	
Contact Person	Dr. Simone Michele Mazza, Santa Cruz Institute for Particle Physics University of California, Santa Cruz 1156 High St., Santa Cruz, CA, 95064, U.S. simazza@ucsc.edu
Institutes	<ol style="list-style-type: none"> 1. University of California Santa Cruz (S.M. Mazza, B. Schumm) 2. FBK (M. Boscardin, M. Centis Vignali, G. Paternoster) 3. CERN (M. Moll, V. Kraus, M. Wiehe, M. Fernandez Garcia, N. Sorgenfrei) 4. UNM (S. Seidel, J. Si, R. Novotny, J. Sorenson, H. Farook, A. Gentry) 5. KIT (M. Caselle, A. Dierlamm) 6. PSI (J. Zhang, A. Bergamaschi, M. Carulla) 7. HEPHY (T. Bergauer, A. Hirtl, M/ Dragicovic) 8. UCG (G. Lastovicka-Medin, V. Backovic, I. Bozovic, J. Doknic) 9. Nikhef (M. van Beuzekom, F. Filthaut, M. Wu, H. Snoek) 10. UZH (B. Kilminster, A. Macchiolo, M. Senger) 11. IHEP Beijing (Z. Liang, M. Zhao, Y. Fan) 12. Manchester (O.A. De Aguiar Francisco, E. Ejopu, M. Gersabeck, A. O.
Total project	101.600 €
RD50 request	50.000 €

1 Abstract

This activity aims at developing a new generation of LGAD technology for applications, featuring: high granularity and radiation hardness. In conventional LGAD sensors, the pixel segmentation is limited by the presence of an inter-pixel resistance. The project goal is to produce segmented thin LGADs (Deep-Junction LGADs) with small pixels down to 100 μm and a 100% gain layer. These devices would provide high spatial resolution preserving at the same time the excellent timing resolutions of 30 ps, already reached with thin LGAD sensor produced at FBK. Furthermore, by adjusting the design by controlling the n/p degradation with radiation damage, this type of radiation-hardness reach of LGADs.

Approved



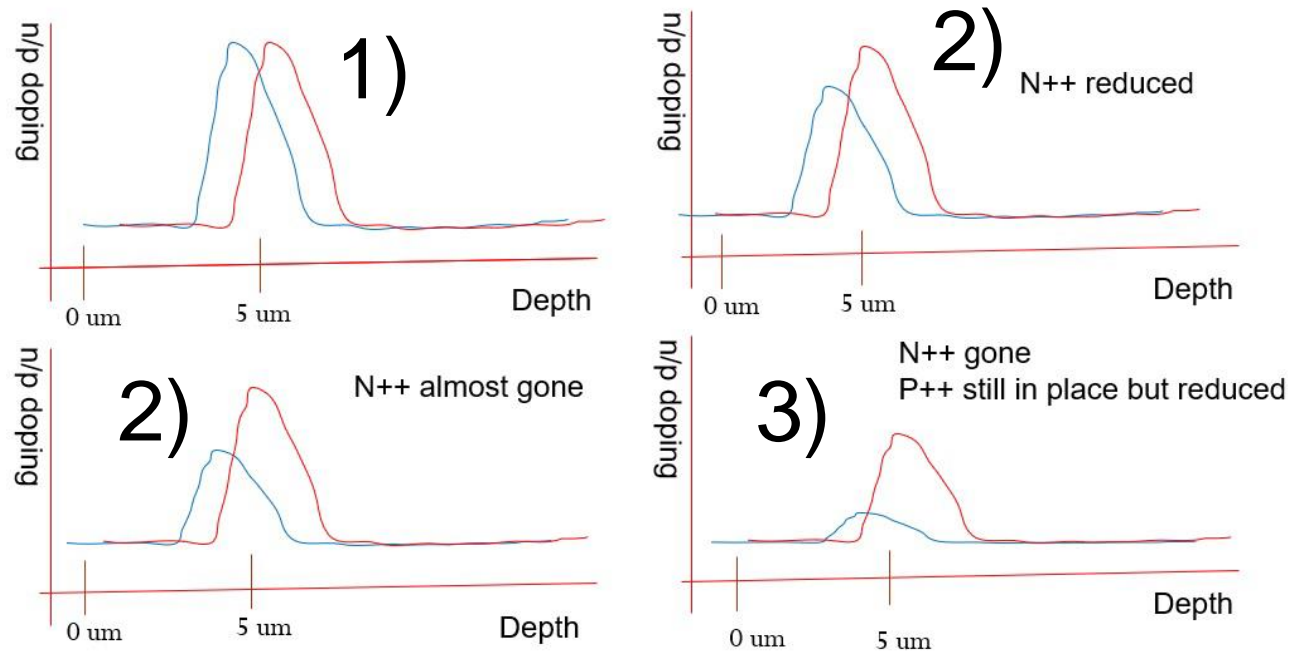
FONDAZIONE BRUNO KESSLER



Toward higher radiation hardness LGAD

Acceptor removal mitigation by layout

- Both the timing resolution and the gain deteriorate with radiation damage due to the acceptor removal mechanism, which reduces the effective doping concentration in the gain layer



- 1) Initial implantation has a 'shallow' (p++ and n++ close together, both highly doped) that is 'deep' in the sensor. The device operates as a "shallow gain layer" (good timing performance)
- 2) With radiation damage the p++ and n++ degrade. The ratio of removal of p++ and n++ can be adjusted with carbon and oxygen implantation respectively
- 3) As n++ degrades faster than p++ the electric field between the deep gain layer and the surface gradually rises.

n++ effective doping layer

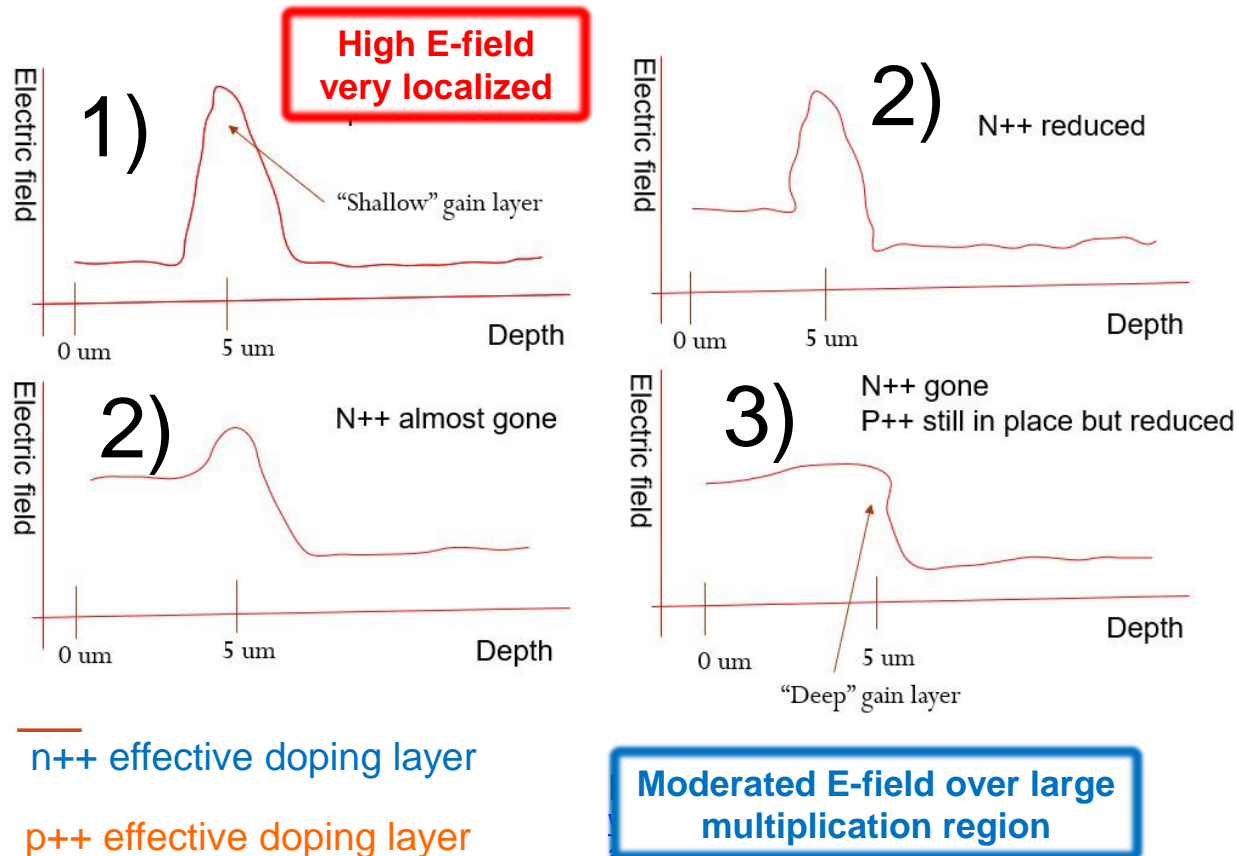
p++ effective doping layer

Patent pending:
[WO2021087237A1 - Deep junction low-gain avalanche detector - Google Patents](#)

Toward higher Radiation hardness LGAD

Acceptor removal mitigation by layout

- Both the timing resolution and the gain deteriorate with radiation damage due to the acceptor removal mechanism, which reduces the effective doping concentration in the gain layer



- 1) very localized and large multiplication charges space. The device operates as a "shallow gain layer" (good timing performance)
- 2) With radiation damage the p++ and n++ degrade, E-field and the multiplication region are balanced
- 3) Moderated E-field distributed over a large multiplication space region (5 μm), which guarantee an adequate multiplication factor also at very high-dose. The device operates as a deep/broad gain layer

Next lecture

Readout electronics of fast detectors